

PRECAMBRIAN GEOLOGY OF THE PICURIS RANGE,  
NORTH-CENTRAL, NEW MEXICO

BY

PAUL WINSTON BAUER

B.S., University of Massachusetts, Amherst, 1978

M.S., University of New Mexico, Albuquerque, 1983

DISSERTATION

Submitted in Partial Fulfillment of the  
Requirements for the Degree of

Doctor of Philosophy in Geology

The New Mexico Institute of Mining and Technology  
Socorro, New Mexico

December, 1987

## ACKNOWLEDGMENTS

I thank my committee members Dr. James M. Robertson, Dr. Jonathan F. Callender, Dr. Jeffrey A. Grambling, Dr. Christopher K. Mawer, and Dr. Kent C. Condie for all aspects of their assistance and guidance. I am particularly grateful to Michael L. Williams for his encouragement, interest, and friendship during the past four years. Other individuals whose contributions were sincerely appreciated are Dr. Rod Holcombe, Dr. Ron Vernon, Dr. Tim Bell, and Dr. Sam Bowring. For assistance in the field I thank Roger Smith, Dave Plummer, Jim Walker, and Rick Lozinsky.

I gratefully acknowledge the financial support provided by the New Mexico Bureau of Mines and Mineral Resources (Frank Kottowski, Director), National Science Foundation Grant EAR 8018506 (to J.F. Callender), the Geological Society of America, the New Mexico Geological Society, Sigma Xi, and the University of New Mexico.

Finally, special thanks to my wife and best friend Joan Resnick, for her support throughout this work.

## ABSTRACT

The Picuris Range in north-central New Mexico contains extensive exposures of Early Proterozoic metamorphosed supracrustal and plutonic rocks. The supracrustal rocks can be divided into three lithostratigraphic groups: the Vadito Group, exposed in the southern part of the range; the felsic schist at Pilar, restricted to the northern part of the range; and the Ortega Group, exposed in the central part of the range. Four distinct granitic plutons, which range in age from 1680 Ma to 1450 Ma, crop out in the southernmost Picuris Range.

The Vadito Group is a stratigraphically complex, heterogeneous sequence of volcanic, volcanoclastic, and clastic sedimentary rocks. In the southwestern Picuris Range, where rocks are best exposed, the Vadito Group consists of three lithostratigraphic units (from north to south: the Marquenas Quartzite, the Vadito schist, and the Vadito amphibolite) that may be separated by bedding-parallel ductile faults and/or unconformities. Granitic plutons which intrude Vadito schist (and perhaps Vadito amphibolite) nowhere intrude the Marquenas Quartzite.

The felsic schist at Pilar consists of homogeneous, feldspathic, quartz-muscovite quartz-eye schist that probably represents metamorphosed, altered, phenocrystic felsic volcanic rocks. No plutons intrude the felsic

schist. These rocks may or may not be equivalent to some part of the Vadito Group.

The Ortega Group is a transgressive, stratigraphically continuous, metamorphosed sequence of basal quartz arenite (Ortega Quartzite), interlayered quartzites and pelitic schists (Rinconada Formation), black phyllites (Pilar Phyllite), and laminated phyllites and schists (Piedra Lumbre Formation) that accumulated in a shallow marine setting. Nowhere are Ortega Group rocks cut by plutons.

Although it is unknown how these three lithostratigraphic groups are related, the Vadito Group and the felsic schist at Pilar occupy similar structural positions below the Ortega Group. The south-dipping boundary between Ortega Group and overlying Vadito Group is a near-bedding-parallel, ductile reverse fault that contains recrystallized quartz-rich mylonites. The south-dipping boundary between Ortega and underlying felsic schist at Pilar is a bedding-parallel, ductile shear zone that contains pristine quartz mylonites. Kinematic indicators suggest that Ortega moved southward over the felsic schist.

Supracrustal rocks have undergone a progressive deformational history that resulted in the formation of three major generations of penetrative structures. All three supracrustal rock groups contain a bedding-parallel schistosity ( $S_1$ ) that is the earliest tectonite fabric recognized. A south-dipping extension lineation ( $L_1$ )

commonly accompanies  $S_1$ . The Ortega Quartzite contains other  $D_1$  structures indicative of localized, bedding-parallel simple shear strain. These shear structures formed throughout much of the ductile deformation history.

Crustal shortening during  $D_2$  generated major tight folds in the Ortega Group (Hondo syncline and Copper Hill anticline) and moderate folding in the Vadito Group. The Hondo syncline is the dominant structure in the mountain range. Most  $F_2$  folds are tight to isoclinal, plunge shallowly westward, and are overturned to the north. Near-bedding-parallel, steeply south-dipping faults and local large-scale imbrication of Ortega Quartzite accompanied  $D_2$ .

$D_3$  is characterized by an intense, pervasive, east-trending schistosity or spaced cleavage ( $S_2^*$  in the Ortega Group) that is the dominant cleavage in most schistose rocks.  $S_2^*$ , which transects  $F_2$  folds in the Ortega Group, probably formed late in the folding history.

$D_1$ ,  $D_2$ , and  $D_3$  structures developed with conditions of approximately coaxial principal strain axes. Throughout the deformation history strain was heterogeneous on all scales.

The preferred stratigraphic/kinematic/tectonic model for the Proterozoic evolution of rocks exposed in the Picuris Range calls for: 1) Vadito Group rocks (or perhaps only part of the Vadito Group) formed in an arc or back-arc setting sometime prior to 1700 Ma; 2) at around 1700 Ma, rifting of this early crust resulted in voluminous felsic

volcanism (felsic schist at Pilar) and plutonism, followed by; 3) crustal stabilization and subsequent accumulation of Ortega Group sediments on some type of continental margin; 4) rocks were buried to 12-15 km depth and subjected to an extended orogenic event, due perhaps to convergence and collision from the south. During  $D_1$ , shear is concentrated between the overriding, mechanically stiff Ortega Quartzite and incompetent felsic schists. As shortening progresses, north-directed shear moves Vadito Group rocks northward over the Ortega Group. As shortening continues, strain evolves from shear-dominated to more homogeneous bulk shortening by nucleation and growth of major folds in the Ortega and Vadito groups. As folding evolves, a well-developed, slightly oblique foliation develops over earlier structures. Late, south-directed shearing occurs along the already highly tectonized Ortega Quartzite-felsic schist boundary.

This model of Proterozoic shearing, folding, and faulting in the Picuris Range is similar to Proterozoic histories recently proposed for nearby uplifts (Tusas Range and Rio Mora area), and is also similar to geologic histories described in a number of Phanerozoic orogenic belts.

## TABLE OF CONTENTS

ACKNOWLEDGMENTS.....	ii
ABSTRACT .....	iii
TABLE OF CONTENTS .....	vi
LIST OF FIGURES .....	xiv
LIST OF TABLES .....	xix
CHAPTER 1. INTRODUCTION .....	1
Purpose and Scope .....	1
Methods .....	4
Access, Physiography, Physical Features, and Map Area.....	6
Previous Work .....	7
CHAPTER 2. GENERAL GEOLOGY .....	13
Regional Geologic Setting.....	13
Local Geologic Setting .....	17
General.....	17
Phanerozoic Rocks.....	17
General.....	17
Paleozoic Rocks.....	19
Del Padre sandstone.....	19
Cenozoic Deposits.....	20
Picuris Tuff.....	20
Tesuque Formation.....	20
Ancha Formation.....	22
alluvium.....	22

Precambrian Rocks.....	23
General.....	23
Basic Precambrian Stratigraphy and Structure.....	23
CHAPTER 3. PRECAMBRIAN STRATIGRAPHY .....	26
General Statement .....	26
Vadito Group .....	30
General field relations and previous work .....	30
Southwestern Picuris Range.....	31
General.....	31
Schist.....	32
Amphibolite.....	32
Marquenas Quartzite Formation.....	33
Other quartzite and conglomerate.....	34
Felsic schists.....	34
Calc-silicates.....	35
Southeastern Picuris Range.....	35
General.....	35
Quartzites and conglomerates.....	36
Amphibolite and biotite schist.....	37
Felsic schist.....	37
Porphyroblastic schist below Ortega.....	39
Andalusite schist.....	39
Felsic Schist at Pilar.....	40
General.....	40
Northwestern Picuris Range (Pilar cliffs).....	41
General.....	41

Quartz-muscovite schist.....	41
Northeastern Picuris Range.....	43
General.....	43
Quartz-muscovite schist.....	43
Eastern block of the Picuris Range.....	44
General.....	44
U.S. Hill.....	44
Comales compground.....	45
Depositional environments of the felsic schist at Pilar and the Vadito Group.....	46
Stratigraphic Position of Marquenas Quartzite.....	47
Ortega Group .....	49
General Statement.....	49
Ortega Quartzite Formation .....	51
General.....	51
Lower quartzite.....	54
Upper quartzite.....	54
Rinconada Formation .....	55
General.....	55
R1/R2 member.....	56
R3 member.....	57
R4 member.....	58
R5 member.....	58
R6 member.....	59
Pilar Phyllite Formation .....	60

Piedra Lumbre Formation .....	61
Sedimentology of the Ortega Group.....	63
Plutonic Rocks .....	65
General.....	65
The Granite of Alamo Canyon.....	65
The Granite of Picuris Peak.....	67
Cerro Alto Metadacite.....	67
Puntiagudo Granite Porphyry .....	68
Rana Quartz Monzonite .....	68
Penasco Quartz Monzonite .....	69
Pegmatites .....	70
Summary of General Field Relations.....	71
CHAPTER 4. GEOCHRONOLOGY .....	76
Introduction.....	76
Previous Work.....	78
Discussion.....	80
CHAPTER 5. GEOMETRICAL FABRIC ELEMENTS.....	82
Introduction .....	82
Compositional layering, $S_0$ .....	83
First Generation of Structures, $D_1$ .....	83
Second Generation of Structures, $D_2$ .....	89
Third Generation of Structures, $D_3$ .....	91
Later Generations of Structures.....	93
CHAPTER 6. METAMORPHISM.....	97
Introduction and previous work.....	97
Metamorphic Mineral Assemblages.....	100

Aluminum Silicate Minerals.....	100
General.....	100
Kyanite.....	100
Andalusite.....	103
Sillimanite.....	104
Discussion.....	107
Other Minerals.....	109
General.....	109
Biotite.....	109
Garnet.....	111
Staurolite.....	115
Chloritoid.....	126
Cordierite.....	126
Other minerals.....	127
Summary.....	128
Garnet-Biotite Thermobarometry.....	128
CHAPTER 7. STRUCTURAL GEOLOGY AND SYNTHESIS.....	133
Introduction .....	133
General statement.....	133
Methods .....	136
Geometries of Domains .....	138
Introduction.....	138
Ortega Group.....	139
Relict sedimentary structures.....	139
First generation of structures, D <sub>1</sub> .....	139
Second generation of structures, D <sub>2</sub> .....	149

Third generation of structures, D <sub>3</sub> .....	157
Fourth generation of structures, D <sub>4</sub> .....	161
Porphyroblast microstructures.....	161
Summary.....	167
Vadito Group.....	168
General.....	168
Relict sedimentary structures.....	168
First generations of structures, D <sub>1</sub> .....	169
Second generation of structures, D <sub>2</sub> .....	171
Third generation of structures, D <sub>3</sub> .....	173
Fourth generation of structures, D <sub>4</sub> .....	174
Southern granitic rocks.....	174
Porphyroblast microstructures.....	175
Discussion.....	177
Felsic Schist at Pilar.....	178
General.....	178
First generation of structures, D <sub>1</sub> .....	179
Second generation of structures, D <sub>2</sub> .....	183
Discussion.....	183
Eastern Block.....	184
General.....	184
Deformational fabrics in the Granite of	
Alamo Canyon.....	185
Deformational fabrics in the Rio	
Pueblo Schist.....	185
Deformational fabrics in the Ortega	

Quartzite.....	186
Summary.....	186
Contacts Between Lithostratigraphic Domains.....	190
Southern contact.....	190
Northern contact.....	193
Picuris-Pecos fault.....	194
Discussion.....	196
Structural Synthesis.....	196
Stratigraphic and Structural Constraints.....	196
Possible Models.....	200
Discussion.....	211
CHAPTER 8. PRECAMBRIAN TECTONIC EVOLUTION.....	214
Introduction.....	214
Depositional Environments.....	215
Vadito Group.....	215
Felsic Schist at Pilar.....	218
Ortega Group.....	219
Discussion.....	220
Constraints on Tectonic Settings.....	220
Possible Tectonic Settings.....	221
Vadito Group.....	221
Felsic Schist at Pilar.....	225
Ortega Group.....	226
Precambrian Tectonic Evolution.....	227
CHAPTER 9. CONCLUSIONS AND SUMMARY.....	230

APPENDICES .....

    Appendix 1. Samples for geochronology in the  
        Picuris Range.....

        Plutonic Rocks.....

            Granite of Alamo Canyon.....

            Granite of Picuris Peak.....

            Cerro Alto Metadacite.....

        Metavolcanic rocks.....

            Vadito quartz-eye schist, southern  
                Picuris Range.....

            Felsic Schist, Pilar cliffs.....

            Rio Pueblo Schist, Comales  
                campground.....

        Metasedimentary rocks.....

            Marquenas quartzite cobbles.....

            R6 schist, southern Picuris Range....

    Appendix 2. Garnet-biotite thermometry and  
        microprobe data.....

REFERENCES CITED .....

## LIST OF FIGURES

Figure	Page
1.1 Location map of Picuris Range.	5
1.2 History of stratigraphic nomenclature for Precambrian rocks in the Picuris Range.	9
2.1 Regional tectonic map of the northern Rio Grande rift.	14
2.2 Generalized map showing Precambrian rocks of north-central New Mexico.	16
2.3 Photomicrograph of Del Padre Sandstone Formation.	21
2.4 Generalized geologic map of the Picuris Range.	24
3.1 Photograph of Vadito Group feldspathic schist.	38
3.2 a. Photograph and photomicrograph of quartz-eye felsic schist at Pilar.	42
3.3 Generalized stratigraphic column of the Ortega Group.	52
3.4 Summary cross-section of stratigraphy in Picuris Range.	72
3.5 Chart of stratigraphic relations in the Picuris Range.	75
4.1 Summary of geochronology in the Picuris Range.	77
5.1 Photographs of primary sedimentary structures in the Ortega Group.	84

5.2	Photograph of transposed layering in Piedra Lumbre schist.	85
5.3	Photomicrograph of $S_1$ foliation in felsic schist at Pilar.	87
5.4	Photograph of down-dip $L_1$ extension lineation in Ortega Quartzite, northwestern Picuris Range.	88
5.5	Photomicrographs of F2 folds in Ortega Group schists.	90
5.6	Photomicrograph of $S_2^*$ crenulating earlier cleavage.	92
5.7	Photographs of third generation lineations in the Ortega Group.	94
5.8	Photograph and photomicrograph of $S_3$ crenulations in Ortega Group schists.	95
6.1	Photomicrograph of kyanite blades with undulatory extinction.	102
6.2	Photomicrograph of fibrolitic sillimanite aggregates in Ortega Quartzite.	106
6.3	Common metamorphic mineral assemblages in the Ortega Group.	110
6.4	Photomicrographs of pre- $S_2^*$ biotite porphyroblasts.	112
6.5	Photomicrograph of garnet containing differently oriented inclusion trails in core and rim.	114
6.6	Photomicrograph of garnet with symmetrical secondary growth.	116

6.7 Photomicrograph of sector zoned staurolite with euhedral core and anhedral rim.	118
6.8 Photomicrograph of staurolite after chloritoid.	119
6.9 Photomicrograph of staurolite porphyroblast with symmetrical secondary growth.	121
6.10 Photomicrograph of "millipede" microstructure in staurolite porphyroblast.	123
6.11 Photomicrograph of staurolite and garnet with concentric quartz inclusion shells.	124
6.12 Photomicrograph of staurolite that preserves spaced cleavage.	125
6.13 Summary of timing relationships between fabric elements and porphyroblast growth in the Ortega Group.	129
6.14 Microprobe profiles across garnet and staurolite.	132
7.1 Generalized geologic map of the Picuris Range.	134
7.2 Contoured stereographic projections of $S_0$ and $L_1$ for Ortega Group rocks.	141
7.3 Photograph of quartz-vein-rich shear zone in Ortega Quartzite.	143
7.4 Photograph of sheath fold in Ortega Quartzite shear zone.	144
7.5 Photograph of small shears in basal Ortega Quartzite.	145
7.6 Photomicrograph of recrystallized quartz mylonite from Ortega Quartzite.	147

7.7	Photomicrograph of pristine quartz ribbon mylonite from R3.	148
7.8	Block-diagram sketch of Hondo syncline showing competent Ortega Quartzite and disharmonic folds in schists.	151
7.9	Contoured stereographic projection and fold sketch of $S_{0/1}$ and $L_2^*$ relationships in the Ortega Group.	153
7.10	Sketch cross-section through Copper Hill anticline.	154
7.11	Sketch cross-section showing imbrication of Ortega Quartzite in northwestern map area.	156
7.12	Sketch, photograph, and stereogram of $S_2^*$ transecting limbs of $F_2$ folds.	158
7.13	Photograph of small near-bedding-parallel $D_2$ or $D_3$ shear zone in Piedra Lumbre schist.	162
7.14	Photomicrographs of zoned staurolite porphyroblast containing two different Si orientations in core and rim.	166
7.15	Stereographic projections of modal $S_{0/1}$ and $S_2$ in Vadito Group rocks.	170
7.16	Photograph and photomicrograph of cordierite schist in Vadito Group.	176
7.17	Photomicrograph of sheared quartz-eye in felsic schist at Pilar.	181
7.18	Summary of structural fabrics in the Ortega Group, Vadito Group, and felsic schist at Pilar.	188

7.19 Synoptic stereographic projections of fabric elements in the Picuris Range.	189
7.20 Photograph of sheared, asymmetric clast in mylonitic Marquenas Quartzite at Ortega-Vadito contact.	191
7.21 Photomicrographs of mylonitic rocks from the Ortega-Vadito contact in the southern Picuris Range.	192
7.22 Photographs of mylonitized contact between Ortega Quartzite and felsic schist at Pilar in the northern Picuris Range.	195
7.23 Sketch of stratigraphic/kinematic model a1.	204
7.24 Sketch of stratigraphic/kinematic model a2.	206
7.25 Sketch of stratigraphic/kinematic model b.	208
7.26 Sketch of stratigraphic/kinematic model d.	210
8.1 Generalized geologic map of Precambrian-cored uplifts in north-central New Mexico.	223

LIST OF TABLES

6.1 Garnet-biotite geothermometry for four samples  
from the northern Picuris Range.....131

## CHAPTER 1. INTRODUCTION

### Purpose and Scope

An important problem in Precambrian geology involves the nature and timing of the formation, growth, and deformation of continental crust. The recent literature contains numerous examples of geologic studies that have successfully reconstructed the Precambrian crustal evolution of an area (Hoffman and Bowring, 1984; Green et al., 1985; McLelland and Isachsen, 1985; Rivers, 1983). Most of the well-documented studies that have examined this topic are multi-faceted, consisting of detailed lithologic mapping in conjunction with a variety of related studies including: U-Pb zircon geochronology, structural geology, geochemistry, metamorphic analysis, and geophysics.

The early Proterozoic history of the southwestern U.S. has been the focus of much recent research. Regional isotopic studies (Nelson and DePaolo, 1985; Silver and others, 1977; Van Schmus and Bickford, 1981; Silver, 1984; Stacey and Hedlund, 1983; Gresens, 1975) and geochemical terrane mapping (Condie, 1978a, 1978b, 1982, 1984, 1985) provide the framework for more detailed investigations into the stratigraphy, sedimentology, petrology, structure, and metamorphism of rocks within smaller areas. In New Mexico,

this more detailed, mapping-based research has been concentrated in the Picuris, Tusas, and Truchas-Rio Mera ranges of northern New Mexico, where distinctive lithostratigraphic rock packages allow both local stratigraphic reconstructions and inter-range correlations. Although each of these areas had been mapped in at least a reconnaissance manner by 1960, many basic questions concerning Precambrian geologic history, environments, and processes remain unanswered.

The Picuris Range, located about 20 km southwest of Taos in north-central New Mexico, has been important in the development of ideas concerning Precambrian geology of northern New Mexico. Several studies have addressed the problems of the stratigraphy and structural evolution in the Picuris Range, including mapping of the entire range (Montgomery, 1953), structural analysis of the southwestern portion of the range (Nielsen, 1972), and a stratigraphic/structural study of a small tract in the Copper Hill area (Holcombe and Callender, 1982). Holcombe and Callender's investigation of stratigraphic and structural relationships in this small area disagreed with previous published interpretations, but the study area was not large enough to resolve critical relations nor to define age relationships and the detailed structural history of the entire Picuris Range. The unresolved questions raised by Holcombe and Callender concerning stratigraphic relations

and deformational history of these and nearby Precambrian rocks provided much of the motivation for the present study. A major tenet of the present study was that earlier difficulties resulted in part from unrecognized structural complexities within the previous areas of study. To resolve these questions, the following topics have been addressed: stratigraphy; nature and style of the early episodes of deformation; significance and timing of the various fabrics; relative and absolute timing of various deformational and metamorphic events; and forces responsible for tectonism.

The primary objectives of this study were to determine the present geometry of Proterozoic strata in the Picuris Range and to thoroughly characterize the Precambrian geologic history, paying special attention to Precambrian deformational events and environments. The secondary objectives have been to apply this knowledge of geometry and kinematics towards understanding the dynamics (physical forces) involved in tectonism, and finally, to attempt to fit the Precambrian geologic history of the Picuris Range into a regional framework within northern New Mexico. These objectives were pursued by detailed geologic mapping and structural analysis of much of the Picuris Range, with collection of rock samples for petrographic analysis and U-Pb zircon geochronology, and by examination of appropriate Proterozoic rocks in other nearby localities.

## Methods

This dissertation is based on detailed geologic mapping at scales of 1:6,000 and 1:12,000 of about 165 sq km (65 sq mi) of the Picuris Range, and laboratory analysis of structural data and rock samples collected in the field. Mapping was done on enlarged U. S. Geological Survey 7.5 minute topographic maps of the Carson, Taos SW, Ranchos de Taos, Trampas, Penasco, and Tres Ritos quadrangles in Taos County (Fig. 1.1).

Field work was done mainly during the summers of 1982-1986. More than 400 oriented and unoriented rock samples were collected, and structural and/or stratigraphic data were recorded at about 600 station locations.

Laboratory study at both the University of New Mexico and New Mexico Institute of Mining and Technology included the following: (1) geometrical analysis of fabric elements recorded both in the field and from oriented laboratory specimens using stereographic projection; (2) compilation of structural maps showing the distribution and variation of attitudes of fabric elements; (3) petrographic examination of about 300 thin sections, with emphasis on timing relationships between fabric development and porphyroblast growth; and (4) selected electron microprobe analysis of 4 garnet-bearing samples. Furthermore, 12 rock samples were selected for U-Pb zircon geochronologic study. Rocks were

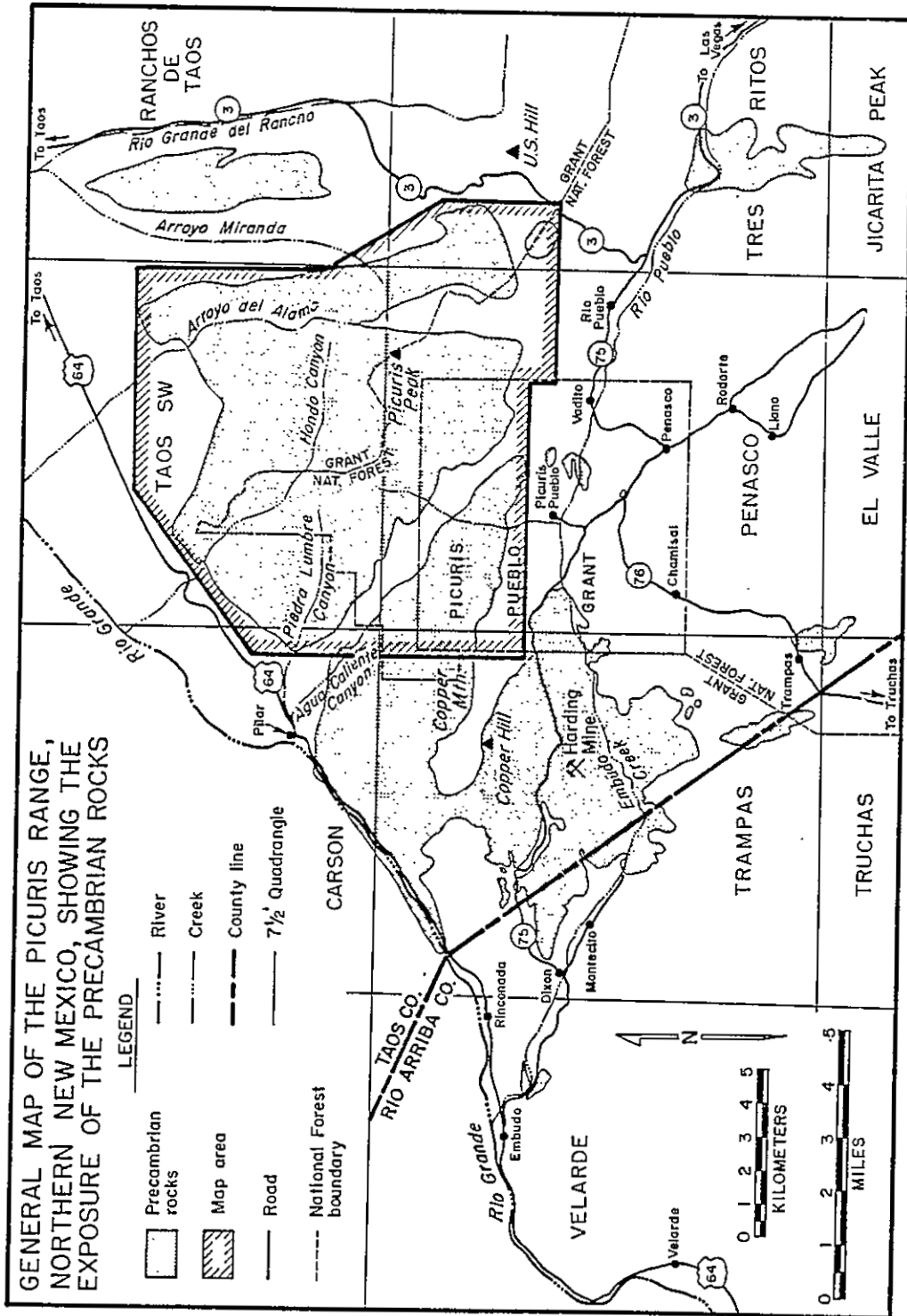


Figure 1.1. General map of the Picuris Range region, showing Precambrian rock exposure and map area.

crushed, ground, and concentrated in facilities of the New Mexico Bureau of Mines and Mineral Resources and the University of New Mexico. Zircon separates are being analyzed by Dr. S. A. Bowring of Washington University in St. Louis.

#### Access, Physiography, Physical Features, and Map Area

Several towns are located around the flanks of the Picuris Range. These towns are linked by three highways that form a triangle around the mountains (Fig. 1.1). Numerous graded and ungraded dirt roads provide access to parts of the mountainous area enclosed by these paved roads. A Forest Service road from Vadito to Picuris Peak provides excellent access to the southeastern Picuris Range. Another Forest Service road from N.M. 75 just west of Penasco to Warm Springs provides access to the central Picuris Range. A primitive road from U.S. 68 into Hondo Canyon provides access to the northern Picuris Range. Several private roads from U.S. 68 provide access to the northeastern Picuris Range. Also, many unimproved dirt roads off N.M. 75 provide access to the Harding Pegmatite Mine area in the southwestern Picuris Range.

Relief of about 1470 m (4800 ft) within the range occurs between the high of 3292 m (10,801 ft) at Picuris

Peak to 1230 m (6000 ft) in the westernmost exposures of Precambrian rock near the town of Dixon. The mountains are rugged, with deep, steep-walled canyons separated by sharp ridges. In general, the range rises to the east towards Picuris Peak, where it drops several thousand feet to a series of north-trending valleys that separate the Picuris Range from the easterly Sangre de Cristo Range.

Physiography in the western half of the range is dominated by narrow east-trending ridges that are underlain by resistant quartzites. To the east, these ridges join the prominent 3050 m (10,000 ft) high north-trending ridge of the eastern Picuris Range.

Climatic conditions and consequently vegetation vary considerably over the range. At lower elevations, and particularly along the southern slopes, precipitation is low and scattered pinon pine and juniper dominate the flora. At higher elevations and in the central canyons, ponderosa pine and aspen form dense forests. Outcrop exposure likewise varies from excellent in many of the dryer regions to poor in heavily forested slopes and valleys.

#### Previous Work

Two major groups of Proterozoic supracrustal rocks are present in the Picuris Range: a metaclastic sequence without

metavolcanic rocks (Ortega Group), and a largely metavolcanic sequence (Vadito Group). Based almost entirely on work done in the southwestern Picuris Range, there have traditionally been two different hypotheses concerning the relative chronology of these sequences in the Picuris Range. One hypothesis holds that the Ortega Group is younger than the Vadito Group, whereas the other maintains that the Vadito Group is younger than the Ortega Group. Figure 1.2 summarizes the additions and modifications various workers have proposed for the stratigraphy of the Picuris Range.

Early work by Just (1937) suggested that the metasedimentary sequence was younger. Montgomery (1953) reinterpreted the field relations of these rocks. He believed that the Vadito rocks unconformably overlay the older Ortega rocks. Miller et al. (1963) recognized a similar stratigraphy in the Truchas Mountains, and Nielsen (1972) retained this relationship during his analysis of Ortega rocks in the Picuris Range. Gresens and Stensrud (1974) noted that a thick metarhyolitic sequence was stratigraphically below the Ortega Quartzite in the northwestern Picuris near the town of Pilar as well as in the eastern Picuris near U.S. Hill. They suggested that the accepted stratigraphic relationship between Ortega and Vadito was suspect. This idea was not accepted by Long (1976) and Scott (1980), both of whom followed Montgomery's original stratigraphy. Subsequently, Holcombe and Callender

Vadito younger than Ortega

Montgomery, 1953		Nielsen, 1972		Long, 1976		Scott, 1980	
Blastose dikes (57)				Pecanitos			
Embudo Granite and pegmatite				Embudo Granite	Panasco qtz. monz. Rana qtz. monz. Punciagudo gran. por. Cerro Alto meta-dac.		
Vadito Formacion	schist member			Vadito Group	Amphibolite	Vadito Group	Marquenas Quartzite
	conglomerate member				schist		
Ortega Form.	Pilar Phyllite Member	Ortega	Pilar Form.	Ortega Group	Piedra Lumbre Formation		Marquenas Quartzite
	Rinconada Schist Member		muscovite phyllite member slate member		Pilar Formation		
	Lower Quartzite (includes metarhyolite, Rio Pueblo Schist) Base unexposed		Rinconada Form.		R <sub>6</sub> R <sub>5</sub> R <sub>4</sub> R <sub>3</sub> R <sub>2</sub> R <sub>1</sub>		

Ortega younger than Vadito

Jusc, 1937	Gressens and Stensrud, 1974		Holcombe and Callander, 1982		This study Bauer, 1987	
Dixon Granite					Panasco qtz. monz. Rana qtz. monz. Punciagudo gran. Cerro Alto metadac.	
Hondo Slate	Ortega Formation	Pilar Phyllite	Ortega Group	Pilar Formation	Ortega Group	Piedra Lumbre
Ortega Quartzite (including the Rinconada schist; Picuris basalts at base of Ortega)		Rinconada Schist		Rinconada Formation		Pilar Phyllite
		Ortega Quartzite		Ortega Quartzite		Rinconada Formation
Hopewell Series (metamorphosed igneous flows with interbedded metasediments; includes the Picuris basalts and the Badito quartzite.)	Metavolcanic-metasedimentary complex (includes Rio Pueblo Schist, metarhyolites) Base unexposed. Ages and structural relationships between metavolc.-metased. complex and Vadito Formation unknown; contact between Marquenas Quartzite and Piedra Lumbre is a fault.		Vadito Group	Piedra Lumbre Formation	Vadito Group	Felsic schist at Pilar (includes Rio Pueblo Schist) Base unexposed
				Marquenas Quartzite		Marquenas Quartzite
				Vadito Schist		Vadito schist
				Vadito Amphibolite		Vadito amphibolite

Figure 1.2. History of stratigraphic nomenclature for Precambrian rocks in the Picuris Range.

(1982) made a detailed structural analysis of rocks adjacent to the Ortega-Vadito contact in the southern Picuris Range. They concluded that the contact was a fault, and that the original stratigraphy of Montgomery needed revision. Their geometric models favored a younger Ortega Group. McCarty (1983) confirmed most of these findings in the Harding Pegmatite Mine area.

The only major regional geologic studies in the Picuris Range that specifically addressed structural problems and interpretations are those of Montgomery (1953) and Nielsen (1972). Montgomery mapped the entire range in reconnaissance fashion and interpreted the structure without benefit of a geometrical analysis or modern petrofabric criteria. His accurate field mapping has proven to be extremely useful during the present study. Montgomery's rock descriptions and interpretations of large-scale structures are excellent and are recommended to readers interested in the early thought on Precambrian rocks in New Mexico. Nielsen's effort involved compilation and field checking of geologic field-camp maps of the western Picuris Range compiled by students and teachers at the University of North Carolina, and a structural analysis of a small area between Copper Hill and the Harding Pegmatite Mine. More local or topical studies include: 1) Holcombe and Callender (1982), who performed a structural analysis in a portion of Nielsen's map area. Although Holcombe and Callender

obtained similar data, their interpretation differed markedly from that of Nielsen; 2) Long (1976), who concentrated on the occurrence of the granitic rocks in the southern Picuris Range, but included a map and structural interpretation of Vadito Group rocks in that area; 3) Scott (1980), who conducted a strain analysis of the Marquenas Quartzite; 4) McCarty (1983), who mapped the structure and petrography of Vadito Group rocks near the Harding Pegmatite Mine; 5) Hurd (1982), who conducted a structural study of the central Hondo syncline in the northwestern Picuris Range; and 6) D.A. Bell (1985), who studied the contact relationships and U-Pb zircon geochronology of granitic rocks in the Harding Pegmatite Mine area.

Prior to 1985, all geochronology in the Picuris Range, with one exception, was based on the Rb-Sr isotopic system, and rocks dated included only the Harding pegmatite and the plutonic bodies south of the Harding Pegmatite Mine. Stacey et al. (1976), Fullagar and Shiver (1973), and Long (1974) all noted that the approximate depositional age of Vadito rocks was 1700 Ma. Based on Rb-Sr geochronology of the "Embudo Granites" (Montgomery, 1953) south of the Harding Mine, Gresens (1972), Fullager and Shiver (1973), and Register (1979) suggested that intermittent intrusion occurred from about 1670 Ma to 1440 Ma. More recent preliminary work using U-Pb zircon chronology suggests two distinct intrusive events for the southern plutons at about

1680 Ma and 1450 Ma (Bell and Nielsen, 1985). L.T. Silver (personal communication in Grambling and Williams, 1985b) reported a U-Pb zircon date of about 1700 Ma for feldspathic quartz-muscovite schist in the Tusas Mountains. Grambling and Williams (1985b) suggested that this age might be appropriate for similar rocks in the Picuris Range which lie below the Ortega Quartzite in cliffs near the town of Pilar.

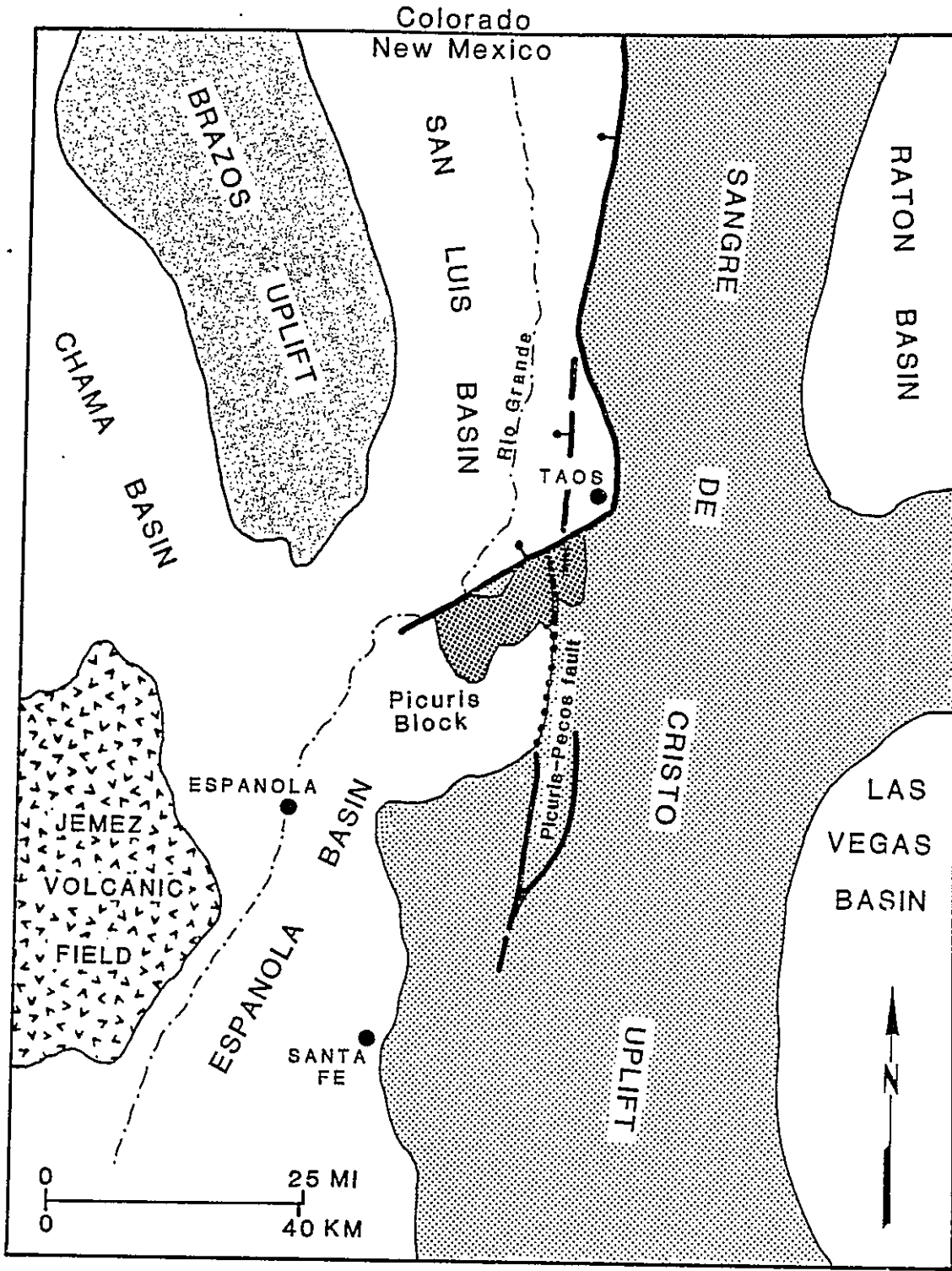
Mineral assemblages in Precambrian rocks of the Picuris Range indicate medium grade (amphibolite facies metamorphism), with peak metamorphic conditions near 530°C, 3.7 kb (Holdaway, 1978), at or near the  $\text{Al}_2\text{SiO}_5$  triple point. Regional metamorphism may have peaked about 1350-1450 Ma ago over much of northern New Mexico (L.E. Long, 1972; P.E. Long, 1974; Gresens, 1975; Callender et al., 1976). Recent work by Grambling (1986) suggested that throughout central and northern New Mexico, subhorizontal isobaric surfaces in Proterozoic rocks preserve consistent P-T conditions of  $4 \pm 0.5$  kb,  $525 \pm 50^\circ\text{C}$ . He proposed that this entire area may have behaved as a coherent cratonic block from mid-Proterozoic until the beginning of Paleozoic sedimentation.

## CHAPTER 2. GENERAL GEOLOGY

### Regional Geologic Setting

The Rio Grande rift consists of a series of linked, north-trending, down-dropped basins that are flanked by generally Precambrian-cored topographic/structural uplifts. In northern New Mexico, the rift lies between the Brazos uplift to the west, and the Sangre de Cristo uplift to the east (Fig. 2.1). Baltz (1978) stated that although some structural elements in the rift are undoubtedly controlled by reactivation of Precambrian and younger features, rift-related deformation does cross-cut some earlier structural trends.

The Picuris Range of north-central New Mexico is a Precambrian-cored, fault-bounded, wedge-shaped uplift that projects westward from the southern Sangre de Cristo Mountains. This isolated, rugged range lies about 20 km southwest of Taos, and includes an area approximately 15 km by 30 km. The Picuris block forms part of the constriction that separates the en echelon Espanola and San Luis basins in the northern Rio Grande rift (Fig. 2.1). The southeastern margin of the San Luis basin is a major hinge fault that separates the east-tilted basinal block from the west-tilted Picuris block (Baltz, 1978). Prior to rifting,



--- FAULT, BAR ON DOWNTHROWN SIDE

Figure 2.1. Generalized regional tectonic map of north-central New Mexico, showing Picuris Block and major faults in the Picuris region. After Baltz (1978).

this region represented a broad Laramide structural high between the Great Plains and the Colorado Plateau (Baltz, 1978).

Surrounding the Picuris Range in north-central New Mexico are several major Precambrian-cored uplifts (Fig. 2.2). To the north is the Tusas Range, and to the northeast is the Taos Range. South and southeast is a large area of Precambrian exposure including the Truchas Range and the Rio Mora uplift.

Montgomery (1963) and Grambling (1979b) suggested that the Picuris block was horizontally offset about 37 km (23 mi) from the Truchas block along the north-trending, dextral, Precambrian Picuris-Pecos fault (Fig. 2.2). The Picuris-Pecos fault has experienced components of dip-slip motion during Paleozoic and early Cenozoic times (Baltz, 1978). Sutherland (1963) noted that the Picuris-Pecos fault may be the eastern margin of the Paleozoic Uncompahgre uplift.

Baltz (1978) showed the Precambrian rocks in the Picuris area as being high in Oligocene and early Miocene time. The present, deeply eroded, Precambrian Picuris block has remained high since Pliocene time.

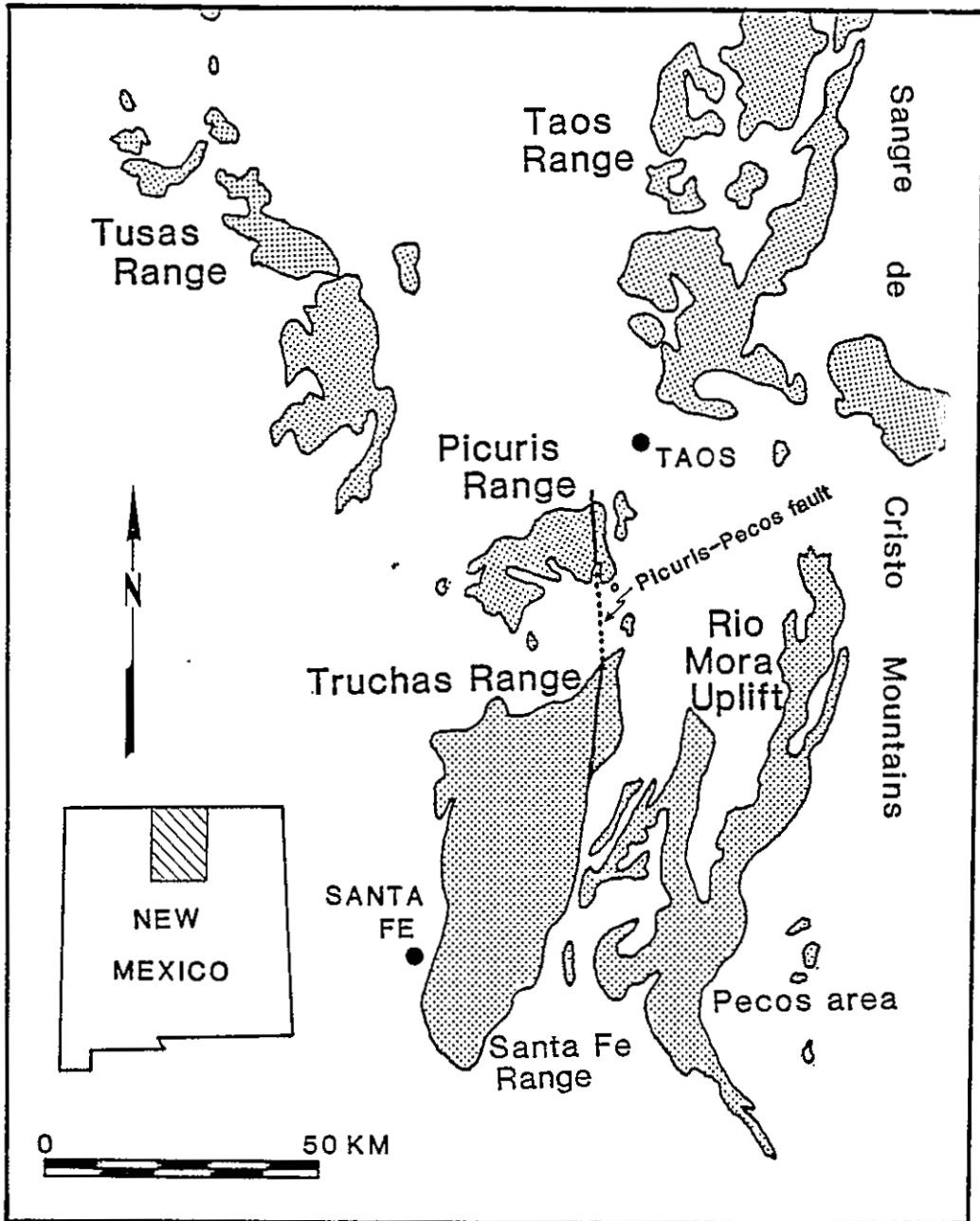


Figure 2.2. Generalized map showing distribution of Precambrian rocks in north-central New Mexico.

## Local Geologic Setting

### General

To the north, west, and south of the Picuris block, basement rocks are bounded by Tertiary sedimentary and volcanic rocks associated with the Rio Grande rift (Steinpress, 1980). These Tertiary units are found within the San Luis basin to the north, and the Chamisal-Penasco re-entrant of the Espanola basin to the south. To the east, basement rocks are either in fault contact with, or are unconformably overlain by Upper Paleozoic sedimentary strata of the southern Sangre de Cristo mountains.

Northwest of the Picuris Range is the 300 m (1000 ft) deep Rio Grande gorge which the Rio Grande has cut through the flat-lying Tertiary sediments and basalts of the Taos plateau (el. 2135 m).

Several Quarternary/Tertiary geomorphic surfaces, which onlap basement rocks and are dissected by arroyos, occur along the northern and southern flanks of the range.

### Phanerozoic Rocks

General. All Paleozoic and Mesozoic sedimentary cover has been eroded from Precambrian crystalline basement rock

in the main block of the Picuris Range. Locally, unconsolidated Cenozoic deposits cover the basement rocks. Paleozoic rocks rest unconformably on Precambrian basement rocks to the east and southeast of the Picuris Range. Farther east, in the Sangre de Cristo Range, tremendous thicknesses of Paleozoic strata conceal the crystalline basement. Relatively thin sedimentary rocks near the Picuris Range range in age from Mississippian to Pennsylvanian. The Pennsylvanian terrigenous sediments in the area were derived mainly from the Uncompahgre highland to the northwest during two major periods of uplift west of the Picuris-Pecos fault (Miller et al., 1963). Sedimentary thicknesses vary considerably due to both Cenozoic tectonics and erosion, and Paleozoic and Mesozoic paleotectonics (Baltz, 1978).

Cenozoic deposits lie unconformably on Precambrian and Paleozoic strata on the northern, western, and southern flanks of the Picuris Range, as well as in topographic lows within the range. Miller et al. (1963) listed the Cenozoic units, from oldest to youngest, as the Picuris Tuff, the Tesuque and Ancha formations of the Santa Fe Group, the Servilleta Formation, stream terraces, and floodplain alluvium. In the area in which Steinpress (1980) made a detailed study of Cenozoic stratigraphy in the western Picuris Range near the town of Dixon, the Santa Fe Group is the primary Cenozoic unit exposed.

Brief summaries of the Phanerozoic deposits found in contact with Precambrian rocks are presented in this chapter. These include the Del Padre Sandstone (Mississippian?), and poorly consolidated Cenozoic units. Other local Paleozoic rocks that are not discussed include the Espiritu Santo Formation (Mississippian?), the Tererro Formation (Mississippian), the Flechado Formation (Pennsylvanian), the Alamitos Formation (Pennsylvanian), and the Sangre de Cristo Formation (Pennsylvanian-Permian). More extensive information may be found in Miller et al. (1963), Steinpress (1980), and Manley (1976).

Paleozoic rocks. The Del Padre Sandstone (Mississippian?) is a non-fossiliferous orthoquartzitic sandstone that rests unconformably on Precambrian rocks (Miller et al., 1963). The type section for the Del Padre is at the junction of Rito del Padre and the Pecos River in the Santa Fe Range. East of the Picuris Range, the Del Padre Sandstone may be easily confused with the Proterozoic Ortega Quartzite, as the Del Padre is highly indurated, orthoquartzitic, locally cross-laminated, locally conglomeratic with rounded clasts of pure quartzite, and well bedded with thin, black, iron oxide-rich layers. Thicknesses of the Del Padre vary considerably in the region. Miller et al. (1963) measured a section 20 m (64 ft) thick in the Rio Pueblo area. The Del Padre is

conformably overlain by, and interfingers with, the Espiritu Santo Formation.

Thin sections of the Del Padre collected from the southeastern map area near the Picuris-Pecos fault show medium-grained, well recrystallized, granoblastic quartz grains that generally contain inequant extinction (Fig. 2.3). Thus the sandstone protolith has recrystallized to a quartzite, and subsequently experienced a moderate amount of strain.

Cenozoic deposits. The Picuris Tuff (Oligocene to lower Miocene) was originally named by Cabot (1938) for tuff and conglomerate that occurred near the town of Vadito. This unit ranges from 60 to 360 m (200 to 1200 ft) in thickness and is composed of interlayered water-laid tuff, coarse conglomerates, clays, and minor basalt flows (Miller et al., 1963). This unit, dated at 24 Ma (Steinpress, 1980), represents the eruption and deposition of Oligocene-lower Miocene volcanoclastics following Eocene erosion. Steinpress noted that the Picuris Tuff is approximately equivalent to the Abiquiu and lower Los Pinos formations, and coincides with the initiation of Rio Grande rifting.

The Tesuque Formation (Miocene to Pliocene), part of the Santa Fe Group, was originally defined near Santa Fe by Baldwin (1956). In the Picuris Range, Miller et al. (1963) described this sequence as buff-colored, poorly sorted,

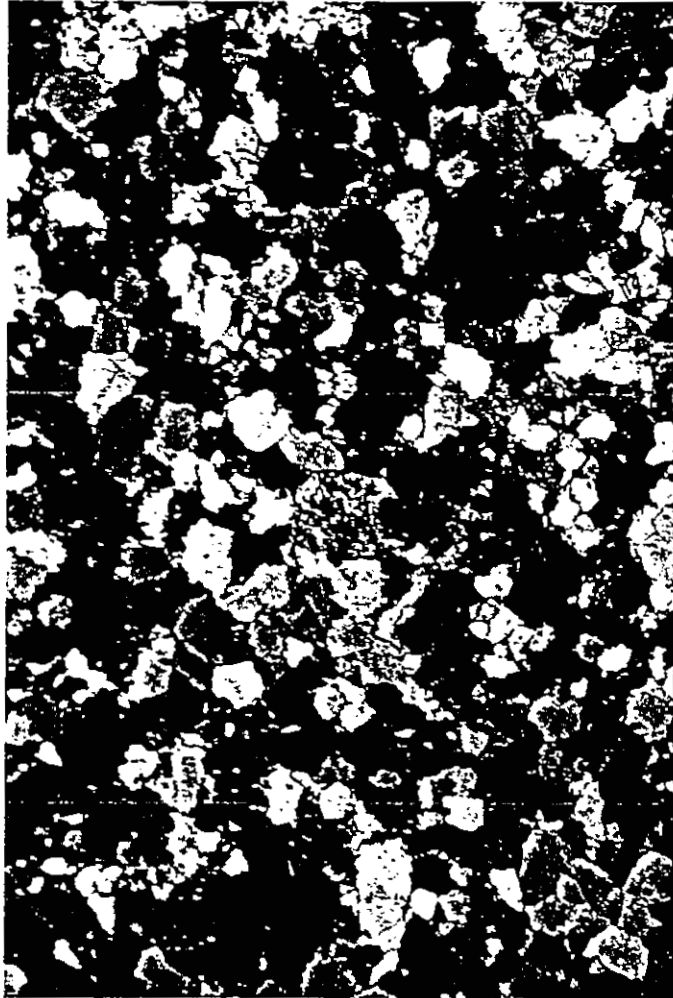


Figure 2.3. Photomicrograph of typical Mississippian(?) Del Padre sandstone from the eastern Picuris Range. Note granoblastic texture, strained individual quartz grains, and single mylonitic grain at center of photograph. Field of view is 14 mm.

weakly consolidated, sand, silt, gravel, volcanic ash, clay, and breccia that ranges in thickness from 150 to 1065(?) m (500 to 3500(?) ft). Much of this unit was derived locally from Paleozoic and Precambrian rocks. Lithologies generally change considerably along strike.

Miller et al. (1963) considered the Ancha Formation to be Quaternary in age and the upper member of the Santa Fe Group. The Ancha consists of fan-deposited sand and gravel of several different ages that overlay the Tesuque Formation. They suggested that this material represented a very large, dissected, once-continuous sheet and could be separated from recent alluvial deposits by position and consolidation. Manley (1976) thought that the Ancha Formation was post-Santa Fe and suggested that it may not be appropriate to name all such gravels the Ancha Formation. Long (1976) followed this suggestion by informally naming these deposits the gravel deposits of Cejita Mesa in the southwestern Picuris Range.

Long (1976) described younger terrace gravels, which presumably were derived directly from the gravel deposits of Cejita Mesa, and brown sand-soil deposits that may have been eolian. The ages of these units are unknown. Steinpress (1980) stated that erosion has dominated the Picuris region in Pliocene and Quaternary time due to the regional uplift of the southern Rocky Mountains. Erosion and deposition of sand and gravel occurs presently in a number of active

streams in and around the Picuris Range. Within the mountain range, recent alluvial and colluvial deposits are common.

### Precambrian Rocks

General. All Precambrian supracrustal rocks in the region appear to be multiply deformed, metamorphosed to amphibolite facies, and of Early Proterozoic age. Intrusive granitic plutons in the southern Picuris Range range in age from about 1680 Ma to 1450 Ma (D.A. Bell, 1985). In general, metasedimentary rocks occur in the north, and metavolcanic and plutonic rocks occur to the south. Several major high-angle faults disrupt the section.

### Basic Precambrian Stratigraphy and Structure

The Picuris Range can be divided into two parts; an eastern, dominantly granitic terrane, and a western, dominantly supracrustal terrane. The north-trending, high-angle Picuris-Pecos fault separates these two terranes. The rocks west of the Picuris-Pecos fault are the focus of this report. The general geology of this area is relatively simple. Three major groups of Precambrian supracrustal rocks are present (Fig. 2.4). The metasedimentary Ortega

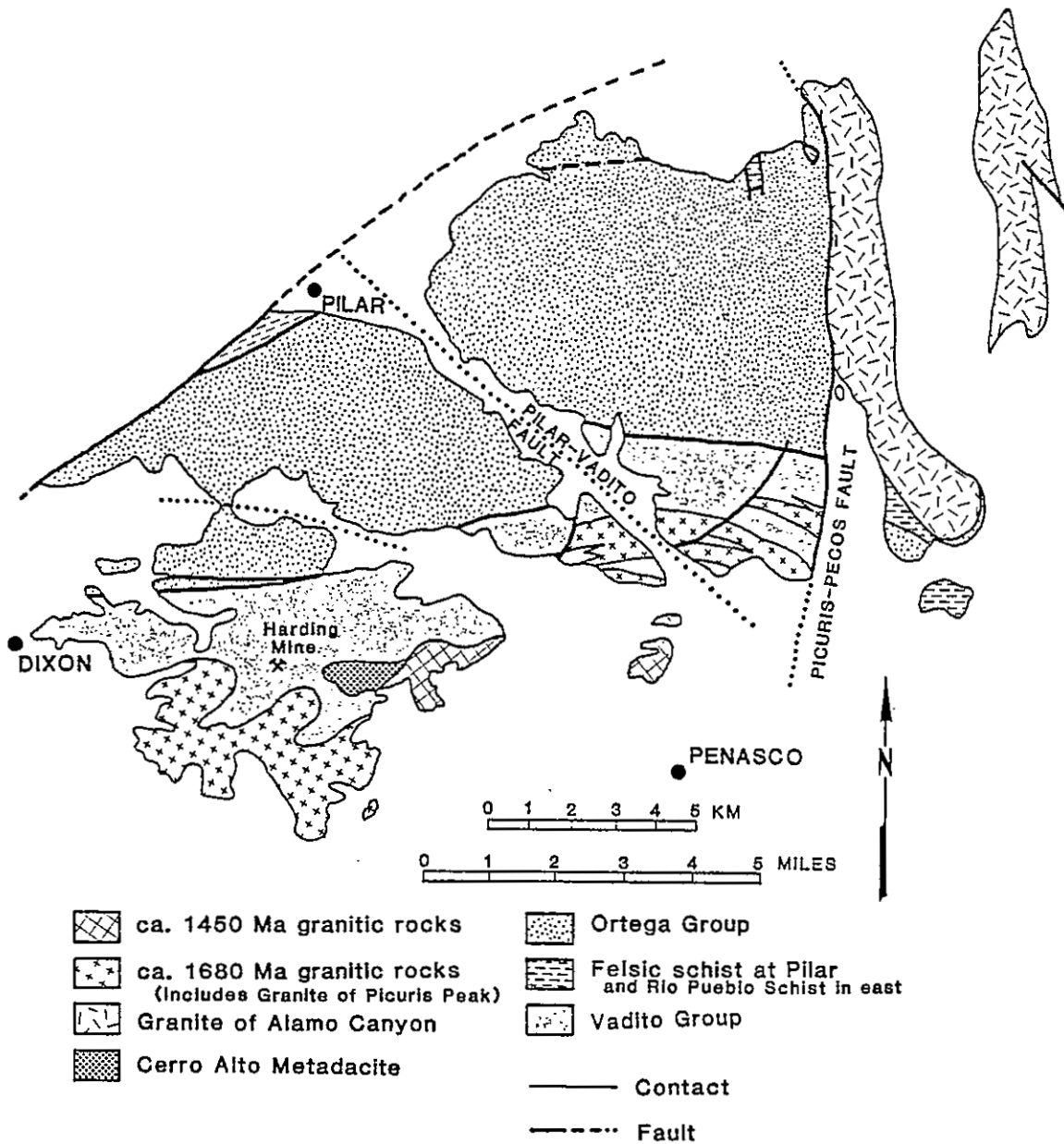


Figure 2.4. Generalized geologic map of Picuris Range, showing the distribution of the major supracrustal rock groups and granitic plutons.

Group (Long, 1976) is the predominant rock group, and consists mainly of resistant quartzites, pelitic schists, and various phyllites. To the south, structurally above the Ortega Group, is the heterogeneous metavolcanic-metavolcaniclastic-metasedimentary Vadito Group, which includes the Marquenas Quartzite (Long, 1976). Intrusive into the southernmost Vadito rocks are at least four granitic plutons which range in age from about 1680 Ma to 1450 Ma (D.A. Bell, 1985). To the north, structurally below the Ortega Group, is a homogeneous sequence of felsic metavolcanic-metavolcaniclastic(?) rocks herein called the felsic schist at Pilar.

Most bedded rocks dip between  $40^{\circ}$  and  $80^{\circ}$  to the south. Stratigraphic and temporal relationships between the three major lithostratigraphic units are uncertain due to tectonization along their mutual contacts. Although all rocks have presumably experienced similar polyphase strain histories, each of the three groups accommodated the strain differently, resulting in the generation of profoundly different tectonite fabrics, geometries, and apparent strain paths.

## CHAPTER 3. PRECAMBRIAN STRATIGRAPHY

### General Statement

The Picuris Range contains exposures of metasedimentary, metavolcanic, and metaplutonic Precambrian rocks. Exposures consist of about 80 percent supracrustal and 20 percent plutonic. The range can be divided into three general blocks separated by major faults (see Fig. 2.4). An eastern block of dominantly plutonic rock, with minor exposures of supracrustal rocks to the south, is separated from a central, dominantly metasedimentary block by the north-trending Picuris-Pecos fault. Complexly layered metavolcanic and plutonic rocks lie in the southern portion of the central block. West and southwest of the central block, across the Pilar-Vadito fault, is the western block, composed of supracrustal rocks in the north, and intrusive granitic rocks in the south.

Stratigraphic nomenclature employed in this paper is based on that proposed by Just (1937), Montgomery (1953), Miller et al. (1963), Nielsen (1972), Long (1976), and Scott (1980). These authors developed a well-defined, consistent stratigraphy for the metasedimentary rock sequence (Ortega Group) in the central and western blocks. Although there is some variation of lithology along strike in these units, nearly all formations and members are readily

distinguishable throughout the range, and younging criteria are generally consistent.

The Ortega Group has been interpreted as a transgressive sequence (Soegaard and Eriksson, 1985) that originally ranged from basal conglomeratic quartz sands, to pure quartz sands, to interlayered sands and shales, to black muds, to calcareous muds and shales. The Ortega Group has an apparent thickness of 3-5 km.

Structurally above, but stratigraphically below, the Ortega Group in the southern Picuris Range is a sequence of complexly interlayered metamorphosed igneous and sedimentary rocks named the Vadito Group by Long (1976). Lithologies within this group change considerably along strike, pinch out and reappear, and probably represent felsic and mafic volcanic rocks interlayered with volcanoclastic and clastic sediments. The minimum apparent thickness of this group is 3-4 km.

In the southern Picuris Range, the volcanic component of the Vadito Group is dominantly mafic. Although feldspathic metavolcanic rocks are common, they are not as voluminous as amphibolites. Thus, the Vadito Group type-section defined by Montgomery (1953), is a mafic-dominated, apparently bimodal volcanic sequence containing interlayered volcanoclastics and sediments. Williams et al. (1986) and Williams (1987) proposed a redefinition of the Vadito Group in northern New Mexico, based mainly on rocks exposed in the

Tusas Range and Rio Mora area in the southern Sangre de Cristo Mountains. They suggested that the Vadito Group be redefined as a felsic volcanic-sedimentary sequence of quartz-muscovite schist, pelitic and feldspathic schist, metaconglomerate, quartzite, and amphibolite correlative over much of northern New Mexico, whose most distinctive feature is quartz-muscovite schist containing feldspar and quartz "eyes". These "eyes" were interpreted to be phenocrysts in altered metatuffs.

This definition is at odds with the type-section in the Picuris Range (Montgomery, 1953). Because stratigraphic relationships between the Vadito Group of the southern Picuris Range and the "Vadito Group" described by Williams et al. (1986) and Williams (1987) are unknown, Montgomery's original nomenclature will herein be retained.

Note that the felsic schist at Pilar, a felsic metavolcanic sequence exposed in the northern Picuris Range, is characterized by quartz and feldspar "eyes". It is possible that these rocks are equivalent to the "Vadito Group" of Williams et al. (1986). The relationship between these rocks and the southern Picuris Vadito Group is unknown; possibilities will be discussed in Chapter 7. Until more precise regional correlations are available, I will continue to use the nomenclature developed by Montgomery for the Picuris Range.

The stratigraphic position of the pelitic schists and

phyllites of the Piedra Lumbre Formation has been extensively debated. Although the most complete, most extensive exposure of Piedra Lumbre Formation occurs as an east-trending strip in the northern Picuris Range, the unit was first described in a relatively thin sliver of exposure in the Copper Hill area.

Long (1976) proposed the name Piedra Lumbre Formation for the laminated schist and phyllite that sit between the Marquenas Quartzite to the south and the Pilar Phyllite to the north. Previous studies noted that the northern and southern exposures of this rock appear to lie in different stratigraphic positions. Holcombe and Callender (1982) observed that although the Piedra Lumbre was stratigraphically similar to rocks in the Ortega Group, it was structurally more appropriately assigned to the Vadito Group. They suggested that faults separated the Piedra Lumbre from rocks on either side. The present study shows that the northern unit is in the correct stratigraphic position, whereas the southern exposure is actually a fault sliver on the southern limb of a minor anticline which is faulted against Vadito Group rocks. The Piedra Lumbre is the youngest unit in the Ortega Group, and rests conformably on the Pilar Phyllite.

Intrusive only into the southern portion of the Vadito Group are at least four distinct plutons; the Cerro Alto Metadacite, the Puntiaquedo Granite Porphyry, the Rana Quartz

Monzonite, and the Penasco Quartz Monzonite (Long, 1976). These rocks are best exposed in the southern half of the western block. Similar rocks intrude Vadito units in the easternmost western block, and the southern part of the central block. Most of the eastern block is composed of a plutonic rock distinct in texture from the western plutons. This body appears to intrude felsic schists in the southernmost part of the eastern block.

Additional and more detailed lithologic descriptions and sedimentological interpretations, are presented in Montgomery (1953, 1963), Nielsen (1972), Gresens and Stensrud (1974), Long (1976), Scott (1980), McCarty (1983), and Soegaard and Eriksson (1985, 1986).

## Vadito Group

### General field relations and previous work

Montgomery (1953) defined the "Vadito Formation" as all Precambrian rocks that overlie the Rinconada Formation in the Picuris Range. Montgomery's conglomerate and schist members of the Vadito were redefined by Long (1976) as the Marquenas Quartzite Formation and the unnamed schist and amphibolite of the Vadito Group, respectively.

Due to the lateral variability of Vadito Group units,

and the different lithologies exposed below the Ortega Quartzite in the northern and southern Picuris Range, the bottom of the Ortega Group is herein defined as being located immediately below the lowermost occurrence of relatively pure orthoquartzite of the basal Ortega Quartzite Formation. In the southeastern Picuris Range, the poorly exposed contact between the Ortega Quartzite and the underlying heterogeneous, more schistose rocks of the Vadito Group is sharp and highly sheared. In the southwestern Picuris Range, the basal Ortega Quartzite is nowhere exposed. Instead, Ortega Group schists are in fault contact with the Vadito Group. In the northern Picuris, the basal Ortega Group is adequately exposed only along the cliffs near Pilar. In this area, the contact with underlying felsic schist at Pilar is also sharp. The fact that very different lithologies underlie the Ortega Quartzite in the north and south is significant and will be discussed in Chapter 7.

The following sections provide brief descriptions of the Vadito Group rocks found in the southwestern and southeastern Picuris Range.

#### Southwestern Picuris Range

General. The area of the Copper Hill-Harding Pegmatite Mine in the southwestern Picuris Range has been the focus of

numerous Precambrian geologic studies. Rocks are well-exposed and easily accessible, and several universities run their undergraduate geology field camps there. Vadito Group rocks in this area consist of schists (35% of area), amphibolites (35% of area), the Marquenas Quartzite Formation (25% of area), other quartzites and metaconglomerates (2% of area), quartz-muscovite schists (2% of area), and calc-silicates (<1% of area).

Schists. Vadito schists contain a large variety of fine-grained, texturally and mineralogically distinct schists, phyllitic schists, and schistose quartzites. McCarty (1983) performed a detailed petrographic study of these rocks and separated out nine distinct schistose units in the Harding mine area. She concluded that these rocks represent a metamorphosed protolith of fine- to medium-grained graywackes interlayered with impure sandstones, shales, volcanoclastic sediments, and basaltic flows that accumulated in a relatively deep-water basin setting. Soegaard and Eriksson (1986) called these schists "orthochemical metasedimentary rocks".

Amphibolites. Amphibolite bodies are scattered throughout the Vadito Group. The thickest and most extensive amphibolite unit occurs just south of the Harding Pegmatite mine. Associated with amphibolites are biotite

schists, quartz-biotite rock, metadacite and felsic schist, and metaquartzite and metachert. These rocks were thoroughly described by Montgomery (1953) and McCarty (1983), who interpreted them as interlayered basaltic flows and volcanoclastic sediments intruded by felsic sills and dikes.

Marquenas Quartzite Formation. The Marquenas Quartzite Formation of Long (1976) is a strip of relatively resistant polymictic metaconglomerate and texturally immature metasediment that is well-exposed in the western end of the western block, and poorly-exposed in the eastern end. Scott (1980) divided the Marquenas into four sub-units. From north to south (top to bottom) these are: 1) a northern metaconglomerate with deformed clasts in a micaceous quartz matrix. Clasts are up to 10 cm long and consist of an average of 66 percent metasedimentary quartzite, 34 percent felsic schist, and traces of vein quartz (J.A. Grambling, personal communication, 1987); 2) a rippled, cross-laminated, micaceous quartzite with isolated pebble layers; 3) a vitreous, cross-bedded massive grey, somewhat micaceous quartzite with scattered pebble layers; and 4) a southern metaconglomerate with deformed orthoquartzite (54%), silicic metavolcanic and quartz-muscovite schist (40%), and white vein quartz clasts (J.A. Grambling, personal communication, 1987) in a micaceous quartz matrix. Quartzite clasts

are up to 1 m in diameter, with aspect ratios averaging 1:2:3 or 1:2:6, with extremes of 1:8:16 for schistose clasts (Montgomery, 1953). Montgomery (1953) also noted that the metaconglomerates coarsen from east to west. Estimates of thickness have ranged from 410 m (Long, 1976) to about 610 m (Montgomery, 1953).

Lithologies and sedimentary structures in the metaconglomerates suggest an origin as proximal alluvial-plain deposits, accumulated during waning flood stages (Soegaard and Eriksson, 1986). The immature quartzites may have been channel deposits in a perennial braided-alluvial plain with water depths greater than 8 m (Soegaard and Eriksson, 1986).

The stratigraphic position of this unit has recently been disputed. This will be addressed in a later discussion section.

Other quartzites and metaconglomerates. Numerous thin, isolated exposures of orthoquartzite and conglomeratic quartzite are scattered south of the Marquesas Quartzite. All of these are similar lithologically to the Marquesas and represent either younger alluvial channel deposits in the Vadito Group, or infolded or faulted Marquesas equivalents.

Felsic schists. Light-colored quartz-feldspar-muscovite rocks are locally found interlayered with other

Vadito Group rocks. Felsic schists commonly contain rounded to sub-rounded quartz grains (quartz-eyes) and/or euhedral to subhedral feldspar megacrysts that probably represent metamorphosed relict phenocrysts. The matrix generally consists of aligned, fine- to medium-grained muscovite laths in mosaics and strung-out patches of fine-grained, granular quartz, plagioclase, and microcline grains. Textures locally suggest tectonic grain-size reduction of an originally coarser-grained felsic protolith. These felsic schists probably represent metamorphosed rhyolites and related rocks, interlayered with locally derived felsic volcanoclastic sediments.

Calc-silicates. Thin, discontinuous calc-silicate horizons occur in a number of places in the northern part of the Vadito section. One of the thickest, described by McCarty (1983), is 1 to 4 m thick, contains quartz, calcite, epidote, thulite, and garnet, and was presumably a manganese-rich limestone.

#### Southeastern Picuris Range

General. Vadito Group rocks in the southeastern Picuris Range differ from those in the southwest in several ways. Biotite-bearing feldspathic and pelitic schists are almost totally lacking in the southeast. White,

feldspathic, quartz-muscovite schists are more abundant and locally thick. "Sheets" of granitic rock are complexly interlayered with the country rocks in marked contrast to the rounded masses of generally discordant granitic rock in the southwest.

Dominant lithologies in this area include quartzite and conglomerate (35% of area), amphibolite (35% of area), feldspathic quartz-muscovite schist (30% of area), and pelitic schist (<1% of area).

Quartzites and conglomerates. Quartzose metasediments in the southeastern Picuris, possibly stratigraphic equivalents of the Marquenas Quartzite, are interlayered with amphibolites, felsites, and granitic rocks. Quartzite xenoliths are common in the granitic rocks, and stringers of granitic rock are common in quartzites. Xenoliths are light tan to white, fine-grained rocks with very small micas, and local thin dark bedding layers. Several quartzitic lithologies are present in this sequence. Massive, vitreous quartzites have cross-beds defined by high concentrations of hematite. Local conglomeratic layers contain flattened clasts up to about 4 cm long. Clasts include: rounded, purple-gray crystalline quartzite; somewhat rounded white quartzite or vein quartz; and dark gray, metallic-looking, fine-grained schist. Dark clasts are most abundant. Some conglomerates contain only very sparsely scattered quartz

clasts in micaceous quartzite matrix. Schistose quartzite crops out locally. There appears to be a general decrease in clast size from west to east.

Amphibolite and biotite schist. Amphibolites are common, and locally grade into black, medium-grained biotite schists. Amphibolites range in texture from rocks containing large, oriented plagioclase laths in a black amphibole matrix, to rocks with many small, somewhat aligned amphibole crystals in a white plagioclase matrix. Biotite schists are less common, well-layered, biotite-quartz rocks. Locally, epidote-rich zones grade into mafic rocks. Most amphibolites probably represent metamorphosed mafic volcanic flows and sills.

Felsic schists. Although felsic schists appear to make up a large proportion of area in the southeastern Picuris, these rocks are not resistant, and thus exposures are scattered and poor quality. In general, these rocks are white, fine-grained, fairly dense, quartz-muscovite schists that commonly contain euhedral feldspar megacrysts and rounded quartz eyes (Fig. 3.1). As in the southwestern Picuris Range, many of these rocks are interpreted to be metamorphosed phenocrystic felsic volcanic rocks.

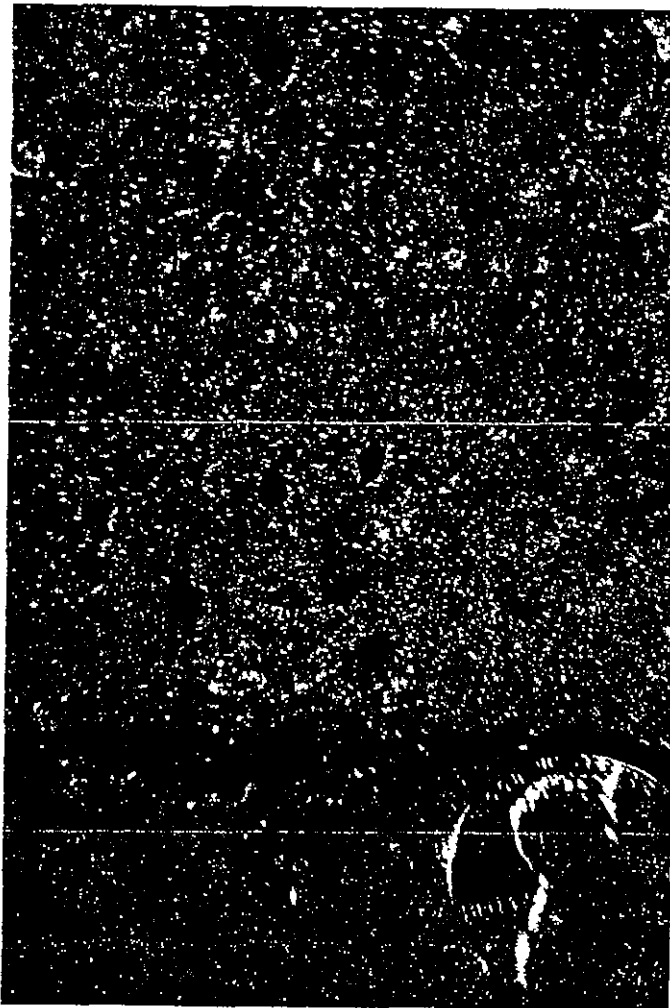


Figure 3.1. Photograph of white felsic schist (HC-542) with flattened, rounded quartz-eyes and euhedral feldspars megacrysts from the Vadito Group, southeastern Picuris Range.

Porphyroblastic schist below Ortega. A schistose horizon commonly underlies the Ortega Quartzite where the base of the quartzite is exposed in the southeastern Picuris Range. This schist is generally coarse-grained, pink to white, strongly crenulated, and contains large blocky altered porphyroblasts of chloritoid(?) in a quartz-muscovite matrix.

In one locality (HC-414), poor exposures of gray and white banded, very fine-grained rock with lens-shaped feldspar pods lie just below the Ortega Quartzite. Thin sections reveal a quartz-rich rock with mylonitic textures.

The origin of these schists is unknown. At least some of the textures are clearly due to shearing and metamorphism rather than to sedimentation.

Andalusite schist. The only pelitic schist identified in southeastern Vadito exposures is a distinctive, black biotite schist containing large knobs of andalusite (HC-518). This unit is only a few meters thick and appears to pinch out along strike in both directions. Possible protoliths for this schist include shale, altered volcanoclastic sediment, or hydrothermally altered volcanic rock.

## Felsic schist at Pilar

### General

Montgomery (1963) defined the Rio Pueblo Schist as the basal "migmatitic quartzite" of the lower quartzite (Ortega Quartzite) of the Ortega Formation in the southeastern Picuris Range, near the town of Rio Pueblo. He considered this feldspathic unit to consist of granitic rock intruded and intermixed with quartzite. He noted that a similar micaceous quartzite crops out in steep cliffs near the town of Pilar. In the cliffs near Pilar, stratigraphically and structurally below Ortega Group rocks, this micaceous quartzite (herein called the felsic schist at Pilar) consists of a sequence of light-colored, pink to white to green quartz-muscovite and quartz-eye schists. With respect to the Ortega Group, the felsic schist at Pilar occupies the same structural position as the Vadito Group rocks in the southern Picuris Range. The felsic schist at Pilar may be: 1) laterally equivalent to the Vadito; 2) a portion of Vadito which is not exposed in the southern Picuris Range; or 3) a totally different package of rocks. These rocks may represent hydrothermally altered, locally reworked, felsic volcanic tuffs and flows (Gresens and Stensrud, 1974).

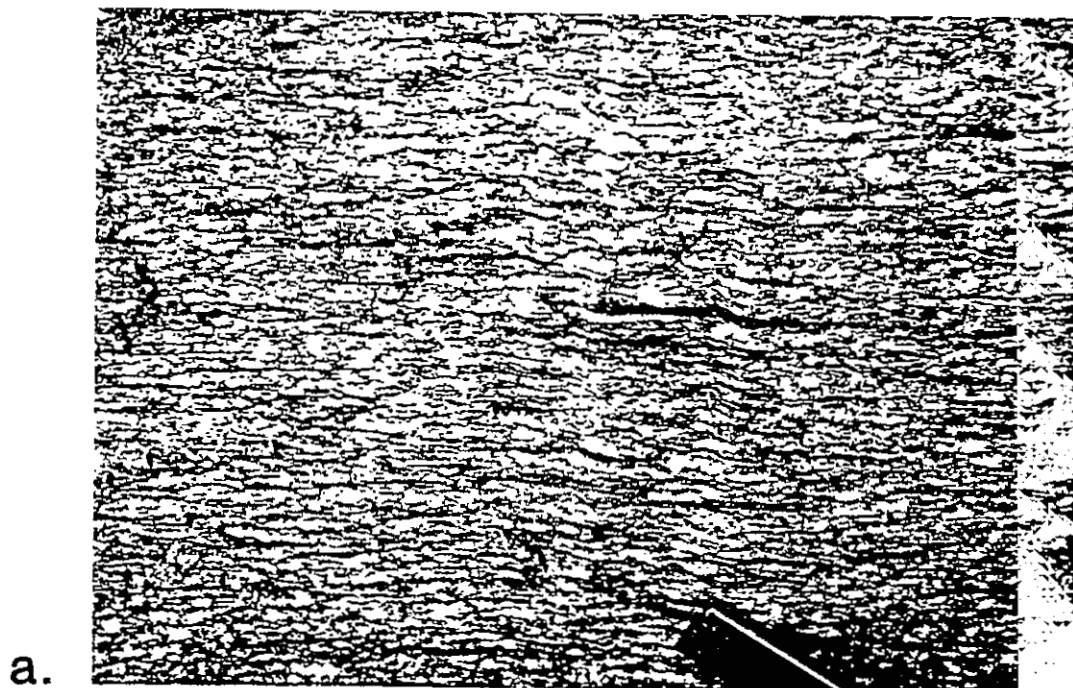
It is important to note that although all of the felsic rocks that Montgomery called Rio Pueblo Schist (including

the felsic schist at Pilar) are very similar, they are texturally distinctive from Vadito Group felsic schists in the southern Picuris Range. In this report felsic schists will be treated separately from type Vadito Group rocks.

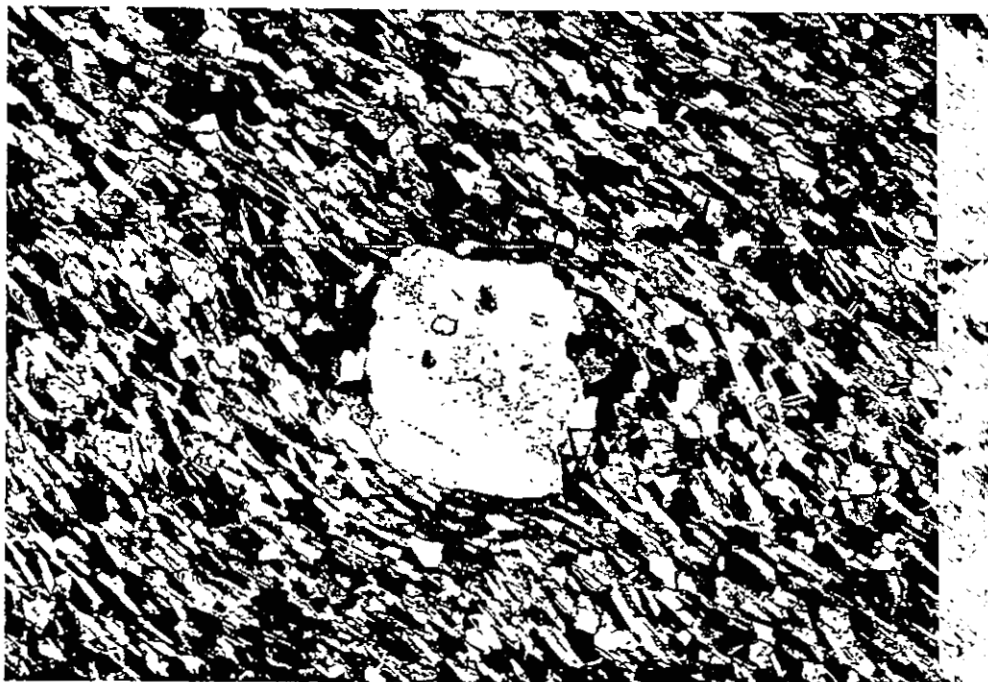
#### Northwestern Picuris Range (Pilar cliffs)

General. The Pilar cliffs are a 450 m (1500 ft), near-vertical escarpment southwest of the town of Pilar, along U.S. highway 64. Excellent exposures of Ortega Quartzite and underlying felsic schist at Pilar occur for several kilometers along the cliffs.

Quartz-muscovite schist. The cliffs near Pilar expose a sharp contact between overlying, right-side-up Ortega Quartzite and feldspathic quartz-muscovite schists and micaceous quartzites of the felsic schist at Pilar. The base of this felsic schist is nowhere exposed. Thin quartzite mylonites occur within the contact zone. Compositional layering in felsic schists is parallel to the Ortega-Vadito contact. Schists are white, light gray, pink, and green, and commonly contain rounded and flattened quartz-eyes (Fig. 3.2). A distinctive pink zone, about 100 m thick, marks the schist immediately below the Ortega Quartzite contact. This zone, which is anomalously high in manganese and rare earth elements, contains such unusual



a.



b.

Figure 3.2. a. Photograph of typical felsic schist at Pilar. Note well-developed, anastomosing foliation. Pen top for scale. b. Photomicrograph of quartz-muscovite, quartz-eye schist from the Pilar cliffs. Foliation has been deflected around the quartz-eye. Section is cut parallel to extension lineation and perpendicular to foliation. Field of view is 4 mm.

minerals as piemontite, thulite, and Mn-andalusite (Grambling et al., 1983, Grambling and Williams, 1985). This distinctive horizon has been traced below the basal Ortega Quartzite in most of the uplifts of northern New Mexico, and may be related to a regional volcanic exhalative event during the waning stages of volcanism, or deep lateritic weathering (Grambling et al., 1983).

In an excellent study that re-examined possible metarhyolite occurrences in northern New Mexico, Gresens and Stensrud (1974) suggested that due to alteration, several metavolcanic units in the Picuris Range had been misinterpreted as metasediments. They cited the rocks in the Pilar cliffs as one of the best examples.

#### Northeastern Picuris Range

General. Two occurrences of feldspathic quartz-muscovite quartz-eye schist have been mapped in the northeastern Picuris Range. Both are very localized exposures of schist within Ortega Quartzite.

Quartz-muscovite schist. The western occurrence is in a small down-dropped fault block within the Ortega Quartzite, where white to pink, quartz-eye schists are exposed. About one kilometer east, in a structurally complex area adjacent to the Picuris-Pecos fault, white,

greenish, and pinkish quartz-muscovite schists appear to be infaulted and infolded with the Ortega Quartzite. In the center of the fold, very fine-grained quartzites, fine-grained quartz-muscovite schists, and metacherts(?) are highly contorted. Both of these exposures are thought to be equivalents of the felsic schist at Pilar.

#### Eastern Block of the Picuris Range

General. There are four isolated exposures of quartz-muscovite quartz-eye schists in the southeastern Picuris, on the eastern side of the Picuris-Pecos fault. Each of these contains rocks similar to those found in the Pilar cliffs and were called Rio Pueblo Schist by Montgomery (1963), who considered them to be migmatitic basal quartzites of the lowermost Ortega Formation.

U.S. Hill. Excellent exposures of well-bedded, white, gray, and pink quartz-muscovite quartz-eye schist are found in open-pit mica mines on an isolated hill of Precambrian rock just west of U.S. Hill. This rock is composed of up to 60 percent coarse white muscovite flakes in a matrix of granular quartz and feldspar. Quartz-eyes are abundant and are consistently flattened in the dominant foliation plane.

North of this hill, similar bedded schists are in contact with granitic rock to the northeast and massive gray

quartzite to the south. Although exposures are poor in the area, several important relationships are clear. Granitic rocks intrude and crosscut layering in the schists, as illustrated by transitional granite-schist rock found along the contact. A Mn-rich horizon occurs stratigraphically below the quartzite, and piemontite and altered porphyroblasts that might be pseudomorphs after Mn-andalusite are found locally along the schist-quartzite contact. It is possible that this contact separates Ortega Quartzite from underlying felsic schist, and is therefore analagous to the tectonic boundary exposed in the Pilar cliffs.

Two kilometers northwest of this exposure is a small hill composed of poorly-exposed, highly-fractured, vitreous quartzite and light-colored quartz-muscovite schist.

Comales campground. A large isolated block of generally poorly-exposed Precambrian rock lies in the extreme southeastern corner of the Picuris Range. New Mexico Highway 3 and the Rio Pueblo pass through the northern end of this block at Comales campground. This somewhat schistose, slightly gneissic, feldspathic quartzite was named Rio Pueblo Schist by Montgomery (1963). However, these rocks could be highly sheared granitic units rather than an originally fine-grained layered rock. White, feldspathic, quartz-muscovite schist crops out in the high

hills to the south, below an exposed section of massive, gray, vitreous quartzite. In the contact zone, porphyroblasts of Mn-andalusite can be found in float.

#### Depositional environments of the felsic schist at Pilar and the Vadito Group

It is necessary to separate the Vadito Group from the felsic schist at Pilar in the Picuris Range due to both their lithologic differences and the uncertainty concerning the manner in which the two sections relate stratigraphically. The felsic schist at Pilar probably represents strained, metamorphosed, and altered rhyolitic flows and tuffs. Rounded quartz eyes and feldspar megacrysts may represent relict phenocrysts. Vernon (1986) suggested that most, if not all, such quartz eyes in deformed rocks are residual phenocrysts, rather than porphyroblasts. Thin sections from throughout this unit consistently show very similar textures of quartz megacrysts in a fine-grained matrix of quartz, muscovite, and feldspar. If the present thickness of this section, a minimum of 300 m, is representative of the thickness of a pile of rhyolites and rhyolitic tuffs, these rocks may have originated proximal to a major felsic volcanic center.

The heterogeneous Vadito Group terrane of feldspathic

and pelitic schists, and amphibolites and related rocks probably represents metamorphosed and complexely interlayered graywackes, basaltic flows and sills, felsic tuffs and sills, and volcanoclastic sediments. Long (1974) described original volcanic textures such as pillows, pillow breccias, and relict vesicles in amphibolites. Duncan and Shore (1984) suggested that some of these rocks are a m $\acute{e}$ lange representing young trench-fill accreted onto continental crust. They recognized turbidity flows, debris flows containing a wide variety of clast sizes, soft sediment folding (but no tectonic folding), and metavolcanics and metacherts. There is no question that the Vadito Group is indeed a terrane of mixed lithology, but it is a highly deformed mixed terrane, and as such requires considerable additional mapping before genetic terms such as melange should be used to describe it.

The fluvial-alluvial protolith of the Marquenas Quartzite appears to be inconsistent with the depositional environment of the Vadito schist.

#### Stratigraphic Position of the Marquenas Quartzite

Soegaard and Eriksson (1986) suggested that the Marquenas Quartzite Formation is younger than both the Vadito and Ortega groups, and actually formed from weathering and erosion of the Ortega Quartzite. Several

relationships observed in this study refute this. Although bedded orthoquartzites are abundant as clasts in the Marquenas Quartzite, no quartzite clasts containing aluminosilicates have been recognized in the Marquenas, suggesting that the very aluminous Ortega Quartzite was not a source for Marquenas rocks (J.A. Grambling, personal communication, 1987). Soegaard and Eriksson's suggestion requires a Marquenas Quartzite wedge in fault contact with Ortega and Vadito rocks. Although the northern Marquenas Quartzite contact is clearly a fault in the Copper Hill area, there is presently no evidence for such a fault along the southern boundary. Furthermore, along strike to the east, possible Marquenas Quartzite equivalents are interlayered with metavolcanic rocks, suggesting that the Marquenas and related quartzites and metaconglomerates are probably part of the Vadito Group. Cross-beds in both the northern and southern quartzite members of the Marquenas Quartzite show tops to the north. However, it should be noted that the disparity in sedimentary environments between the fluvial-alluvial Marquenas Quartzite and the deeper water graywackes of the Vadito schist in the Copper Hill-Harding Mine area suggests that the quartzite and schist are separated by an unconformity or a fault. This however, does not imply that the Marquenas was derived from the Ortega Group and is the youngest supracrustal unit in the range.

## Ortega Group

### General Statement

The Ortega Group is a 4+ km thick transgressive sequence of mature terrigenous metasedimentary rocks that crop out in most of the major Precambrian-cored uplifts of northern New Mexico. Just (1937) defined the Ortega Quartzite in the Tusas Range, and correlated it to a section of similar quartzite in the Picuris Range. Montgomery (1953) redefined the sequence as the Ortega Formation, which consisted of three members: the Lower Quartzite; Rinconada Schist; and Pilar Phyllite. Nielsen (1972) further subdivided the Ortega sequence into the Ortega Quartzite, the Rinconada Formation with six members, and the Pilar Formation with a slate and a muscovite phyllite member. Long (1976) proposed raising the Ortega Formation to group status, and the two members of the Pilar Formation to the Piedra Lumbre and Pilar formations. Although this nomenclature has remained unchanged, the relative positions of some of these units has been debated. The most complete section of the Ortega Group in the Picuris Range is located in the northern map area.

The youngest Ortega Group unit in the Picuris Range is the Piedra Lumbre Formation. The correct stratigraphic position of the Piedra Lumbre Formation has been uncertain,

as the northern and southern exposures of this rock appear to lie in different stratigraphic positions. Montgomery (1953) mapped the Piedra Lumbre Formation as part of the Pilar Phyllite member of the Ortega Formation, and included the large northern exposure with the uppermost schists of the Rinconada. Nielsen (1972) called this unit the muscovite phyllite member of the Pilar Formation, and correlated it with the northern exposures. He considered the thin quartzites in the northern outcrops as equivalents of the quartzites in the Vadito Group of the southern Picuris Range. Long (1976) proposed the term Piedra Lumbre Formation for the exposures near Copper Hill of layered schist and phyllite that sit between the Marquenas Quartzite to the south and the Pilar Phyllite to the north. Holcombe and Callender (1982) noted that although the Piedra Lumbre was lithologically similar to rocks in the Ortega Group, it was structurally more appropriately assigned to the Vadito Group. They suggested that faults separated the Piedra Lumbre from rocks on either side. Hurd (1982) examined a small area in the northern Picuris Range, and determined that no Vadito Group rocks were present in the map area, and no faults existed between Piedra Lumbre and Pilar units in the map area. Bauer (1984) tentatively proposed that the unit in the north should informally be called the Hondo schist until more was known about its relationship to the Piedra Lumbre type section. He also suggested that if the

two units are correlative, then the fault that exists between Piedra Lumbre and Pilar in the south, does not exist in the north. Within the map area, the Pilar Phyllite contact is gradational up into the Piedra Lumbre, and the quartzites previously interpreted as Vadito quartzites by Nielsen (1972) are actually layered within the lower Piedra Lumbre schist. The present study shows that the northern unit is in the correct stratigraphic position, whereas the southern exposure is actually a fault sliver on the southern limb of a minor anticline.

Ortega Group metasediments take up most of the northern two thirds of the Precambrian exposures in the range. Regional dips are consistently between  $40^{\circ}$  and  $80^{\circ}$  south.

Because the Ortega Group contains a remarkably consistent stratigraphy over the entire range, the remainder of this section presents a single set of lithologic descriptions of Ortega Group rocks for the Picuris Range. A generalized stratigraphic column of the Ortega Group is shown in Figure 3.3.

#### Ortega Quartzite Formation

General. The name Ortega was first used by Just (1937) for the spectacular quartzites of the Ortega Mountains in the Tusas Range. Montgomery (1953) later used Ortega Formation to include the entire section of metaclastic rocks

	FORMATION	MEMBER	LITHOLOGY	THICK. (m)
	GROUP	PIEDRA LUMBRE	Quartzite	Micaceous, cross-bedded quartzite
Schist			Fine-grained, laminated, garnet-staurolite schist and phyllite. Local black slates and calc-silicates.	
PILAR PHYLLITE			Black, graphitic phyllite and slate. Local white schist layers. Basal blue-black quartzite.	200 - 600
RINCONADA		R6	Qtz-mu-bi-gr-stl phyllitic schist	40 - 100
		R5	Massive, micaceous, white to gray quartzite; blue crystalline quartzite.	80 - 200
	R4	Reddish, small qt-stl schist	27 - 70	
	R3	Tan-white micaceous, X-bedded quartzite. Massive blue quartzite.	60 - 100	
	R1/2	Mu-stl schist with large twinned stl. Bi-mu-andalusite schist.	120 - 255	
ORTEGA	ORTEGA	Upper	Massive, clean, medium-grained, crystalline, white to gray cross-bedded quartzite. Local aluminous schist layers	1000 - 1200
	QUARTZITE	Lower	Gray quartzite and reddish weathering, coarsely granular cross-bedded quartzite. Local gt-bearing black quartzites. Conglomeratic at base.	

Figure 3.3. Generalized stratigraphic column for the Ortega Group. Modified from Nielsen, 1972; Long, 1976; and Grambling, 1985b).

in the Picuris Range, and called the thick basal quartzite the "Lower Quartzite". Nielsen (1972) named this Lower Quartzite the Ortega Quartzite Formation.

In this report the Ortega Quartzite Formation is subdivided into two mappable members informally called the lower and upper quartzites. These members are discernable over the entire Picuris Range.

The two major east-trending bands of Ortega Quartzite exposed in the Picuris Range are slightly offset along strike by two northwest-striking faults that are covered by unconsolidated Cenozoic sands and gravels. Several small, isolated exposures of orthoquartzite crop out east of the Picuris-Pecos fault in the southeastern part of the range. Exposures of Ortega Quartzite are generally excellent, due to its highly resistant nature. The quartzite invariably forms high ridges and peaks. Thicknesses of Ortega Quartzite of about 1200 m are fairly constant throughout the range, except for an area in the northwestern part of the map area, where the quartzite has an apparent thickness of more than two kilometers. This is inconsistent with the average regional thickness of Ortega Quartzite of 1.0 to 1.5 km, and is probably due to tectonic doubling along a high angle fault. The upper and lower quartzite members are repeated in this section. No such schist is recognized elsewhere within the Ortega Quartzite of the Picuris Range.

Lower quartzite. The lower quartzite generally consists of brick-red to brownish-red, granular, crystalline, medium- to coarse-grained, weathered-looking grains of quartz. This unit is commonly highly fractured, with coarse black iron-oxide layers defining bedding and cross-laminations. Locally, dark quartzite horizons contain medium-sized, altered garnet porphyroblasts, and basal quartzites contain small, rounded clasts of white vein quartz, quartzite, and felsic schist. The thickness of this unit is approximately 500 to 600 m.

Upper quartzite. The upper part of the Ortega Quartzite is gray to grayish white, coarse-grained, vitreous, massive, clean, cross-bedded quartzite. Layering and cross-bedding are defined by black layers of iron-oxide minerals. Aluminosilicate minerals (especially kyanite and sillimanite) are ubiquitous throughout the quartzite. Aluminosilicates are locally concentrated in thin bedding-parallel schistose layers. Locally, in the Hondo Canyon area, these aluminous layers are composed of up to 75 percent kyanite crystals. Near Copper Hill, similar horizons contain 70 percent andalusite porphyroblasts (J.A. Grambling, personal communication, 1987). Common accessory minerals in the quartzite are ilmenite, hematite, tourmaline, epidote, muscovite, kyanite, sillimanite, and zircon.

The lower quartzite is less resistant to weathering than the upper quartzite, and is commonly found as crumbly, iron-stained float. The contact between upper and lower Ortega Quartzite is defined by a poorly exposed, 5- to 10-m thick, schistose layer which generally forms canyons or saddles.

### Rinconada Formation

General. The Rinconada Formation consists of a sequence of interlayered pelitic schists and orthoquartzites that lie stratigraphically above the Ortega Quartzite. Nielsen (1972) divided this formation into the R1 schist, R2 schist, R3 quartzite, R4 schist, R5 quartzite, and R6 schist members. Because R1 and R2 appear to differ only in metamorphic mineralogy, not in bulk chemistry, Grambling (1986b) has suggested that a better terminology is Rs1, Rq1, Rs2, Rq2, Rs3; where Rs1 includes R1 and R2. For this report, five members R1/R2, R3, R4, R5, and R6 will be used.

The members of the Rinconada Formation are remarkably consistent in thickness, lithology, and texture over the two east-trending bands of exposure in the range. Quartzite occurs locally in schist members, and thin pelitic schists are invariably interlayered in quartzite members.

Protoliths for the Rinconada were probably sands and shales

that accumulated in deltaic, fluvial, and shallow marine settings (Soegaard and Eriksson, 1985).

R1/R2 member. Because these schists are easily weathered and eroded, exposures are generally poor. The best exposures in the northern band occur where Hondo Canyon cuts across the strike of Rinconada units (Plate 1). The best exposures in the southern band occur in the Copper Hill area. Montgomery (1963) estimated thickness of 60-105 m (200-350 ft) for R1, and 60-150 m (200-500 ft) for R2.

Traditional definitions of R1 and R2 depended on the presence of large andalusite porphyroblasts in biotite-muscovite "salt and pepper" R1 schist, and garnet and staurolite porphyroblasts in R2 muscovite-biotite schist. In general, especially in the Copper Hill area, these criteria are consistent; however in the northern Picuris there is some mineralogical and textural variability in these units.

In the Copper Hill area, the Ortega Quartzite grades into R1 schists over a 5-m-thick zone of intercalated quartzite and schist. The lowermost schists of R1/R2 contain abundant knobby andalusite and cordierite porphyroblasts up to 6-7 cm across. Andalusites are less abundant upwards, where schists consist of black biotite books in muscovite-quartz matrix. R2 begins where porphyroblasts of staurolite coexist with andalusite. R2

schists are relatively uniform in texture. Large twinned staurolite crystals weather out of a medium-grained muscovite-quartz-garnet-biotite schist. Locally near Copper Hill, the basal R2 contains a 1 m thick resistant, gray quartzite horizon. Garnets are small and euhedral, and although they remain constant in size, they become more abundant up-section. R2 schists become more quartz-rich at the top of the member, where they grade into the R3 quartzite member.

R3 member. The northern band of R3 contains exposures that range from excellent in the west to average in the east. Good exposures occur along most of the southern band. The R3 quartzite is highly resistant to weathering, and commonly forms prominent, steep-sided ridges.

From bottom to top, the R3 member consists of:

- 1) tan to white, micaceous, cross-bedded quartzite;
- 2) massive, vitreous, crystalline, bluish-gray quartzite;
- 3) friable brown quartzite;
- 4) slabby gray to white quartzite;
- 5) quartzite containing thin layers of staurolite-garnet-muscovite-quartz schist and knobby grey plagioclase schist;
- 6) friable tan to brown quartzite, which grades up to the R4 schists.

In the Copper Hill area, the R3-R4 contact is marked by a

massive, 1-m-thick layer of dark blue-black quartzite. Thicknesses of R3 range from 60 to 100 m.

R4 member. Northern exposures of the R4 schists are fair to poor. Exposures around Copper Hill are excellent and extensive. The R4 schists tend to underlie canyons and saddles between the bounding, more resistant quartzite members.

R4 schists are characteristically fine- to medium-grained, reddish weathering, gray to silver, garnet-staurolite-muscovite-biotite-quartz schists. Quartz-rich versus biotite-rich layers are common. Small euhedral garnets are concentrated in thin reddish layers, whereas staurolite porphyroblasts are scattered throughout. Thicknesses range from 25 to 70 m.

R5 member. The R5 quartzite member crops out extensively over most of the two bands of Rinconada Formation. This rock forms prominent ridges and steep slopes. From bottom to top, the R5 consists of:

- 1) massive, micaceous, white to gray quartzite;
- 2) massive blue crystalline quartzite;
- 3) massive, resistant gray-black quartzite and white quartzite;
- 4) massive, gray to white, locally cross-bedded vitreous quartzite with thin staurolite schist horizons;

- 5) pure quartzite, interlayered tan, cross-bedded quartzite and massive, blue quartzite;
- 6) tan micaceous quartzite, massive blue quartzite, friable quartzite, massive quartzite which grades up into R6 schist member.

In general, the R5 member has more localized cross-beds and is more massive than the R3 member. Thickness range from 80 to 200 m.

R6 member. Although the R6 member is easily weathered and eroded, it is a prominent lithology that crops out extensively over both the northern and southern bands of exposure. In general the R6 is well banded, gray to red, quartz-muscovite-biotite-garnet phyllite to schist. This rock type is commonly strongly crenulated. In the northern exposures, medium-sized porphyroblasts of staurolite are commonly concentrated in layering. Interlayers of garnet-rich and quartz-rich rock contain small red-brown euhedral garnet porphyroblasts. Garnet forms up to 40 percent of some of the garnet-rich layers. Cleavage surfaces in muscovite-rich phyllitic horizons exhibit a characteristic gray to silver sheen. Good graded bedding occurs locally. Basal R6 schists contain local, thin black quartzite beds. Although minor textural and mineralogical variations are numerous, this unit is lithologically distinctive with respect to the other Rinconada schists. The upper contact

of the R6 with the overlying Pilar Phyllite is marked by a very distinctive, several meter thick, blue-black garret quartzite. Thicknesses of R6 range from 40 to 100 m.

### Pilar Phyllite Formation

Just (1937) originally included the Pilar Phyllite Formation as the Hondo Slate. Montgomery (1953) renamed the Hondo Slate as the Pilar Phyllite Member of the Ortega Formation. Nielsen (1972) separated a slate member from a muscovite phyllite member (later to become the Piedra Lumbre Formation) in the Pilar Formation. Long (1976) proposed group status for the Ortega, and broke out the Pilar Formation and Piedra Lumbre Formation.

The Pilar Formation is exposed in two major and two minor localities in the Picuris Range. Lithologies are identical in all areas, with the exception of the occurrence of somewhat more phyllitic rock in parts of the southwestern exposure. The Pilar is a distinctive, black, compact, very fine-grained, quartz-rich carbonaceous slaty phyllite. Brown to yellow iron-staining commonly occurs locally. In some areas, small, elongate, flattened cavities appear on cleavage surfaces, and thin white, schistose layers, which probably represent bedding, cut the homogeneous black phyllite. McCarty (1983) mapped a 15-m-thick, brick-red phyllitic layer in the southwestern exposure.

On the average, the Pilar consists of about 50 percent small (less than 0.1 mm) streaky quartz grains and lenses and small veins of coarser quartz, 25% very fine opaque grains that are mainly graphite, and 25% very fine-grained (less than 0.05 mm) aligned muscovite laths. Relict porphyroblasts occur in some rocks. Minor minerals include sphene and traces of biotite. Apparent thicknesses of Pilar Phyllite range from 200 to 600 m in the Hondo syncline area.

Most workers agree that these rocks represent reduced, carbonaceous black shales that were deposited in some type of oxygen-starved basin.

#### Piedra Lumbre Formation

Although the most complete, most extensive exposure of Piedra Lumbre Formation occurs as an east-trending strip in the northern Picuris Range, the unit was first described in a relatively thin sliver of exposure south of Copper Hill. The Piedra Lumbre Formation as originally described in the Copper Hill area consists of dark-colored, fine-grained, carbonaceous, muscovite-biotite phyllite with garnet porphyroblasts and local calc-silicate and thin quartzite horizons. Based on transposition structures, Holcombe and Callender (1982) suggested that layering in the Piedra Lumbre is tectonic rather than original sedimentary. Although this may be true in much of the section, original

graded bedding is locally preserved. In the Copper Hill area, the contact between Piedra Lumbre and Pilar is very sharp, with Pilar rocks appearing highly deformed. In the Hondo syncline, the contact is gradational with numerous calc-silicates and dark, unusual lithologies marking the transition zone.

Piedra Lumbre lithologies in the Hondo Syncline are more diverse than at Copper Hill, and probably include more of the original stratigraphic section. The thickness of the Piedra Lumbre in the syncline is not measureable due to folding and a lack of marker horizons, and no stratigraphic younging features are preserved. Most of rock in the Piedra Lumbre consists of thinly banded, fine- to medium-grained, garnet- and/or staurolite-bearing quartz-muscovite-biotite schist, phyllite, and metasiltstone. Excellent graded beds are found locally. Lithologies are variable along strike, but one 50-m-thick section measured up from the Pilar Phyllite consists of: gray, laminated schists; laminated schistose quartzite and phyllitic schist with small cross-beds; gray schist; yellow, cross-bedded quartzite with 5 cm cross-beds; gray phyllitic, garnet-bearing schist; and massive quartzite with finely laminated garnet-plagioclase bands. The contact zone between Pilar and Piedra Lumbre contains interlayered black slate and phyllite, fine schists, metasiltstones, cross-bedded knobby plagioclase schists, quartz-rich black metasiltstone, amphibole schist,

dark calc-silicates, quartzites, and various phyllites. Montgomery (1953) made complete petrologic descriptions of the calc-silicate and related rocks from the Piedra Lumbre Formation in the Copper Hill area. Thicknesses of Piedra Lumbre sections are difficult to estimate due to extremely high amounts of internal deformation. The apparent thickness of Piedra Lumbre Formation in the Hondo syncline ranges from 200 m to 400 m. The top of the Piedra Lumbre Formation has been removed by weathering and erosion, so these are minimum estimates.

In general, schists of the Piedra Lumbre contain less garnet, are more resistant to weathering, are darker, and are more heterogeneous than the R6 schist member of the Rinconada Formation. Piedra Lumbre protoliths include laminated, thinly interlayered quartz sandstones and siltstones, and carbonaceous shales.

#### Sedimentology of the Ortega Group

The most thorough sedimentological analysis done in Precambrian rocks in New Mexico was made by Soegaard and Eriksson (1985) on the Ortega Group of northern New Mexico. Based on facies analyses in the Tusas, Picuris, Truchas, and Pecos areas, they concluded that the Ortega Group accumulated on a shallow marine shelf that sloped gently to the south and southeast. No evidence of subaerial exposure

was found, so sediments were considered subtidal shelf deposits. These rocks represent a transgression in which sediment input initially matched basin subsidence, but which ended with the drowning of the outer shelf and deposition of black basinal muds (Pilar and Piedra Lumbre formations). No Proterozoic supracrustal rocks younger than the Piedra Lumbre have been identified in any of these ranges. Soegaard and Eriksson (1985) found that sedimentary structures were dominated by storms on the outer shelf, and tides on the inner shelf. Very low shelf slopes are inferred due to the lack of shallow-water turbidites.

Soegaard and Eriksson (1985) noted that depositional models for accumulation of thick quartz arenites and lesser mudrocks such as the Ortega Group are not well constrained, because no modern analogs have been found. In the geologic record, very thick sandstones and quartzites are restricted to the Lower Paleozoic, the Proterozoic, and the late Archean. Most thick, pure quartz sandstones probably form in a relatively long-lived, tectonically stable setting during a major sea-level rise. Influx of mature terrigenous quartzose sediment must be balanced by the relative sea-level rise.

## Plutonic Rocks

### General

The suite of granitic rocks in the southern Picuris Range was originally named the Dixon Granite by Just (1937) during his reconnaissance mapping. Montgomery (1953) called these rocks, and similar rocks to the south in the Truchas Range, the Embudo Granite. In a detailed field, petrologic, and geochemical study of these rocks, Long (1976) subdivided four major intrusive units which he named, from oldest to youngest, Cerro Alto Metadacite, Puntiaquedo Granite Porphyry, Rana Quartz Monzonite, and Penasco Quartz Monzonite. In addition to these four units from the southern Picuris Range, at least two other intrusive bodies are exposed in the map area in the eastern half of the range. In this report, these are informally called the Granite of Alamo Canyon and the Granite of Picuris Peak (see outcrop distributions in Fig. 2.4).

### The Granite of Alamo Canyon

East of the Picuris-Pecos fault are two large, north-south elongate, partially fault-bounded exposures of plutonic rock which are separated by a strip of Cenozoic sedimentary rocks. In many of the best-exposed, non-faulted

areas, thin zones of steeply-dipping Precambrian orthoquartzite and Pennsylvanian sandstone, limestone, and shale separate the Granites of Alamo Canyon from the surrounding Cenozoic sediments.

Although both the eastern and western granitic bodies show textural variation from place to place, these rocks resemble one another and are probably the result of a single intrusive event. The eastern block generally consists of pink to white, medium-grained, weathered looking, mica-rich granitic rock with euhedral megacrysts of feldspar. The western block is more heterogeneous. In the northern half, black flattened amphibolite lenses float within a pinkish, fine- to medium-grained granitic rock. These granitic rocks are always weathered looking, fairly equigranular, and commonly crumbly. In places, this rock could easily be mistaken for an arkose. In the south, this unit appears intrusive into Rio Pueblo quartz-eye schist. The Granites of Alamo Canyon nowhere cut basal Ortega Group quartzites. Pegmatites are voluminous in the southernmost granitic exposures just northwest of U.S. Hill.

All of the granitic rocks east of the Picuris-Pecos fault contain at least one tectonic foliation. Commonly three closely-spaced, orthogonal joint sets cause this rock to weather into small, angular blocks.

## The Granite of Picuris Peak

In the southeastern Picuris Range, on the west side of the Picuris-Pecos fault, medium- to coarse-grained granitic rocks, herein called the Granite of Picuris Peak, are interlayered with supracrustal Vadito Group country rock. Blocks of orthoquartzite within the plutonic rock suggest an intrusive relationship between the two. Contacts between granitic rock and supracrustal rock invariably trend east, parallel to bedding in the country rock.

The Granite of Picuris Peak shows a variety of local textures ranging from coarse-grained, pink feldspar-rich rock to white, quartz-rich rock. In thin section, these rocks show interlocking mosaics of microcline, plagioclase, quartz, biotite, and iron-oxide minerals. Most samples exhibit considerable alteration of feldspars and mica.

## Cerro Alto Metadacite

The Cerro Alto Metadacite is a fine-grained, gray, foliated, stock-like body that sits within Vadito Group supracrustal rocks. Montgomery (1953) included this rock with the unit he mapped as "Vadito Conglomerate-felsite" (Vcf). Long (1976) described isolated sills of metadacite in nearby amphibolites, and found xenoliths of metadacite in nearby granitic rocks. Granitic rocks appear to cut the

main metadacite body, and thus Long concluded that the metadacite is the oldest granitic body in the southern Picuris. D.A. Bell (1985) found no evidence for later intrusion of the Cerro Alto Metadacite by the Puntiaquedo Granite Porphyry or the Rana Quartz Monzonite, and concluded that the Cerro Alto body was contemporaneous with the Vadito amphibolite.

#### Puntiaquedo Granite Porphyry

Long (1976) has described the Puntiaquedo Granite Porphyry as consisting of subequant, subhedral, Carlsbad-twinned, 1 cm-long, microcline phenocrysts, and rounded quartz phenocrysts in a plagioclase, K-feldspar, biotite, muscovite matrix. Modally, the rock ranges from quartz monzonite to granodiorite.

The pluton is massive, and cross-cuts Vadito Group schists and amphibolites along sharp contacts. The intrusion nowhere penetrates Ortega Group rocks. D.A. Bell (1985) found that the Puntiaquedo intrudes the Vadito schists, but does not intrude the Vadito amphibolite.

#### Rana Quartz Monzonite

The Rana Quartz Monzonite is the most widely exposed of the plutonic rocks in the southern Picuris Range. Contacts

with the other granitic bodies are poorly exposed, but Long (1976) noted inclusions of Puntiaquedo in the Rana, suggesting that the Rana is younger. The Rana is generally foliated, medium-grained biotite quartz monzonite to granodiorite, with a discontinuous fine-grained, gradational border zone (Long, 1976). This body also is strongly discordant with Vadito Group country rocks.

As with the Puntiaquedo pluton, D.A. Bell (1985) suspected that this unit intrudes Vadito schists, but not Vadito amphibolites. In the one area where the Rana pluton is in contact with the Vadito amphibolite, the fine-grained border zone that everywhere else rims the pluton is absent. D.A. Bell (1985) proposed that this contact is an unconformity separating older Vadito schists and granitic plutons, from younger Vadito amphibolites. The Puntiaquedo-Rana contact is a fault in most places. In unfaulted areas, the Rana pluton intrudes Puntiaquedo rocks.

#### Penasco Quartz Monzonite

Long (1976) found the Penasco Quartz Monzonite to be the youngest plutonic body in the southern Picuris Range. The Penasco is generally conformable with Vadito Group rocks in its northern exposure. Penasco rocks are less foliated than the other granitic rocks in the area. It is a biotite-sphene quartz monzonite to granodiorite, that locally

contains abundant, large (up to 9 cm long) megacrysts of Carlsbad-twinned microcline, and mafic xenoliths along its borders.

D.A. Bell (1985) found that the Penasco pluton intrudes the Cerro Alto Metadacite, the Vadito schists, and the Vadito amphibolites.

### Pegmatites

Pegmatites are common in the southwestern Picuris Range, and cut all granitic rock types. Long (1974) divided them into five groups: 1) small, simple pegmatites with microcline, quartz, albite, muscovite, and green beryl; 2) larger, variably-zoned bodies with unusual mineralization (e.g. the Harding Pegmatite); 3) small, zoned bodies of albite, quartz, and muscovite; 4) small dikes of pegmatite-aplite; and 5) medium-sized dikes of K-feldspar, plagioclase, quartz, and tourmaline. These pegmatites commonly cut across abundant, deformed quartz veins that occur widely in most rock types.

Several, 2 to 4-m-thick, concordant, simple pegmatites of quartz-microcline-albite-muscovite have intruded Pilar Phyllite in the west-central map area. These pegmatites are aligned within the hinges of macroscopic folds, but are not themselves folded.

## Summary of General Field Relations

The Picuris Range contains three supracrustal rock sequences and at least five different plutonic bodies. In all rocks, compositional layering and foliations dip an average of  $60^{\circ}$  south. Cross-beds in Vadito Group quartzites suggest an overall younging to the north. Thus, as illustrated by a cross-section through the Picuris Range, the Vadito Group structurally overlies and stratigraphically underlies the Ortega Group (Fig. 3.4). The felsic schist at Pilar structurally and stratigraphically underlies the Ortega Group. Thus, the Vadito Group and the felsic schist at Pilar occupy identical stratigraphic positions with respect to the Ortega Group. The nature of the relationships among all three of these terranes is unknown.

The Vadito Group is extensively intruded by syntectonic granitic plutons. No plutons intrude Ortega Group rocks or the felsic schist at Pilar (however, the base of the felsic schist is not exposed). The pre-tectonic Cerro Alto Metadacite intrudes the amphibolite unit of the Vadito Group, but not the schist unit. The syntectonic Puntiaquedo and Rana plutons intrude the schist unit but not the amphibolite unit (D.A. Bell, 1985). The post-tectonic Penasco pluton intrudes both the schist and amphibolite units of the Vadito Group. These relationships suggest that the Vadito Group is not a simple, continuous stratigraphic

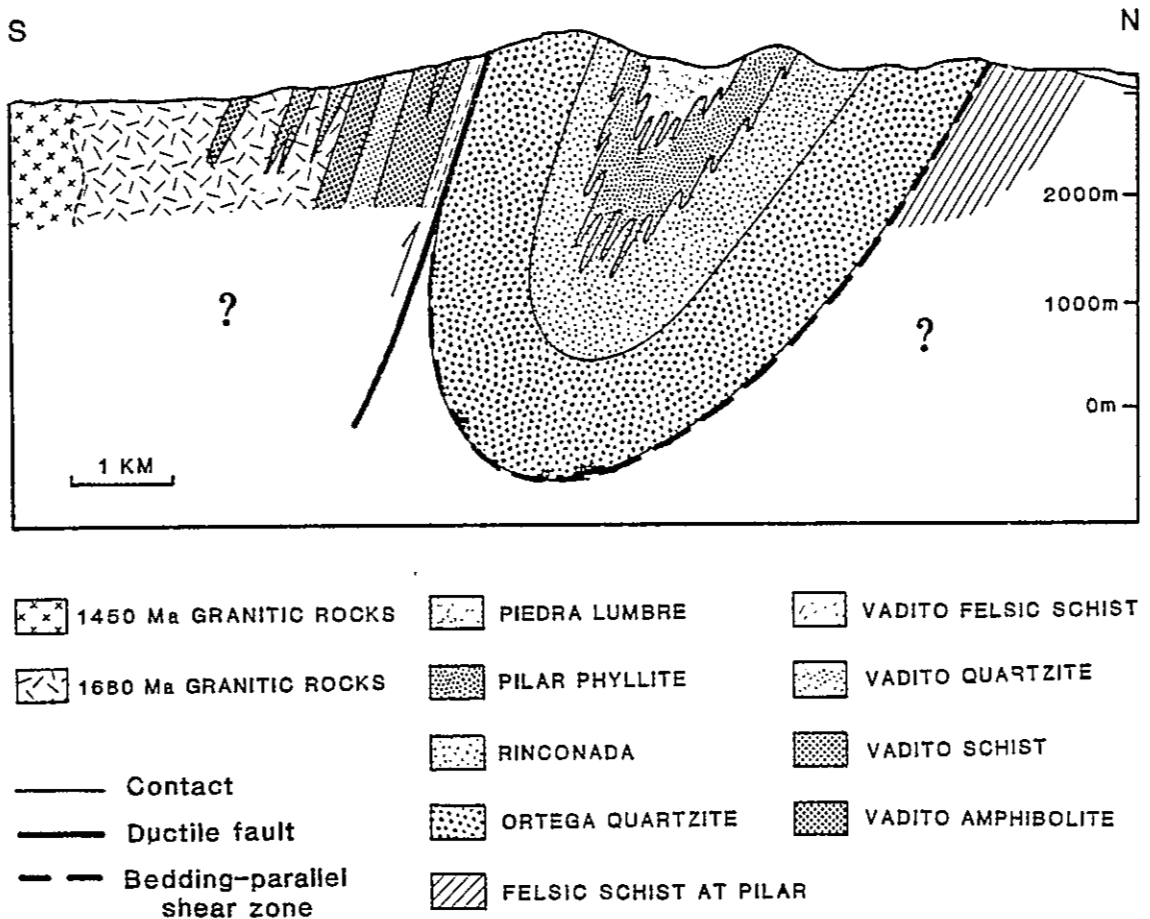


Figure 3.4. Generalized south-north cross-section through the Picuris Range. No vertical exaggeration. See text for discussion.

package, but rather contains faults and/or unconformities separating different lithostratigraphic units.

The quartz-eye felsic schist at Pilar is similar to part of the redefined "Vadito Group" that Williams et al. (1986) described in the Tusas, Taos, and Rio Mora areas. Parts of the more mafic Vadito Group in the southern Picuris Range are similar to the older mafic metavolcanic sequences found in the Tusas Range (Moppin metavolcanic series), the Santa Fe Range (Pecos greenstone belt), and the Taos Range. Williams (1987) suspected that each of these may be separate older greenstone-type terranes of different ages. If mafic rocks in the southern Picuris Range are such a terrane, it is probably best to maintain the original Vadito Group name because it may be a rock group without stratigraphic equivalents.

The Vadito Group as a whole is unlike both the mafic metavolcanic packages, and the felsic pre-Ortega packages. None of the older mafic terranes contain thick orthoquartzites such as the Marquenas Quartzite Formation of the Picuris Range. None of the other felsic packages are intruded by granitic plutons. Thus the Vadito Group of the Picuris Range is anomalous. D.A. Bell (1985) suggested that a major unconformity separated the Vadito schists from the Vadito amphibolites. He suggested that this unconformity was subsequently folded. Early, near-bedding parallel ductile faults cut Vadito and Ortega rocks to the north. It

is possible that the contact that D.A. Bell (1985) suspected was a folded unconformity is actually a folded fault or series of folded faults in the Vadito Group. If so, these faults may have juxtaposed rocks from totally different tectonic terranes (i.e. the amphibolite, schist, and metaconglomerate/quartzite units of the Vadito Group). Furthermore, the very different sedimentary environments represented by Vadito schist and Marquenas Quartzite suggest that the boundary between schist and metaconglomerate is an unconformity or a bedding-parallel fault.

The southern Picuris Range Vadito Group may consist of fragments of various lithostratigraphic sequences. This may be the reason that the Vadito Group possesses characteristics of both types of pre-Ortega terranes. Alternatively, there are two other possibilities to account for the incongruity: 1) there is more lithologic variety to either the felsic or mafic terrane (or both) than has previously been recognized; or 2) the entire Vadito Group of the southern Picuris Range is entirely distinct from both the felsic and older mafic metavolcanic terranes. For this paper, these rocks will be considered as a single package called the Vadito Group, *sensu stricto* (Fig. 3.5).

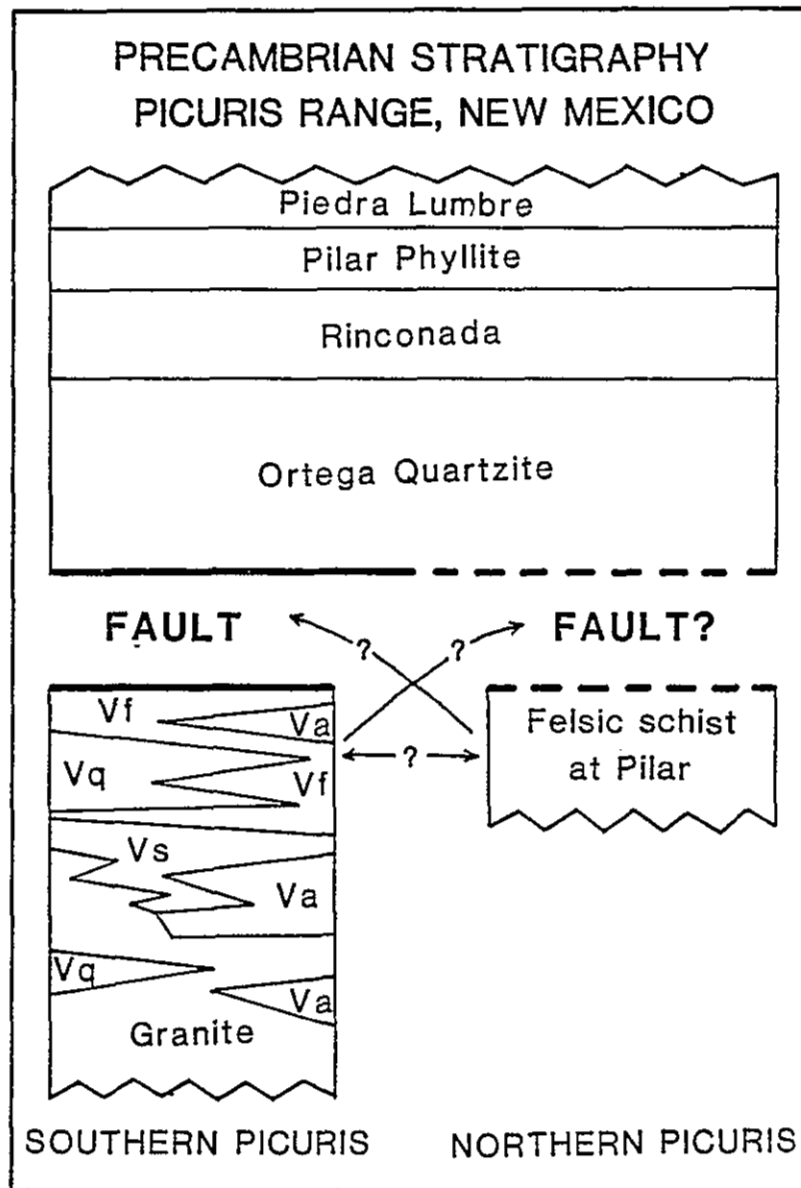


Figure 3.5. Possible stratigraphic relationships among the Ortega Group, Vadito Group, and the felsic schist at Pilar in the Picuris Range. The felsic schist at Pilar may be equivalent to some of the Rio Pueblo Schist of Montgomery (1963). Vf = Vadito Group felsic schist. Va = Vadito amphibolite. Vs = Vadito schist. Vq = Marquenas Quartzite and similar Vadito Group quartzites and metaconglomerates.

## CHAPTER 4. GEOCHRONOLOGY

### Introduction

Prior to this study, no attempts have been made to date crystallization ages of supracrustal rocks in the Picuris Range. No U-Pb zircon ages have been published for any unit of the Vadito Group of the southern Picuris Range, and no absolute ages are available for deposition of the Ortega Group because no metavolcanic rocks exist in the section. Several recent U-Pb zircon dates have been reported for plutonic rocks in the southern Picuris Range, and one study has examined detrital zircons in the Ortega Quartzite. The remaining geochronology in the Picuris Range has been limited to the K-Ar and Rb-Sr isotopic systems. L.T. Silver (personal communication in Grambling and Williams, 1985b) reported a U-Pb zircon age of about 1700 Ma for felsic metavolcanic rocks in the Tusas Mountains. Grambling and Williams (1985b) suggested that these rocks could be correlative with the felsic schist at Pilar. All previously published Picuris Range geochronology is summarized in Figure 4.1.

Ma	U-Pb zircon	Rb-Sr whole rock	K-Ar
1200		1234 $\pm$ 63 Embudo (miner. 1238 $\pm$ 23 isochron) (1)	1235 $\pm$ 19 Biotite, SE of Trampas (3)
1300			1335 Muscovite in simple peg (3)
1400		1370 $\pm$ 30 Harding Peg. (6)	
	1450 Penasco (7) 1470 $\pm$ 20 Penasco (4)	1430 Penasco (2) 1440 $\pm$ 160 Rana (6)	
1500		1550 $\pm$ 140 Puntiaquedo (6)	
1600	1630 Cerro Alto (7)		
	1665 "Rio Pueblo Schist" 1673 $\pm$ 5 Rana (7)	1670 Rana (2)	
1700	1684 $\pm$ 1 Puntiaquedo (7)	1709 $\pm$ 41 "Embudo Granite" (1)	
1800	1830 $\pm$ 21 detrital zircons, Ortega Quartzite (5)		
1900			

(1) Fullager and Shiver, 1973

(2) Long, 1974

(3) Gresens, 1975

(4) Long, 1976

(5) Maxon, 1976

(6) Register, 1979

(7) Bell, 1985

Figure 4.1. Summary of previous geochronologic work in the Picuris Range. Ages recalculated using decay constants of Steiger and Jager (1977).

## Previous Work

The first geochronologic investigation of rocks in the Picuris Range consisted of K-Ar and model Rb-Sr study of muscovite and lepidolite from the Harding Pegmatite (Aldrich et al., 1958). Samples yielded an average value of approximately 1300 Ma for the age of the pegmatite. Upon reinterpretation of these data, Long (1976) proposed that the Rb-Sr mineral isochron suggested that the pegmatite may be as old as 1375 Ma. Register (1979) found an Rb-Sr age of  $1370 \pm 30$  Ma for the Harding Pegmatite.

Gresens (1975) determined an Rb-Sr age of about 1335 Ma for pegmatitic muscovite in the southern Picuris Range.

Fullagar and Shiver (1973) produced an Rb-Sr whole-rock isochron analysis of the "Embudo Granite" in the southern Picuris Range. Long (1976) suspected that the resultant age of  $1673 \pm 41$  Ma was actually a composite age of several different plutons. Upon reinterpretation of field relations of these samples, Long (1976) deduced poorly constrained ages of 1673 Ma for the Rana Quartz Monzonite, and 1400 Ma for the Penasco Quartz Monzonite. Fullagar and Shiver also derived mineral isochrons of  $1208 \pm 63$  and  $1212 \pm 23$  for "Embudo Granites". Fullagar and Shiver (1973) suggested that a thermal event may have reset the system at about 1200 Ma. Long (1976) also suspected that the significance of these ages is uncertain due to partial or total resetting of

the Rb-Sr and K-Ar isotopic systems.

Gresens (1975) found K-Ar biotite dates of  $1235 \pm 19$  Ma in rocks southeast of the town of Trampas.

Gresens (1975) proposed the following history for Precambrian rocks in the southern Picuris Range: intrusion of the "Embudo Granite" at 1673 Ma; tectonism and metamorphism at 1425 Ma; a thermal event at 1350 Ma; and tectonism and hydrothermal activity at 1250 Ma. Long (1976) postulated that the overlap of K-Ar and Rb-Sr dates represented a thermal event at 1220-1250 Ma.

In a Rb-Sr geochronologic study of granitic rocks in the southern Picuris Range, Register (1979) reported dates of  $1550 \pm 140$  Ma for the Puntiaugudo Granite Porphyry, and  $1440 \pm 160$  for the Rana Quartz Monzonite.

Two workers have reported U-Pb zircon crystallization ages for rocks in the Picuris Range. Maxon (1976) sampled detrital zircons in the Ortega Quartzite from two localities in the cliffs near Pilar. Several different shapes of zircon populations were recognized. Concordia diagrams contained upper and lower intercepts of  $1830 \pm 21$  and 436 Ma, respectively. The age of  $1830 \pm 21$  Ma is a minimum age of crystallization of zircons in some igneous rock from some unknown source area, and a maximum age for deposition of the Ortega Quartzite.

D.A. Bell (1985) performed U-Pb zircon chronology on the four granitic plutons in the southwestern Picuris Range.

He reported dates of  $1684 \pm 1$  Ma for the Puntiaquedo Granite Porphyry,  $1673 \pm 3$  Ma for the Rana Quartz Monzonite, about 1630 Ma for the Cerro Alto Metadacite, and about 1450 Ma for the Penasco Quartz Monzonite.

## Discussion

These Rb-Sr and K-Ar dates may be minimum estimates of crystallization ages due to isotopic resetting during thermal overprinting. Resetting is not a problem with the U-Pb zircon dates reported in recent investigations. Therefore, 12 samples for geochronology were collected for the present study. A preliminary U-Pb zircon date has thus far been generated for only one sample. A sample of Rio Pueblo Schist from the type-section at Comales campground in the southeastern Picuris Range yielded a relatively concordant age of about 1665 Ma (S.A. Bowring, personal communication, 1986). The rock dated is texturally different from the felsic schist at Pilar, and may not be equivalent. Ages of the remaining samples will be reported in a future publication.

Ten of these samples should yield ages of crystallization for various volcanic and plutonic units in the Picuris Range. The other two samples are from metasedimentary rocks. One is designed to investigate detrital zircons in quartzite clasts from the Marquenas

Quartzite Formation, and the other was collected to investigate the age of peak metamorphism in the Ortega Group.

The timing of metamorphism and deformation of Precambrian rocks in northern New Mexico has previously been attempted with the Rb-Sr system. Rb-Sr whole-rock and mineral isochron studies in conjunction with detailed structural-metamorphic work have been used to determine absolute ages of structural-metamorphic events in multiply deformed-metamorphosed rocks (Black et al., 1979; Marjoribanks and Black, 1974). Deformational events that cause strong penetrative cleavages are sufficient to homogenize Rb isotopes over a large scale. By carefully collecting samples whose fabrics are dominated by some known schistosity, whole-rock and mineral isochrons can yield data on the thermal-structural history of the rock. Ward and Grambling (1985), who successfully applied this technique to rocks in northern New Mexico, reported an age of around 1425 Ma for development of a strong syn-metamorphic crenulation cleavage in schists, and a cooling rate of 2-3°C/Ma at depth. Although this strong crenulation cleavage may correspond to a similar fabric in schists of the Picuris Range, concurrence of development of these fabrics is not required.

Appendix 1 describes the zircon separation method used for the present study and the 12 geochronology samples.

## CHAPTER 5. GEOMETRIC FABRIC ELEMENTS

### Introduction

Multiple microscopic and mesoscopic tectonite fabrics are developed to various degrees in most of the Proterozoic rocks in the Picuris Range. Correct identification and interpretation of these fabrics is critical to the structural analysis. This chapter defines and describes the various fabric elements in Precambrian rocks of the Picuris Range. It is important to note that the character of the fabrics themselves varies between areas, and between lithologies within an area. In these cases, range-wide correlation of specific fabric elements becomes difficult.

The deformational episodes that produced a characteristic set of structures and fabric elements are identified as  $D_1$ ,  $D_2$ , and  $D_3$ . This terminology is not meant to suggest that the area was subject to distinct pulses of deformation. There may have been considerable temporal overlap of formation of these "generations" of structures.

Folding events are denoted  $F_1$ ,  $F_2$ , etc., with associated cleavages  $S_1$ ,  $S_2^*$ ,  $S_2$ , etc.  $L_{10}$  and  $L_{20}$  are intersection lineations of surfaces designated by subscripts.  $L_1$  and  $L_2$  are extension lineations formed during  $D_1$  and  $D_2$  respectively.

## Compositional Layering, $S_0$

In most rocks, compositional layering is thought to represent original stratigraphic layering. Orthoquartzites in both the Ortega Group and the Vadito Group commonly contain well preserved cross-laminations (Fig. 5.1a). Schists of the Piedra Lumbre Formation locally preserve graded bedding in which metamorphism has caused coarsening of the pelitic portion, and thus a "reverse" grainsize grading (Fig. 5.1b).

In some areas, compositional layering does not correspond to sedimentary layering. Holcombe and Callender (1982) suggested that much of the layering in the sliver of Piedra Lumbre exposed south of Copper Hill was structurally transposed. This is clearly the case locally in many of the schistose units of the Picuris Range (Fig. 5.2).

Most quartzose rocks fracture along compositional layers rather than later cleavages. Over most of the range,  $S_0$  strikes east, and dips around  $60^\circ$  south.

## First Generation of Structures, $D_1$

The earliest recognized cleavage,  $S_1$ , appears as a schistosity in quartzites and micaceous quartzites. Within the matrix of most schists,  $S_1$  appears to have been

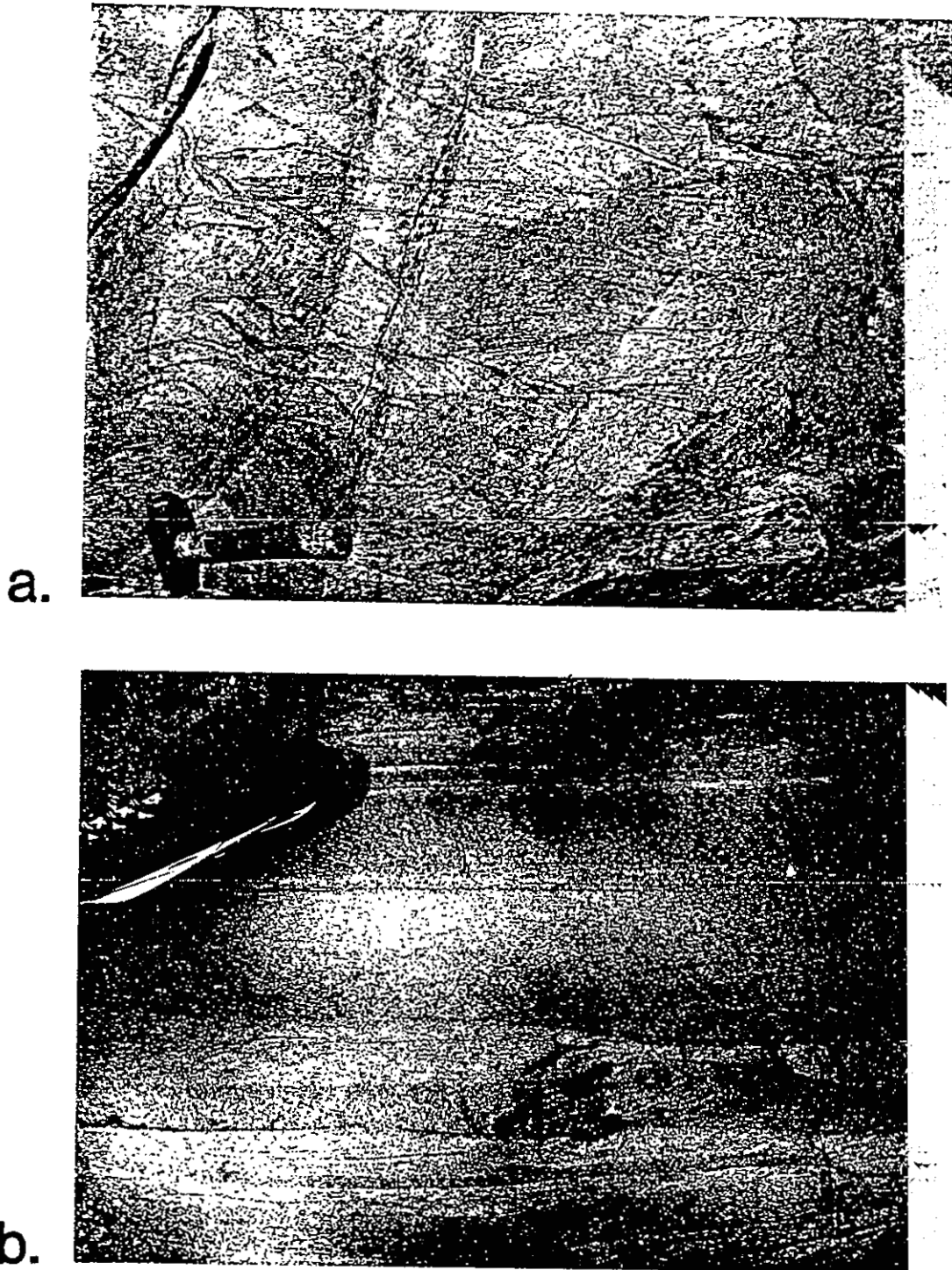


Figure 5.1. Photographs of primary sedimentary structures in Precambrian rocks of the Picuris Range. a. Overturned cross-beds in Ortega Quartzite. b. Overturned graded bedding in the Piedra Lumbre Formation.

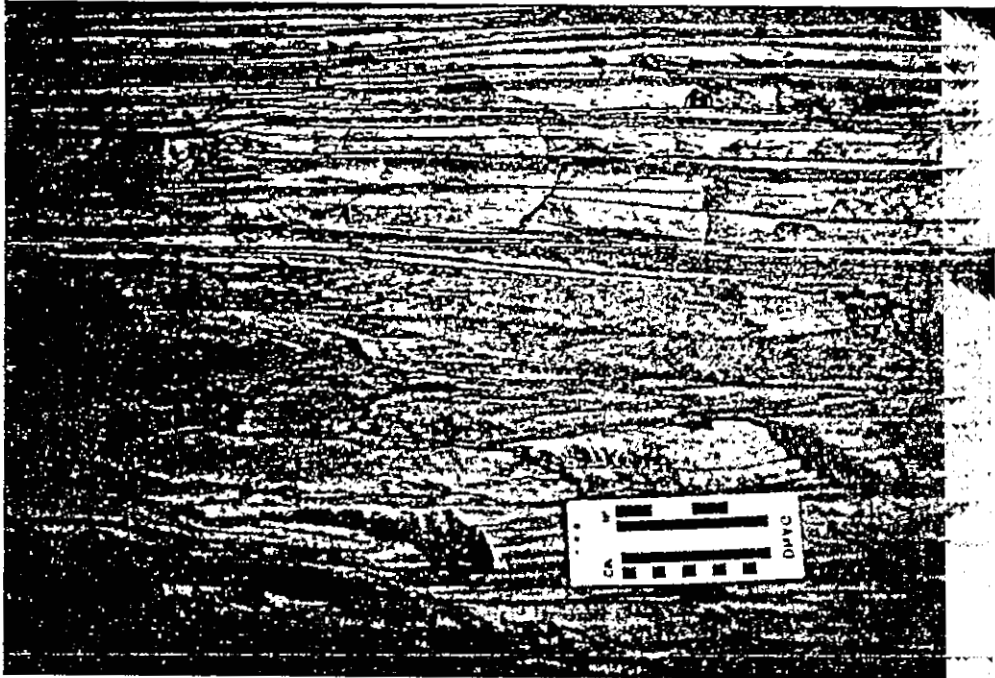


Figure 5.2. Photograph of transposed layering and  $F_1$ (?) folds in Piedra Lumbre Formation, southwestern Picuris Range.

destroyed by subsequent cleavage formation. Porphyroclasts in some schists contain inclusion trails interpreted to be remnants of  $S_1$ . In the quartzites,  $S_1$  is generally parallel or sub-parallel to compositional layering, and is responsible for the mica sheen visible on bedding surfaces in quartz-rich rocks. In the felsic schist at Pilar, the dominant foliation is bedding-parallel, and is interpreted as  $S_1$  (Fig. 5.3). In these schists,  $S_1$  is defined by aligned muscovite, opaque minerals, inequant quartz grains, and flattened quartz and feldspar megacrysts. This  $S_1$  corresponds to the  $S_1$  of Nielsen and Scott (1979) and Holcombe and Callender (1982).

The earliest imposed lineation,  $L_1$ , is generally a down-dip mineral elongation best seen in the quartzites and quartz-eye schists near the Vadito-Ortega contact (Fig. 5.4). Commonly, elongate grains of kyanite, sillimanite, and quartz define this extension lineation. In Marquenas Quartzite Formation metaconglomerates the down-dip orientation of stretched pebble clasts may represent  $L_1$ . This lineation does not correspond to the composite  $L_1$  of Nielsen and Scott (1979), who defined  $L_1$  as the intersection between  $S_1$  and  $S_2$ .

$F_1$  folds are uncommon. None have been unequivocally identified in the map area. Small, intrafolial, isoclinal folds in the Piedra Lumbre Formation south of Copper Hill may be  $F_1$  folds. These  $F_1$  folds correspond to the rootless,

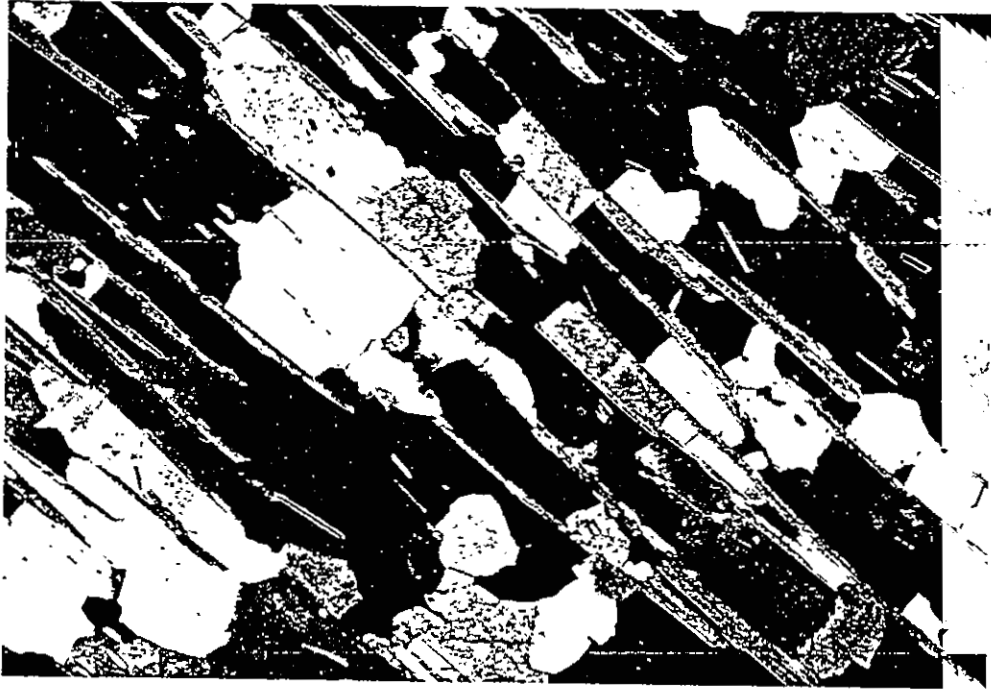


Figure 5.3. Photomicrograph of  $S_1$  foliation in quartz-muscovite, felsic schist at Pilar. Field of view is 3.4 mm.

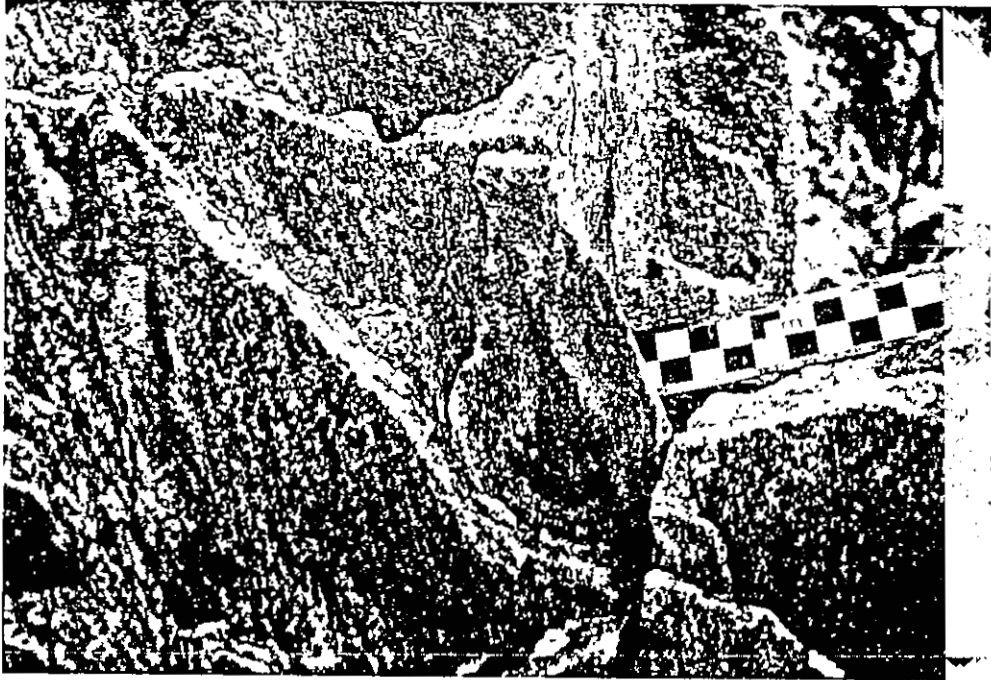


Figure 5.4. Photograph of down-dip  $L_1$  extension lineation on  $S_1$  surfaces in Ortega Quartzite, northwestern Picuris Range.

intrafolial folds of Nielsen and Scott (1979) and McCarty (1983).

### Second Generation of Structures, $D_2$

The  $S_2$  cleavage appears as either a crenulation cleavage or a schistosity.  $S_2$  is rarely the dominant cleavage in rocks of the Picuris Range. In most schistose rocks,  $S_2$  has been totally destroyed by  $D_3$  structures. In quartzose rocks, which do not preserve cleavages well,  $S_2$  appears locally as a crenulation cleavage.  $S_2$  is generally at a low angle to compositional layering. This  $S_2$  does not correspond to the  $S_2$  of either Nielsen and Scott (1979) or Holcombe and Callender (1982). Instead, the presently defined  $S_2$  is intermediate between their  $S_1$  and  $S_2$ .

The  $L_2$  extension lineation is parallel or sub-parallel to the  $L_1$  lineation and contains aligned biotite, quartz, kyanite, sillimanite, and tourmaline. The  $L_{20}$  intersection lineation is extremely difficult to separate from later intersection lineations. These lineations do not correspond to the  $L_2$  and  $L_{20}$  intersection lineations of Nielsen and Scott (1979) and Holcombe and Callender (1982).

$F_2$  folds are common, range from tight to isoclinal, and range in size from microscopic to map-scale (Fig. 5.5). In quartz-rich rocks,  $S_1$  is folded by  $F_2$  folds. Axial surfaces

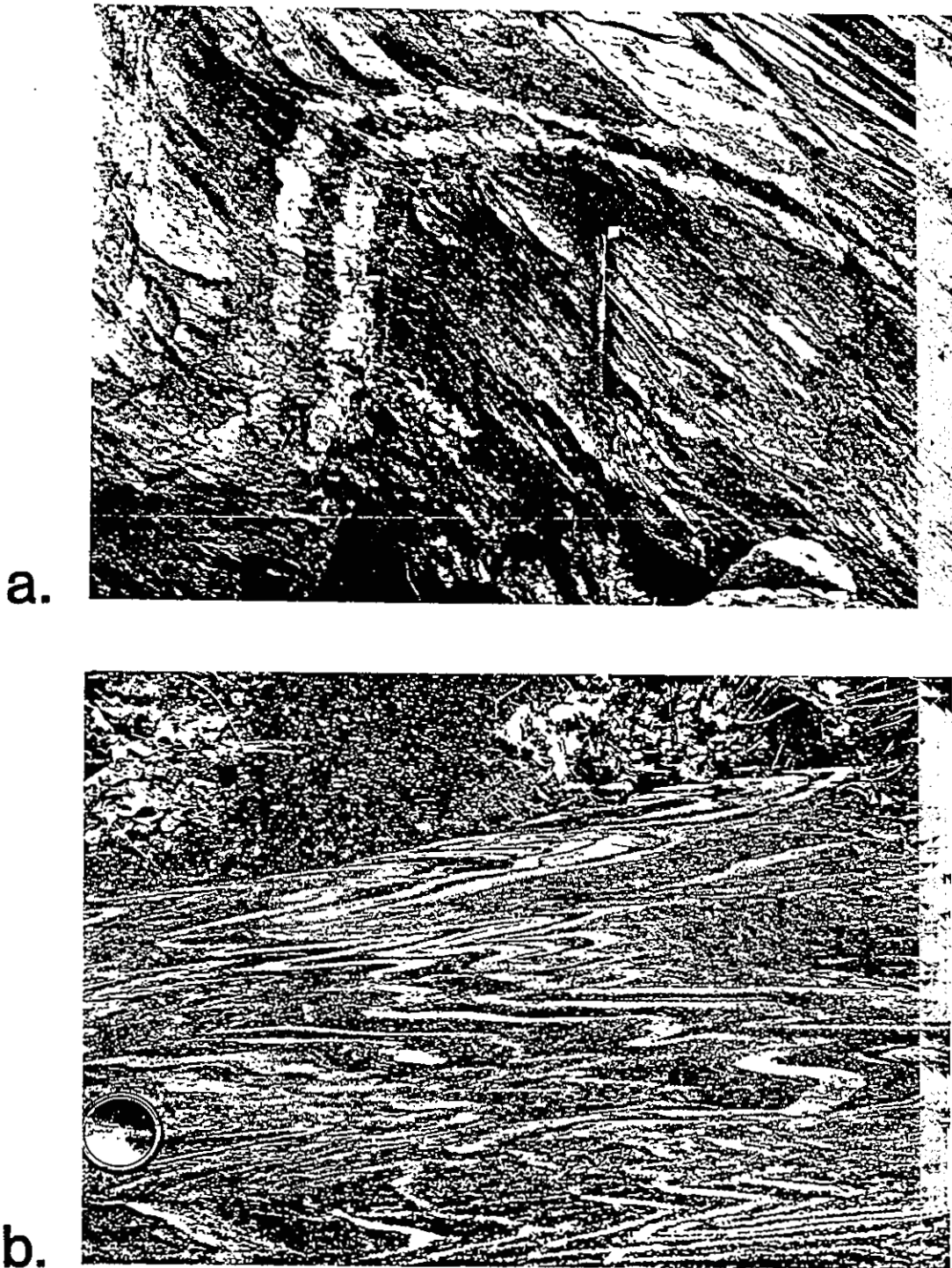


Figure 5.5. Photographs of F<sub>2</sub> folds. a. Photograph of open F<sub>2</sub> antiform with well developed axial plane cleavage from the Piedra Lumbre Formation. b. Photograph of tight, disharmonic F<sub>2</sub> folds in the Piedra Lumbre Formation.

are generally reclined to the north, with dips southerly from  $40^{\circ}$  to  $80^{\circ}$ . Commonly, at the outcrop scale,  $F_2$  folds are identified only by the occurrence of a strong  $S_3$  cleavage that transects both limbs of the fold. These  $F_2$  folds correspond to the  $F_2$  structures described by Nielsen and Scott (1979) and Holcombe and Callender (1982).

### Third Generation of Structures, $D_3$

The  $S_2^*$  cleavage is the dominant cleavage in nearly all rocks of the Ortega Group. Most schistose rocks break along the  $S_2^*$  surfaces.  $S_2^*$  is generally oriented within  $20^{\circ}$  of compositional layering. In schists,  $S_2^*$  is well-developed, and is commonly the youngest visible cleavage. In more quartzose rocks  $S_2^*$  may be a crenulation cleavage. Rarely, quartz-mica schists preserve an intermediate stage of cleavage formation, in which an  $S_2$  schistosity has been microfolded and differentiated into mica-rich and quartz-rich zones of an  $S_2^*$  crenulation (Fig. 5.6).  $S_2^*$  is defined by aligned muscovite, biotite, opaque minerals, tourmaline, and flattened quartz grains. This  $S_2^*$  corresponds to the  $S_2$  of Nielsen and Scott (1979) and Holcombe and Callender (1982).

$L_2^*$  is a moderately well-developed extension lineation in some schists, defined primarily by aligned biotite and/or



Figure 5.6. Photomicrograph of vertically spaced  $S_2^*$  which has crenulated an earlier oblique  $S_2(?)$  cleavage.

tourmaline grains (Fig. 5.7a).  $L_2^*$  is the dominant intersection lineation in most rocks, and is generally parallel to the hinges of  $F_2^*$  folds within any local area.  $L_2^*$  is most evident as compositional bands on  $S_2^*$  cleavage surfaces in thinly layered schists (Fig. 5.7b). The  $L_2^*$  and  $L_2^*$  lineations correspond to the  $L_2$  of Nielsen and Scott (1979) and the  $L_{20}$  of Holcombe and Callender (1982).

$F_2^*$  folds are rare. In some cases, at the outcrop scale, where the fold contains an axial plane schistosity but lacks the "transecting"  $S_2^*$  cleavage,  $F_2$  and  $F_2^*$  folds cannot be told apart. Locally, on the overturned limb of the Hondo syncline, north of Warm Springs, it appears that  $F_2^*$  folds have overprinted  $F_2$  structures (Plate 1). These  $F_2^*$  folds do not correspond to any fold generation described by Nielsen and Scott (1979) and Holcombe and Callender (1982).

#### Later Generations of Structures

At least two generations of non-penetrative (on an outcrop scale) structures post-date  $D_3$  structures in the region. Strain accumulation associated with these structures appears to be minor. The major late structure appears as local, weak, cross-cutting crenulations in some schists (Fig. 5.8). Associated with these are intersection

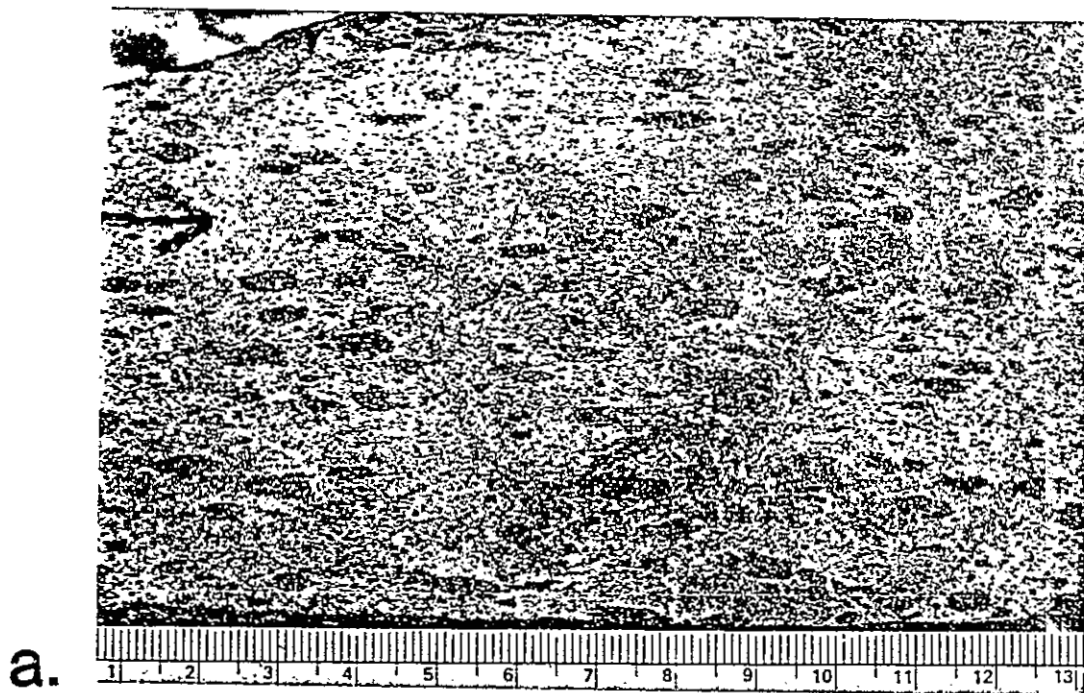


Figure 5.7. Photographs of second generation lineations in the Ortega Group. a.  $L_2^*$  biotite extension lineation on  $S_2$ . Scale bar is in cm. b.  $L_2^*$  intersection lineation on  $S_2$  surface.

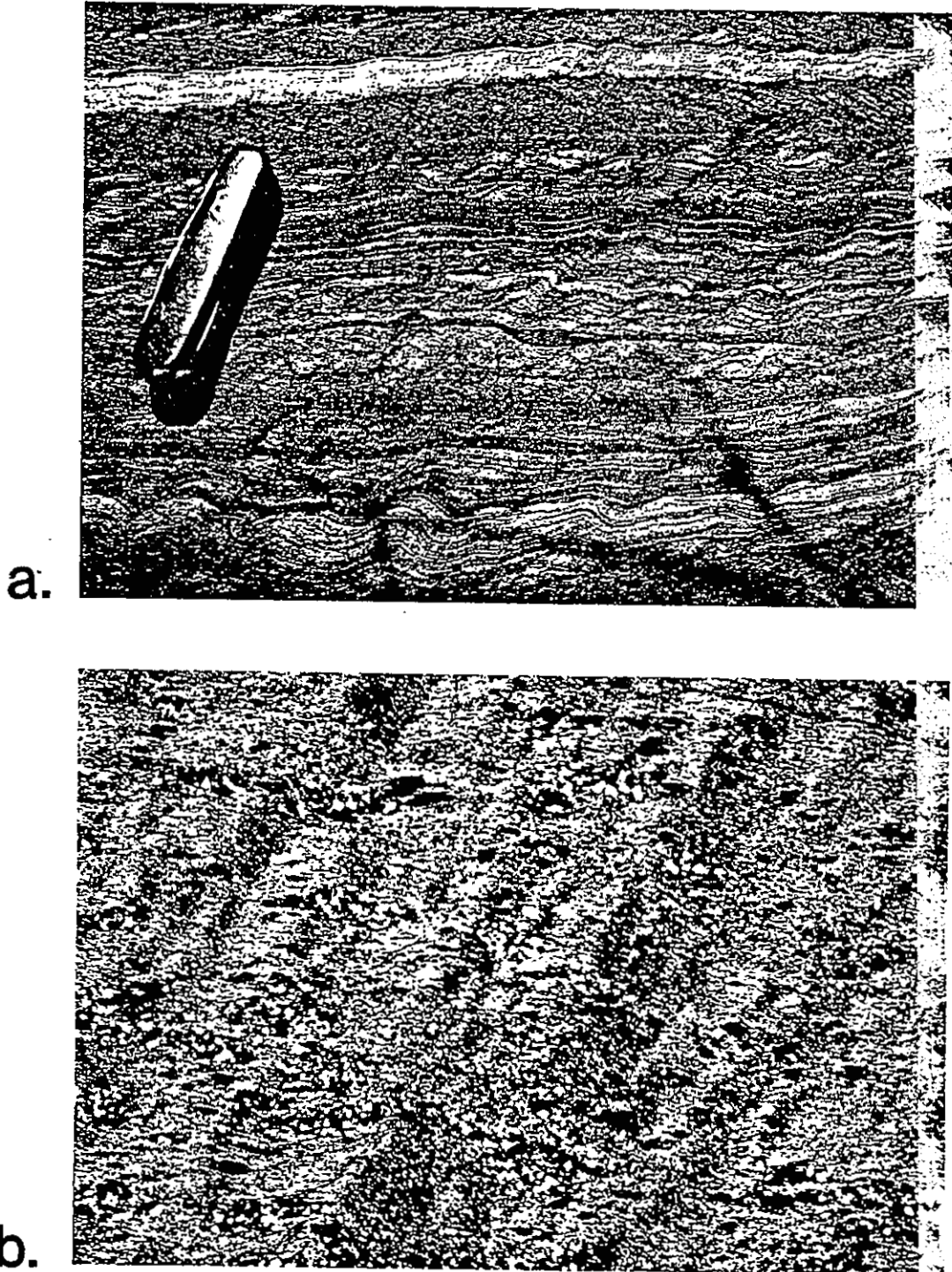


Figure 5.8. a. Photograph of S<sub>3</sub> crenulation cleavage in Piedra Lumbre schist. b. Photomicrograph of S<sub>3</sub> crenulation cleavage in Rinconada schist. Field of view is 8 mm.

lineations and very open folds. In a regional sense, these features trend north-south, approximately perpendicular to the earlier structures. These structures correspond to the  $S_3$ ,  $L_3$ , and  $F_3$  structures of Nielsen and Scott (1979), and the  $S_3$ ,  $L_{30}$ , and  $F_3$  structures of Holcombe and Callender (1982). Within the map area, none of the fourth generation ductile offset features of Nielsen and Scott (1979) were recognized.

## CHAPTER 6. METAMORPHISM

### Introduction and Previous Work

Although the metamorphism of rocks in the Picuris Range has never been rigorously examined, all previous studies have agreed that Ortega and Vadito group rocks have been regionally metamorphosed to middle amphibolite facies. Metamorphic index minerals are abundant throughout both groups, and all three aluminum silicate polymorphs are found in rocks of the Ortega Group.

Montgomery (1953) described a metamorphic history of medium- to high-grade dynamo-thermal regional metamorphism, widespread hydrothermal metamorphism, and retrograde metamorphism. In the Ortega Group, Montgomery traced isograds separating sillimanite, kyanite, and staurolite zones. These isograds were coincident with lithologic contacts.

Nielsen (1972) related intensity of metamorphism to timing of deformational events. He found that prograde regional metamorphism peaked between the F2 and F3 deformations, and that a regressive peak occurred after the F4 event.

Holdaway (1978) performed a metamorphic study of Ortega Group rocks. He described  $\text{Al}_2\text{SiO}_5$  triple point conditions,

and documented key assemblages of chloritoid + kyanite, andalusite + sillimanite, chloritoid + staurolite, and kyanite + andalusite. Based on these assemblages, he concluded that metamorphism had peaked at about 530°C, 3.7 kb in the Picuris Range.

Long (1976) reported on conditions of metamorphism of Vadito Group rocks in amphibolites, pelitic schists, and calc-silicates. Various mineral assemblages permitted him to deduce upper temperature and pressure limits of about 600°C and 3.7 kb. Long also developed a model for the P-T path with respect to the deformational history. In this model, temperature increased at about 40°C per kb of pressure, towards the aluminum silicate triple point (Holdaway, 1971), until achieving peak conditions between the F2 and F3 deformational events of Nielsen (1972). Following the metamorphic peak, several highly conjectural retrogressive stages of the P-T path were proposed by Long (1976), in which P and T varied considerably on a small scale during an overall isothermal pressure decrease.

McCarty (1983) also examined metamorphism in Vadito Group rocks. She concluded that P and T increased during F1 and F2 deformations, until peaking during or after F2 with the growth of biotite, andalusite, and cordierite(?) porphyroblasts. Peak temperature was between 525°C and 600°C, and peak pressure was 3.7 kb. These estimates are compatible with Holdaway's (1978) estimates in the Ortega

Group. McCarty noted that because andalusite may not be pure  $\text{Al}_2\text{SiO}_5$ , triple point pressures may be slightly above 3.7 kb. Peak conditions were followed by retrogression and alteration of andalusite to muscovite, cordierite to muscovite+chlorite, and growth of garnet and staurolite porphyroblasts. After garnet growth, further retrogression resulted in alteration of biotite to chlorite.

Grambling and Williams (1985a) investigated aluminum silicate phase relations in Precambrian rocks of north-central New Mexico. In the Picuris Range, they found that kyanite-andalusite-sillimanite assemblages in the Copper Hill region preserve conditions of  $3.8 \pm 0.5$  kb and  $505 \pm 3^\circ\text{C}$ .

All of these P-T estimates for the Ortega and Vadito rocks suggest that both groups were metamorphosed to near triple point conditions after the time of major folding in the Picuris Range.

Peak P-T conditions and the various mineral assemblages in Precambrian rocks in the Picuris Range are well established, so rather than repeat previous work on assemblages and possible metamorphic reactions, the following sections of this chapter will emphasize the distribution of aluminum silicate polymorphs, the timing of mineral growth with respect to fabric development in the Ortega Group, and possible P-T paths for these rocks.

Relative timing criteria between porphyroblasts and

matrix are based mainly on those described by Vernon (1978), Olsen (1978), T.H. Bell (1985), and Bell et al. (1986), Bell and Rubenach (1983), Wilson (1971), Williams and Schoreveld (1981), Zwart (1962), and Spry (1969).

## Metamorphic Mineral Assemblages

### Aluminum Silicate Minerals

General. Kyanite, andalusite, and sillimanite are common minerals in quartzites and schists of the Ortega Quartzite and Rinconada formations. In many rocks two of these polymorphs appear to stably coexist. Near Copper Mountain (M.L. Williams, personal communication, 1987) and in a few locations in the northwestern map area, all three may stably coexist. Holdaway (1978) also noted that all three coexist in the Hondo syncline area. The occurrence of these minerals seems to be a function of both lithology and variations in P-T topology.

Kyanite. Kyanite is a common mineral in the Ortega Quartzite and Rinconada formations. Along the northern exposure of Ortega Quartzite, kyanite generally either coexists with sillimanite, or occurs alone in quartzites and aluminous schist layers within quartzite. Less commonly,

kyanite coexists with andalusite, and in one locality in the map area, kyanite coexists with andalusite and sillimanite. Along the southern exposure of Ortega Quartzite Formation, kyanite either coexists with andalusite, or is found alone in quartzites. Where kyanite is found in quartzites and schists of the Rinconada Formation in the central map area, it occurs either alone, or coexisting with andalusite.

Kyanite grains are generally elongate subhedral blades or euhedral prismatic crystals. Grains range in length from less than 0.5 mm to greater than 15 mm. Inclusions in kyanite are generally not abundant. Some grains have been partly altered to sericite or pyrophyllite.

Kyanite grains are typically aligned in the dominant foliation in the rock. Typically, in quartzites, kyanite-rich layers are parallel and spaced between quartz-rich matrix. In schistose quartzites, foliations wrap around isolated kyanite grains. Nearly all kyanites show domainal and/or undulatory extinction (Fig. 6.1). In many rocks, kyanite grains define a strong, down-dip extension lineation. In other rocks, kyanites have overgrown and preserved preexisting foliations defined by small aligned inclusions of iron-oxide.

The evidence suggests that most, if not all, kyanite growth occurred prior to or during formation of the dominant cleavage ( $S_2^*$ ) in these rocks. Kyanite growth may have coincided with the  $D_1$  strain that produced a strong down-dip

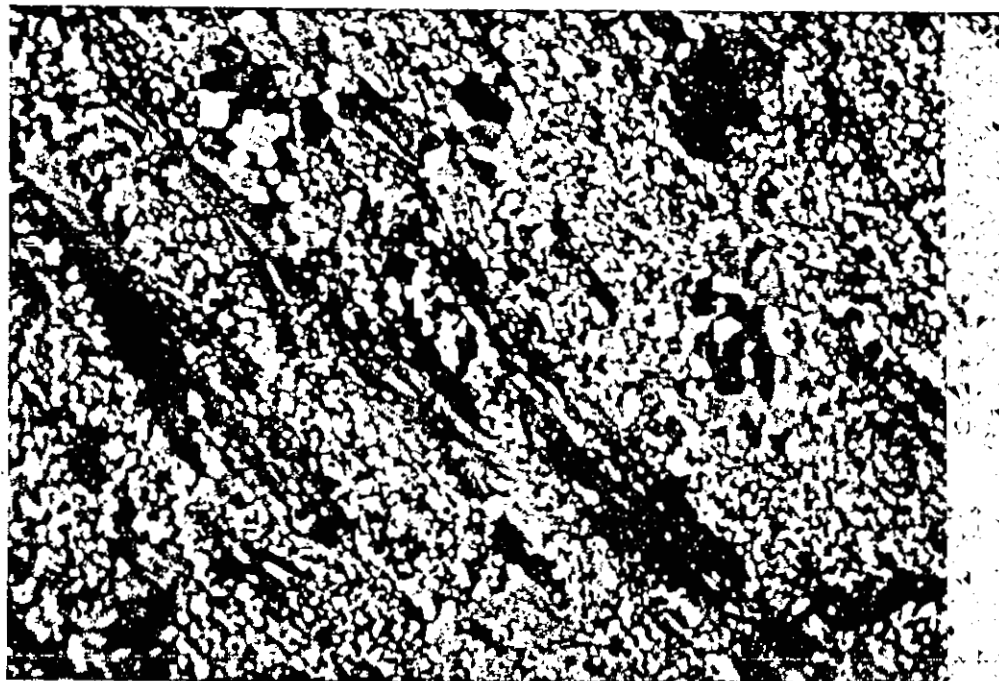


Figure 6.1. Photomicrograph of strained kyanite blades aligned in  $S_1$  and  $L_1$ . Section is cut parallel to  $L_1$  and perpendicular to  $S_1$ . Field of view is 10 mm.

extension. Kyanite appears to have remained stable (or persisted metastably) during most of the subsequent metamorphic/tectonic history of the rocks.

Andalusite. Large porphyroblasts of andalusite are found in many of the schistose units of the Rinconada and Ortega Quartzite formations. In particular, andalusite is abundant in the R1/R2 schist that lies just above the Ortega Quartzite Formation. Andalusite occurs in the northern and southern bands of Rinconada Formation, and local pelitic Vadito schist beds in the southern map area. Andalusite is the only common aluminum silicate mineral in Vadito Group rocks. Montgomery (1953) mentioned coexisting andalusite and sillimanite in an unlocated area in Vadito rocks of the southern Picuris Range.

Typically, in schists, andalusite porphyroblasts are dark, vaguely rounded, poikiloblastic knobs that can be up to 8 cm in diameter. Rounded quartz inclusions are invariably abundant within andalusites. Commonly, these inclusions are prolate, and are aligned in a relict foliation. Other common included minerals are biotite, muscovite, iron-oxide mineral, and garnet. Most commonly, andalusite is accompanied by kyanite. No rocks containing andalusite and sillimanite without kyanite have been found. Alteration of andalusite is rare.

Andalusite porphyroblasts generally have equant shapes,

and are therefore not aligned or flattened in the dominant foliation. The schistose matrix of most rocks warps around andalusites. Well-defined inclusion trails of elongate quartz typically are continuous with the surrounding matrix foliation,  $S_2^*$ . In one rock, this included relict foliation appears to have been a crenulation cleavage. Andalusite has therefore trapped an intermediate stage of  $S_2^*$  development. Other andalusites contain relict folds ( $F_1$  or  $F_2?$ ) defined by quartz inclusions or opaque minerals. Most andalusites are optically continuous in spite of their sponge-like textures. In most rocks where andalusite and kyanite coexist, relative timing relationships between the two are ambiguous.

Andalusite has overgrown an early foliation ( $S_1$  or  $S_2?$ ), and coincides with development of the dominant  $S_2^*$  foliation in schists.

Sillimanite. The occurrence of sillimanite is more restricted than that of either kyanite or andalusite. In the map area, sillimanite is found only in the northern exposure of Ortega Quartzite Formation. Within these rocks it has grown in both quartzite and aluminous schist. Grambling and Williams (1985a) also reported sillimanite occurrences in the Ortega Group east of Copper Hill and near the town of Pilar.

Sillimanite occurs as both fibrolitic aggregates of

radiating acicular crystals and strongly lineated fibrolitic bundles (Fig. 6.2). Aggregates range in size from 1.0 to 3.0 mm, whereas individual crystals are generally less than 0.4 mm long. The cores of these bundles are pure, coarse fibrolite, whereas the rims contain only minor amounts of long, needle-like fibrolite. Sillimanite occurs either as the lone aluminum silicate polymorph, or with kyanite, although one thin section from the northwestern map area contains all three polymorphs. In some thin sections, where sillimanite coexists with kyanite, sillimanite needles extend across kyanite grain boundaries, whereas in other thin sections where they coexist, sillimanite grains do not cross kyanite grain boundaries. Sillimanite and andalusite without kyanite are not found in the map area. In some rocks, sillimanite is replaced by fine, fibrous grains presumed to be pyrophyllite.

Although some sillimanite bundles are randomly oriented, most show a slight flattening in the plane of the dominant  $S_2^*$  foliation. Within and around sillimanite aggregates, sillimanite crystals invariably cross quartz grain boundaries. Many sillimanite crystals show some amount of internal strain through undulatory extinction.

Some well-lineated samples of Ortega Quartzite show a strong alignment of sillimanite grains in the  $L_1$  extension direction. These grains are interpreted to have grown pre- to syn- $D_1$ .

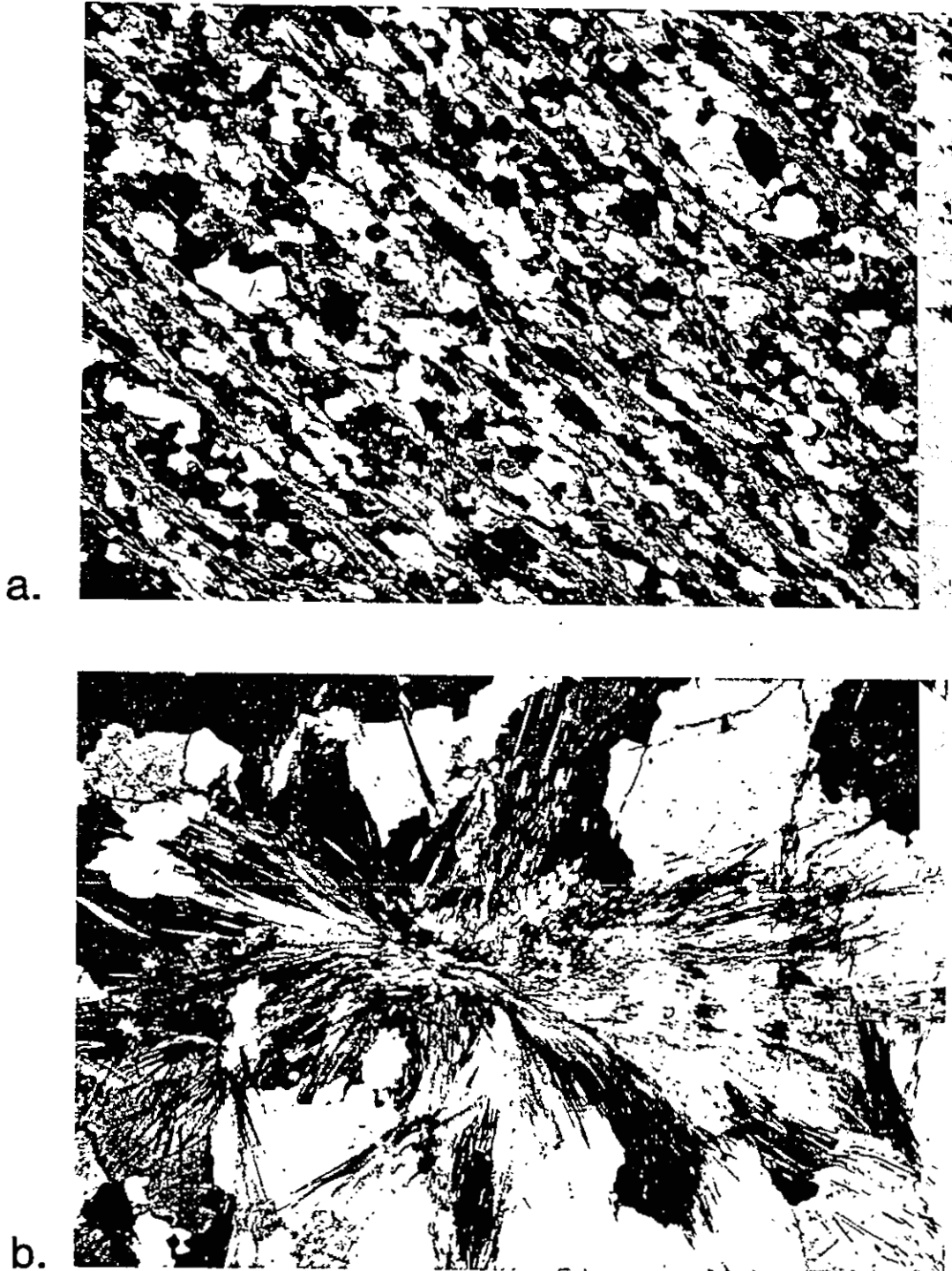


Figure 6.2. a. Photomicrograph of fibrolitic sillimanite aggregates strongly aligned in  $L_1$ , from Ortega Quartzite, northern Picuris Range. Section is cut parallel to  $L_1$  and perpendicular to  $S_1$ . Field of view is 14 mm. b. Photomicrograph of fibrolitic sillimanite bundles in Ortega Quartzite. Field of view is 3.4 mm.

It appears that sillimanite has grown in the Ortega Quartzite throughout much of the deformational history. However, because the  $D_1$  strain is heterogeneous, absolute timing relationships are uncertain. Vernon (1987) noted that if sillimanite aggregates grow in regions of low strain (e.g. quartz-rich rock), then their growth is not related to strain in terms of the bulk heterogeneous shortening model of Bell (1981). Random bundles do not necessarily imply post-deformational growth on scales larger than a thin section. Therefore, in these quartzites, sillimanite may be pre- or syn-kinematic with respect to  $D_3$ , but may remain unstrained due to the heterogeneity of strain. Alternatively, if  $D_1$  structures developed throughout much of the early deformational history, the lineated sillimanite could have grown at almost any time. Although timing relationships remain unclear, sillimanite was probably stable over much of the deformational history.

Discussion. There appears to be a difference in the occurrence of aluminum silicate phases in the northern and southern exposures of Ortega Quartzite Formation in the map area. Stratigraphy and lithologies are identical across the northern and southern limbs of the Hondo syncline. On the southern limb, kyanite coexists with andalusite. On the northern limb, kyanite coexists with sillimanite, and locally with both sillimanite and andalusite. Grambling and

Williams (1985a) suggested that these variations correspond to variations in elevation across an area containing sub-horizontal isograds, with kyanite occurring at the highest elevations, andalusite (+ kyanite) at intermediate elevations, and sillimanite ( $\pm$  kyanite and andalusite) at the lowest elevations.

Andalusite, kyanite, and probably sillimanite are pre-kinematic with respect to the dominant  $S_2^*$  foliation in most rocks. Kyanite grains are generally aligned in a first generation extension lineation ( $L_1$ ), and exhibit undulose extinction. Andalusite typically has overgrown and preserved an early foliation ( $S_2?$ ). Based on these relationships, kyanite is interpreted as having grown syn-kinematically with respect to  $D_1$ , and andalusite has grown late syn-kinematically or post-kinematically with respect to  $D_2$ .

In strongly lineated Ortega Quartzite, sillimanite appears to have grown pre- to syn- $D_1$ . In other samples, sillimanite appears to have grown syn- to post- $D_3$ . Because  $D_1$  structures probably developed at different times in different areas, the absolute timing of mineral growths outside of small areas is uncertain.

In the map area, kyanite grew during shearing of the Ortega Quartzite and Rinconada formations. Although folding of the Hondo syncline may have post-dated kyanite growth, the present large-scale variations in aluminum silicate

distribution across the axis of the Hondo syncline are probably due to variations in elevation of rocks on the two limbs. Sillimanite is exposed in the deeper rocks at lower elevations on the northern limb, whereas kyanite is exposed in the shallow rocks at higher elevations on the southern limb.

### Other Metamorphic Minerals

General. Schists and quartzites of the Ortega Group contain a large variety of shapes and sizes of many different mineral phases. This section will concentrate on relationships between tectonite fabrics and porphyroblastic phases found within the map area. Common metamorphic mineral assemblages found in Ortega Group rocks are given in Figure 6.3.

Biotite. Biotite is common in schistose rocks throughout the range. Most Piedra Lumbre and Rinconada formation schists contain 10 to 15 percent biotite. Grain sizes range from about 0.1 mm to more than 5.0 mm, with an average size of about 0.6 mm. Most biotites are blocky, euhedral to subhedral, and do not contain significant amounts of inclusions. Commonly, biotite grains cut across boundaries between other minerals. Locally, chlorite is intergrown with biotite.

	QUARTZ	MUSCOVITE	CHLORITE	BIOTITE	GARNET	STAUROLITE	CORDIERITE	CHLORITOID	PLAGIOCLASE	KYANITE	ANDALUSITE	SILLIMANITE	FE-OXIDE	TOURMALINE	OTHER
PIEDRA LUMBRE	●	●	●	●	●	●							●	●	
	●	●	●	●	●				●				●		calcite
	●	●		●				●					●		calcite
	●	●	●	●	●										trem.-zols.-cc- ksparsphene
PILAR PHYLLITE	●	●		●			●						●		carbonaceous material
	●	●		●									●		
R6	●	●		●	●	●							●		
	●	●			●	●				●			●		
	●	●		●	●								●		
R5	●	●		●									●		
	●	●		●									●	●	
	●	●		●		●				●			●		
R4	●	●		●	●	●							●		
R3	●	●				●				●	●		●	●	
	●	●	●	●											
	●	●	●										●		
R1/2	●	●		●							●		●		
	●	●	●		●			●		●		●	●		
	●	●		●					●				●		
	●	●		●	●	●			●				●		
ORTEGA QUARTZITE	●	●								●		●	●		
	●	●								●	●		●		
	●	●				●						●	●		
	●	●								●			●		
	●	●					●			●		●	●		
	●	●			●	●							●		
	●	●		●				●	●				●		

Figure 6.3. Common metamorphic mineral assemblages found in rocks of the Ortega Group.

From sample to sample, there is considerable range in the orientation of biotite grains with respect to strain fabrics. This probably reflects multiple stages of biotite growth during the deformational history. Several thin sections display two generations of biotite growth distinguished by orientation and grain size. Typically, large biotite porphyroblasts are flattened in the dominant  $S_2^*$  foliation. These grains tend to show undulose extinction, have strong quartz-rich pressure shadows at both ends, and lie within the anastomosing  $S_2^*$  foliation. Numerous small, elongate biotite crystals in the matrix are generally aligned obliquely to  $S_2^*$ . The timing of these small grains with respect to the larger grains is uncertain. In one sample of Piedra Lumbre Formation schist (HC-62), biotite porphyroblasts in fine-grained micaceous matrix have been flattened and sheared (Fig. 6.4). In another highly folded Piedra Lumbre sample, a biotite-rich compositional layer has been folded around a strong  $S_2^*$ (?) axial plane cleavage. Biotite grains in this layer are spaced and aligned in the cleavage.

At least one period of biotite growth was pre-kinematic with respect to  $S_2^*$ . Large biotite grains are aligned within an anastomosing  $S_2^*$  cleavage. Some appear to be sheared as well. Other smaller biotites may be either predate or postdate growth of the large pre- to syn- $S_2^*$  biotite grains.

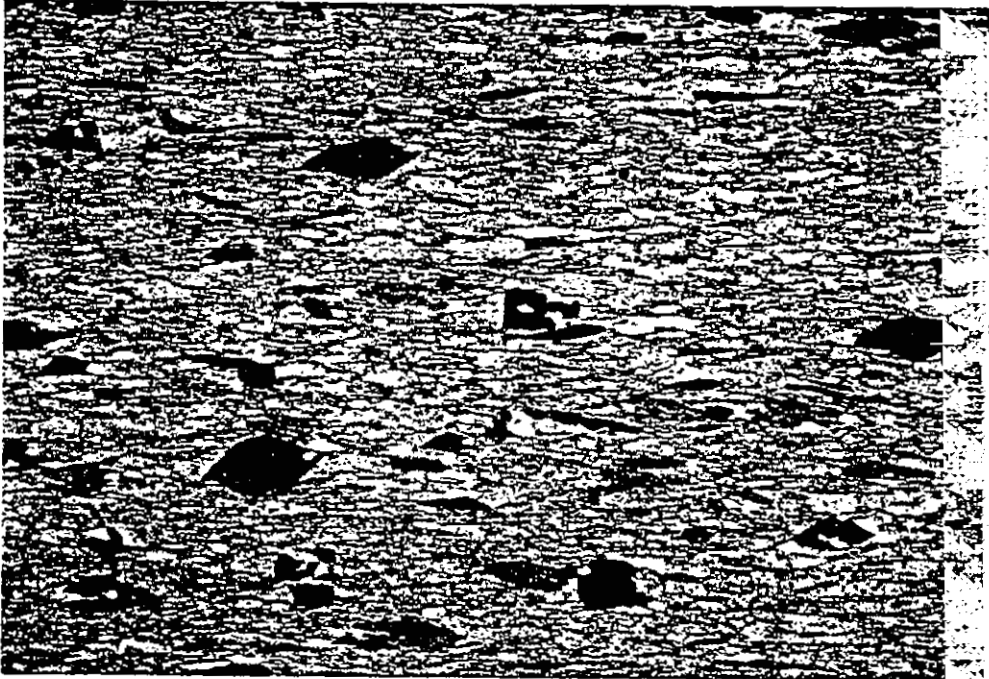


Figure 6.4. Photomicrograph of sheared biotite fish in Piedra Lumbre schist, showing dextral shear. Field of view is 4 mm.

Garnet. Porphyroblasts of garnet are abundant throughout the Picuris Range in schists and some quartzites. Garnets are especially well developed in schists of the Piedra Lumbre Formation and the R6 member of the Rinconada Formation. Several horizons in the Piedra Lumbre Formation contain thin layers of schist that are up to 60 percent garnet porphyroblasts.

Garnet crystals range in size from less than 1.0 mm to more than 4.0 mm. Although most garnets are euhedral, some grains, especially in quartzites, are sub- to anhedral. In general, garnets from Ortega Group rocks in the map area tend to be relatively inclusion-free. Typically, garnets that do contain inclusions tend to have relatively inclusion-rich cores and inclusion-free rims. Quartz is the most abundant inclusion. Other included minerals are biotite, chlorite, and zoisite. Alteration of garnet is uncommon. In garnet-staurolite schists, garnets are commonly found within the larger staurolites.

In schists, the dominant foliation ( $S_2^*$ ) is generally warped around the equant garnet porphyroblasts. Rarely, quartz inclusion trails within garnets show complex microstructures. In the cores of garnets, inclusions define a relict foliation that is oriented at a high angle to the foliation in the matrix. In some samples, the core foliation is bent into a rim orientation that merges with the matrix foliation (Fig. 6.5). These inclusion

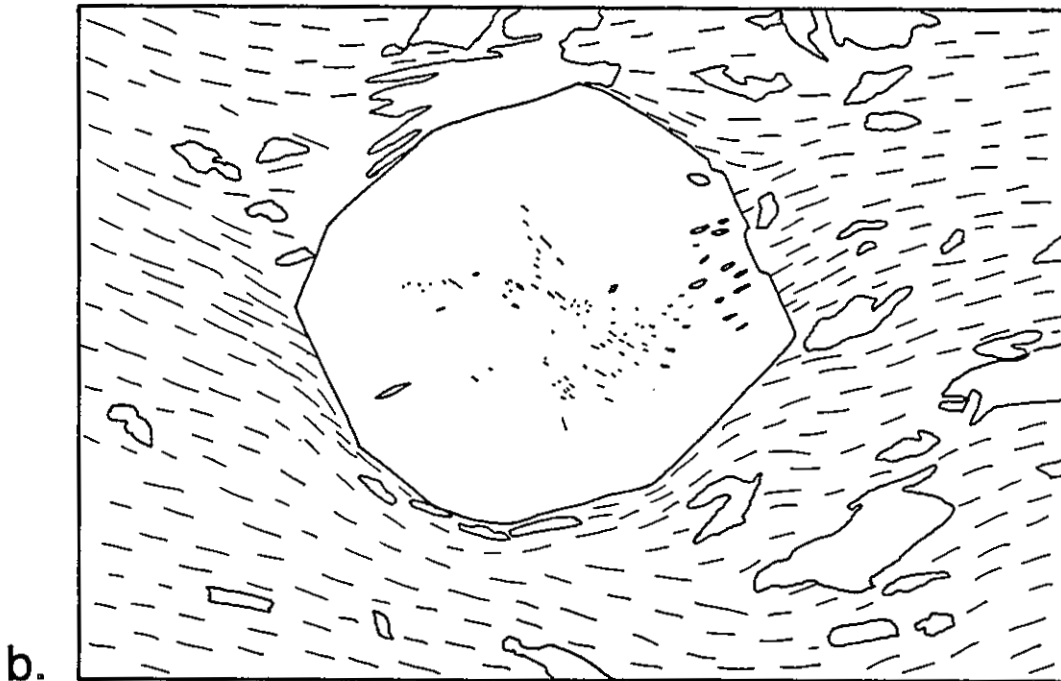


Figure 6.5 a. Photomicrograph of garnet porphyroblast containing different orientations of quartz inclusions in core and rim. Section is cut normal to  $L_1$ . Field of view is 3.4 mm. b. Sketch.

microstructures are more suggestive of non-rotational inclusion patterns (T.H. Bell, 1981, 1985; Bell and Rubenach, 1983; Bell et al., 1986) than the garnet porphyroblast rotation patterns described by Rosenfeld (1968, 1970), Schoneveld (1977), and Powell and Vernon (1979).

An unusual, relatively uncommon garnet microstructure is shown in Figure 6.6. A garnet core containing a relict foliation oriented normal to the matrix foliation is bracketed on two sides by a secondary garnet growth in which the relict foliation is at right angles to the core foliation. This secondary growth foliation is parallel to, and merges with the matrix foliation. This type of porphyroblast structure has been described by Bell (1931) as indicative of a deformational history involving bulk, inhomogeneous shortening.

Most garnet porphyroblasts appear to be at least as old as pre- to syn-D3, but due to their equant shapes, and the general scarcity of good internal microstructures, relative ages of growth remain uncertain. Locally, there is evidence for two stages of garnet porphyroblast growth. The first stage preserved a second(?) generation foliation, whereas the second stage preserved a third generation foliation.

Staurolite. Staurolites are abundant in schists of the Piedra Lumbre and Rinconada formations. They occur



Figure 6.6. Photomicrograph of garnet porphyroblast containing symmetrical secondary growths.  $S_2^*$  in matrix is horizontal. Garnet core contains "millipede" microstructures defined by quartz inclusion trails. Section is cut normal to  $L_1$ . Field of view is 4 mm.

throughout the Picuris Range and form the most spectacular porphyroblasts and porphyroblast microstructures of any mineral. Smaller, less spectacular crystals occur in quartzites of the Ortega Quartzite Formation.

Staurolite prisms range in length from less than 1.0 mm to more than 25.0 mm. Superb twinned staurolite crystals including simple twins, compound twins, and right-angle crossed twins are found in the R4 member of the Rinconada Formation in the northern part of the map area. Sector-zoned patterns of inclusions are also common in many of the larger staurolite crystals in the Ortega Group. Commonly, the large poikiloblastic staurolites are concentrically zoned by multiple stages of growth (Fig. 6.7). Between successive growth zones, sizes, densities, and textures of inclusions vary considerably. In general, cores are euhedral, less inclusion-rich, and contain larger inclusions than the sub-to anhedral rims. Quartz and iron-oxide minerals are the most commonly included minerals. Other inclusions consist of smaller amounts of garnet, biotite, and muscovite. Several staurolites appear to have replaced small, euhedral prisms of chloritoid (Fig. 6.8). One sample contains staurolite porphyroblasts that have overgrown a folded fine-grained carbonaceous layer and the coarser-grained quartz-muscovite matrix (HC-457A). Staurolite crystal morphologies are profoundly different for the two growth mediums. In the graphitic layer, staurolites are euhedral, whereas in the

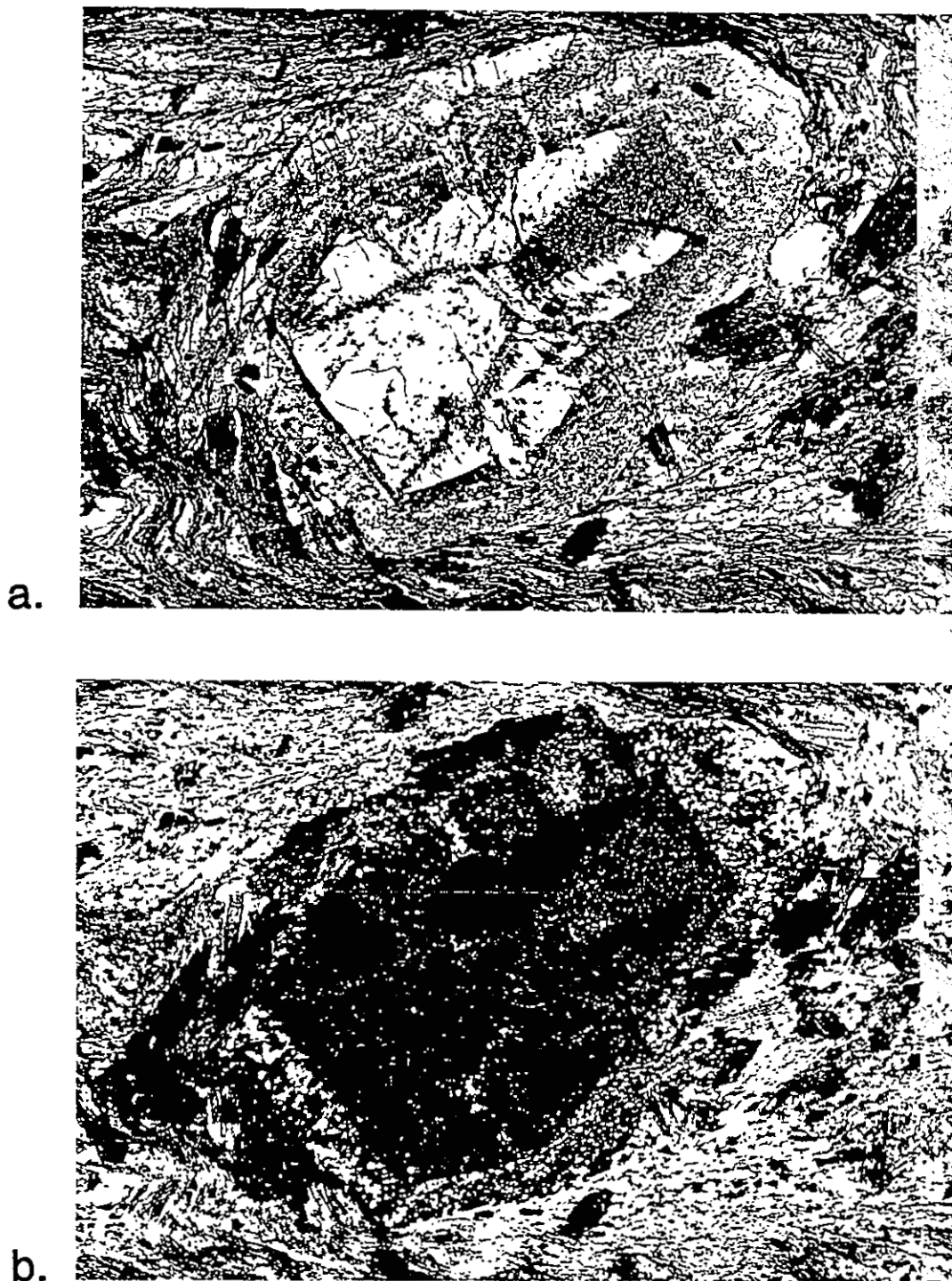


Figure 6.7. Photomicrographs of staurolite porphyroblast with sector-zoned inclusion patterns in euhedral core mantled by secondary subhedral rim. Field of view is 14 mm. a. Plane light. b. Cross polarized light.

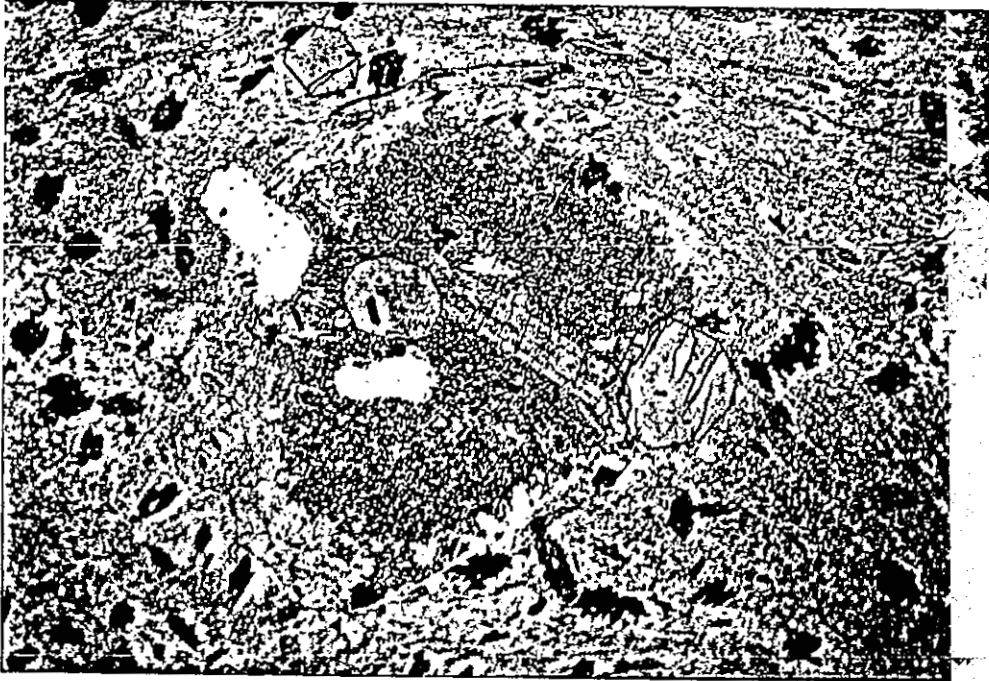


Figure 6.8. Photomicrograph of staurolite after chloritoid, in biotite-staurolite-garnet R4 schist. Field of view is 14 mm.

matrix, staurolites are anhedral. The reason for this is unknown.

Staurolite porphyroblasts exhibit a narrow range of relationships with respect to matrix tectonite fabrics. Most staurolite crystals are generally not aligned in the dominant foliation ( $S_2^*$ ). Matrix foliations generally abut upon the ends of staurolites, and slightly wrap around the sides of staurolites. Relict foliation trails in the cores of staurolite grains merge with trails in the rims of grains. In turn, these rim trails merge with the matrix foliation. Successive orientations of included trails generally lie at high angles to one another.

Staurolites have also been found that contain similar unusual microstructures as described above for the garnets with two-staged growth. A euhedral, zoned staurolite porphyroblast is "bracketed" by symmetrical secondary anhedral staurolite growth in R4 schist (HC-450) (Fig. 6.9). The euhedral part of the staurolite contains an inclusion-free core surrounded by an inclusion-rich rim. Quartz inclusions in the secondary growth define a relict foliation that is nearly perpendicular to the dominant matrix foliation ( $S_2^*$ ). Inclusion trails in the secondary growths define a relict foliation ( $S_i$ ) that is oblique to both the euhedral staurolite rim foliation and  $S_2^*$ . This foliation is truncated by  $S_2^*$  where  $S_2^*$  abuts against the staurolite (Fig. 6.9b). In the strain shadows, where  $S_2^*$  is only

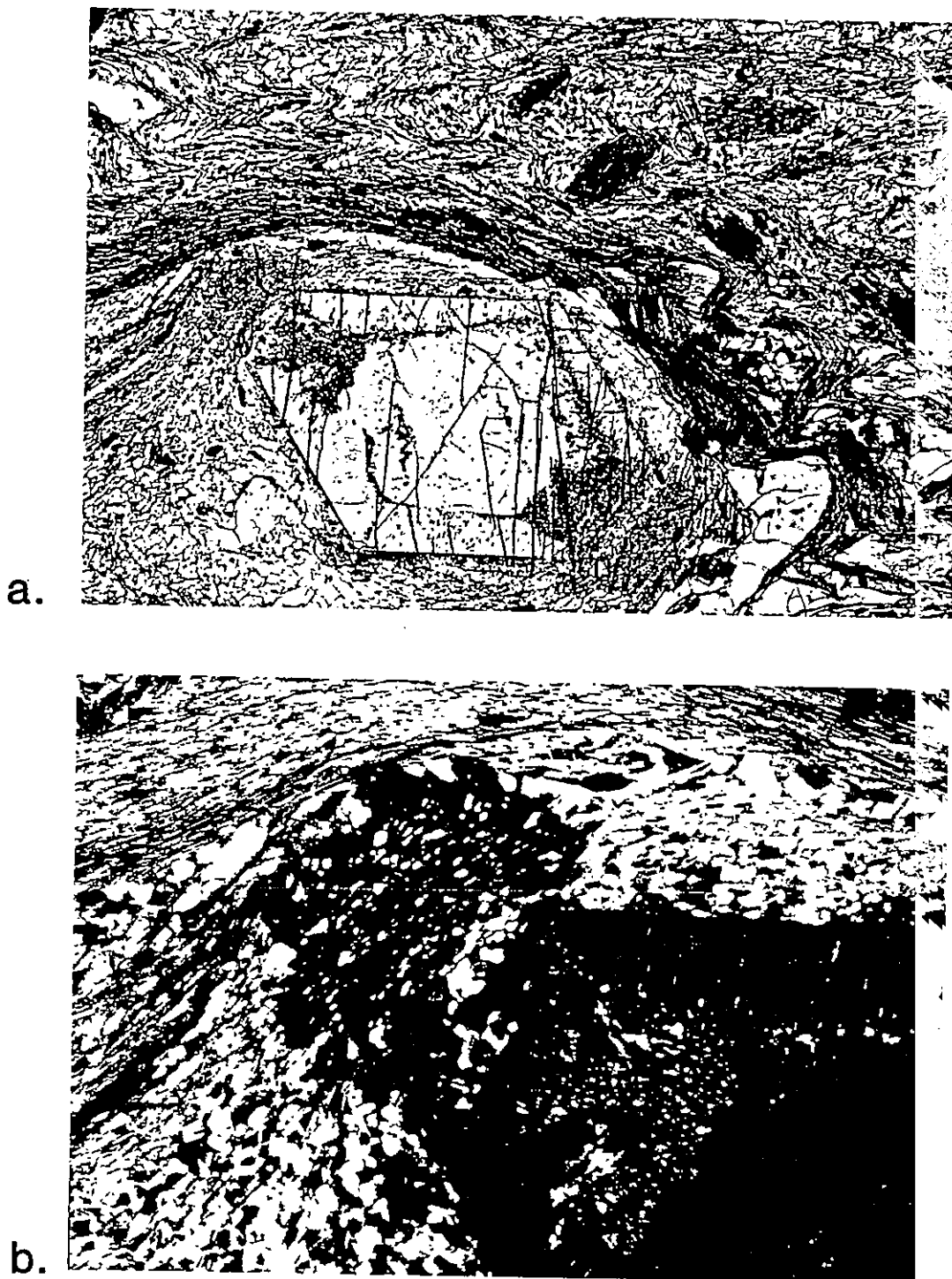


Figure 6.9. a. Photomicrograph of large staurolite with two stages of growth and complex fabric relationships. Field of view is 12 mm. b. Close-up view of left side of staurolite porphyroblast in cross polarized light. See text for discussion. Section is cut normal to  $L_1$ . Field of view is 4 mm.

weakly developed, the secondary growth Si merges with the matrix foliation.

A sample of Piedra Lumbre garnet-staurolite schist in the central map area (HC-64) contains staurolite crystals with an included foliation oriented at about  $30^{\circ}$  from the vertical matrix schistosity (Fig. 6.10). One possible interpretation of this microstructure is of staurolite rotation after overgrowth of the included foliation.

In one schist sample of Rinconada Formation (HC-377), approximately equal sized staurolite and garnet porphyroblasts coexist. Both minerals contain a concentric ring of quartz inclusions at approximately equal distances from the porphyroblast edges (Fig. 6.11). This implies that both porphyroblasts grew together (at same growth rates?), and for some unknown reason incorporated the quartz inclusions during a certain stage of growth.

Several staurolites preserve relics of spaced cleavages. In the staurolites the originally quartz-rich cleavage segregations are now quartz-inclusion-rich, whereas the originally mica-rich cleavage segregations are now quartz-inclusion-poor (Fig. 6.12). In most of these examples, the relict spaced cleavage (stage 4 to 5 of Bell and Rubenach's model of cleavage formation, 1983) is parallel to the dominant  $S_2^*$  schistosity (stage 6 of Bell and Rubenach's model of cleavage formation, 1983) in the rock matrix. These relationships suggest that an earlier,



Figure 6.10. Photomicrograph of staurolite porphyroblast with  $S_1$  at about  $30^\circ$  to  $S_2^*$  in matrix. This geometry may indicate rotation of the porphyroblast. Piedra Lumbre Formation schist. Section is cut normal to  $L_1$ . Field of view is 6 mm.

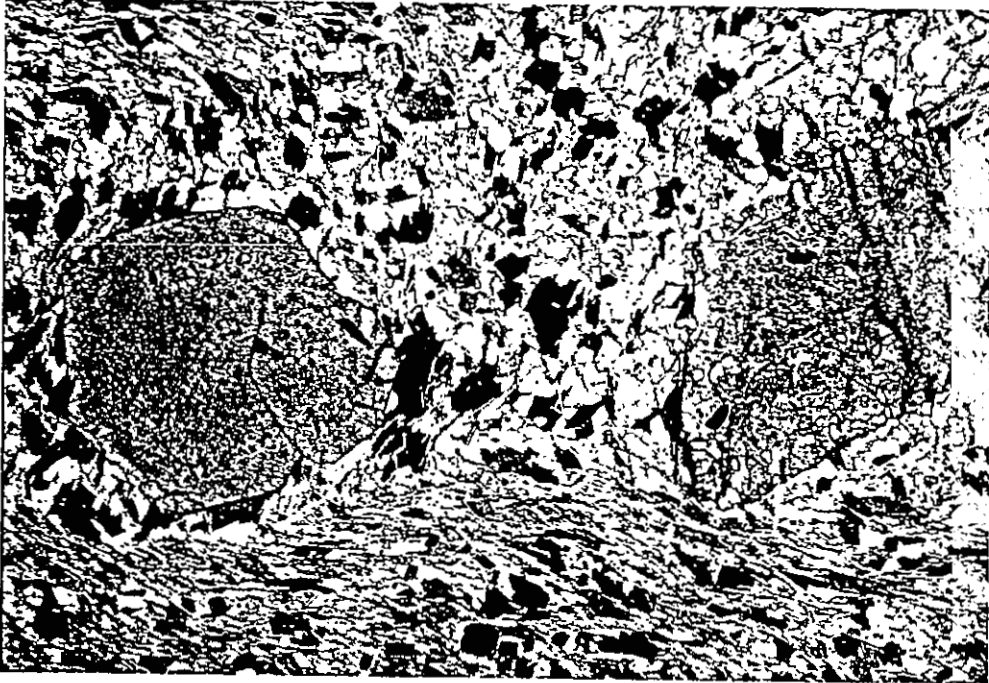


Figure 6.11. Photomicrograph of R6 schist with staurolite and garnet porphyroblasts. Both minerals contain concentric quartz-rich inclusion trails about 0.4 mm from rims. See text for discussion. Section is cut normal to  $L_1$ . Field of view is 6 mm.

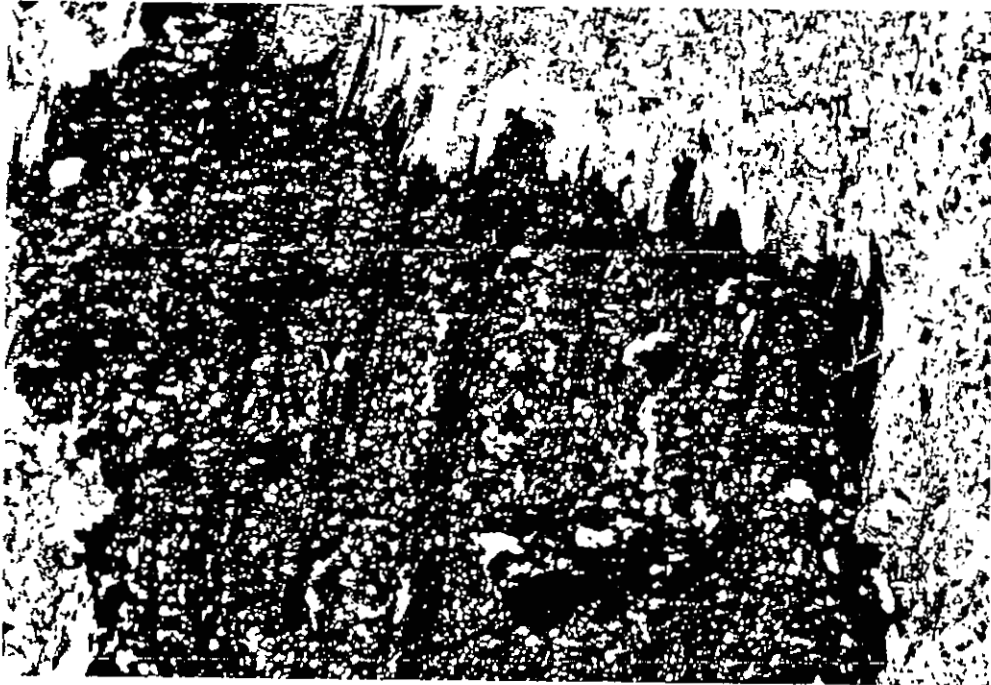


Figure 6.12. Photomicrograph of staurolite at extinction that preserves relict spaced cleavage. Well-developed  $S_2^*$  schistosity in matrix is parallel with  $S_1$ . Note muscovite beard around edge of staurolite. Section is cut normal to  $L_1$ . Field of view is 4.5 mm.

pre-porphyroblast stage of  $S_2^*$  was a differentiated spaced cleavage that has not been reoriented during evolution into a schistosity.

Most staurolite porphyroblasts seem to have grown pre- or syn-D3. Staurolites contain inclusion trails that represent either pre- $S_2^*$  foliations, or intermediate stages of  $S_2^*$  orientation and development. In some rocks, distinct stages of staurolite growth are demonstrated by rims and cores with distinctly different textures. In a few rocks, primary growth of staurolite was followed closely(?) by a secondary staurolite growth. Microstructures in these rocks are similar to structures described by T.H. Bell (1985) and Bell et al. (1986) as indicative of strain partitioning and cleavage reactivation.

Chloritoid. Chloritoid porphyroblasts are uncommon in Ortega Group rocks in the map area. The Piedra Lumbre and the Ortega Quartzite formations contain some chloritoid.

Chloritoid grains range in size from less than 0.1 mm to more than 2.0 mm. In calc-silicate rocks of the Piedra Lumbre Formation, chloritoids are unstrained, poikiloblastic grains with calcite(?) inclusions. In Ortega Quartzite Formation, poikiloblastic chloritoid contains quartz and opaque inclusions. Although the timing of chloritoid growth in these rocks is uncertain, pseudomorphic staurolite has replaced chloritoid in Rinconada Formation rocks.

Cordierite. Small amounts of cordierite are found in the Ortega Quartzite Formation within the map area. Most cordierite grains are anhedral and contain abundant small inclusions. Commonly, these inclusions define a relict foliation that is parallel to that of the matrix. This cordierite is interpreted as having formed syn-D3.

A Vadito schist unit northeast of the Harding Pegmatite Mine contains enormous (up to 15 cm long) subhedral porphyroblasts of cordierite. The dominant schistosity in this rock is bent around these porphyroblasts. In thin section, cordierite is seen to contain complex relict microstructures including either multiple foliations or S-C tectonites (Berthé et al., 1979). In this locality cordierite has grown prior to D3.

Other metamorphic minerals. Plagioclase is common in Vadito Group and felsic schist at Pilar units, and less common in Ortega Group rocks of the Picuris Range. In Ortega Group rocks small, anhedral plagioclase grains preserve a relict foliation, and appear to have grown pre-D3.

Iron-oxide minerals, common in most Ortega Group lithologies, exhibit the entire range of timing relationships with respect to deformational fabrics.

Piemontite crystals occur in the felsic schist at Pilar, and in the southeastern map area near U.S. Hill.

Grains are small, euhedral prisms that are invariably aligned within the dominant foliation. Assuming that this foliation is S<sub>1</sub>, then piemontite is pre- to syn-D<sub>1</sub>.

Summary. Within the map area, the distribution of many pelitic minerals appears to be more related to original sediment composition than lateral variations in P-T topology. Within the map area, 700+ m of local relief is present. Less resistant, porphyroblast-rich pelitic schists tend to occupy topographic lows, whereas more resistant, porphyroblast-poor quartzites and slates tend to occupy topographic highs. Where pelitic schists of the Rinconada and Piedra Lumbre formations do occur at high elevations, biotite, garnet, and staurolite porphyroblasts persist, suggesting that what local relief there is has not affected pelitic mineralogy. Porphyroblasts of biotite, garnet, and staurolite grew repeatedly before and during the D<sub>3</sub> phase of deformation. Other porphyroblasts such as chloritoid, cordierite, and plagioclase may also have grown prior to D<sub>3</sub>. A summary of timing relationships between fabric elements and porphyroblast growth for various rocks of the Ortega Group is given in Figure 6.13. The usefulness of this diagram is limited by two factors. Timing relationships are only useful within a local area, and the development of D<sub>1</sub>-style structures probably overlapped in time with development of D<sub>2</sub> and D<sub>3</sub> structures.

	S1	S2	S2*	S3
KYANITE	—————	---		
ANDALUSITE		-----	---	
SILLIMANITE	—————	-----	-----	---
BIOTITE	-----	-----	-----	---
GARNET	---	-----	-----	---
STAUROLITE		-----	-----	-----
CHLORITOID	-----	---		
CORDIERITE			-----	
PLAGIOCLASE	-----	-----	---	
FE-OXIDES	-----	-----	-----	---
CHLORITE				-----
MUSCOVITE	-----	-----	-----	-----
QUARTZ	-----	-----	-----	-----

Figure 6.13. Summary of timing relationships between fabric elements and porphyroblast growth for rocks in the Crtega Group.

## Garnet-biotite Thermobarometry

Most rocks in the map area show minimal retrograde metamorphic effects. Four porphyroblastic samples from the Ortega Group were selected for quantitative geothermobarometry and P-T path analysis. Chemical analyses were performed by M.L. Williams on the automated electron microprobe in the Geology Department at the University of New Mexico. Samples yielded garnet-biotite temperatures of about 500°C, at pressures of around 4 kb (Table 6.1).

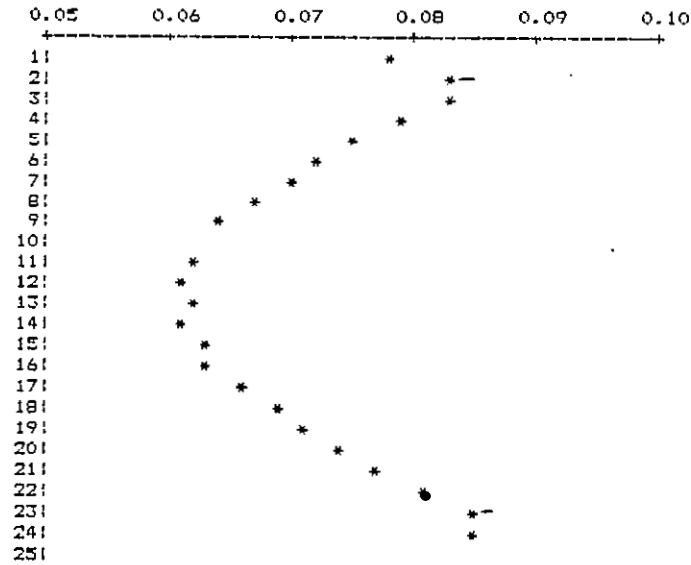
Microprobe traverses across garnet, as shown by the profiles in Figure 6.14, suggest that no significant jumps in P-T conditions have interrupted a continuously changing P-T path. This quantitative finding supports the petrologic observations and interpretations that deformation and metamorphism were continuous, punctuated only by porphyroblast growth rate changes and/or strain rate changes.

<u>Sample</u>	<u>(Fe/Mg)Bi</u>	<u>(Fe/Mg)Gt</u>	<u>K<sub>D</sub></u>	<u>P(Kb)</u>	<u>T(°K)</u>	<u>T(°C)</u>
64	2.86	19.30	0.148	4	777	503
377	3.24	22.21	0.146	4	771	498
385	3.03	19.27	0.157	4	793	520
454	2.46	19.80	0.124	4	729	455

Table 6.1. Garnet-biotite geothermometry results from four samples of garnet-biotite schist in the map area. Calculations are based on those described by Ferry and Spear (1978).

HCCBS AND 64 E TR EACH 24-Nov-86 10:13 PM  
 Garnet Data Set: 1 Trav Length: 1246 Step Length: 51.9

X<sub>Mg</sub> / (X<sub>Mg</sub> + X<sub>Fe</sub>)



HCCBS AND 64 E TR EACH 24-Nov-86 10:13 PM  
 Garnet Data Set: 1 Trav Length: 1246 Step Length: 51.9

Percent Spessartine:

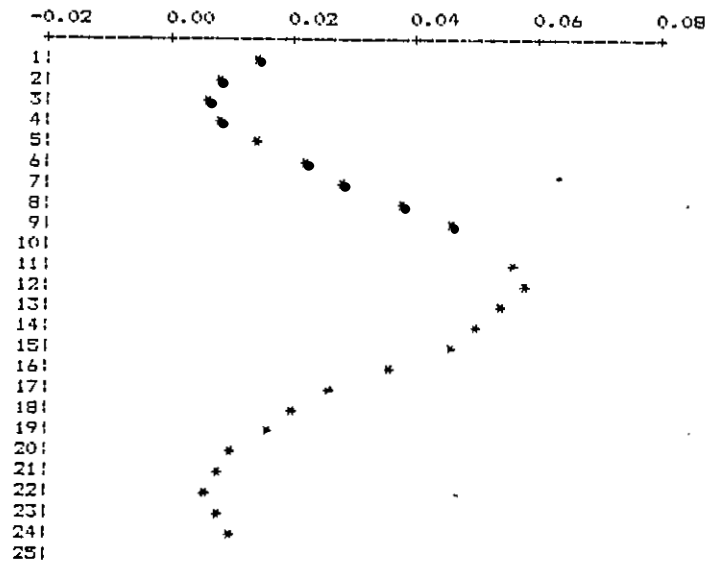


Figure 6.14. Microprobe profiles across porphyroblasts in Ortega Group schists. Data are courtesy of M.L. Williams.

## CHAPTER 7. STRUCTURAL GEOLOGY AND SYNTHESIS

### Introduction

#### General statement

Deformational styles vary considerably within Precambrian rocks of the Picuris Range. These variations occur to some degree within individual lithostratigraphic groups, but more noticeably among rock groups. For this structural synthesis, the Picuris Range has been divided into three domains. These domains are the Ortega Group, which comprises most of the central portion of the Picuris Range; the Vadito Group, which lies to the south of the Ortega Group; and the felsic schist at Pilar, which lies to the north of the Ortega Group (Fig. 7.1). A southern contact separates the Ortega rocks from felsic schist at Pilar rocks, and a northern contact separates Ortega rocks from Vadito rocks.

A domainal approach is essential because lithology, deformational style, and possibly tectonic setting differ among the Ortega, Vadito, and felsic schist sequences, and it is possible that none of the three are related in an original stratigraphic manner. The southern and northern domainal contacts are characterized by ductile shear.

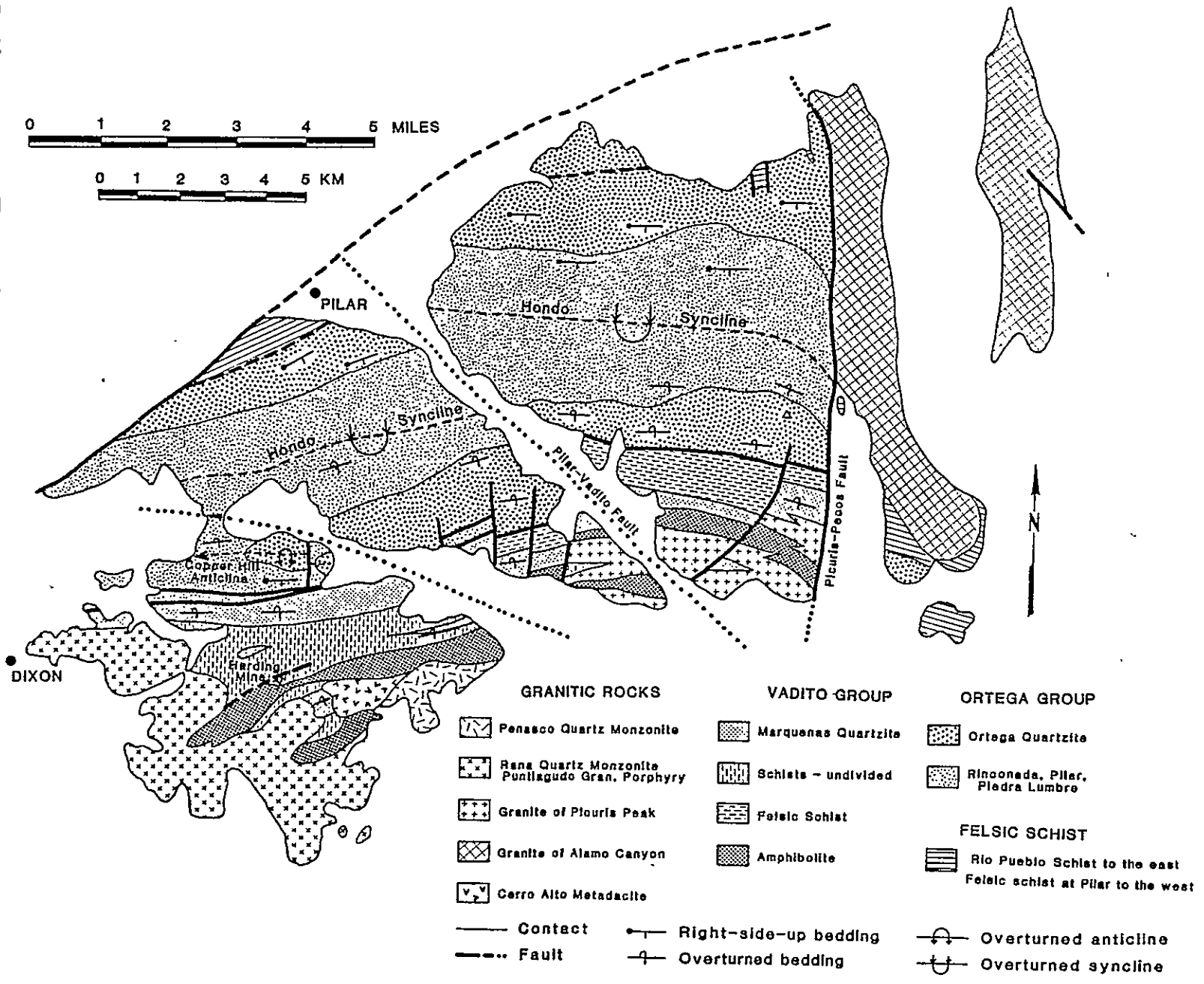
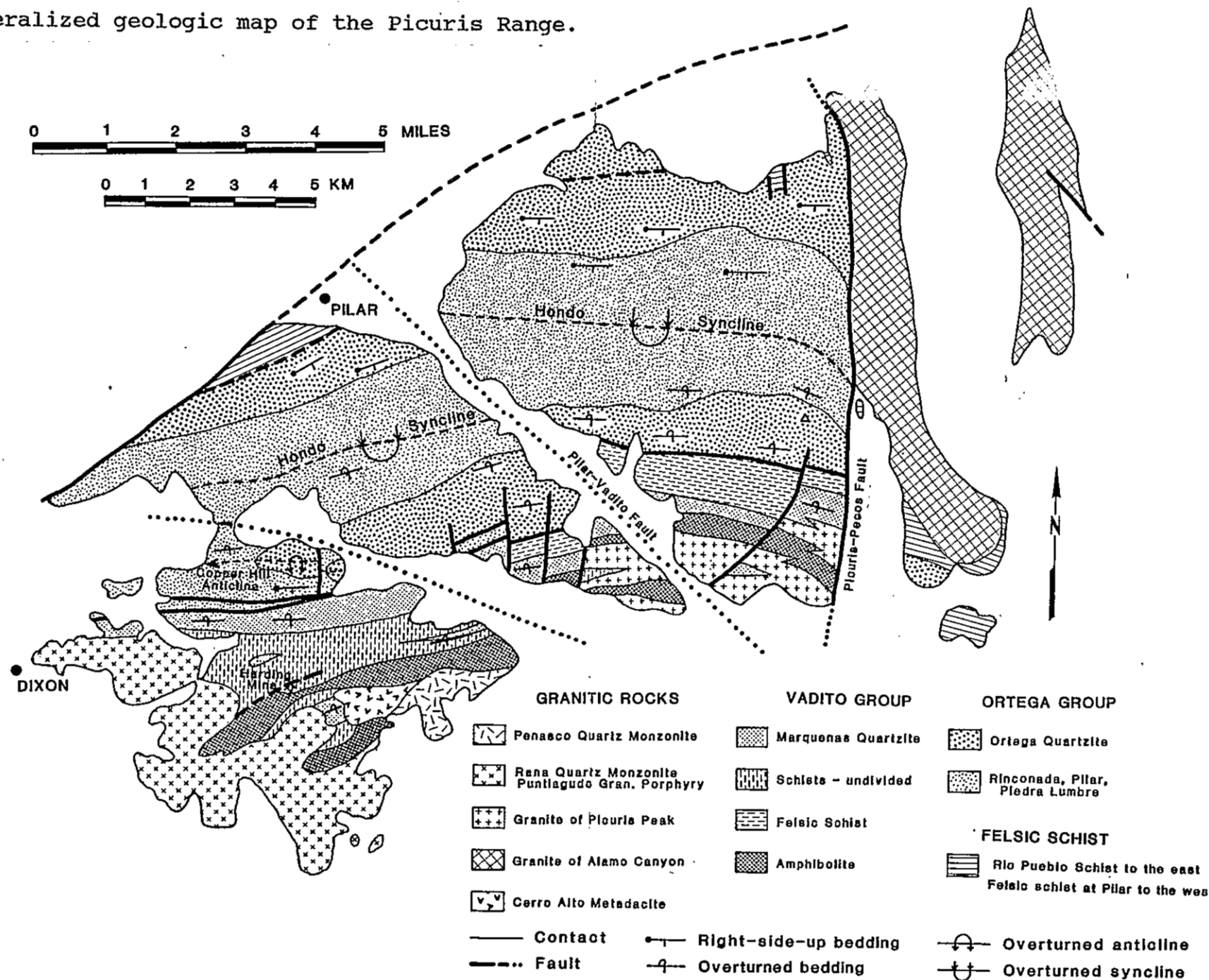


Figure 7.1. Generalized geologic map of the Picuris Range.



Within each domain, the various generations of structures have been catalogued. It is important to note that although the structures are sub-divided into generations, the strain history responsible for these structures is probably due to a progressive deformation. Because of this, structures and fabrics that seem to have formed together are referred to as a generation of structures rather than a deformational event.

Regardless of the seemingly diverse structural histories of the domains, all three major supracrustal rock groups will be reconciled in a single comprehensive kinematic model for the entire range. This model involved a complex interplay of progressive folding and shearing in a mid-crustal, ductile environment under medium-grade metamorphic conditions, and is presented at the end of this chapter.

Two of the most persistent questions regarding the Precambrian geology of the Picuris Range are: 1) what are the stratigraphic relationships, if any, between major lithostratigraphic rock packages in the range; and 2) what are the Precambrian structural histories of these packages? Answers to these questions lead to models outlining the evolution and tectonic setting of the range and place the range in a regional framework.

Although previous studies of the stratigraphy and structure of Proterozoic rocks in the Picuris Range are

numerous, detailed models of the kinematics and dynamics are few. This is due mainly to uncertainties and inconsistencies concerning the basic geology of rocks in the range. This in turn is largely due to the heterogeneity of strain within and between major rock groups, and the presence of previously unrecognized faults and ductile shear zones. The most important Precambrian shear zones in the Picuris Range are bedding-parallel, and are accordingly difficult to recognize and interpret. Some workers have described relatively simple strain histories whereas others have described complex polyphase histories.

It has recently become apparent that these problems and complications are characteristic of all five of the isolated Precambrian uplifts in northern New Mexico that have been mapped and analyzed in some detail (Williams, 1987; Grambling et al., in prep.). In each range, workers have described early, ductile shear zones which have subsequently been folded and faulted.

## Methods

Methods employed in this study include detailed mapping, and thin section and microstructural analysis. Thin sections were generally cut normal to the foliation, and both parallel and normal to intersection or extension lineations. All stereograms are lower hemisphere equal-area

projections, contoured to 1 percent of area.

Serious problems can arise when correlating generations of structures between domains (P.F. Williams, 1985). If lithologies and stratigraphies differ, the character of imposed structures and fabrics may also differ. If terranes have experienced somewhat different structural histories, or identical structural histories under different structural conditions, it may be difficult to match corresponding structures and fabrics. In the Picuris Range, previous interpretations concerning the number of fabric-forming events, and relative timing of those events have varied from study to study. Overprinting relationships are the best criteria for determining structural history (P.F. Williams, 1985). Foliation overprinting relationships are not as reliable as fold interference patterns. Other useful criteria in certain areas are deformational style and orientation patterns. Because fold interference patterns are rare in the Picuris Range, most correlations of structural history among the three domains depend on foliation overprinting, deformational style, and orientation patterns.

## Geometries of Domains

### Introduction

The three major stratigraphic/structural domains in the Picuris Range (Vadito Group, felsic schist at Pilar, and Ortega Group) are shown in Figure 7.1. Granitic plutons that intrude only the southern part of the Vadito Group are included in the Vadito Group domain. A fourth, poorly understood domain consists of all of the rocks that crop out east of the Picuris-Pecos fault. This eastern block is considered a separate domain, even though it may contain stratigraphic equivalents of one or more of the other domains. It is not clear how this domain fits into the regional picture, and it will not be emphasized in this dissertation.

The Ortega Group is a well-layered metasedimentary sequence dominated by a >1000m thick, resistant basal quartzite. The Ortega Group is structurally characterized by major folds which are overprinted by a slightly oblique, penetrative, reactivated cleavage.

The felsic schist at Pilar is a homogeneous sequence of layered feldspathic quartz-muscovite "quartz-eye" schists. This unit is structurally dominated by a single, layer-parallel foliation which is probably mylonitic.

The Vadito Group is a complexly interlayered

metavolcanic-metasedimentary sequence which is characterized by heterogeneous units that thicken, thin, and pinch-cut along strike. Vadito Group rocks contain a strong foliation that is axial planar to tight, moderately sized folds.

### Ortega Group

Relict sedimentary structures. Well-preserved cross-beds in many quartzites, and graded beds in some schists and phyllites provide excellent stratigraphic control in the Ortega Group. With the exception of the southern Copper Hill area and local regions of minor folding, younging criteria are consistent with the major fold structure. On the northern limb of the Hondo syncline, strata dip and young to the south. On the southern limb of the Hondo syncline, strata dip to the south and young to the north. In the Copper Hill area, on the southern limb of the Copper Hill anticline, beds dip and young to the south (Fig. 7.1).

First generation of structures, D<sub>1</sub>. The earliest generation of structures in the Ortega Group is characterized by fairly small-scale, near-bedding-parallel, high shear-strain features. These structures are most evident in quartzites and quartz-rich rocks at or near the basal Ortega Quartzite Formation. Within the map area,

folding does not appear to be an important component of  $D_1$  strain.

Nielsen (1972) and Nielsen and Scott (1979) suggested that because stratigraphic and structural facings were consistent, the first-generation of structures represents one limb of a large recumbent fold. In the Picuris Range, no evidence of closure on such a fold has been recognized.

The only penetrative  $D_1$  feature is a bedding-parallel schistosity ( $S_1$ ) in micaceous quartzites (Fig. 7.2). Commonly associated with this schistosity is a strong south-plunging extension lineation ( $L_1$ ) on  $S_1$  surfaces (Fig. 7.2).  $L_1$  is defined by either elongate quartz grains, or aligned crystals of sillimanite, kyanite, and tourmaline. This lineation generally plunges down-dip. Bedding-parallel foliations are common in rocks from multiply deformed Proterozoic terranes (Holst, 1985; Hobbs et al., 1976), and debate continues over whether they are the result of a primary depositional fabric or a tectonite fabric. Holst (1985) reported such a fabric in metasediments of the Proterozoic Thomson Formation of Minnesota. He concluded that it was a tectonic foliation clearly related to other early tectonite structures. The  $S_1$  fabric in the Picuris Range is also related to other early deformational features, and is considered a tectonic foliation. These other  $D_1$  structures are described in the following paragraphs.

The Ortega Quartzite contains one-meter-thick-or-less,

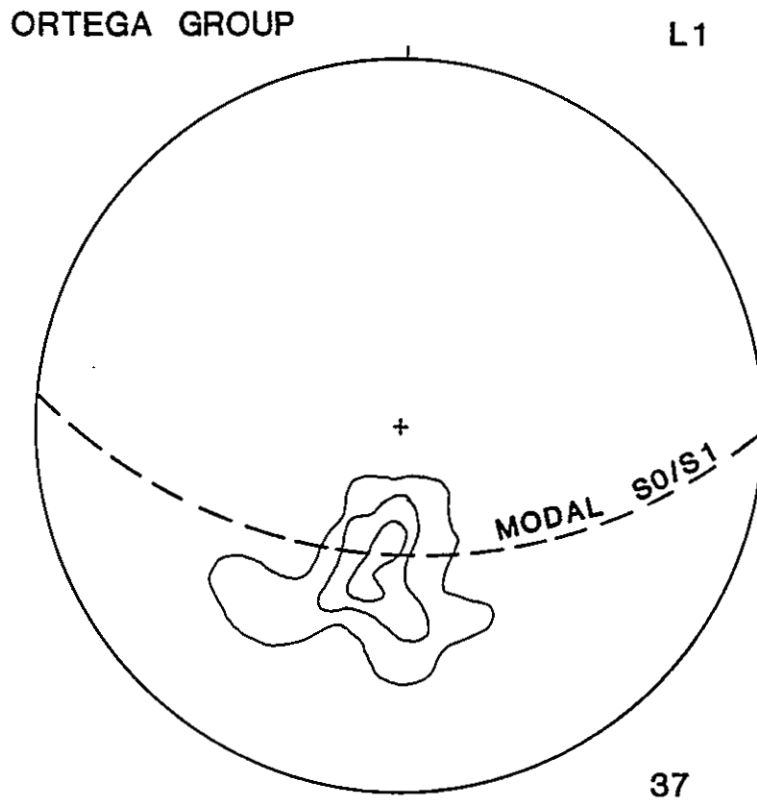


Figure 7.2. Contoured, equal-area stereographic projection of  $L_1$  and  $S_0/S_1$  in Ortega Group rocks.

bedding-parallel zones of deformed vein quartz surrounded by an anastomosing aluminous schist matrix. Highly contorted quartz layers and aligned quartz pods (Fig. 7.3) indicate that these features are zones of high shear strain. It is not known whether the vein quartz and aluminous schist were concentrated in these zones during deformation or prior to deformation. Metamorphosed aluminous "shale drapes" are commonly found within the Ortega Quartzite (Soegaard and Eriksson, 1985). Roering and Smit (1987) reported a clear relationship between the occurrence of vein quartz and bedding-parallel shear zones in quartzites from the Witwatersrand Supergroup, South Africa. In these zones, quartz veins developed during shear deformation.

In one locality in the northwestern map area, a quartz-vein-rich shear zone contains a fold structure interpreted to be a sheath fold. This fold is only exposed in two dimensions, but is consistent with a sheath fold profile cut perpendicular to the transport direction (Fig. 7.4). Sheath folds in which the fold axis is parallel to the extension lineation are common in mylonite zones (Bell and Hammond, 1984; Cobbold and Quinquis, 1980; White et al., 1980; Carreras et al., 1977; Quinquis et al., 1978; Berthé and Brun, 1980).

The basal Ortega Quartzite in the Pilar cliffs area contains zones of abundant, small, concave shear planes that are sub-parallel to compositional layering (Fig. 7.5).

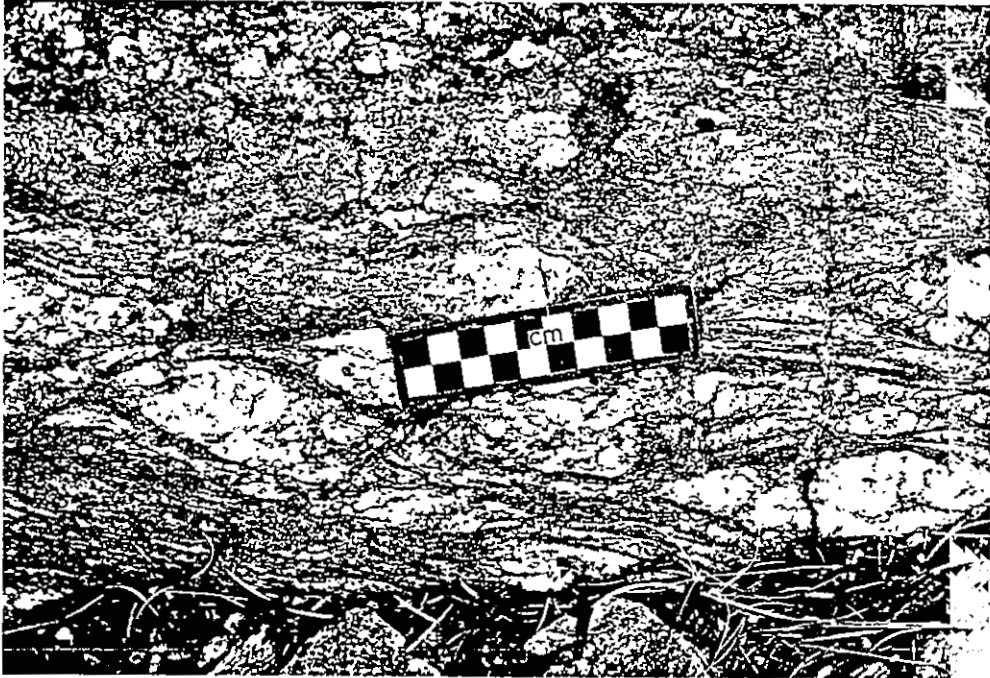


Figure 7.3. Photograph of bedding-parallel, quartz-vein-rich shear zone in the Ortega Quartzite. Quartz pods are surrounded by anastomosing, aluminum silicate-rich schist.

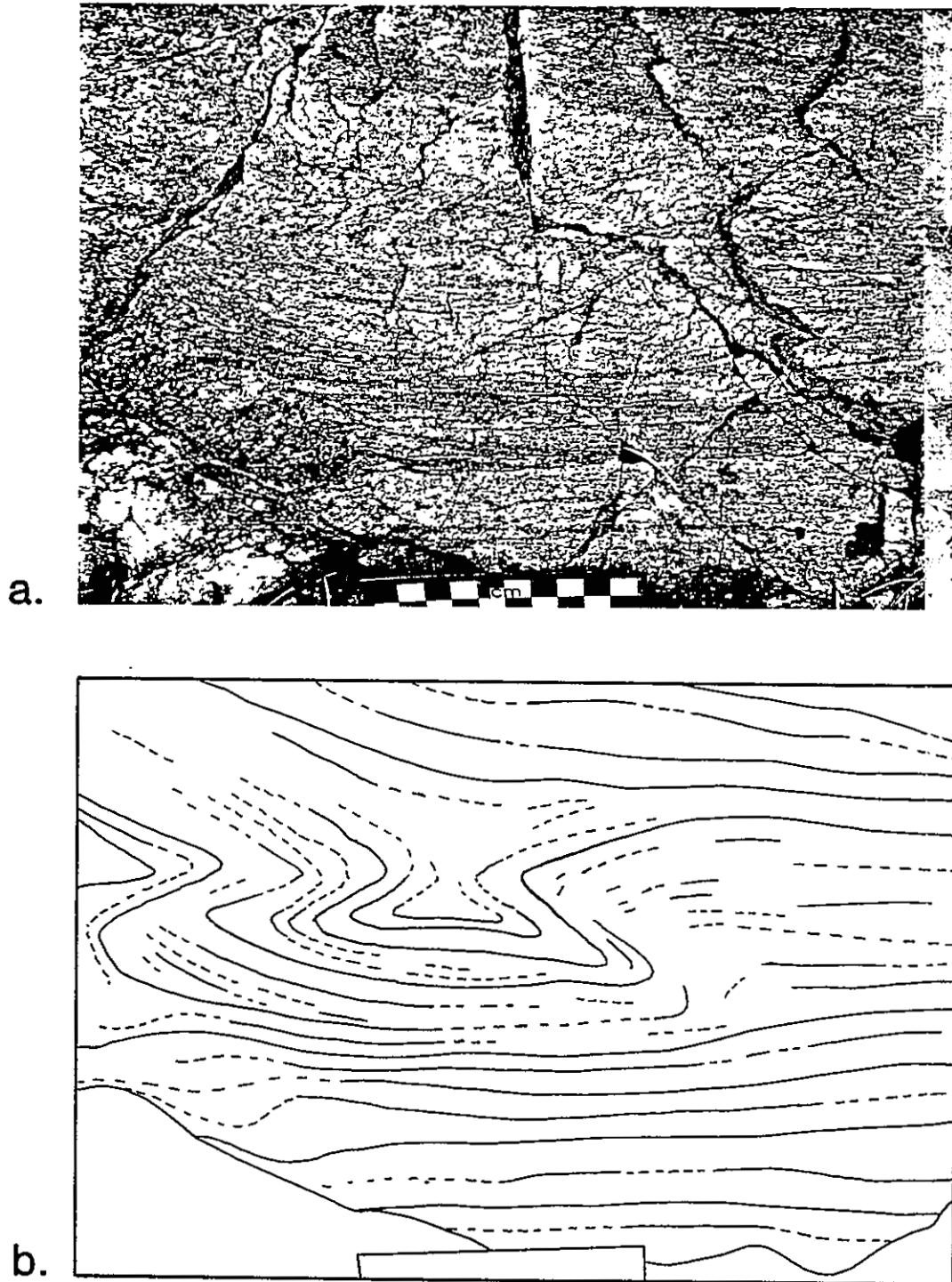


Figure 7.4. a. Photograph of sheath fold in Ortega Quartzite shear zone. Rock face on which fold is exposed is normal to the extension lineation. b. Sketch.

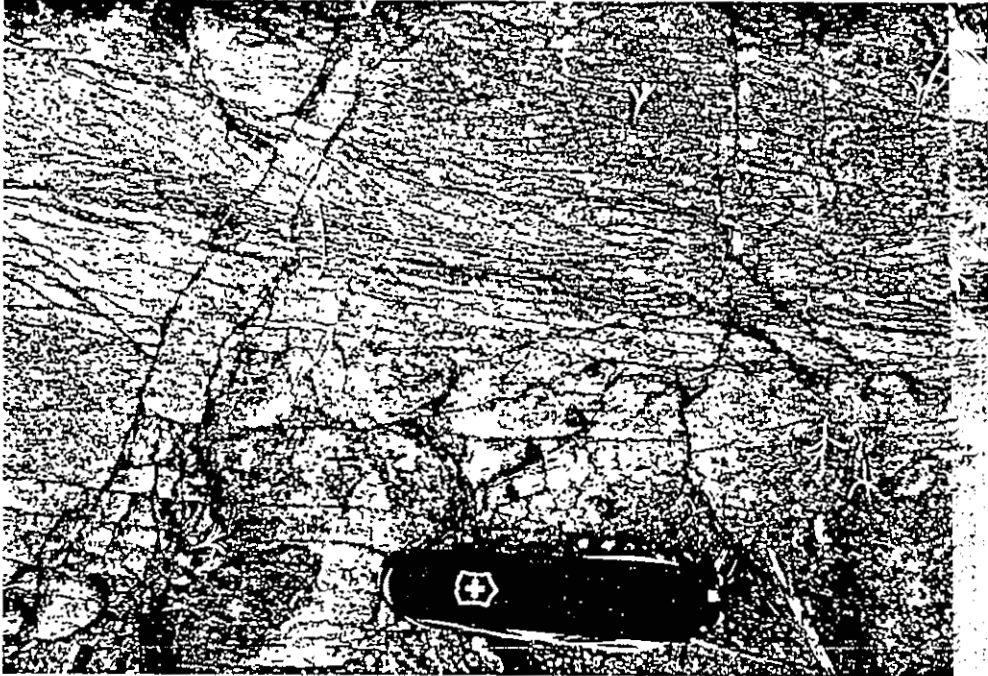


Figure 7.5. Photograph of small shears in basal Ortega Quartzite from the Pilar cliffs, northwestern Picuris Range.

These arcuate features are defined by reduced grain size rather than by compositional variations. Sense of shear is not discernable. These features are similar to narrow shear zones found in non-foliated quartzites in the Witwatersrand Supergroup (Roering and Smit, 1987).

Mylonite zones are important  $D_1$  structures. Quartz mylonites are found locally in the Ortega Quartzite (HC-366) (Fig. 7.6). These rocks appear to have undergone grain size reduction by ductile processes. All contain an intense foliation and well-developed extension lineation. Such structures generally imply conditions of high, localized, simple shear strain (Tullis et al., 1982).

Pristine quartz ribbon mylonites are found locally in quartzites within the Rinconada Formation and the basal Ortega Quartzite in the Pilar cliffs. These mylonites show no evidence of post-kinematic coarsening or annealing of quartz grains (Fig. 7.7). These types of structures are only recognized in extremely pure quartzites. Although in style and orientation these quartz ribbon mylonites resemble other  $D_1$  structures, the lack of annealing suggests that they developed late in the metamorphic history. Perhaps these fabrics are  $D_1$  mylonites that were reactivated syn- or post- $D_3$ .

All of these features found in quartz-rich lithologies suggest a (early?) deformational history of near bedding-parallel progressive simple shearing along discrete zones.

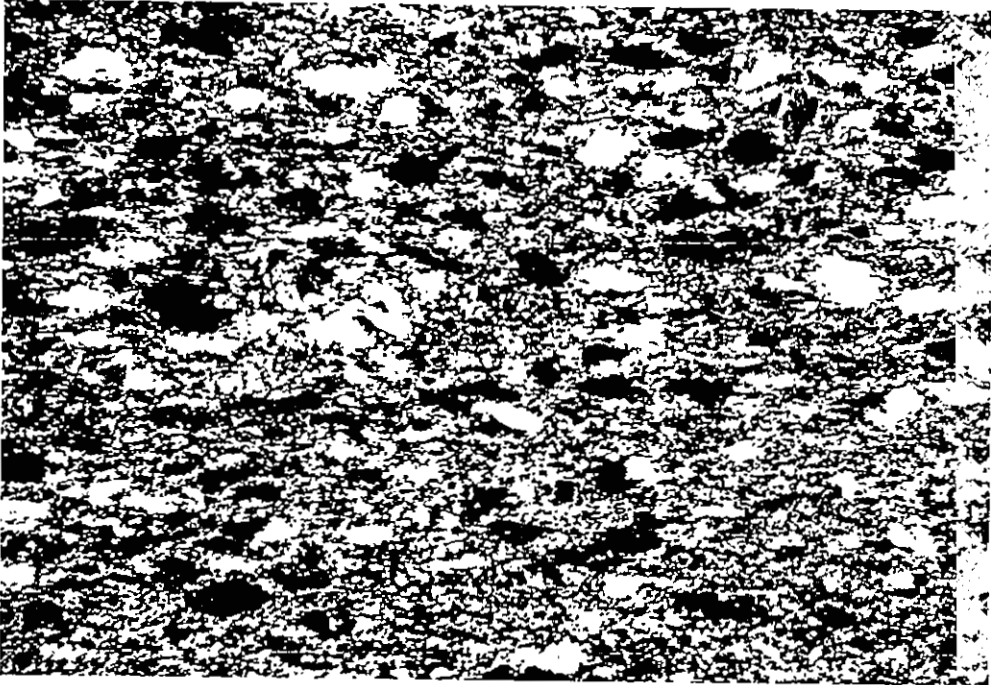


Figure 7.6. Photomicrograph of recrystallized quartz mylonite from the Ortega Quartzite. Field of view is 16 mm.

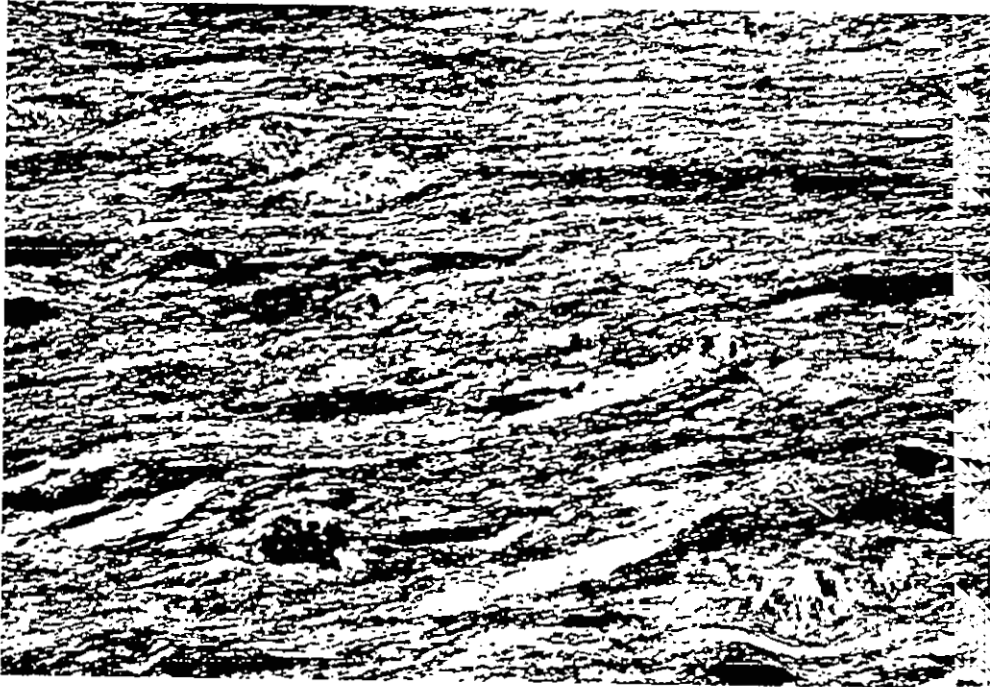


Figure 7.7. Photomicrograph of pristine quartz ribbon mylonite from R3 quartzite in the north-central Picuris Range. Section is cut parallel to the extension lineation and normal to the mylonitic foliation. Field of view is 16 mm.

It is reasonable to assume that considerable  $D_1$  shear strain was also partitioned into the schistose lithologies, where evidence of these features has been destroyed by later deformation. Some schists however do contain evidence of  $D_1$  fabrics preserved as microstructures in some pre- $D_2$  porphyroblasts. These features will be described in a following section.

Strain conditions suitable for the formation of some of these  $D_1$ -type structures presumably continued at least into  $D_2$  time. This overlap is well illustrated by occurrences of the  $D_1$  extension lineation. In some areas these lineations are folded around  $F_2$  folds, suggesting that they are pre- $F_2$ , whereas in other adjacent areas they sit within axial planes of  $D_2$  folds, suggesting that they are syn- $F_2$ . Other structures such as the quartz vein shear zones, which everywhere follow folded compositional layering, may only have formed early in  $D_1$ .

Second generation of structures,  $D_2$ . The dominant expression of the second generation of deformation is folding on all scales. Most  $F_2$  folds are now upright, tight to isoclinal, variably-plunging structures. On a macroscopic scale  $D_2$  is best illustrated by the Hondo syncline. This fold is the dominant structure in the mountain range, and affects the entire Ortega Group. It is a tight, shallowly west-plunging fold with axial surface

dipping due south at about  $65^{\circ}$ . Dip values of modal  $\epsilon_0$  ranges from an average of  $66^{\circ}$  on the northern limb to  $60^{\circ}$  on the southern limb. On a map scale, as illustrated by the shape of the thick, mechanically stiff Ortega Quartzite Formation, this fold geometry is simple. In detail however, thinly interlayered units above the Ortega Quartzite, with differing competency contrasts, have folded disharmonically and noncylindrically (Fig. 7.8). Folding mechanisms range from nearly pure buckling (Hudleston, 1986) in the Ortega Quartzite, to dominantly passive folding (Hudleston, 1986) in subordinate schists and phyllites. Several map-scale minor folds and fault-related complications are evident in the Hondo syncline. In particular, these structures are concentrated on the overturned, tectonically thinned, southern limb of the fold in the Rinconada and Pilar Phyllite formations. Most of the faults in the area north of Warm Springs are bedding-parallel, and because they are associated with abundant minor folds, they cause enormous complexities in local mapping of stratigraphy.

Outcrop-scale folds in the Ortega Group are extremely common.  $F_2$  folding is especially spectacular in the colorful, finely laminated schists, metasiltsstones, and phyllites of the Piedra Lumbre Formation in the nose of the Hondo syncline. Although small-scale  $F_2$  folds show significant variation in hinge orientation, hinge lines consistently lie within the plane of compositional layering.

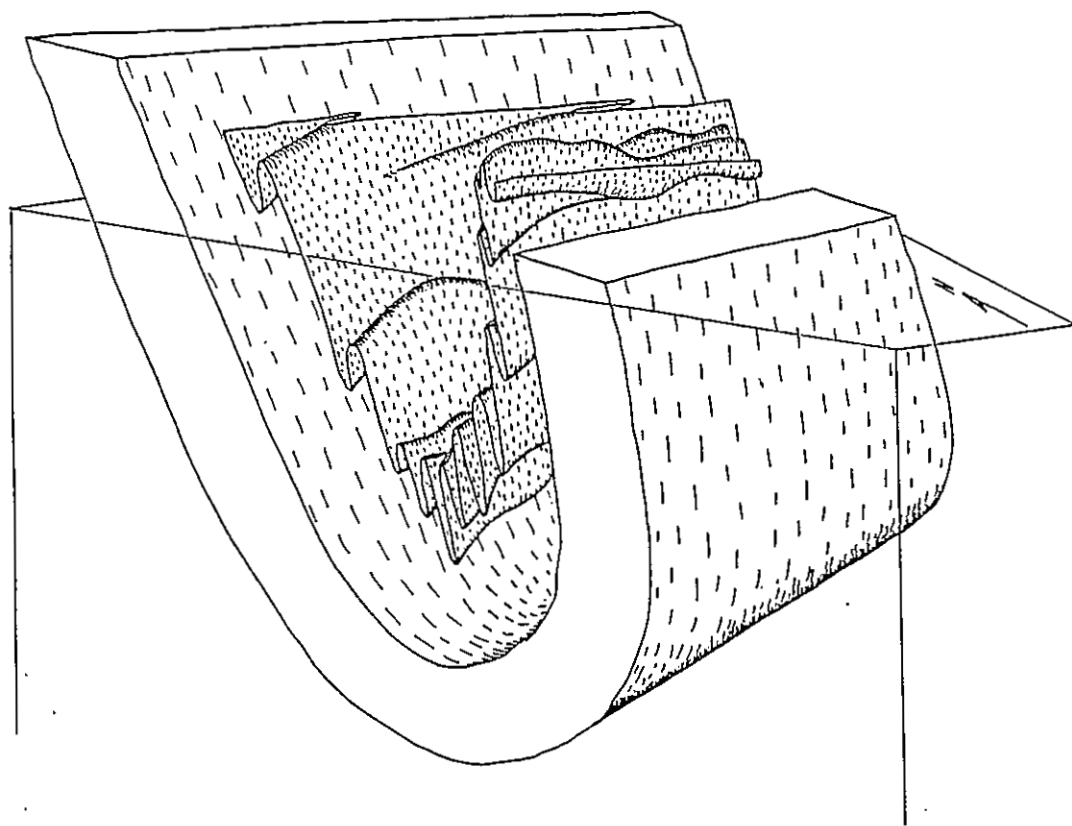


Figure 7.8. Block-diagram sketch of Hondo syncline showing thick, competent Ortega Quartzite fold, and disharmonic, noncylindrical folds in less competent schists. Fold is approximately 6 km across.

This effect is illustrated by stereographic projections of compositional layering and  $L_2^*_{0/1}$  lineation (Fig. 7.9).

One fold of particular interest is the Copper Hill anticline in the southwestern Picuris Range. This structure has been the focus of numerous studies, and is unique in that it is the only large anticline recognized in the Ortega Group of the Picuris Range. The structure plunges about  $20^\circ$  to the west, and folds a tectonite fabric along with compositional layering. Thin sections of Rinconada schist from the hinge area shows an axial plane crenulation cleavage cutting an earlier schistosity ( $S_1?$ ) and compositional layering. In style and orientation the Copper Hill anticline resembles other  $F_2$  folds.

The Copper Hill anticline contains extensive copper mineralization localized in the upper portion of the Ortega Quartzite (Williams, 1982). It is possible that the Copper Hill anticline is separated from adjacent rocks by high-angle reverse(?) faults as shown in Figure 7.10. The Copper Hill structure may therefore be an uplifted minor fold of the Hondo syncline.

The axial plane cleavage ( $S_2$ ) associated with  $F_2$  folding is generally either obscured by the  $S_2^*$  fabric, or not developed. Where exposed,  $S_2$  is difficult to distinguish from the later  $S_2^*$ . As will be discussed in the following section, although  $S_2^*$  is generally not axial planar to  $F_2$  folds in the Ortega Group, it was probably

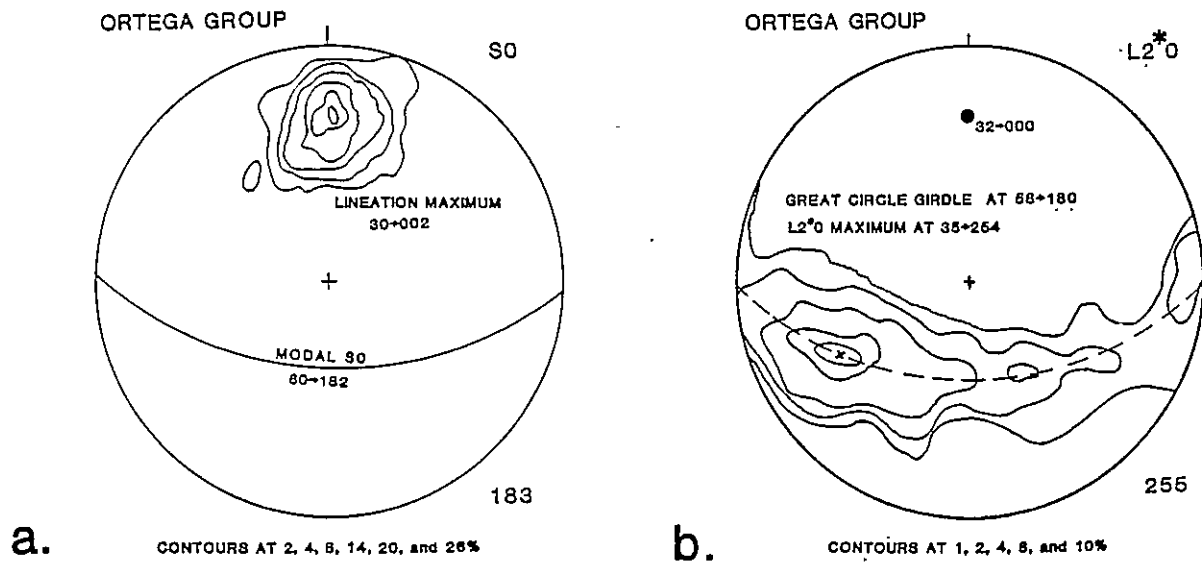


Figure 7.9. a. Contoured stereographic projection of  $S_0/S_1$  in Ortega Group. b. Contoured stereographic projection of  $L_2^*0$  in Ortega Group. c. Sketch of  $F_2$  fold geometry in Ortega Group that illustrates  $S_0/S_1$ - $L_2^*0$  relationships. See text for discussion.

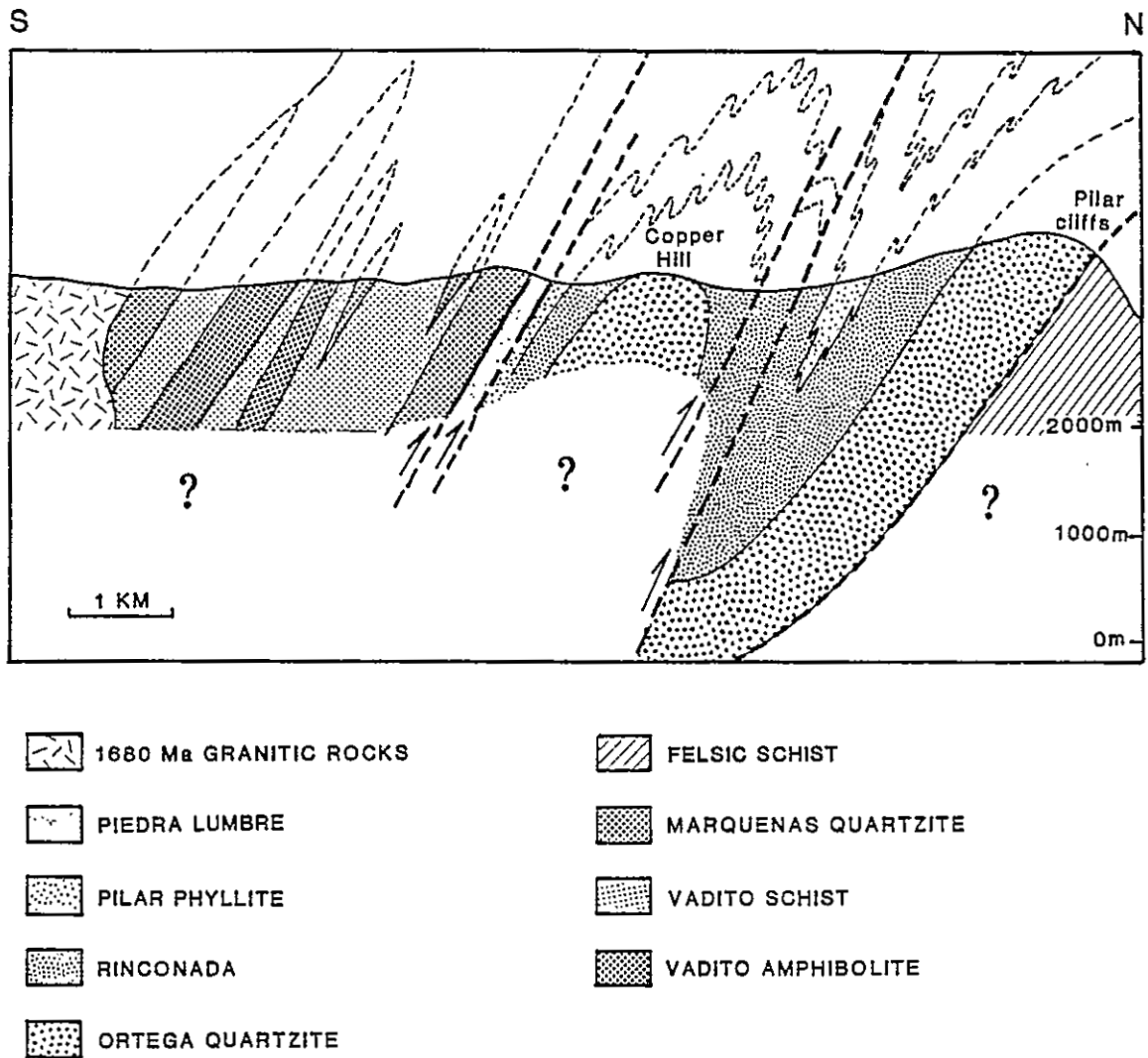


Figure 7.10 Sketch cross-section through the Copper Hill area, showing possible relationship between the Copper Hill anticline and adjacent rocks.

developed late in the  $F_2$  folding process, and is therefore called  $S_2^*$  rather than  $S_2$ . Identification of  $S_2$  is certain only where the overprinting  $S_2^*$  fabric is weak, and the  $S_2$  cleavage can be observed axial planar to an  $F_2$  fold.

Within the northwestern map area, the apparent thickness of the Ortega Quartzite Formation approaches two kilometers. Everywhere else in the range, this formation is not much more than one kilometer thick. In this area, Ortega Quartzite stratigraphy is repeated across a biotite schist horizon that sits approximately where the base of the quartzite should occur. The mica foliation in the biotite schist is oriented at  $72^\circ$  to  $235^\circ$ . Compositional layering in Ortega Quartzite dips about  $50^\circ$  south to the south of the biotite schist, and about  $65^\circ$  south to the north of the biotite schist. This area probably represents an imbrication and tectonic thickening of the Ortega Quartzite (Fig. 7.11). Although the timing of faulting is unknown, its style suggests  $D_1/D_2$  deformation. Very similar imbrication features in the Ortega Quartzite have been described by Williams (1987) in the Tusas Range, and by J.A. Grambling (personal communication, 1987) in the Rio Moya and Guadalupita areas.

A minimum estimate of  $D_2$  shortening within the Ortega Group, made by comparing the fold profile of the Ortega Quartzite with an unfolded reconstruction, yields values of

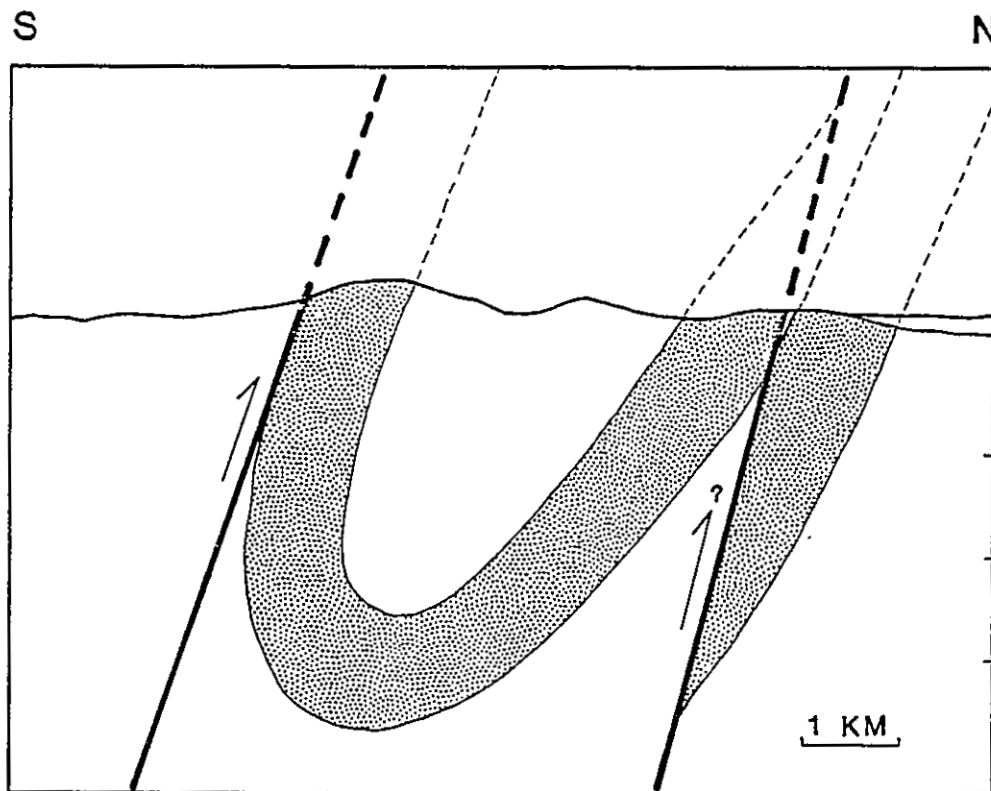


Figure 7.11 Sketch cross-section showing imbrication of Ortega Quartzite in northwestern map area. Age of faulting is unknown, but may be related to  $D_2/D_3$ .

about 65 percent shortening. This estimate neglects the shortening effects of tangential longitudinal shortening and shearing.

Third generation of structures,  $D_3$ . The third generation of structures is dominated by a slightly oblique, penetrative foliation ( $S_2^*$ ) that has overprinted earlier features.  $S_2^*$  is the dominant cleavage in nearly all schist outcrops in the Ortega Group.  $S_2^*$  appears as both a schistosity and a crenulation cleavage locally, and typically is not axial planar to  $F_2$  folds. Figure 7.12a illustrates the manner in which  $S_2^*$  transects these structures. Because  $S_2^*$  is generally the dominant cleavage in outcrop, and lies slightly oblique to  $D_2$  axial surfaces, many measurements of the bedding-cleavage structural vergence relationships across the Hondo syncline are potentially misleading. In order for the bedding-cleavage rule to be useful, folding and cleavage formation must be synchronous (Borradaile, 1978). In terms of the major fold structure, vergence measurements show that although the stratigraphy requires synclinal closure, most vergence data indicate anticlinal closure. Evidence of this can be found at the outcrop scale where minor  $F_2$  folds in the Pilar Phyllite Formation are transected by an overprinting  $S_2^*$  cleavage (Fig. 7.12b). If a well-developed  $S_2$  cleavage ever existed, it has been destroyed or reactivated by  $S_2^*$ .

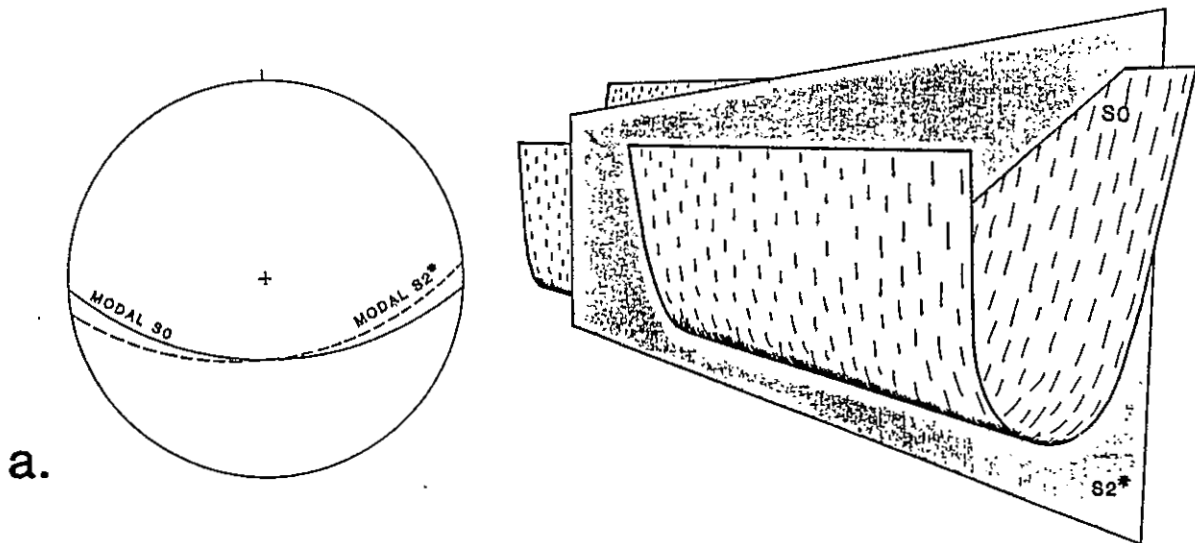
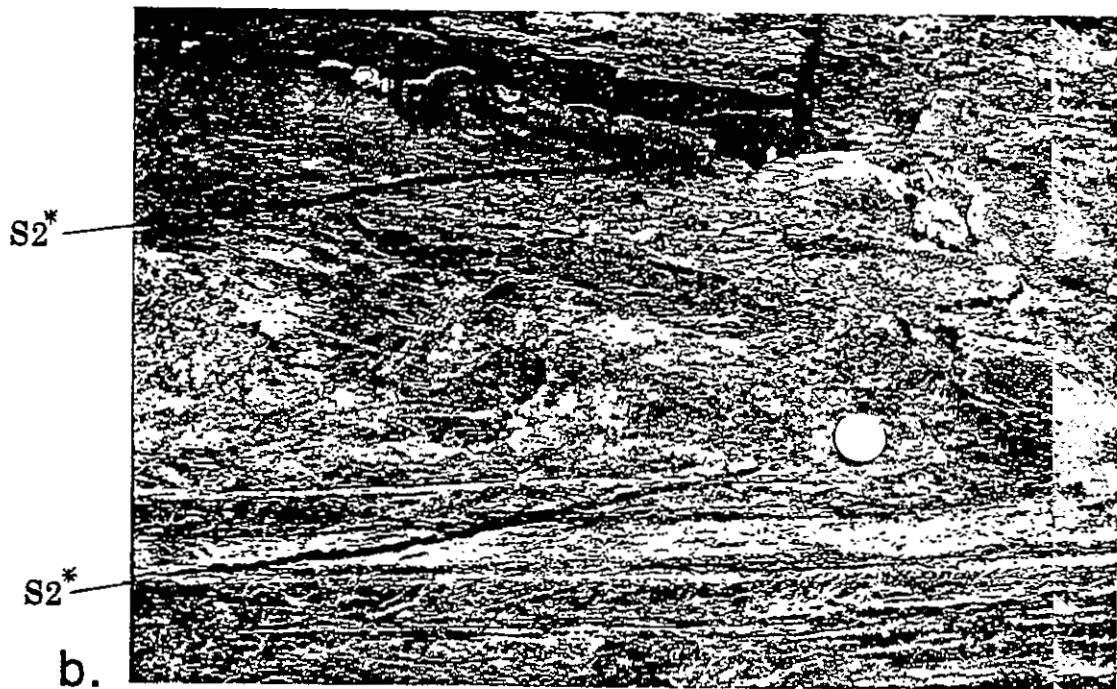


Figure 7.12. a. Sketch and stereogram showing the nature of  $S_2^*$  transection of  $F_2$  folds. b. Photograph of  $S_2^*$  transecting  $F_2$  fold in the Pilar Phyllite. Black marker lines parallel the trace of  $S_2^*$ .

Borradaile (1978) proposed a method of describing the nature of fold transection. According to his scheme, the Hondo syncline is an example of "case 1", with a dihedral angle between the fold hinge and cleavage plane of about 10-15°. There is debate concerning the interpretation of the relative timing of a transecting cleavage and fold development. Powell (1974) and Borradaile (1978) noted that transected folds are not uncommon, and that one method of development involves a time lag between the inception of folding and development of the cleavage. Alternatively, Duncan (1985) stated that there existed no evidence to suggest that transected folds are not just the effect of superimposed deformations. He noted that to prove transection, it must be shown that folding and cleavage formation were formed during a single deformational event, and not during a polyphase deformational history. Although geometrical fabric relationships in the Picuris Range do not permit unambiguous conclusions regarding the absolute timing of  $F_2$  folds and the  $S_2^*$  cleavage, porphyroblast microstructures described below suggest a continuum of deformation during  $D_2$  and  $D_3$ . This implies that the transecting  $S_2^*$  cleavage formed either late in  $F_2$  or immediately after  $F_2$  folding.

Unambiguous examples of  $F_2^*$  folds are not common. Examples of apparent map-scale  $F_2^*$  folds possibly exist on the southern limb of the Hondo syncline, within the R6 unit

of the Rinconada Formation, and the Pilar Phyllite Formation. Two sets of complex folds, on the southern limb of the Hondo syncline, exhibit the wrong sense of asymmetry for the major west-plunging Hondo syncline structure. Axial surfaces of these folds parallel the  $S_2^*$  cleavage orientation. Plunges of these folds are unknown. If they plunge eastward, then they are consistent with the major structure.

The dominant intersection lineation in Ortega Group rocks appears to be  $L_2^*0$ . This is speculative because  $L_{20}$  and  $L_2^*0$  are essentially identical in style. The stereographic projection of  $L_{20}/L_2^*0$  defines a great-circle girdle which corresponds to compositional layering (Fig. 7.9b). The point maximum at  $35^\circ$  to  $242^\circ$  suggests that many measured  $F_2/F_2^*$  folds plunge southwest, consistent in orientation with the larger structures.

Minor fold axes commonly develop oblique to the regional trend of major folds (Sanderson, 1973). This effect does not imply that the principal strain axes rotated during folding. Sanderson (1973) found that oblique fold axes can develop under conditions of constant principal strain axis orientation. In a highly deformed Proterozoic terrane in the southern Lake Superior region, fold axes have rotated towards the bulk extension direction, and plot as a great-circle distribution on a stereogram (Sedlock and Larue, 1985). Such progressive reorientations of fold axes

are common in deformed terranes throughout the world (Pfiffner, 1981; Speed and Larue, 1982; Miller et al., 1982; Williams, 1978), and such an interpretation is proposed for rocks in the Ortega Group of the Picuris Range.

Mesoscopic, near bedding-parallel shears represent another important component of  $D_2/D_3$  strain. In the Piedra Lumbre schist, such shears truncate small,  $F_2$ -style folds (Fig. 7.13). In the Warm Springs area of the west-central map area, numerous near bedding-parallel shears disrupt stratigraphy. It is suspected that these structures are more abundant than can be demonstrated by mapping of stratigraphic relationships. Because some of these shears appear to cut  $F_2$  folds, they may be more closely associated in time with  $D_3$  rather than  $D_2$ .

Fourth generation of structures  $D_4$ . Several late, nonpenetrative, cross-cutting sets of structures have locally overprinted earlier fabrics. These are characterized by generally north-trending crenulations and kink folds in schists (see Fig. 5.8). The strains involved in these events are relatively small in comparison to  $D_1$ ,  $D_2$ , and  $D_3$  strain.

Porphyroblast microstructures. Large porphyroblasts of staurolite, garnet, biotite, plagioclase, and andalusite are abundant in schistose units of the Ortega Group.

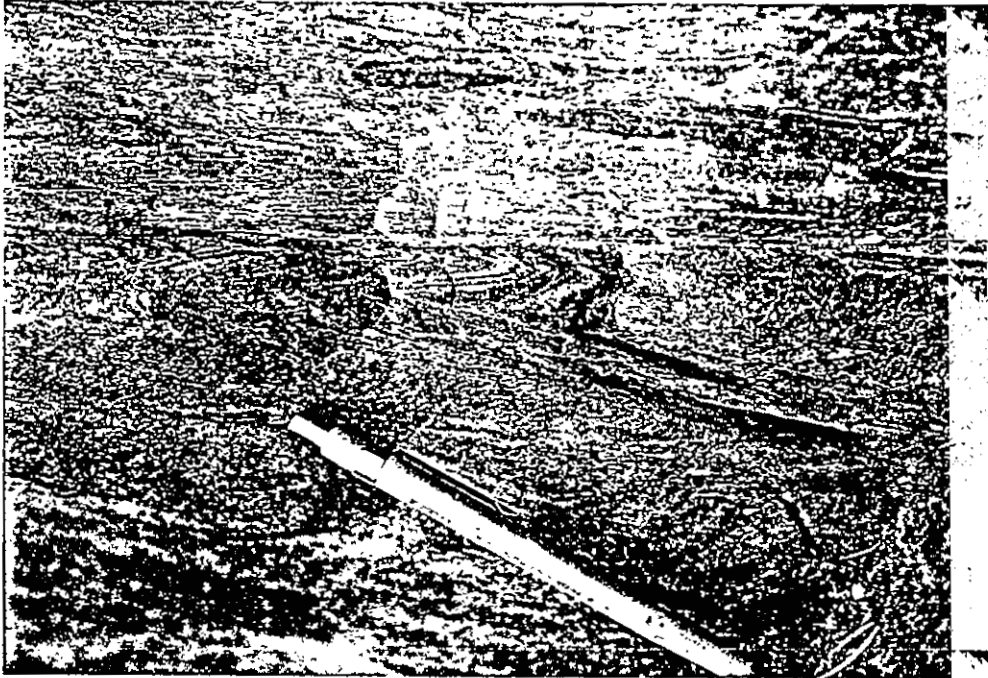


Figure 7.13. Photograph of small near-bedding parallel,  $D_2$  or  $D_3$  shear in Piedra Lumbre Formation. Shear cuts  $F_2(?)$  fold.

Microstructures are common, and especially useful, in staurolites and garnets from the R6 schist and the Piedra Lumbre Formation.

Certain porphyroblasts clearly overgrow, and preserve as inclusion trails, earlier fabrics that may have been destroyed within the matrix. Typically, interpretations of these microstructures are ambiguous. Nonetheless, porphyroblast/microfabric relationships yield important information that may not be obtainable by any other method. One of the most intriguing subjects involves the relative timing of metamorphism and the various generations of structures. Do the generations of structures recognized in the rocks represent separate consecutive orogenic episodes, several pulses of strain during one orogeny, or a continuum of straining during evolving metamorphic conditions? Although common, well-preserved porphyroblast microstructures in staurolites and garnets from the Ortega Group can help answer such questions, it should be noted that because absolute relationships must vary in time and space across orogens, methods for establishing the relative timing of deformational events can only be applied locally (P.F. Williams, 1985).

Euhedral garnet porphyroblasts, which range in size from less than 1 mm to 5 mm are found in a variety of lithologies of the Ortega Group. In many units, garnets are concentrated in the most aluminous layers. Generally,

garnets are relatively inclusion-free. Where inclusions are present, concentrations are greatest in garnet cores.

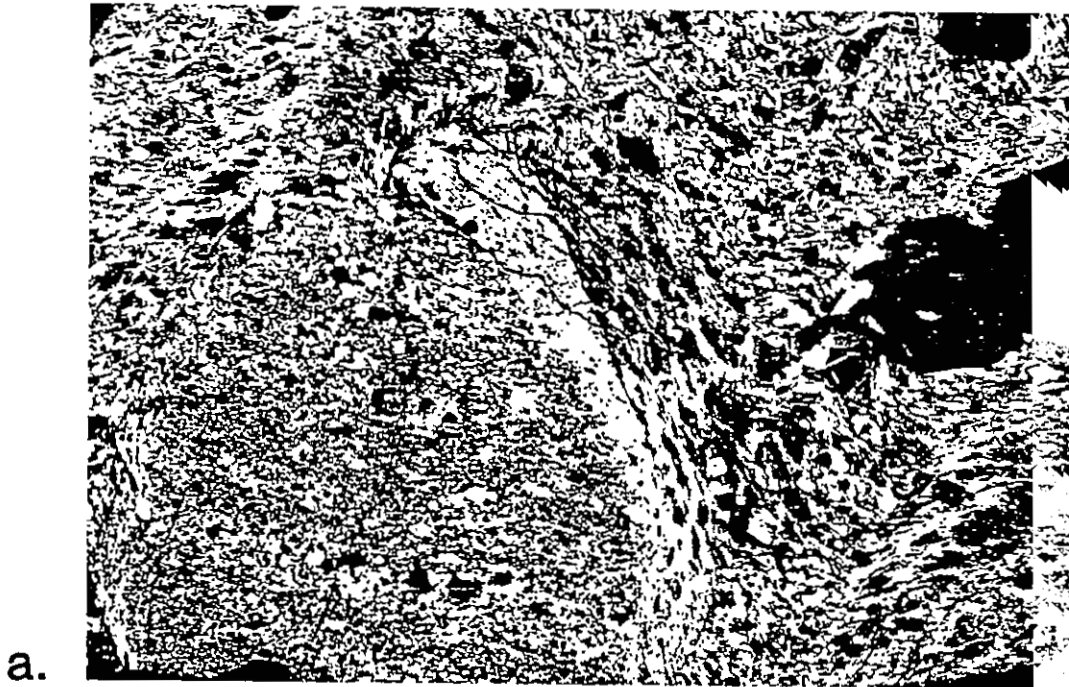
Typical inclusions include small grains of quartz, biotite, plagioclase, muscovite, staurolite, and Fe-oxide. Inclusion trails representative of relict foliations are rare. Where present, these trails are generally curved. At garnet rims, the inclusion trails merge into and are continuous with the dominant mica foliation in the matrix (see Fig. 6.5). These types of inclusion trails are similar to those described by T.H. Bell (1985) and Vernon (1978) which are representative of a foliation that has been rotated or reactivated by a subsequent foliation (T.H. Bell, 1985; Vernon, 1978).

Inclusion trails everywhere seem to merge into the younger orientations, rather than to be truncated. These phenomena imply that deformation and metamorphism were continuous during and slightly after porphyroblast growth.

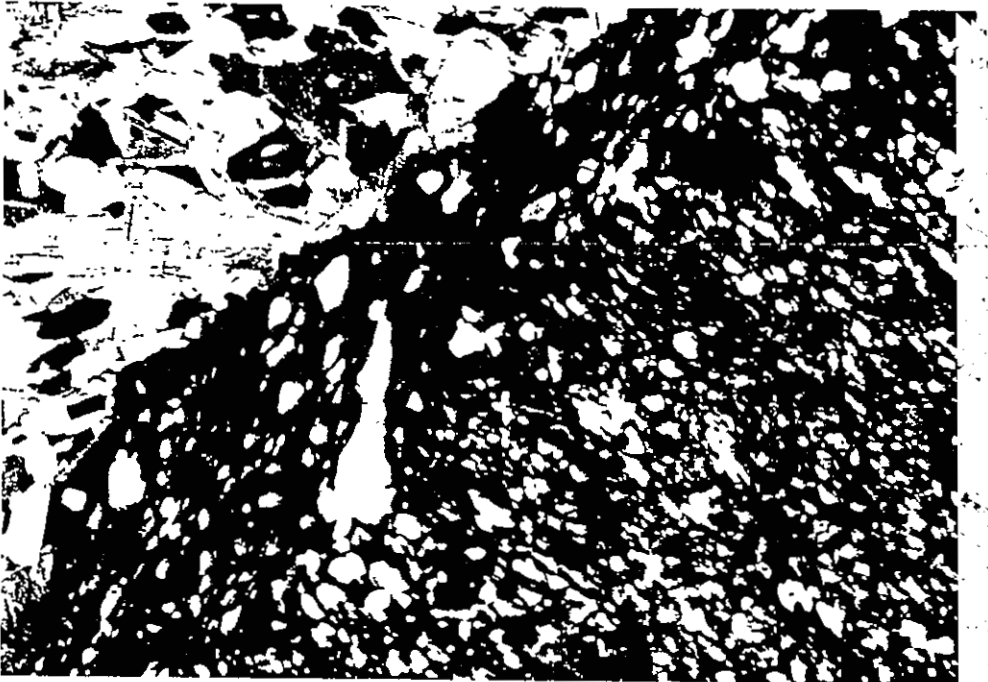
Staurolite porphyroblasts ranging in size from less than 1 mm to greater than 3 cm are abundant in Ortega Group schists. An enormous variety of staurolite shapes exists. The most anhedral crystals are typically highly poikiloblastic with rounded quartz inclusions. Staurolites are commonly twinned and/or sector zoned, and contain aligned quartz inclusion trails (see Fig. 6.7). Most staurolites are unstrained; some are slightly strained. In schists, the dominant foliation ( $S_2^*$ ) wraps around the randomly oriented staurolite porphyroblasts. Zoned crystals

typically contain euhedral cores with small quartz inclusions surrounded by a sub- to anhedral mantle that contains larger quartz inclusions.

A number of intriguing microstructural relationships exist between matrix foliations, growth zones in staurolites, and internal foliations. The most revealing staurolite porphyroblast (HC-450) is a zoned crystal that contains two orientations of a relict foliation (Fig. 7.14). The core contains a high density of small quartz inclusions that define straight foliation trails. The rim of the porphyroblast contains a lower density of larger, elongate quartz inclusions that define a slightly curved foliation trail. At the edge of the porphyroblast, these curved trails merge into a coarse matrix foliation, which in turn is bent into the dominant rock foliation ( $S_2^*$ ). This  $S_2^*$  is perpendicular to foliation trails preserved in the staurolite rim, and parallel to foliation trails preserved in the staurolite core. Close examination reveals that the core foliation actually bends into and merges with the rim foliation across the sharp core-rim boundary. One interpretation of these microstructures is that the porphyroblast rotated and grew in stages, preserving successive apparent orientations of a relatively constant foliation orientation. A second possible interpretation of these microstructures involves successive reorientation of foliation with respect to a non-rotational staurolite



a.



b.

Figure 7.14. Photomicrograph of large, zoned staurolite porphyroblast in R6 schist. Core contains horizontal inclusion trails that bend into vertical rim inclusion trails.  $S_2^*$  in matrix is horizontal. Field of view is 14 mm. b. Close-up of upper left portion of staurolite under cross polarized light. Section is cut normal to  $L_1$ . Field of view is 3.4 mm. See text for discussion.

porphyroblast. In this scheme, the staurolite growth is punctuated by orthogonal reorientations of foliation. The relative rates of porphyroblast growth and strain might be important in producing these microstructures. In either case, the relict included foliations may or may not represent successively earlier foliations (i.e.  $S_2$  and  $S_1$ ).

Both of these interpretations suggest that for this rock sample of Piedra Lumbre Formation at least part of the deformational history was progressive rather than episodic. Similar microstructural relationships are observed in other Ortega Group schists.

These petrologic observations and interpretations support the quantitative garnet-biotite P-T analysis presented in Chapter 6 that suggests that deformation and metamorphism were continuous, punctuated only by porphyroblast growth rate changes and/or strain rate changes. All porphyroblasts show a tendency for quartz inclusions to progressively coarsen from core to rim to matrix. This implies that minerals were continually recrystallizing and growing during prograde metamorphism.

Summary. Field and petrologic evidence from the Ortega Group suggests a deformation history of early, low-angle, near bedding-parallel, localized progressive simple shear that evolved into large-scale, upright folding and faulting, which in turn evolved into strong, slightly oblique,

overprinting foliation formation. There probably existed considerable temporal overlap of structural development associated with changing deformation conditions. In particular,  $D_1$  shearing persisted well into the time dominated by  $D_2$  folding, development of the  $S_2^*$  cleavage probably occurred late in  $F_2$  folding, and mylonites formed in some quartzites as late as or later than  $D_3$ .

#### Vadito Group.

General. The present structural investigation concentrated more on Ortega Group rocks than on Vadito Group rocks. This section on Vadito Group structures and fabrics will therefore draw mainly on previous studies by Nielsen and Scott (1979), Holcombe and Callender (1982), and McCarty (1983).

Relict sedimentary structures. Structurally useful sedimentary structures are limited mainly to cross-beds in the Marquenas Quartzite and other smaller orthoquartzite bodies scattered throughout the Vadito Group. All beds dip to the south and most young to the north. The only region where overall stratigraphic younging is inconsistent between the Ortega and Vadito groups is in the Copper Hill area. As noted earlier, in this area Ortega Group rocks young to the

south. Thus, at least locally, the contact between the Ortega and Vadito groups must be a shear zone.

First generation of structures, D<sub>1</sub>. Rocks in the Vadito Group contain an S<sub>1</sub> bedding-parallel foliation defined mainly by aligned micas in quartzose rocks. S<sub>1</sub> was recognized by Nielsen (1972), Nielsen and Scott (1979), Scott (1980), Holcombe and Callender (1982), and McCarty (1983). Associated with S<sub>1</sub> is a locally well-developed down-dip extension lineation (L<sub>1</sub>) defined by aligned quartz, muscovite, and biotite grains on S<sub>1</sub> surfaces, and probably by aligned, constricted clasts in metaconglomerates.

Mylonitic quartzites and highly strained rocks are common along the Ortega-Vadito contact. In recrystallized, mylonitized Marquenas Quartzite, kinematic indicators such as asymmetric clasts indicate that the Marquenas Quartzite has moved up and to the north relative to the Ortega Group. Although the timing of onset of this shearing is unknown, it is consistent with D<sub>1</sub>-D<sub>2</sub> conditions.

Stereographic projections from Holcombe and Callender (1982) and McCarty (1983) show the orientation of S<sub>0/1</sub> in the western Vadito Group (Fig. 7.15a).

In the relatively poorly exposed Vadito Group rocks in the southern map area, no F<sub>1</sub> folds were recognized. Vadito Group F<sub>1</sub> folds have only rarely been described. McCarty (1983) reported rare intrafolial "hooks" in amphibolite

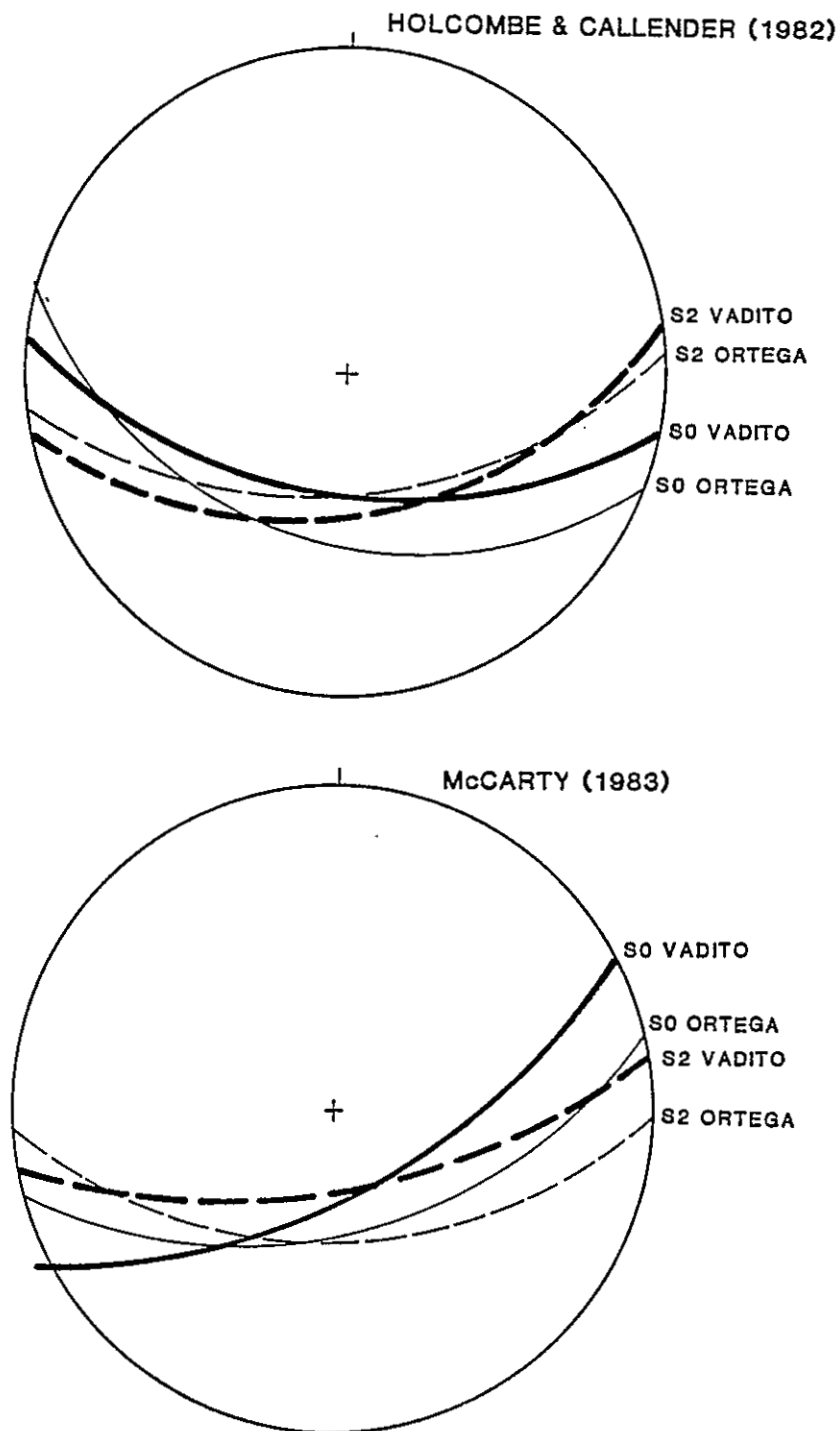


Figure 7.15. Stereographic projection of modal  $S_0$  and modal  $S_2$  in Ortega and Vadito Group rocks. From a) Holcombe and Callender (1982) and b) McCarty (1983). This  $S_2$  may be equivalent to  $S_2^*$  in this report.

lenses which may represent relict  $F_1$  folds. Although Nielsen (1972) proposed that evidence for large, recumbent isoclinal folds is present locally where  $S_1$  cuts tightly folded  $S_0$ , no megascopic or macroscopic  $F_1$  folds have been reported. As in the Ortega Group, the  $D_1$  deformation in the Vadito Group is thought to be characterized by near bedding-parallel shearing, rather than by folding.

Second generation of structures,  $D_2$ . A well-developed, regionally penetrative foliation is the dominant tectonite fabric in most rocks of the Vadito Group. This foliation is a schistosity in some rocks and a crenulation cleavage in others. Although in both style and orientation this foliation is consistent with  $S_2^*$  described in the Ortega Group, previous workers in the southwestern Picuris Range have reported that this cleavage is axial planar to  $F_2$  folds in the Vadito Group. Mesoscopic  $F_2$  folds are relatively common in the Vadito Group, though not as abundant or spectacular as those in the Ortega Group. In the Harding Pegmatite Mine area, where the Vadito rocks are best exposed, several workers have described map-scale folds. Montgomery (1953) mapped a tight, upright synclinal and anticlinal pair. McCarty (1983) described two generations of fold structures, including rare mesoscopic  $F_2$  structures that occur as tight, upright folds in schists. These are equivalent to Montgomery's map-scale fold pair. McCarty

defined six megascopic  $F_2$  folds by structural vergence relationships and lithologic similarities. D.A. Bell (1985) did find opposing cross-beds in small quartzite bodies on either side of the Vadito amphibolite, and reported folds similar to those of McCarty. As described by these workers, the mesoscopic Vadito Group folds are similar in style and orientation to the  $F_2$  structures described above in the Ortega Group.

The question of post- $D_1$  cleavage correlation between Ortega and Vadito group rocks remains unresolved. In the Ortega Group,  $S_2^*$  transects  $F_2$  folds, and  $S_2$  is either weak or reactivated. In the Vadito Group,  $F_2$  folds are cut by an axial planar cleavage ( $S_2$ ) that is identical to the Ortega Group  $S_2^*$ . Is  $S_2^*$  in the Ortega Group equivalent to  $S_2$  in the Vadito Group? Although further analysis of Vadito Group rocks is required to resolve this question, interpretative microstructural relationships in Vadito schist may provide some important clues.

Holcombe (in prep.) has described and interpreted an important set of microstructures in oriented thin sections of Vadito Group quartz-muscovite-biotite schist. Biotite porphyroblasts have overgrown earlier fabric elements in such a way that individual generations of strain can be examined. Holcombe found that a relatively minor  $D_2$  coaxial bulk shortening produced an axial plane cleavage ( $S_2$ ) at  $23^\circ$  to an  $S_1$  schistosity.  $S_2$  is a schistosity rather than a

crenulation cleavage. He interpreted these features to mean that  $S_2$  was pirated from  $S_1$  by grain shape changes, and  $F_2$  microfolds were modified  $F_1$  folds.  $S_2$  transects  $F_1$  folds.

This history is remarkably similar to that previously described in Ortega Group rocks within the map area, with one important difference. In Ortega rocks, a third generation cleavage ( $S_2^*$ ) has reactivated  $S_2$  and transected  $F_2$  folds. Is it possible that in the Vadito schist, the strong  $S_2$  schistosity has obliterated evidence of  $D_1$  fabrics? If so, then the folds in Holcombe's thin section could be  $F_2$ , and the transection cleavage  $S_2^*$ . Further evidence that these folds are actually  $F_2$  folds is based on fold style.  $F_2$  folds are common, tight to isoclinal, and upright, whereas  $F_1$  folds are rare and intrafolial. The folds described by Holcombe are more similar to  $F_2$  than to  $F_1$ . If this is the case, then at least some Ortega and Vadito group rocks have probably experienced identical strain histories in  $D_2$  and  $D_3$ .

Third generation of structures,  $D_3$ . There exists some evidence to suggest that the dominant  $S_2$  cleavage in Vadito Group rocks is equivalent to the  $S_2^*$  in the Ortega Group. At least on the microscopic scale, the dominant cleavage transects  $F_2$ -style folds. If so, then  $S_2$  in the Vadito Group is equivalent to the third generation  $S_2^*$  in the Ortega Group. To date, no good evidence of an Ortega Group

S<sub>2</sub> equivalent has been recognized in Vadito Group rocks. Stereographic projections from Holcombe and Callender (1982) and McCarty (1983) show the orientation of the "S<sub>2</sub>" cleavage in the western Vadito Group (Fig. 7.15b)

Fourth generation of structures, D<sub>4</sub>. The latest phase of ductile structures in Vadito Group rocks are identical to the fourth phase in the Ortega Group. These consist of cross-cutting, non-penetrative crenulations and kinks in schistose rocks.

Southern granitic rocks. Two distinct ages of granitic plutons intrude Vadito Group rocks in the southern Picuris Range. These are the Puntiaquedo Granite Porphyry (1684 ± 1 Ma) and Rana Quartz Monzonite (1674 ± 5 Ma), and the Penasco Quartz Monzonite (about 1450 Ma) (D.A. Bell, 1985). A fourth intrusive body, the Cerro Alto Metadacite, is locally exposed in the southernmost Picuris Range. Both of the older granitic rocks are strongly foliated and contain anastomosing zones of high shear strain. Foliation trends of east to northeast are consistent with the regional trend of S<sub>2</sub> in the Vadito Group. The younger Penasco Quartz Monzonite contains only a weakly developed foliation which is also consistent in orientation with the regional S<sub>2</sub> in the Vadito Group. The Cerro Alto Metadacite contains a strong east-trending penetrative foliation defined mainly by

aligned biotite grains.

Interpretation of relative timing relationships between intrusion of granitic plutons and deformation is complicated by such variables as emplacement depth, grain size, degree of crystallinity, and possible deformation mechanisms. Nonetheless, comparisons based on style and orientation yield approximate timings of pluton emplacement relative to strain. The Rana and Puntiaquedo plutons were certainly emplaced pre-D<sub>2</sub> and possible as early as pre- to syn-D<sub>1</sub>. The Penasco pluton was probably intruded syn- to late-syn-D<sub>3</sub>. The Cerro Alto body was emplaced at least pre-D<sub>2</sub>, and possibly pre-D<sub>1</sub>.

Porphyroblast microstructures. An unusual schist exposed west of the Harding Pegmatite Mine area contains abundant, large (up to 15 cm in diameter) rounded, subhedral porphyroblasts of cordierite. Thin sections across these cordierites show complex microstructures outlined by quartz inclusions (Fig. 7.16). These inclusions delineate two obvious relict foliation trails that unfortunately are not clear enough to show relative timing relationships. The cordierite porphyroblasts are pre-kinematic with respect to the dominant foliation (S<sub>2</sub>) in the rock matrix. One possible interpretation of the microstructures is that they represent relict successive overprinted foliations that formed prior to growth of the cordierite. The inclusion

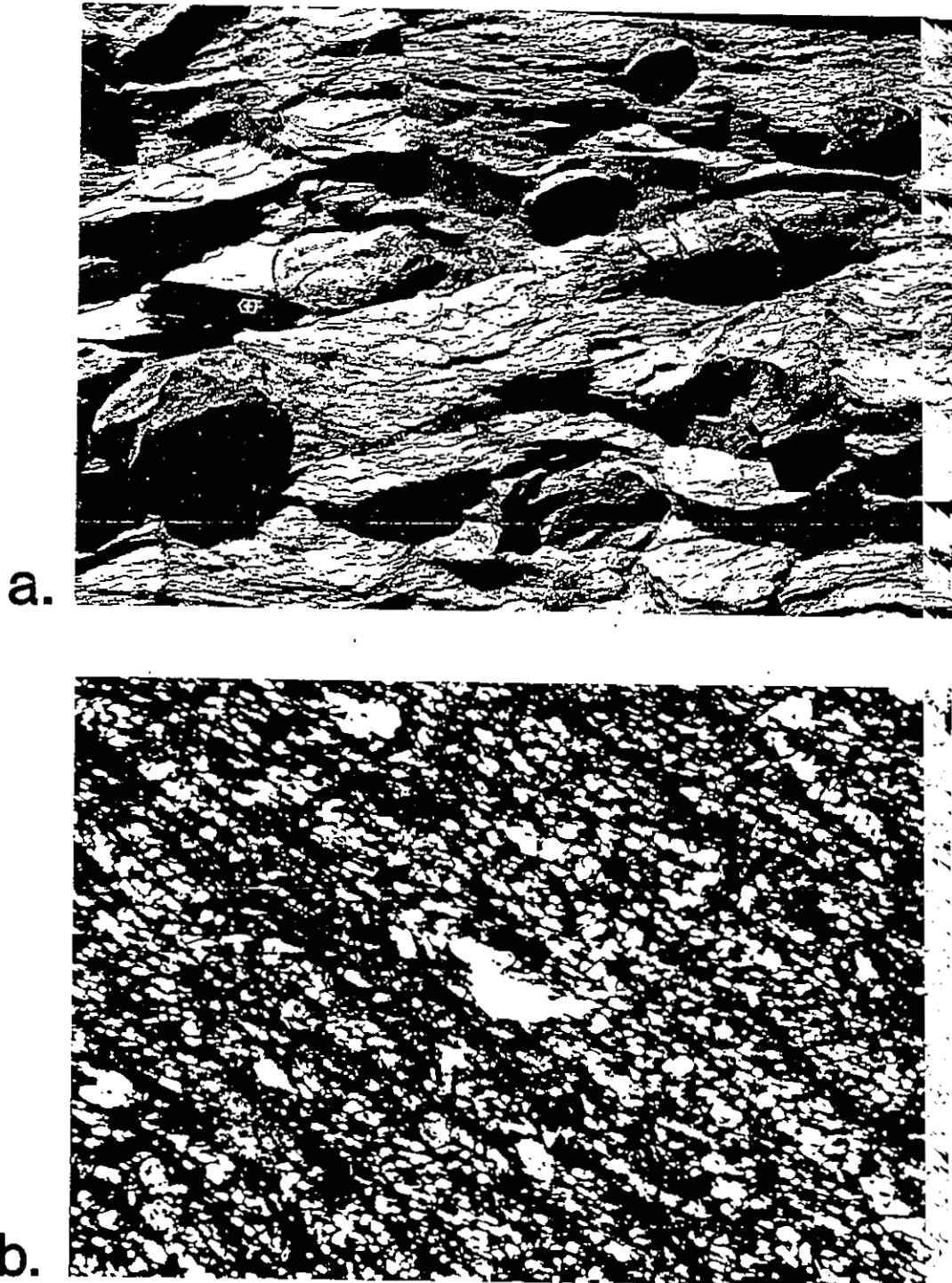


Figure 7.16. a. Photograph of large, rounded cordierite porphyroblasts in Vadito schist, southwestern Picuris Range. b. Photomicrograph of complex microstructures in cordierite porphyroblast defined by elongate quartz inclusions. Field of view is 3.4 mm. See text for discussion.

trails are straight, so porphyroblast growth was rapid relative to the strain rate. Alternatively, they may represent relict  $D_1$  S-C planes (Berthé et al., 1979) or shear bands (White et al., 1980). In either case, these microstructures suggest a complex pre- $D_2$  (or  $D_3$ ) history for these rocks.

Discussion. Although interpretation of structures in the Vadito Group is limited by poor exposures and complex volcanic/sedimentary stratigraphy, the  $D_1$ - $D_2$ - $D_3$  strain history is comparable with that recorded in the Ortega Group. Vadito rocks lack the major folds found in the Ortega Group; the strain instead probably is expressed by many bedding-parallel  $D_2$  faults present in Vadito rocks, yet unrecognized due to the absence of reliable stratigraphy.

The contact between the Ortega Group (Piedra Lumbre Formation) and the Vadito Group (Marquenas Quartzite Formation) is a near bedding-parallel, mylonitic shear zone south of Copper Hill, and along strike to the east, south of Copper Mountain. South of Copper Hill, near state highway 75, a two-meter-wide pod of Pilar Phyllite is caught up in the shear zone. To the east, near the Picuris-Pecos fault, quartzose mylonites lie at and just below the Ortega-Vadito contact.

McCarty (1983) found that the orientation of  $S_0/S_1$  in the Vadito and Ortega groups differed consistently by  $14^\circ$  in

the contact region south of Copper Hill. Holcombe and Callender (1982) and McCarty (1983) noted that the  $S_2$  cleavage that overprints  $S_0/S_1$  is similarly oriented in both groups. They suggested that the apparent structural vergence change measured across the contact was due to the  $S_2$  cleavage overprinting a preexisting  $S_0/S_1$  orientation difference. This implies that the faulting responsible for juxtaposing right-side-up Ortega rocks against overturned Vadito rocks occurred post- $D_1$  and prior to  $D_3$ . One possibility is that ductile faulting was associated with the late  $D_1$  shear and/or the major  $D_2$  folding.

#### Felsic schist at Pilar

General. The felsic schist at Pilar is a homogeneous sequence of feldspathic quartz-muscovite schist and megacrystic quartz-muscovite "quartz-eye" schist exposed in the cliffs near Pilar. These rocks may correlate with the Rio Pueblo Schist located in several isolated outcrops in the southeastern corner of the range. These rocks are well-layered on a range of scales. On a mesoscopic scale, thick sections of pink schist are interlayered with light green schist and white schist. On a finer scale, individual layers differ in the shade of pink or green or white, in the proportion of white megacrysts, and the relative proportions of quartz and muscovite.

The upper pinkish portion of this unit contains anomalously high concentrations of Mn, Fe, Al, and many rare earth elements (Coddington et al., 1983). This geochemical zone may have originated by hydrothermal Mn enrichment of seawater during the waning stages of volcanism, with subsequent deposition of Mn on and with clay minerals (Williams, 1987).

Although it is possible that portions of the felsic schist at Pilar are locally reworked volcanoclastic metasediments, no primary sedimentary structures have been recognized. The contact with the overlying Ortega Quartzite is abrupt, and no transitional rocks are present.

First generation of structures, D<sub>1</sub>. The dominant tectonite fabric in the felsic schist at Pilar is a well-developed, somewhat anastomosing foliation (S<sub>1</sub>) this is parallel to compositional layering in the overlying Ortega Group. This is the earliest fabric recognized in these rocks, and in many areas is the only foliation visible. A south-dipping extension lineation (L<sub>1</sub>) defined by elongate quartz, muscovite, and tourmaline grains is ubiquitous on S<sub>1</sub> surfaces. Although S<sub>1</sub> has the appearance of a mylonitic fabric, in thin section, quartz and muscovite crystals are recrystallized. It is possible that this fabric formed through a process of dynamic recrystallization.

White megacrysts of quartz and rare feldspar in the

schist are interpreted as relict, metamorphosed phenocrysts. Although locally these grains may appear relatively euhedral, all megacrysts show some evidence of internal strain. Typically, the grains are flattened in the foliation plane, and elongate in the extension direction. In the extreme cases, quartz megacrysts are highly flattened with distinct asymmetric tails of dynamically recrystallized quartz grains (Fig. 7.17). These quartz porphyroclasts lie isolated in relatively homogeneous matrix of fine-grained quartz and muscovite. Such asymmetric "eyes" are reliable kinematic indicators of shear (Simpson and Schmidt, 1933; Simpson, 1986; Lister and Snoke, 1984). According to the classification system of Passchier and Simpson (1986), these porphyroclasts are  $\sigma_a$ -type. This type of structure is thought to represent conditions in which the recrystallization rate is large relative to the strain rate (Passchier and Simpson, 1986). Such structures are useful as sense of shear indicators if they have monoclinic symmetry, matrix grain size is small with respect to porphyroclast size, matrix fabric is homogeneous, deformational history is simple, and the thin section is cut parallel to the extension direction. The felsic schist at Pilar samples seem to satisfy all of these requirements. All of the asymmetric porphyroclasts recognized in thin section from schist samples in the Pilar cliffs suggest sinistral shear as viewed towards the west. This implies

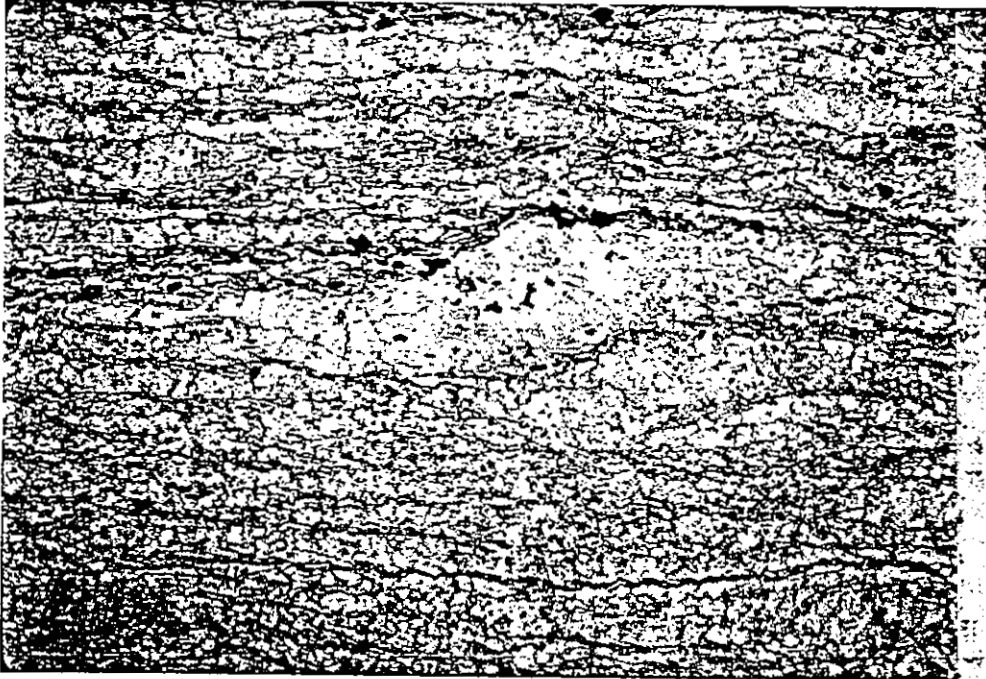


Figure 7.17. Photomicrograph of asymmetric quartz-eye in felsic schist from the Pilar cliffs. Thin section is oriented with south to the right and up to the top. Sense of shear is top to the south (dextral). Section is cut parallel to the extension lineation and normal to the foliation. Field of view is 15 mm.

that the Ortega Quartzite has moved southward over the felsic schist at Pilar. The timing of this movement is unknown.

Immediately below the base of the Ortega Quartzite, near the top of the Pilar cliffs, lie a variety of pink and gray pure quartz mylonites. The mylonitic foliation is bedding-parallel and well-developed quartz extension lineations plunge gently to the south. These structures differ from those in the underlying schistose rocks in an important way. Whereas the schists are well recrystallized with granoblastic textures, the quartzites show no evidence of post-kinematic annealing. The quartz mylonite structures may be younger than the shear structures in the schists. Alternatively, they may have formed synchronously, whereupon for some unknown reason the quartzites successfully resisted later coarsening during peak metamorphism. Preliminary work on sense of shear in these mylonites suggests that the Ortega Quartzite moved southward over the felsic schist at Pilar.

No unequivocal  $F_1$  folds were found in the felsic schist at Pilar. In one locality on the Pilar cliffs, dark, thin interlayers of tourmaline-rich rock pinch out parallel to  $S_1$ . It is not known if these represent intrafolial, isoclinal  $F_1$  folds, original depositional pinch-outs, or local hydrothermal alteration.

Second generation of structures, D<sub>2</sub>. Locally, the dominant S<sub>1</sub> schistosity is overprinted by a slightly oblique crenulation cleavage (S<sub>2</sub>). Intensities of S<sub>2</sub> range from gentle warpings of S<sub>1</sub> to a strong, penetrative crenulation of S<sub>1</sub>. No F<sub>2</sub>-style folds were recognized in the felsic schist at Pilar, apart from these gentle warpings of layering.

Discussion. The contact between Ortega Quartzite and felsic schist at Pilar is a zone of highly concentrated shear strain. A large portion of this strain may have been partitioned into the underlying felsic schist. Textures in the felsic schist are probably due to a combination of an originally well-layered tuff that has been subjected to later layer-parallel shear. Although mesoscopic textures are mylonitic, thin sections typically reveal granoblastic quartz and feldspar textures. This may have been due to dynamic recrystallization during shearing, as is common in many shear zones. The Ortega Group apparently moved southward over the felsic schist at Pilar during some, or much, of the ductile deformation history. Quantitative estimates of displacement along this discontinuous ductile shear zone are not possible, due to the absence of offset marker beds or piercing points.

The presence of the Mn-rich layer at the top of the felsic schist at Pilar suggests that little if any of the

uppermost part of the schist section has been cut out by shearing. In a relatively undisturbed section of the same contact in the Tusas Range, this Mn-horizon sits just below the Ortega Quartzite at the top of a transitional quartzite-schist sequence (Williams, 1987). If transitional rocks ever existed in the Pilar cliffs, they have subsequently been sheared out.

The felsic schist at Pilar and the Vadito Group are nowhere in contact in the Picuris Range, and therefore structural and stratigraphic relationships between the two remain unknown.

#### Eastern Block.

General. The eastern block of the Picuris Range is separated from the western block by the north-trending, high-angle Picuris-Pecos fault. The western block is dominated by two north-south elongate exposures of fine-grained, crumbly granitic rock informally called the Granite of Alamo Canyon. In the southern end of the western granitic block, granitic rocks intrude felsic schists that Montgomery (1963) called Rio Pueblo Schist. Although these schists are similar to felsic schists exposed in the Pilar cliffs, they are more muscovitic and less resistant than the Pilar rocks. A Mn-rich horizon has been mapped adjacent to a pure, cross-bedded quartzite. Although exposures are poor

and the contact zone is nowhere visible, this quartzite appears to be equivalent to the Ortega Quartzite. The manner in which these rocks relate to those in the western block is unclear.

Deformational fabrics in the Granite of Alamo Canyon.

Deformational fabrics are obscure in the Granite of Alamo Canyon. In the southern areas, the strong  $S_1$  foliation in Rio Pueblo Schist is continuous into granitic rocks. Farther north, this foliation is somewhat variable in orientation, perhaps due to reorientation by drag along the Picuris-Pecos fault. Locally, an earlier foliation is visible in some outcrops. This foliation is defined as a vague layering of white versus pinkish bands, and may represent an original flow foliation.

Several fine-grained, lensoid, well-foliated amphibolite bodies lie within the northern half of the western block of the Granite of Alamo Canyon. Granitic rocks around the amphibolites are commonly coarse-grained and laced with epidote mineralization. The age and origin of these amphibolites is unknown.

Deformational fabrics in Rio Pueblo Schist. Structures within these rocks are identical to those in the Pilar cliffs area. Rare kinematic indicators suggest that quartzites moved southward over Rio Pueblo Schist.

Deformational fabrics in Ortega Quartzite. On the southern end of the granitic block, grey quartzites are highly fractured, and bedding and cross-bedding orientations are inconsistent within small areas. The contact with Rio Pueblo Schist is nowhere exposed.

### Summary

Rocks in each of the three major domains have experienced polyphase strain histories. Rocks in the Ortega Group provide evidence for early shearing and faulting during  $D_1$ , major folding and ductile faulting during  $D_2$ , and intense cleavage formation and faulting(?) during  $D_3$ . Rocks in the Vadito Group locally contain evidence for an identical deformational history. Differences include fewer map-scale folds in Vadito rocks, and less transection of  $F_2$  folds by  $D_3$  cleavage. In the Vadito Group, the potential exists for abundant bedding-parallel faults. Rocks in the felsic schist at Pilar are dominated by structures characteristic of bedding-parallel shear strain. In the Picuris Range, this may occur because of the proximity of all felsic schist exposures to the mechanically stiff, overlying Ortega Quartzite during shearing. Pristine quartz ribbon mylonites along the basal Ortega Quartzite contact probably formed late in the metamorphic history. The Ortega

Quartzite has folded primarily by large-scale buckling, whereas thinner, less competent lithologies have folded primarily by passive folding mechanisms.

Although a single polyphase deformational history is sufficient to explain all structures in all three lithostratigraphic groups, structural correlations are difficult due to the fact that each group has responded differently to strain, and each preserves a unique deformational style. These structural variations are summarized in Figure 7.18, and a synoptic stereographic projection is given in Figure 7.19.

Porphyroblast microstructures and P-T microprobe profiling suggest that this deformational history was progressive under prograde metamorphic conditions. This progressive history was punctuated by changes in porphyroblast growth rate and/or strain rate.

The ductile shear structures recognized below the Ortega Group in the northern and southern Picuris Range support the suggestion that neither of these boundaries represents a primary depositional contact. If these contacts are major shear zones, than different rock packages may be juxtaposed across them.

	ORTEGA GROUP	VADITO GROUP	FELSIC SCHIST AT PILAR	
D <sub>1</sub>	S <sub>0</sub>	Primary compositional layering.	Primary compositional layering.	
	S <sub>1</sub>	Bedding-parallel schistosity best preserved in quartz-rich rocks; parallel to ductile shear zones.	Bedding parallel schistosity best preserved in quartz-rich rocks.	Bedding-parallel schistosity mylonitic; dominant foliation; anastomosing; contains asymmetric prophyroclasts.
	L <sub>1</sub>	Well-developed extension lineation in Ortega Quartzite; south-plunging.	Extension lineation, well-developed in Marquesas Quartzite; south-plunging.	Pervasive extension lineation; south-plunging.
	F <sub>1</sub>	Small, intrafolial, isoclines in Piedra Lumbre.	Small, intrafolial hooks in amphibolite.	
D <sub>2</sub>	S <sub>2</sub>	Rare, poorly preserved schistosity or crenulation cleavage in some schists.	Dominant foliation in most rocks; well-developed schistosity or crenulation; NNE-trending. May be equivalent to S <sub>2</sub> * in Ortega Grp.	
	L <sub>20</sub>	Trace of S <sub>0</sub> on S <sub>2</sub> surfaces; difficult to distinguish from L <sub>2</sub> * <sub>0</sub> .	Dominant intersection; trace of S on S <sub>2</sub> . SE-plunging.	
	F <sub>2</sub>	Major folding on all scales; Copper Hill anticline and Hondo syncline; large folds plunge SW; overturned to N.	Major folding in schist and amphibolite; plunge gently SE.	Minor open folds?
D <sub>3</sub>	S <sub>2</sub> *	Dominant foliation; schistosity or crenulation cleavage; transects F <sub>2</sub> folds; NNE-trending; may be equivalent to S <sub>2</sub> in Vadito Group.		Cross-cutting relatively weak spaced cleavage.
	L <sub>2</sub> * <sub>0</sub>	Dominant intersection; trace of S <sub>0</sub> on S <sub>2</sub> ; describes great circle girdle coincident with S <sub>0</sub> on stereogram.	D <sub>3</sub> structures in Ortega Group may be equivalent to D <sub>2</sub> structures in Vadito Group.	Vague trace of S <sub>2</sub> on S <sub>1</sub> .
	F <sub>2</sub>	Minor folds; difficult to distinguish from F <sub>2</sub> .		
D <sub>4</sub>	S <sub>3</sub>	Weak, cross-cutting, non-penetrative crenulation, N to NW-trending; best seen in schists.	Weak cross-cutting, non-penetrative crenulation; N-trending.	Rare, weak, cross-cutting non-penetrative crenulation, N-trending.
	L <sub>30</sub>	Non-penetrative; trace of S <sub>0</sub> on S <sub>3</sub> .	Non-penetrative; trace of S <sub>0</sub> on S <sub>3</sub> .	Non-penetrative, trace of S <sub>1</sub> on S <sub>3</sub> .
	F <sub>3</sub>	Small kink folds in schists.	Small kink folds.	Small kink folds.

Some fabrics in Vadito Group are from McCarty (1983).

Figure 7.18. Summary and comparison of structural fabrics in the Ortega Group, Vadito Group, and felsic schist at Pilar. It is unknown whether S<sub>2</sub> in the Vadito Group is equivalent to S<sub>2</sub> or S<sub>2</sub>\* in the Ortega Group.

## ORTEGA GROUP

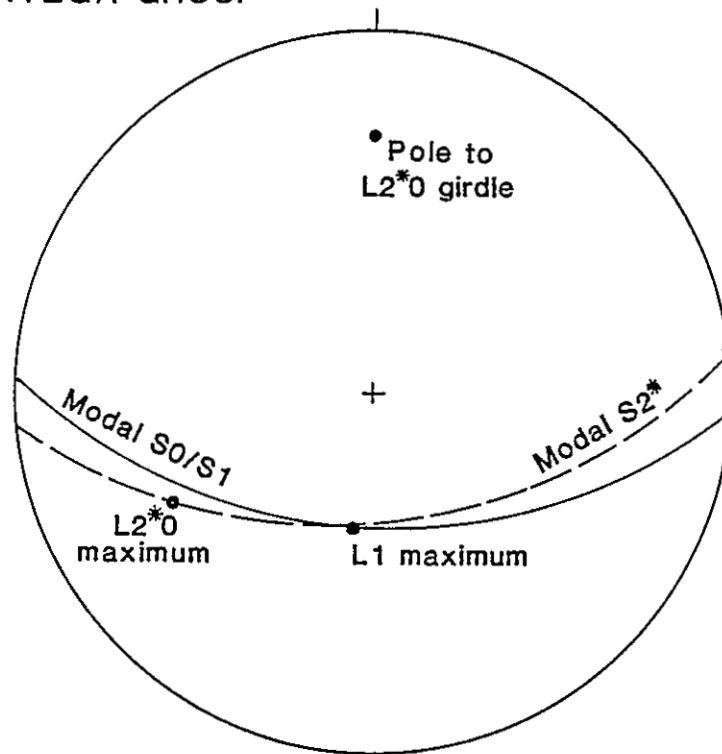


Figure 7.19. Synoptic equal-area stereographic projection of  $D_1$ - $D_2$ - $D_3$  fabric elements in Ortega Group rocks, Picuris Range.

## Contacts Between Lithostratigraphic Domains

## Southern Contact

At Copper Hill, right-side-up Ortega Group rocks and inverted Vadito Group rocks are juxtaposed along a near bedding-parallel, ductile shear zone. There was some component of dip-slip motion along this zone between  $D_1$  and  $D_3$  time. Kinematic indicators in the Marquenas Quartzite suggest that at least one ductile component of motion along this fault zone consisted of north-trending shear (Fig. 7.20). To the east, along the same contact, fault slivers of upper Ortega Group are caught between mylonitic Ortega and Vadito rocks. Near the Picuris-Pecos fault, where Vadito and Ortega rocks appear most stratigraphically continuous, mylonites occur just below the Ortega Quartzite (Fig. 7.21). These data all point to a highly tectonized Ortega-Vadito boundary, perhaps with extended or repeated ductile shearing. The amount of slip along this zone is unknown, but must be considerable, judging from juxtaposition of inverted stratigraphic sections in the Copper Hill area. The direction of motion along this zone could be either northward or southward, but the southerly dip, along with the northerly vergence of all major folds in the range suggests some (late  $D_1$ ?) component of transport to the north. However, it should be noted that in the inner parts



Figure 7.20. Photograph of asymmetric clast in metaconglomeratic Marquenas Quartzite at the Ortega-Vadito contact. Asymmetry suggests dextral shear of Vadito rocks northward over Ortega rocks. Mylonitic foliation dips  $45^{\circ}$  to the south (left in photo).

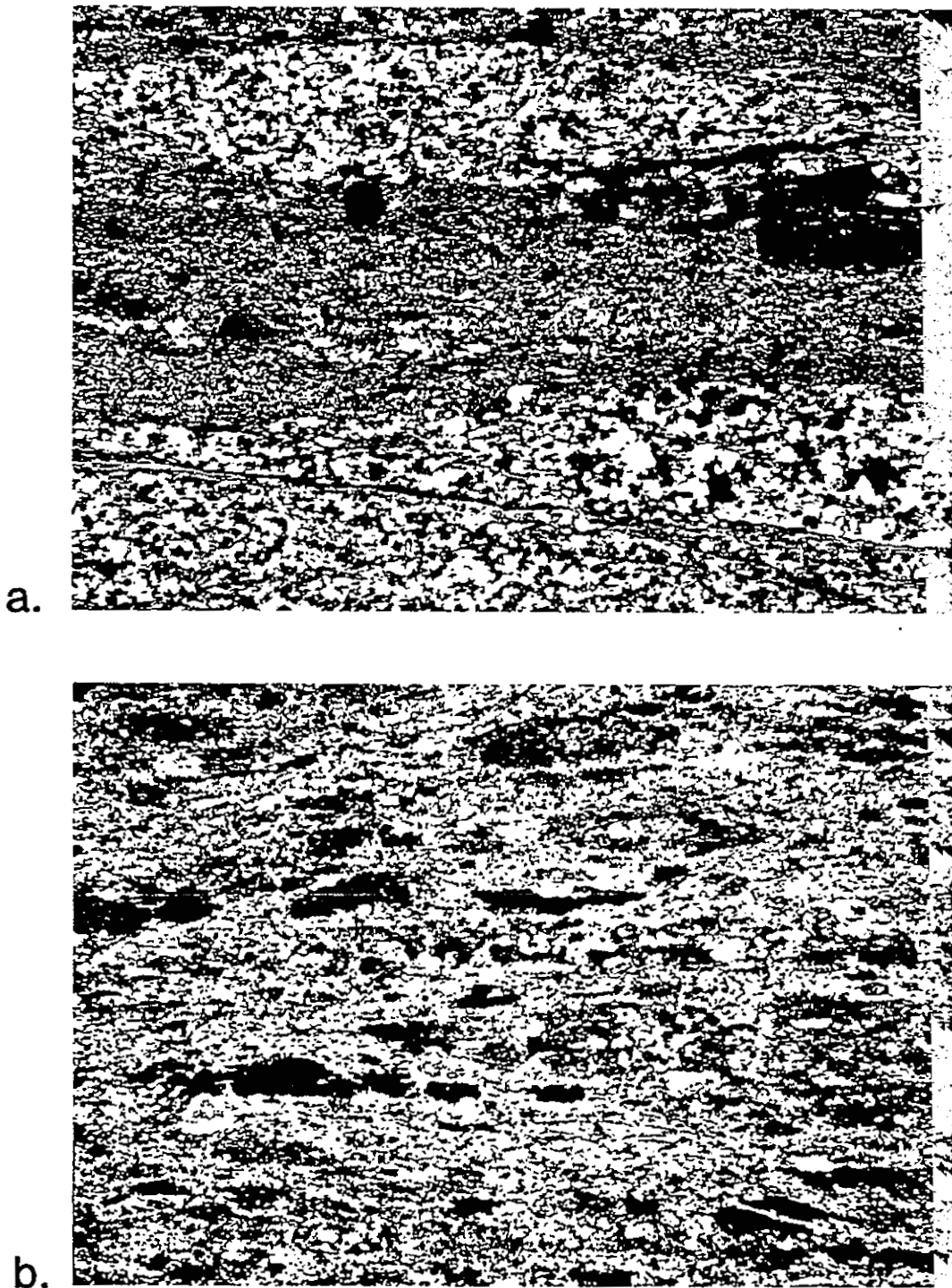


Figure 7.21. Photomicrographs of mylonitic rocks from the Ortega-Vadito contact in the southern Picuris Range.  
a. Marquenas quartzite in the western part of the range. Field of view is 14 mm. b. Vadito schist from the eastern part of the range. Field of view is 16 mm.

of orogenic belts, the steepness of faults may be due to later folding rather than to original orientation (Coward, 1983). Therefore, the pre-D<sub>2</sub> dip of this shear zone may have been any value to either the north or south. Other similar boundaries in northern New Mexico dip to the south, suggesting that unless all such zones have been reversed by later folding, some transport along this zone was northward.

#### Northern Contact

The contact between the felsic schist at Pilar and overlying right-side-up Ortega Quartzite is abrupt and well-exposed in the Pilar cliffs. The quartzite contains small shears near the contact, and thicker, schistose shear zones within the basal quartzite. The felsic schist at Pilar contains mylonitic textures and asymmetric quartz-eyes (see Fig. 7.17). Kinematic indicators suggest that Ortega rocks moved southward over the felsic schist. Because early shear features appear to be especially well preserved in these rocks, this southward shear may represent the earliest observed component of strain. The northward transport deduced along the southern boundary may therefore be a later component of D<sub>1</sub> motion. Alternatively, the geometry of the structures involved may be more complicated than imagined. Perhaps movements along these shear zones were synchronous, but occurred in a complex thrust or back-thrust setting.

Fine-grained quartz ribbon mylonites at the Ortega Quartzite-felsic schist at Pilar contact show no sign of post-kinematic recrystallization (Fig. 7.22). These rocks probably represent syn- to post-D<sub>3</sub> mylonites in a zone that has experienced prolonged or repeated ductile simple shear.

It is unknown how the strain was distributed among the contact, the schists, and the quartzite. A geochemical marker horizon that characterizes the upper 100 m of the felsic schist at Pilar (and equivalent rocks regionally) is present in these outcrops, suggesting that little if any of the uppermost part of the felsic schist section has been removed by shearing.

#### Picuris-Pecos Fault

A third important shear boundary that juxtaposes different Precambrian rock types is the north-trending, high-angle Picuris-Pecos fault. This fault separates Ortega Group on the west from the Granite of Alamo Canyon on the east. Ortega Group metasediments are bent southward near the fault (Plate 1). Because no apparent fracturing is associated with this drag folding, dextral movement probably occurred during the Proterozoic ductile deformation history. A breccia zone of mixed Ortega Group lithology, which occurs along most of the fault zone in the map area, probably represents a later, more brittle component of motion.

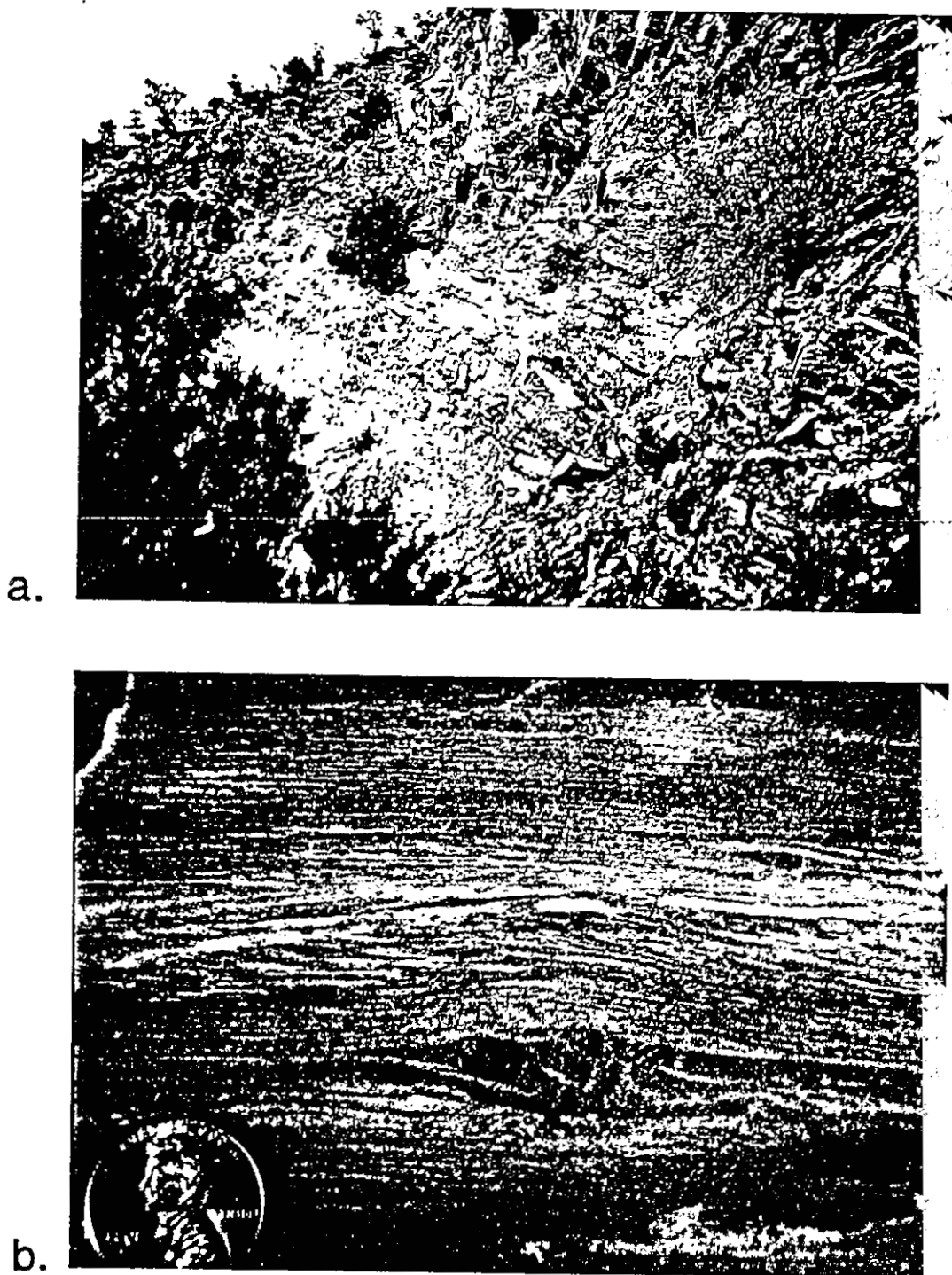


Figure 7.22. a. Photograph of contact between gray Ortega Quartzite above and pink felsic schist below. Mylonitic quartz ribbon quartzites occur within the contact zone. b. Photograph of mylonitic quartzite from within the contact zone.

## Discussion

All contact zones of Ortega Group with underlying rocks have been highly tectonized along bedding-parallel ductile shear zones. In the southwestern Picuris Range, where displacement must be large, primary stratigraphic relationships between Ortega and Vadito are probably not preserved. In the north, where displacement need not be large, a primary depositional stratigraphy between Ortega and felsic schist is probably more closely preserved. However, in the north, the transitional quartzite-schist sequence seen elsewhere in northern New Mexico is absent.

The fact that the exact natures of these zones remain unknown precludes the possibility of developing a unique model for the evolution of the Picuris Range. Nevertheless, a listing of important geological constraints can help minimize the number of potential models.

## Structural Synthesis

### Stratigraphic and Structural Constraints

1) There are three supracrustal rock packages present in the Picuris Range: a) a heterogeneous sequence of bimodal volcanic, volcanoclastic, and clastic sedimentary

rocks (Vadito Group); b) altered, metamorphosed felsic volcanic rocks deposited around 1700 Ma(?) (felsic schist at Pilar); and c) a transgressive sequence of sediments deposited (on the felsic schist at Pilar?) in a shallow marine, continental shelf environment (Ortega Group).

2) It is unknown how the Vadito and felsic schist units relate stratigraphically to the Ortega Group.

The boundary between the Ortega Group to the north and Vadito Group rocks to the south is a near bedding-parallel, high-angle shear zone that might have been active over much of the deformation history. Basal Ortega Quartzite overlies the felsic schist at Pilar along a zone of high shear strain. Although the amount of bedding-parallel displacement that has occurred along this low-angle shear zone is unknown, possibly, the felsic schist at Pilar occupies an approximately correct stratigraphic position with respect to the Ortega Group.

3) The Vadito Group and felsic schist at Pilar are not juxtaposed anywhere. Both lie structurally below the basal Ortega Quartzite.

4) Granitic plutons intrude some Vadito Group rocks, but nowhere intrude Ortega or felsic schist at Pilar units.

5) Older granitic plutons are highly tectonized, whereas the youngest pluton is only weakly foliated. These older plutons are at least syn-D<sub>2</sub>, and may be as early as pre- or syn-D<sub>1</sub>. The youngest pluton is weakly foliated, and is probably syn- to late-syn-D<sub>3</sub>.

6) All rocks appear to have experienced lower to middle amphibolite facies metamorphism, with peak metamorphic conditions of about 4 kb and 500°C, coinciding with or slightly post-dating S<sub>2</sub>\* cleavage development.

7) Supracrustal rocks have undergone a common progressive deformational history that resulted in the formation of three major generations of structures.

D<sub>1</sub> is characterized by localized zones of high simple shear strain, rather than by large fold structures.

D<sub>2</sub> involved macroscopic folding in the Ortega Group, moderate folding in the Vadito Group, and minor folding in the felsic schist at Pilar. Extensive, near-bedding-parallel faulting probably accompanied D<sub>2</sub>.

D<sub>3</sub> was characterized by formation of a strong cleavage (S<sub>2</sub>\*) that slightly transects Ortega Group F<sub>2</sub> folds, and is now the dominant cleavage in most schistose rocks of the Ortega and Vadito groups. S<sub>2</sub>\* reactivated and cannibalized preexisting S<sub>1</sub> and S<sub>2</sub> foliations. The effects of D<sub>3</sub> on the felsic schist at Pilar were minor.

All three of these fabric forming events developed under conditions of approximately coaxial principal strain axes.

8) The major structure in the Picuris Range is the gently west-plunging, tight to isoclinal, northward verging  $F_2$  Hondo syncline in the Ortega Group.

The Copper Hill anticline is thought to be a minor, parasitic fold on the Hondo syncline that has been uplifted along high-angle  $D_2/D_3$  reverse faults.

9) In the north-central Picuris Range, the Ortega Quartzite is doubled in thickness by what may have been a  $D_1$  or early  $D_2$  fault imbrication.

10) Kinematic indicators such as asymmetric "quartz-eyes" in the felsic schist at Pilar suggest a component of movement of Ortega Quartzite southward over the felsic schist at Pilar. This is opposite to the northward vergence sense indicated by kinematic indicators along the Ortega-Vadito contact and  $D_2/D_3$  folds in the Ortega and Vadito groups. The south-directed movement may represent a later component of motion than the northern movement.

## Possible Models

The above constraints limit the number of possible kinematic/stratigraphic models for the evolution and joining of the three major lithostratigraphic terranes in the Picuris Range. Models presented in the following two sections are founded on the following two major points:

1) Different rock sequences occupy identical structural positions beneath Ortega Group on the northern (felsic schist at Pilar) and southern (Vadito Group) limbs of the Hondo syncline.

2) There exist five general possibilities for the nature of the relationship between the Ortega Group, the felsic schist at Pilar and the Vadito Group:

- a) all three groups are related in an original, primary stratigraphic manner. Within this model, there are three possible stratigraphic relationships:
- b) Ortega and felsic schist are related in an original, primary stratigraphic manner;
- c) Ortega and Vadito are related in an original, primary stratigraphic manner;
- d) Vadito and felsic schist are related in an original, primary stratigraphic manner;
- e) none of the three are related in an original, primary stratigraphic manner.

Models invoking these five general possibilities are

presented in the following kinematic/stratigraphic models section, and then critically examined in the discussion that follows. All models involve a complex interaction of faulting, shearing, and folding.

Well-constrained stratigraphic relationships in nearby ranges may aid in limiting the number of variables in these models. In the Tusas Range, in less tectonized regions, the Ortega Group appears to grade stratigraphically downward into a felsic metavolcanic-metasedimentary sequence of rock characterized by quartz-muscovite "quartz-eye" schists (Williams, 1987). Portions of this unit resemble the felsic schist at Pilar of the northern Picuris Range, and the Mn-rich marker horizon is present in both places at the top of the uppermost felsic sequence. If this represents a regionally-developed stratigraphically continuous package, then all models that do not place the felsic schist at Pilar stratigraphically below the Ortega Group can be eliminated. Two of the five general possibilities can thus be eliminated: c) and e). Additionally, one of the three subdivisions within possibility a) can be eliminated. It is important to note that although the correct stratigraphy may have Ortega Group resting stratigraphically on felsic schist at Pilar, in the northern Picuris Range the contact between the two is sharp and has been tectonized. It is not known whether in this area the original contact is abrupt rather than transitional as it is in the Tusas Range, or whether

some portion of the upper portion of the felsic schist at Pilar has been faulted out. It should also be noted that other portions of the "Vadito Group" in the Tusas Range resemble lithologies in the Vadito Group of the southern Picuris Range (M.L. Williams, personal communication, 1987).

One further point with respect to the likelihood of these two lithostratigraphic groups representing an original primary stratigraphic sequence concerns tectonic settings. The progression from felsic volcanism (felsic schist at Pilar) to transitional rocks (absent in the northern Picuris Range) to stable shelf sedimentation (Ortega Group) is common in modern extensional tectonic settings. On the other hand, the progression from mafic volcanism and graywacke deposition (Vadito Group of southern Picuris Range, exclusive of the Marquenas Quartzite) to stable shelf sedimentation represents an uncommon evolution of tectonic settings. Thus, modern examples of tectonic progressions are consistent with an interpretation that favors development of the felsic schist at Pilar/Ortega Group stratigraphy.

Each of the remaining models includes some component of  $D_1$  sub-horizontal ductile shear strain, which was concentrated below the Ortega Quartzite. On the scale of the Picuris Range, this shearing may or may not have resulted in significant disruption of the stratigraphic section by low-angle ductile faulting. Although the figures

depicting possible kinematic histories do not show these structures, all models include the possibility of such faulting.

Model a) All three major rock groups are stratigraphically related. In this case, there are two possible stratigraphic scenarios:

1) Ortega is in primary stratigraphic contact with underlying felsic schist at Pilar, which is in primary stratigraphic contact with underlying Vadito.  $D_1$  sub-horizontal shearing concentrated beneath the Ortega Quartzite is followed by  $D_2$  folding and syn- or post- $D_2$  reverse faulting along the southern limb of the Hondo syncline (Fig. 7.23). This ductile fault brings Vadito Group rocks against Ortega Group in the southern Picuris Range. Locally, in the Copper Hill area, southward-younging Ortega Group rocks on the southern limb of the parasitic Copper Hill anticline are juxtaposed against inverted Vadito Group rocks.

Advantages:

- a) consistent with the observed geology;
- b) permits the possibility of complex faulting in the Vadito Group separating Marquenas Formation, schist, and amphibolite;
- c) permits the Vadito Group to be any age older than the felsic schist at Pilar, and permits

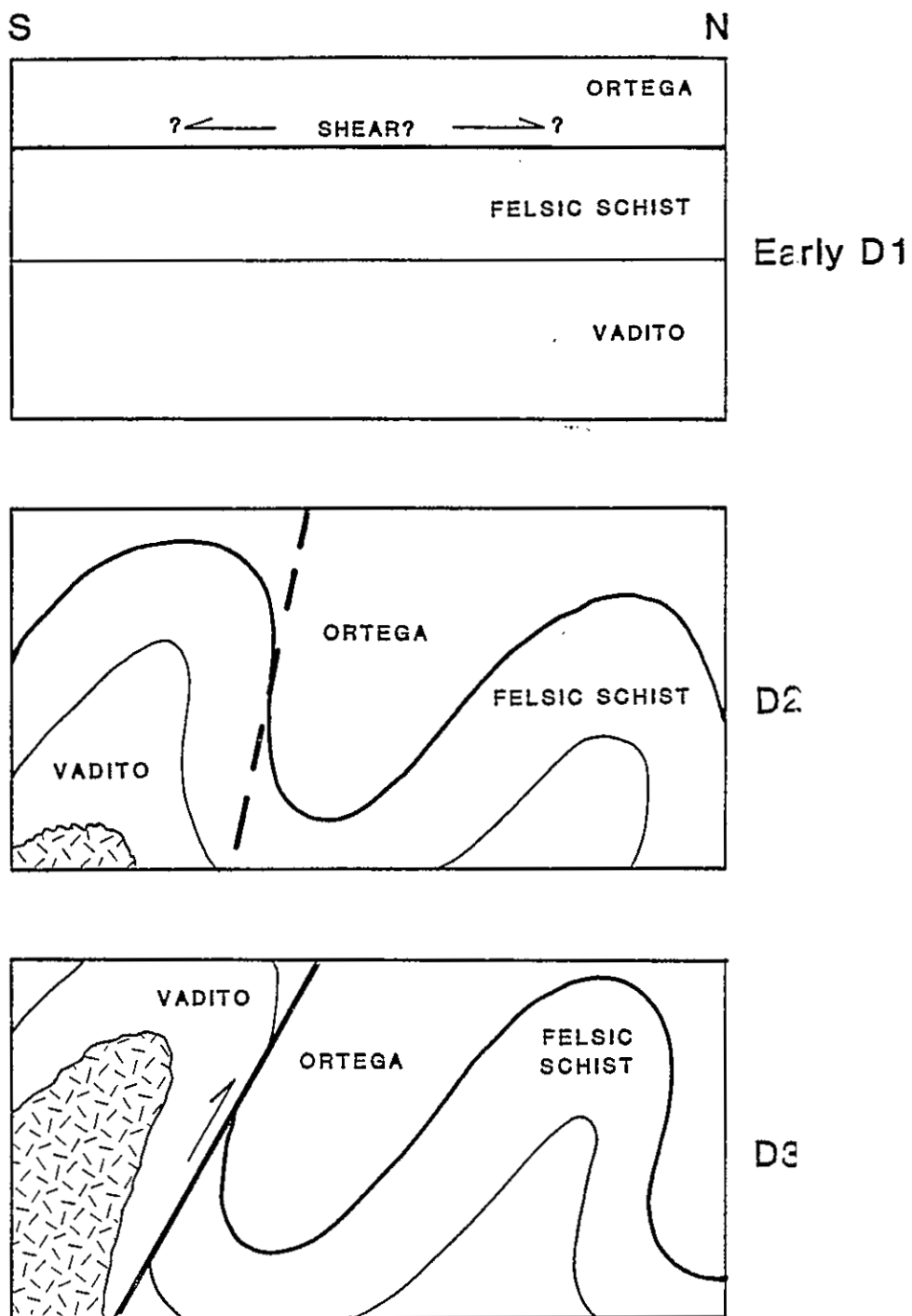


Figure 7.23. Stratigraphic/kinematic model a1. See text for discussion.

their contact to be either conformable or unconformable.

Problems:

a) requires that no granitic intrusions penetrated through the Vadito Group into the overlying felsic schist. Although this is no problem with respect to the pre- or syn-D<sub>1</sub> 1680 Ma plutons, it is more of a problem with respect to the syn-D<sub>3</sub> 1450 Ma pluton. During intrusion of the 1450 Ma pluton, country rocks were already folded, and therefore intrusions could have penetrated Vadito, felsic schist, and even Ortega rocks assuming same level of emplacement.

2) Ortega is in primary stratigraphic contact with an underlying, stratigraphically complex Vadito/felsic schist metavolcanic terrane. This model is similar to the above model, but differs in that it calls for north to south lithologic variations of a stratigraphically equivalent felsic schist at Pilar/Vadito Group (Fig. 7.24). It assumes that an original facies variation existed from a thick felsic metavolcanic section in the north to a mixed metasedimentary, mafic-felsic metavolcanic section to the south. The felsic schist and Vadito are stratigraphic equivalents, perhaps analogous to a variation from

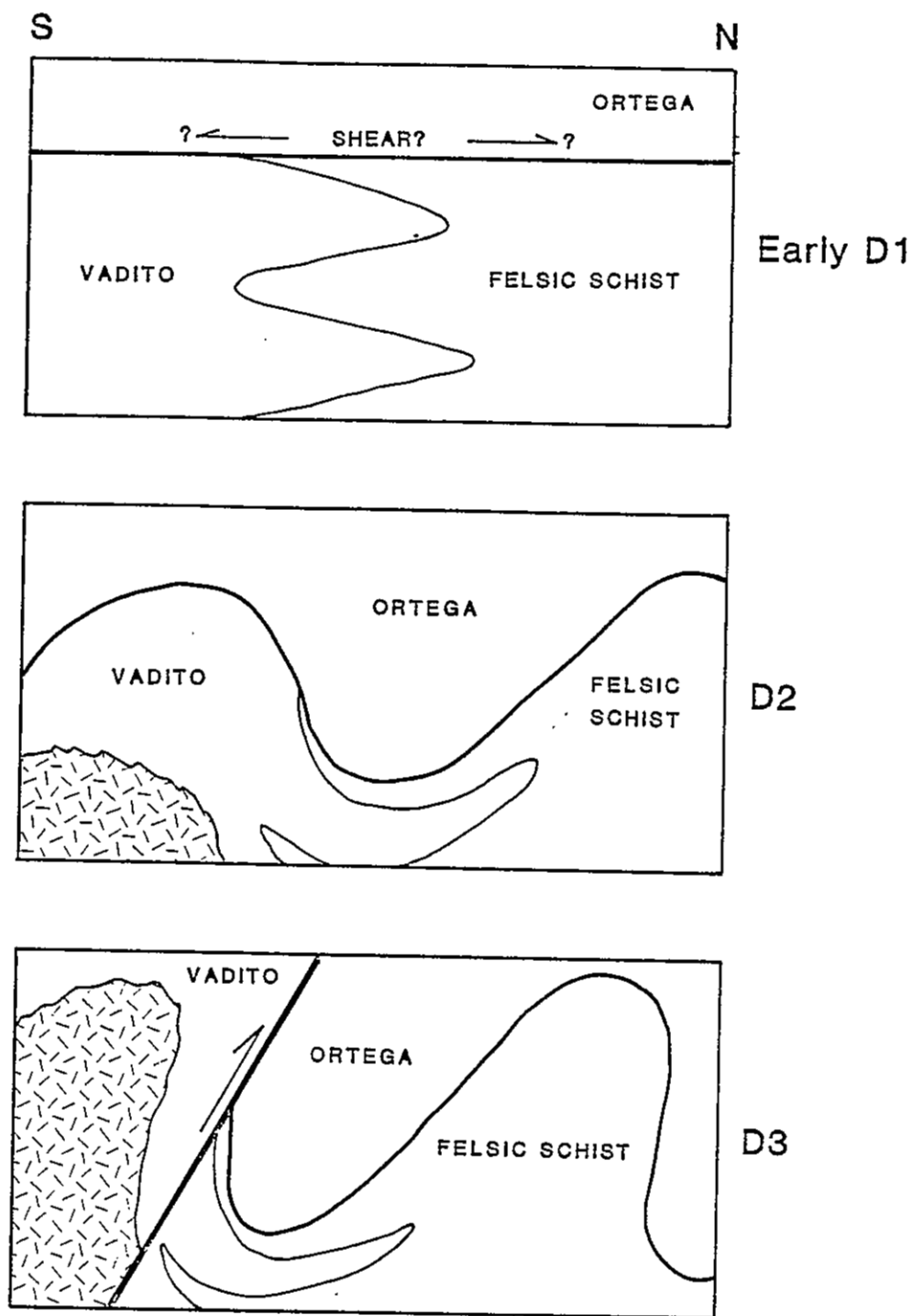


Figure 7.24. Stratigraphic/kinematic model a2. See text for discussion.

homogeneous cauldron fill to heterogeneous outflow sheets. This sequence was blanketed by Ortega Group sediments. Folding of the section would result in the observed apparent lithologic asymmetry. Reverse faulting along the southern limb of the Hondo syncline juxtaposes inverted Vadito and right-side-up Ortega rocks.

Advantages:

- 1) consistent with the observed geology.

Problems:

- 1) requires a special case where the fold hinge corresponds with the facies change.

Model b) Ortega and felsic schist are in original stratigraphic contact. A major fault is present between the Ortega/felsic schist package and the Vadito Group (Fig. 7.25). This south-dipping fault transported the Vadito Group northward over the Ortega Group in the southern Picuris Range. The timing of this fault can range anywhere from earliest  $D_1$  to latest  $D_2$ . Displacement along the fault must have been large.

Advantages:

- 1) consistent with the observed geology;
- 2) the Vadito Group can be older, younger, or identical in age to the Ortega/felsic schist sequence;
- 3) the Vadito Group can itself be a composite

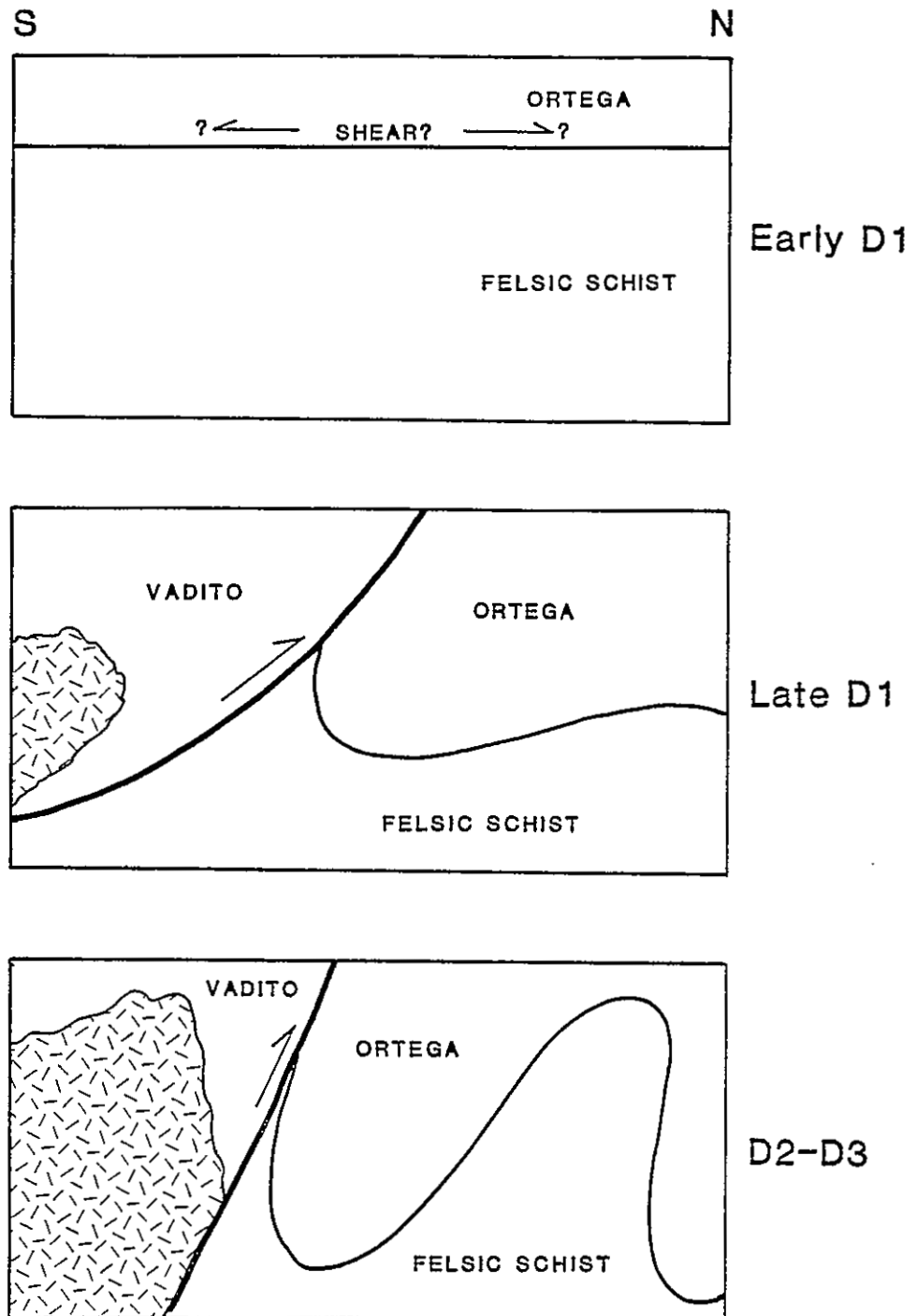


Figure 7.25. Stratigraphic/kinematic model b. See text for discussion.

terrane of Marquesas Quartzite Formation,  
Vadito schist, and Vadito amphibolite;

- 4) granitic plutons have intruded the Vadito Group only, because the Vadito and Ortega/felsic schist groups were not adjacent during granitic emplacement.

Problems:

- 1) no problems identified.

Model d) Felsic schist and Vadito are in primary stratigraphic contact. The manner in which the felsic schist and Vadito Group are related is not specified for this model. A major thrust fault must exist between the Ortega Group and the felsic schist/Vadito package (Fig. 7.26). In this model the Ortega Group was thrust (southward?) over the metavolcanic felsic schist/Vadito terrane.

Advantages:

- 1) consistent with observed geology.

Problems:

- 1) granitic rocks might be expected to have intrude both the felsic schist and Vadito sequences.

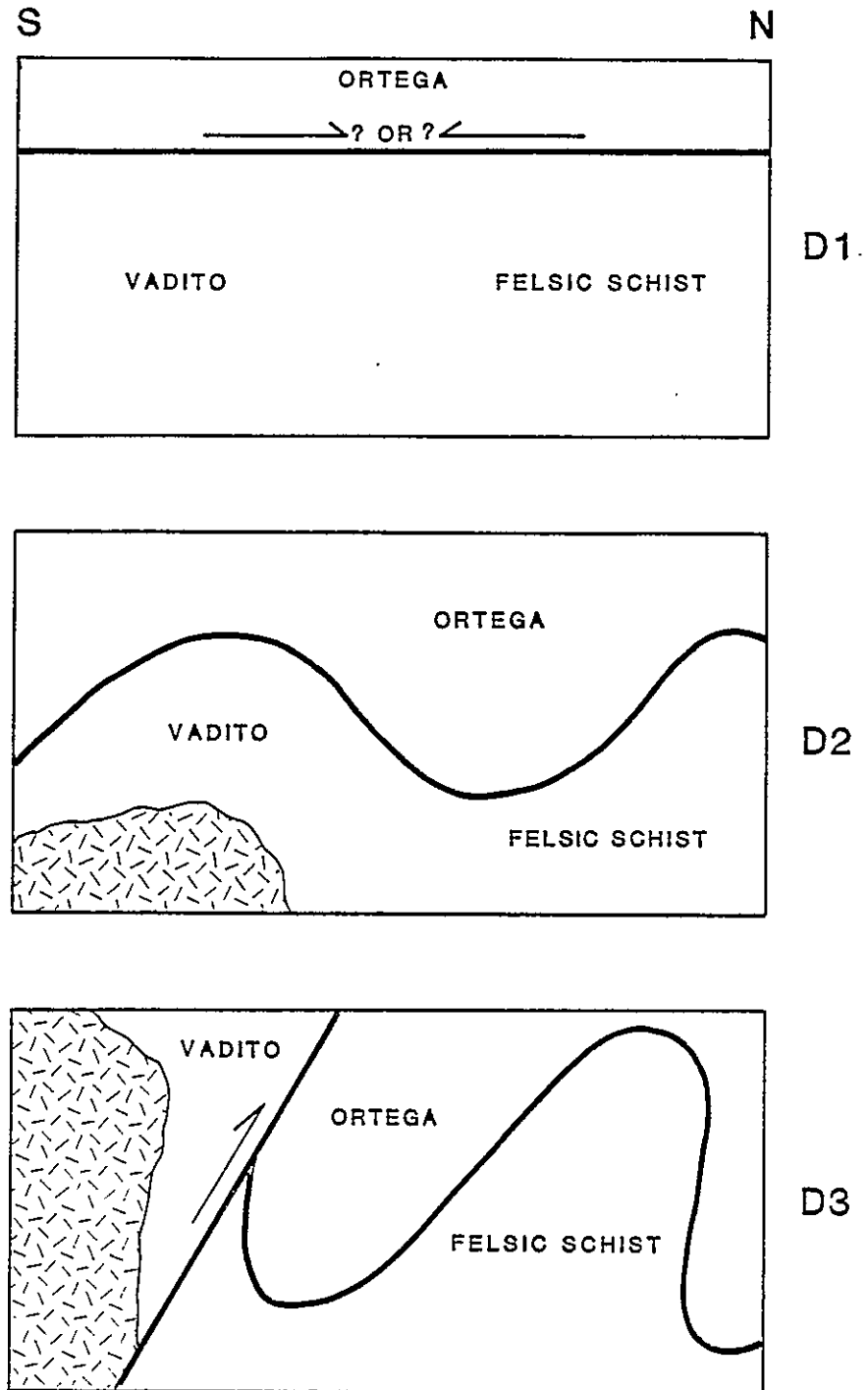


Figure 7.26. Stratigraphic/kinematic model d. See text for discussion.

## Discussion

Although each of these models is adequate to explain the observed geologic relationships in the Picuris Range, one most easily accomodates all data sets, and displays no serious drawbacks. This is model b), in which the Vadito Group has been displaced northward over the Ortega/felsic schist package along some type of ductile shear zone. During faulting, the Vadito Group may have either moved primarily vertically from a deeper structural level, or moved mainly horizontally along a flat shear zone. Both scenarios provide an explanation for the fact that plutons intrude Vadito rocks and do not intrude Ortega/felsic schist rocks. Ortega/felsic schist rocks were spatially removed from or above the zone of granitic emplacement. Similar models of evolution of Precambrian rocks in the Picuris Range have recently been published by Bauer (1987) and Holcombe et al. (1985). As a variation on this model, as the Vadito Group moved northward over the already folded Ortega Group, the Ortega Group was correspondingly moving northward over the felsic schist. This idea is borrowed from a kinematic model developed by Williams (1987) for similar rocks in the Tusas Range.

Realizing that all of these models contain common structural elements is probably more important than attempting to rigidly defend one particular model. All

possible models involve deformational histories containing ductile shearing, folding, and faulting. Early shearing was low-angle and near bedding-parallel. Some imbrication may have occurred. Shearing apparently continued well into (and perhaps after) the phase of deformation dominated by upright folding. Coincident with the folding, reverse faulting disrupted stratigraphy locally and may have juxtaposed lithotectonic units.

The major juxtaposition of lithostratigraphic groups probably occurred early in the history, when shearing and horizontal transport dominated. Most stratigraphic-structural complications that occurred within the major rock groups were related to folding and ductile reverse(?) faulting.

During shearing, high shear strains were concentrated below the Ortega Quartzite and within schists. All models can accommodate reactivation of mylonitic zones or progressive mylonitization along the basal Ortega Quartzite throughout the deformation history. During crustal shortening, thick, mechanically stiff layers such as the Ortega Quartzite (and the Marquenas Quartzite?) responded by forming large-scale buckle folds and local imbrications. More thinly interbedded layers with contrasting competencies responded in a more ductile manner by complex, noncylindrical, passive folding. Williams (1987) concluded that strain development was profoundly dependent on

proximity to the Ortega Quartzite in the Tusas Range. This is probably true in the Picuris Range as well.

This deformational history occurred in a Proterozoic, mid-crustal setting at depths of approximately 10 to 15 km. A complex interaction of shearing, folding, and faulting may be characteristic of many such orogenic events of any age. Crustal shortening in the northern Appalachian belt, and the Alpine and Himalayan belts has resulted in the developments of similar fault/fold/shear structures.

Williams (1987) and Grambling et al. (in prep.) have identified very similar strain histories in correlative lithostratigraphic terranes in the Tusas, Taos, Rio Mora, and Truchas areas. Both lithologic associations and subsequent deformational environments may have been laterally continuous over much of northern New Mexico during some of early Proterozoic time.

## CHAPTER 8. DEPOSITIONAL HISTORY AND TECTONIC SETTING

### Introduction

The three major rock packages in the Picuris Range will be treated separately for several important reasons. Dominant lithologies (and presumably protoliths) differ among the three groups. The Vadito Group contains metavolcanic, metavolcaniclastic, and clastic metasedimentary rocks; the felsic schist at Pilar consists of felsic metavolcanic rocks; and the Ortega Group is composed of clastic metasedimentary rocks. Structural styles also differ among the three sequences, and all major contacts are ductile shear zones. Lastly, the Vadito and felsic schist at Pilar units are nowhere in contact in the Picuris Range.

The Vadito Group presents an additional complexity in that it may contain several different rock packages separated by bedding parallel shear zones, or unconformities. However, crucial contacts between metavolcanic and clastic metasedimentary packages are poorly exposed in the southern Picuris Range, and much work remains to be done.

Deductions concerning possible tectonic settings for terranes containing igneous rocks are facilitated by

comparative analysis of rock chemistry. To date, no geochemistry on supracrustal rocks in the Picuris Range has been published. In lieu of such geochemistry, evidence for tectonic settings of major rock packages must come from a consideration of individual lithologic assemblages and their depositional environments.

### Depositional Environments

#### Vadito Group

In the southwestern part of the Picuris Range, the three major Vadito Group units, from north to south, are the Marquenas Quartzite, the Vadito schist, and the Vadito amphibolite. In the southeastern part of the range, a major component of felsic schist is present, and all lithologies are more complexly interlayered than to the west.

The Marquenas Quartzite consists of polymictic metaconglomerate and texturally immature quartzite. Soegaard and Eriksson (1986) suggested that the orientation of trough cross beds in the Marquenas Quartzite indicates a provenance to the south of the Picuris Range. Shearing and folding may have invalidated a straightforward interpretation of transport direction in this unit. Clasts in metaconglomerates consist of approximately 66 percent

quartzite, 34 percent felsic schist, and small amounts of vein quartz, mafic schist, and calc-silicate rock. The quartzite clasts characteristically are devoid of aluminum silicate minerals, and were therefore not derived from the Ortega Quartzite. The geographic source for all of the material in the Marquenas Quartzite is unknown. These rocks were deposited on an alluvial plain by a number of braided-fluvial processes (Soegaard and Eriksson, 1986).

The Vadito schist unit includes a large variety of fine-grained phyllitic schists and micaceous quartzites, interlayered with lesser amounts of felsic schist, amphibolite, and quartzite. Rare cross beds are present in the quartzites. The Vadito schist has been interpreted to represent a sequence of fine- to medium-grained graywackes, micaceous quartz sandstones, pelitic shales, minor basalts flows, and volcanoclastic sedimentary rocks that has been intruded by minor felsic and mafic sills and dikes (McCarty, 1983). A likely depositional setting for these rocks is in a continental shelf basin or intracratonic basin in which the accumulation of graywacke material is punctuated by influx of quartz sands, pelitic muds, volcanoclastic sediments, and minor volcanic rocks.

The Vadito amphibolite of the southwestern Picuris Range consists of two main amphibolite bodies; a large body to the south of the Vadito schist, and a smaller body to the southeast. At least five lithologic units can be mapped out

in the Vadito amphibolite (McCarty, 1983). Based on pillow structures, pillow breccias, and relict amygdules, Long (1974) interpreted these amphibolites to represent metamorphosed mafic volcanic rocks. McCarty (1983) suggested the Vadito amphibolite unit was a volcanic sequence of mafic flows and volcanoclastic sedimentary rocks intruded by felsic dikes and sills. The pillow structures reported by Long (1974) indicate that at least some of these mafic flows erupted in a submarine setting.

The contact between the Marquenas Quartzite and the Vadito schist is nowhere well-exposed. If the boundary represents a primary depositional surface of conglomerate atop graywacke, then the contact must be unconformable due to the disparity of depositional environments between Marquenas Quartzite and Vadito schist. In the uppermost Vadito schist a calc-silicate horizon is present. If the Marquenas Quartzite and Vadito schist are unconformable, then this horizon could represent a weathering surface on the top of the eroded Vadito schist section.

The contact between Vadito amphibolite and Vadito schist is generally poorly exposed. In some areas the two are separated by a bedding-parallel fault zone. Based on the presence or absence of cross-cutting granitic plutons, it has been suggested that an unconformity separates the amphibolite and schist units (D.A. Bell, 1985). This discontinuity could just as easily represent an early shear

zone. To date, no structures indicative of early, localized shearing have been identified between the Vadito amphibolite and the plutons that intrude the Vadito schist.

Alternatively, this contact may represent a continuous depositional contact. A progression from accumulation of mafic volcanics and volcaniclastics (Vadito amphibolite) to deposition of graywackes with minor quartzose sediments and intrusions (Vadito schist) represents a typical evolution of depositional settings. Further work is clearly needed to resolve stratigraphic and structural relationships within the Vadito Group. For the following tectonic discussion, the Vadito Group ( $\pm$  the Marquenas Quartzite) will be considered as a single lithotectonic package.

#### Felsic schist at Pilar

In the Pilar cliffs, the felsic schist at Pilar is a texturally monotonous sequence of feldspathic, quartz-eye, quartz-muscovite schist. The only appreciable variation in mineralogy is due to Mn and rare earth element enrichment in the uppermost 30 m of the section (Coddington et al., 1983). Textures throughout the sequence are consistent with a felsic volcanic protolith such as rhyolitic ash-flow tuff. Although no geochemistry has been reported for these rocks, rocks with similar texture, mineralogy, and stratigraphic

position from the Tusas Mountains exhibit trace-element chemistries similar to modern felsic volcanic rocks in continental rifts or continental margin back-arc basins in or near continental crust (J.M. Robertson, personal communication, 1987).

### Ortega Group

Of the three supracrustal packages in the Picuris Range, the sedimentology of the Ortega Group is the most studied, and its depositional setting is best documented. The Ortega Group consists of a thick basal quartzite which is overlain by interlayered pelitic schists and quartzites, black graphitic phyllite, and laminated pelitic phyllites and schists. Pervasive primary sedimentary structures confirm a sedimentary origin for these rocks, and provide reliable stratigraphic younging information. The Ortega Group was deposited on a broad, continental, shallow marine shelf during an overall transgression (Soegaard and Eriksson, 1985). Soegaard and Eriksson (1985, 1986) suggested that the shelf sloped gently to the south and southeast, and received a continuous influx of sediment from the north and northeast during prolonged subsidence. Sedimentologic evidence for shallow gradients in Ortega Group rocks throughout northern New Mexico suggests that the shelf break must lie to the southeast of the Truchas-Rio

Mora area (Soegaard and Eriksson, 1985). Soegaard and Eriksson (1986) concluded that the basal quartzite of the Ortega Group accumulated in a stable tectonic environment.

## Discussion

### Constraints on tectonic settings

Relative and absolute ages of rocks in the Picuris Range only loosely constrain possible tectonic settings of the three major rock groups. With one possible exception, no supracrustal rocks in the Vadito Group have been dated. The possible exception is the Cerro Alto Metadacite (ca. 1673 Ma, D.A. Bell, 1985), a shallow to extrusive body which appears to intrude the Vadito amphibolite. U-Pb zircon ages of about 1685 Ma (D.A. Bell, 1985) for the Rana and Puntiaquedo plutons, which intrude Vadito schist, yield a minimum age for deposition of at least part of the Vadito Group. Grambling and Williams (1985b) noted that an unpublished U-Pb zircon age of about 1700 Ma by L.T. Silver for feldspathic quartz-muscovite schist in the Tusas Mountains could be correlable with the felsic schist at Pilar. This date probably represents the crystallization age of the felsic volcanic protolith. In the Picuris Range, no radiometric dates have been reported for deposition of Ortega Group rocks. If the Ortega Group did rest in primary

stratigraphic contact with the felsic schist at Pilar prior to shearing along the contact zone, then the Ortega Group probably accumulated shortly after 1700 Ma.

Deformational styles and structural histories of the three major rock groups do not help constrain possible individual tectonic settings, because structures recognized in each of the groups are compatible with all groups having been deformed during a single progressive deformational event. It is also true, however, that mylonitic ductile shear zones which separate the Ortega Group from the Vadito Group and felsic schist at Pilar allow for the possibility that any or all of the three sequences evolved in widely different places at different times.

Preliminary metamorphic studies suggest that the Vadito Group and Ortega Group have experienced similar most recent P-T histories. If these groups have been juxtaposed tectonically, then it is possible that both groups with different metamorphic histories have been overprinted by a common post-assembly metamorphic peak. Additional work on P-T paths within rock groups will aid in resolving this question.

#### Possible tectonic settings

Vadito Group. The tectonic setting of the Vadito Group is the most poorly constrained of the three major rock

sequences in the Picuris Range. With the possible exclusion of the Marquenas Quartzite, the Vadito Group is lithologically similar to several scattered, mafic metavolcanic sequences that have been described as the Moppin Metavolcanic Series of the Tusas Mountains (Barker, 1958; Wobus and Manley, 1982; Williams, 1987), the Pecos greenstone belt of the southern Sangre de Cristo Mountains (Robertson and Moench, 1979), and an exposure of mafic rocks in the central Taos Range (Reed, 1984) (Fig. 8.1). These mafic sequences range in age from about 1765 Ma for the Taos Range (S.A. Bowring, personal communication in Williams, 1987) to about 1720 Ma for felsic metavolcanic rocks in the Pecos greenstone belt (Bowring and Condie, 1982). A minimum age for the Moppin Metavolcanic Series of about 1755 Ma (L.T. Silver, personal communication in Williams, 1987) results from an age of the Maquinita Granodiorite, which may intrude the Moppin rocks. These mafic sequences generally contain bimodal volcanic suites, and are in contact with pre- to syn-tectonic, generally calc-alkalic plutons. Each of these occurrences is dominated by mafic metavolcanic rocks that probably formed in an arc or back-arc setting (Bingler, 1974; Robertson and Moench, 1979; Klich, 1983; Soegaard and Eriksson, 1986; Grambling and Ward, 1987; Williams, 1987). If the Vadito Group represents the remains of a similar lithotectonic package, then these rocks are probably the oldest terrane in the Picuris Range. Although

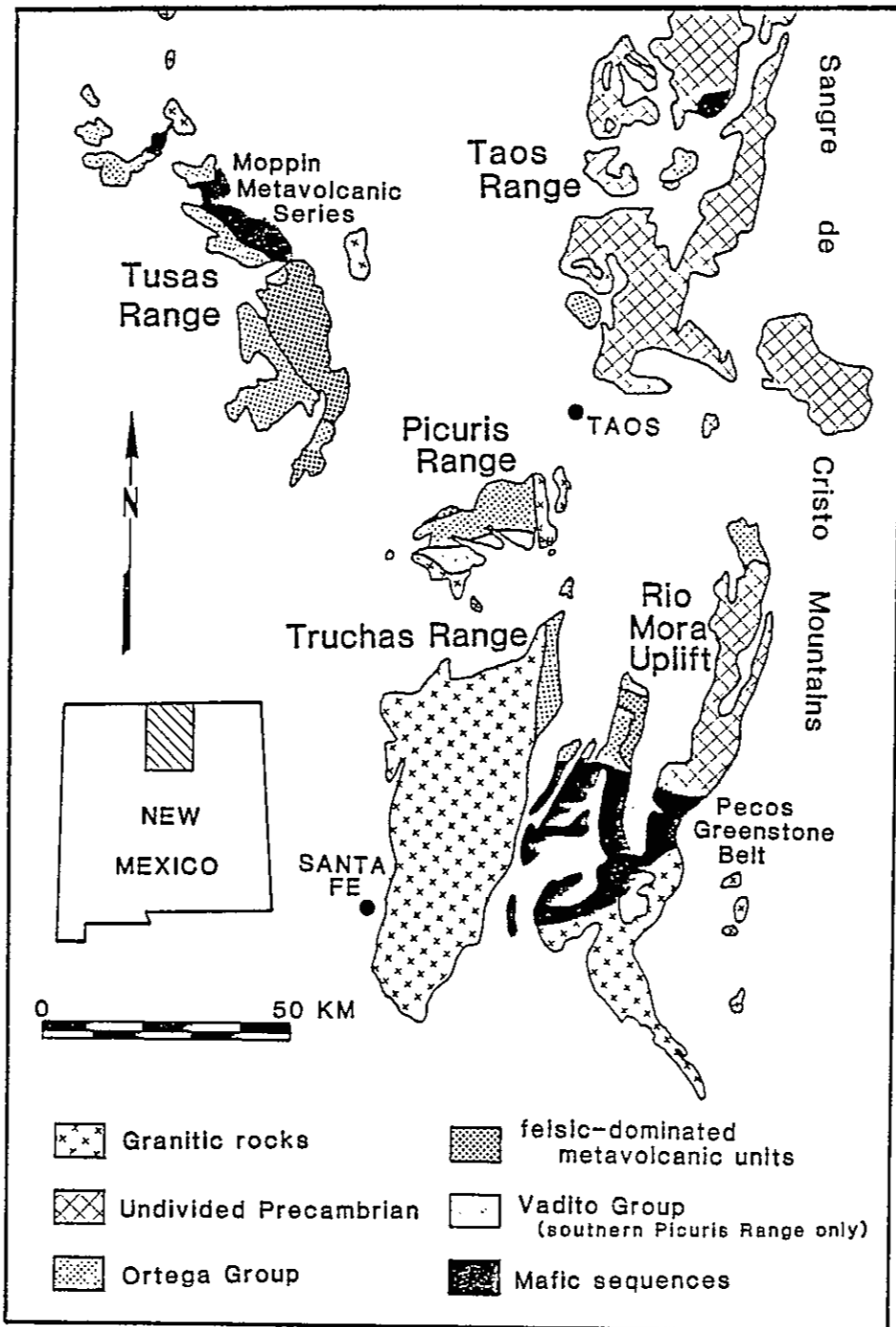


Figure 8.1. Generalized geologic map of Precambrian-cored uplifts in north-central New Mexico. Modified from Williams (1987).

no geochemistry exists for Vadito Group rocks in the Picuris Range, it is possible that this sequence of rocks represents the type II supracrustal assemblage of Condie (1982). This assemblage consists of bimodal volcanics-quartzite-arkose assemblages, and represents "lithosphere-activated continental rifts or aborted mantle-activated rifts" (Condie, 1982, p. 341).

It is not clear how the Marquenas Quartzite and similar orthoquartzites of the Vadito Group fit into this tectonic picture. Neither the Moppin nor the Pecos mafic sequences contains appreciable thicknesses of orthoquartzite and metaconglomerate. Therefore, if the Marquenas unit is an original part of the Vadito Group, and if the Vadito Group is tectonically equivalent to the Pecos or Moppin terrane, then the Vadito Group of the southern Picuris Range is a variety of mafic arc or back-arc association that has not previously been described in the southwestern U.S. However, Soegaard and Eriksson (1986) proposed that the Marquenas section comprised a distinct lithostratigraphic sequence that is in fault contact with Ortega rocks to the north and Vadito rocks to the south. This idea is plausible. Alternatively, the Marquenas Quartzite might rest unconformably above an older mafic Vadito section. In either of these two cases, the tectonic setting of the Marquenas Quartzite is unknown.

Felsic schists at Pilar. Textures in the felsic schist at Pilar suggest a phenocrystic felsic volcanic protolith. Similar 1700 Ma felsic metavolcanic rocks in the Tusas Range have geochemical signatures similar to modern felsic volcanic rocks in continental rifts or continental margin back-arcs in or near continental crust (J.M. Robertson, personal communication, 1987). On a more regional scale, felsic volcanic rocks of this age in the southwestern U.S. contain trace element chemistries characteristic of modern "continental rift systems and back-arc basins in or near continents" (Condie, 1986, p. 857). The felsic schist at Pilar probably represents part of the extensive 1680 to 1700 Ma volcanic-sedimentary terrane that is found in New Mexico and Arizona (Conway and Silver, 1986; Condie, 1986).

The base of the felsic schist at Pilar is not exposed. It is not known what type of continental crust was rifted, and what the felsic schist at Pilar was deposited on. One possibility is that basement to the felsic schist at Pilar is Vadito Group or equivalent rock. The absence of clastic sediments and mafic volcanics, and the lack of identifiable structures such as growth faults in the felsic schist at Pilar suggest that this unit accumulated after the most active phases of rifting.

Rocks similar to the felsic schist at Pilar lie stratigraphically beneath the Ortega Group in most of the major Precambrian-cored uplifts of northern New Mexico. It

is possible that these voluminous felsic volcanic rocks represent the final stage of stabilization of continental crust prior to Ortega Group deposition, and may also have provided one component of source material for the enormous thickness of quartz sand that blanketed the region at about 1700 Ma.

The Ortega Group. The Ortega Group, which is regionally exposed in northern New Mexico and perhaps in central New Mexico as well (Bauer and Williams, 1985), is probably the youngest regionally exposed Precambrian supracrustal lithostratigraphic package in northern New Mexico. The Ortega Group belongs to the 1650 to 1750 Ma quartzite-pelite terrane of the southwestern U.S. (Condie, 1986), and developed subsequent to rifting on a stable continental shelf during a first-order sea level rise (Soegaard and Eriksson, 1985). On a regional scale, detrital zircons from the Ortega Quartzite range in age from about 1850 to 1700 Ma (Maxon, 1976; Aleinikoff et al., 1985; S.A. Bowring, personal communication in Williams, 1987). This range of ages implies that one source component of the Ortega Quartzite was from the underlying felsic volcanic rocks, and another component was derived from elsewhere (Williams, 1987). It is possible that the Ortega Group could be assigned to supracrustal assemblage I of Condie (1982). Such as assemblage consists of quartzite-carbonate-

shale, is characterized by extensive cross-bedded quartzite with lesser amounts of carbonate, shale, and siltstone, and reflects either "stable continental margins or stable craton interiors" (Condie, 1982, p. 348). Because the top of the Ortega Group is not exposed, it is unknown what, if any, rocks were deposited above the Piedra Lumbre Formation. Possibly, carbonates accumulated within the uppermost Ortega Group.

#### Precambrian Tectonic Evolution

The Picuris Range geological summary that follows is based on available data from the Picuris Range, similarities with adjacent terranes in northern New Mexico, and a general outline of Precambrian history of the southwestern U.S. by Silver (1987).

- >1700 Ma
- 1) The Vadito Group accumulates in an arc or back-arc setting (on oceanic lithosphere?). The Vadito Group is tectonically equivalent to mafic metavolcanic assemblages in the Moppin Metavolcanic Series, Taos volcanics, or Pecos greenstone belt.
  - 2) The arc system matures and is accreted to the North American craton.

- 1700 Ma 3) The primitive continental crust is rifted. Successor basins form during rifting.
- 4) The felsic schist at Pilar is deposited within a northeast-trending chain of felsic volcanic-plutonic centers on or near the continental crust. These igneous rocks interfinger with subsequent transgressive proximal basin sediments.
- <1700 Ma 5) The thick Ortega Group sediments accumulate on the felsic schist at Pilar in a stable continental shelf setting. Basin subsidence matches sediment influx during a first-order sea level rise.
- 1680 Ma 6) Extensive plutonism with emplacement of granitic bodies in the Vadito Group.
- 1650-1450 Ma 7) Extensive, prolonged tectonism with approximately north-south crustal shortening. Possibly due to accretion of a microcontinent with the southwestern U.S. at about 1640 Ma (Condie, 1987). South-verging simple shear strain was concentrated below the mechanically stiff Ortega Quartzite. With progressive shortening, north-verging ductile shear zones and large folds develop. The Vadito Group moves northward over the Ortega Group along a ductile shear zone. It is possible that this setting is analogous to that described in the Pecos-Rio Mora area by Grambling and Ward (1987), in which the Pecos

greenstone belt has been thrust northward over younger Ortega Group and underlying felsic rocks along a south-dipping ductile fault. Deformation has waned by the time anorogenic plutons are emplaced in the Vadito Group at about 1450 Ma.

<1450 Ma 8) Horizontal isothermal and isobaric surfaces are superimposed on structures. At some later time, rocks are uplifted to their present structural levels and exhumed.

## CHAPTER 9. CONCLUSIONS

1) There exist three major supracrustal rock packages in the Picuris Range: a) The Vadito Group, *sensu stricto*, a heterogeneous sequence of metamorphosed bimodal volcanic, volcanoclastic, and clastic sedimentary rocks; b) the felsic schist at Pilar, scattered exposures of relatively homogeneous feldspathic quartz-muscovite schists containing distinctive "eyes" of quartz and feldspar, that probably represent metamorphosed, altered phenocrystic felsic volcanic rocks; and c) the Ortega Group, an overall transgressive, thick, stratigraphically continuous, metamorphosed sequence of basal quartz arenite, interlayered quartzites and pelitic schists, black phyllites, and laminated phyllites and schists that accumulated in a shallow marine setting.

The felsic schist at Pilar is similar to one component of the "Vadito Group" rocks that Williams et al. (1985) described in the Tusas, Taos, and Rio Mora areas. Parts of the more mafic Vadito Group in the southern Picuris Range are similar to the older mafic metavolcanic sequences found in the Tusas Range (Moppin metavolcanic series), the Santa Fe Range (Pecos greenstone belt), and the Taos Range.

2) It is unknown how these three lithostratigraphic

units relate to one another. The south-dipping boundary between Ortega and Vadito group rocks in the southern Picuris Range is a near-bedding-parallel, ductile reverse fault. Mylonitic structures indicative of simple shear occur all along this zone.

In the northwestern Picuris Range, in the cliffs near Pilar, the basal Ortega Quartzite overlies the felsic schist at Pilar along a low-angle zone of high ductile shear strain. The amount of bedding-parallel displacement that has occurred along this shear zone is unknown.

3) The Vadito Group to the south, and the felsic schist at Pilar to the north occupy identical structural positions with respect to the overlying Ortega Group. Both lie structurally below the basal Ortega Quartzite Formation.

4) The stratigraphic position of the Piedra Lumbre Formation is found to be above the Pilar Phyllite, and is therefore the youngest unit of the Ortega Group. The section of Piedra Lumbre Formation that is the type-section in the southern Picuris Range, is actually a fault sliver trapped between the Pilar Phyllite and the Marquenas Quartzite.

5) There exists some preliminary evidence, based mainly on intrusive relationships, to suggest that a major

fault or unconformity separates the Vadito amphibolite from the Vadito schist. A disparity in probable depositional settings indicates that the Vadito schist and Marquenas Quartzite are separated by either a fault or an unconformity. It is therefore suggested that the Vadito Group may be a composite of different rock groups juxtaposed along bedding-parallel faults and/or unconformities. If such faults exist, they must predate  $D_3$ , as the contacts are folded by  $D_3$  folds.

6) Although Ortega Group rocks locally contain concordant, simple pegmatite bodies, no intrusions into Ortega rocks have been found in the Picuris Range.

7) All rocks appear to have experienced lower to middle amphibolite facies metamorphism. Kyanite, andalusite, and sillimanite coexist in the Ortega Group in the Hondo syncline area. Porphyroblasts of biotite, garnet, and staurolite have experienced multiple stages of growth during the ductile strain history of Ortega Group rocks. All three of these minerals grew both pre- $D_3$  and syn- to post- $D_3$ . Kyanite, andalusite, biotite, staurolite, and sillimanite(?) all grew early in the strain history, prior to  $D_3$ .

8) Supracrustal rocks have undergone a progressive deformational history that resulted in the formation of three major generations of structures.

$D_1$  is characterized by localized zones of high simple shear strain, rather than by large fold structures.

The second generation of structures,  $D_2$ , involved major folding in the Ortega Group, and moderate folding in the Vadito Group. The Hondo syncline and the Copper Hill anticline are both  $F_2$  folds.  $D_2$  involved considerable near-bedding-parallel faulting.

In the northcentral Picuris Range the Ortega Quartzite has been tectonically doubled by what may have been a  $D_1$ ,  $D_2$ , or  $D_3$  imbrication. Similar shearing occurred beneath the Ortega Quartzite in the northern Picuris Range.

The third generation of structures,  $D_3$ , is characterized by an intense, pervasive, east-trending schistosity or crenulation cleavage ( $S_2^*$  in the Ortega Group) that is the dominant cleavage in most schistose rocks.  $S_2^*$  has rotated and reactivated the earlier cleavages. Based on relict crenulation cleavages preserved in porphyroblasts, the  $S_2^*$  schistosity has at least locally passed through an earlier crenulated stage of development. Minor  $F_2^*$  folds are recognized in the Ortega Group.

All three of these phases of deformation developed under conditions of approximately coaxial principal strain axes, and probably with considerable temporal overlap.

9) The major structural feature in the Picuris Range is the gently west-plunging, tight to isoclinal, northward verging  $F_2$  Hondo syncline in the Ortega Group. The Copper Hill anticline is thought to be a minor, parasitic fold on the Hondo syncline.

10) Kinematic shear indicators in the felsic schist at Pilar suggest that the Ortega Quartzite moved southward over felsic schist sometime during  $D_1$ . This is opposite to the vergence sense recorded by kinematic indicators along the Vadito-Ortega boundary and the attitudes of  $D_2/D_3$  folds. This south-directed shear may have been the earliest component of movement in the Picuris Range during  $D_1$ . It may also represent regional transport, as similar movements have been reported from the Tusas and Taos ranges.

Pristine quartz ribbon mylonites at the Ortega-felsic schist at Pilar contact indicate that south-directed shearing occurred, at least locally, late in the metamorphic history.

11) The Copper Hill anticline is a gently west-plunging  $F_2$  fold that dies out, or is faulted out, to the east. This fold is anomalous, and may be a parasitic fold on the Hondo syncline that has been uplifted along steeply south-dipping  $D_2/D_3$  reverse faults.

12) The older Rana and Puntiaquedo plutons (ca. 1680 Ma) in the southern Picuris Range are certainly pre-D<sub>3</sub>, and may be as early as pre- or syn-D<sub>1</sub>.

The "anorogenic" 1450 Ma Penasco Quartz Monzonite is probably syn- to late-syn-D<sub>3</sub>.

The Granite of Picuris Peak in the southeastern Picuris Range is probably related to the ca. 1680 Ma plutons to the west.

The Granite of Alamo Canyon resembles granitic rocks in the eastern Tusas Range that have been tentatively correlated with the Tres Piedras Granite.

13) Stratigraphic and structural observations and interpretations listed above limit the number of kinematic/stratigraphic models possible for the evolution and accretion of the three major lithostratigraphic terranes in the Picuris Range. All models involve a complex interaction of faulting, shearing, and folding in the mid-crustal environment. In the best model, early south-directed shear is concentrated between the overriding, mechanically stiff Ortega Quartzite and the relatively incompetent felsic schist at Pilar. With progressive crustal shortening, north-directed(?) ductile faulting (thrusting?) transports Vadito Group rocks northward over the Ortega Group-felsic schist at Pilar lithostratigraphic package. As shortening continues, the deformational style

evolves from heterogeneous  $D_1$  shearing to more homogeneous bulk shortening by nucleation and growth of major folds in the Ortega and Vadito groups. The Ortega Quartzite-felsic schist at Pilar contact remains a zone of intense bedding-parallel simple shear throughout much of the deformation history. As  $D_2$  folding evolves (and locks up?) an intense, slightly oblique  $S_3$  cleavage is superimposed on earlier structures in Ortega Group rocks. Near bedding-parallel, steeply south-dipping faulting which may have reactivated  $D_1$  structures, accompanied the  $D_2$  and  $D_3$  phases of deformation.

14) The felsic schist at Pilar is lithologically and geochemically similar to felsic schists in the Tusas, Rio Mora, and Taos ranges. Geochemistries and textures of these rocks are consistent with modern continental extensional systems. The felsic schist at Pilar and related rocks may have accumulated on rifted, pre-1700 Ma basement that is not exposed in the Picuris Range.

15) The Vadito Group as a whole is dissimilar to other pre-Ortega sequences in northern New Mexico. The southernmost mafic portion of the Vadito in the Picuris Range is similar to mafic metavolcanic terranes in northern New Mexico that are geochemically similar to modern arc or back-arc settings. The northern metaconglomeratic-felsic schist portion is most similar to the felsic package that

underlies the Ortega Group in the Tusas Range. Therefore, if the Vadito Group is a tectonic composite of different lithostratigraphic sequences, it may contain old mafic arc-related basement rocks and young rift-related rocks.

16) The Ortega Group accumulated depositionally above the felsic schist at Pilar on a stable continental shelf in a shallow marine environment during a major sea-level rise.

17) One possible model for the tectonic evolution of rocks in the Picuris Range begins with accretion of mafic(?) continental crust as arcs or back-arcs prior to about 1700 Ma. At around 1700 Ma, rifting of this crust results in production of voluminous felsic volcanism, followed by crustal stabilization sufficient to permit accumulation of mature shallow marine sediments along the continent margin. These rocks were buried to moderate crustal levels and subjected to an extended orogenic event, due perhaps to convergence and collision from the south. This extended orogeny resulted in formation of three major generations of structures which are developed to various degrees in the three lithostratigraphic groups of rocks now exposed in the Picuris Range. The extreme heterogeneity of strain on all scales that characterizes Proterozoic rocks in the Picuris Range and adjacent uplifts is the effect of this orogeny on supracrustal and plutonic rocks at mid-crustal levels.

## Appendix 1. Descriptions of geochronology samples

Samples ranging from 75 to 210 lbs were collected from outcrop exposures. Samples were crushed, pulverized, and separated at laboratories in the Department of Geology at Washington University, and the New Mexico Bureau of Mines and Mineral Resources at New Mexico Institute of Mining and Technology. Magnetic and heavy liquid separations were done at Washington University and the Department of Geology at the University of New Mexico. Zircons were hand-picked by M. Williams, P. Bauer, and students at Washington University. U-Pb chemistry and mass spectrometry were performed by Dr. S. A. Bowring at Washington University.

### Plutonic Rocks

Granite of Alamo Canyon. Montgomery (1953) correlated these rocks with the granitic rocks of the southern Picuris Range (the Embudo Granite). Textures, intrusive relationships, and deformational fabrics differ between the Granite of Alamo Canyon and the four plutons in the southwestern Picuris Range. Williams (1987) tentatively correlated a similar pluton in the eastern Tusas Range with

the 1654 Ma (Maxon, 1976) Tres Piedra Granite of the northern Tusas Range. Therefore, the age of the Granite of Alamo Canyon is important in both a local and regional perspective.

Granite of Picuris Peak. The Granite of Picuris Peak is a highly tectonized, complex intrusion that is intimately interlayered with Vadito Group lithologies. This granite is very similar to the c.a. 1680 Ma Rana and Puntiaquido plutons in the southwestern Picuris Range.

Cerro Alto Metadacite. Mappers in the Harding Pegmatite Mine area have generally agreed that field relationships support the interpretation that the Cerro Alto Metadacite is the oldest of the four granitic plutons emplaced in Vadito Group rocks (Long, 1976; R.J. Holcombe, personal communication, 1984; McCarty, 1983). However, D.A. Bell (1985) reported a preliminary U-Pb zircon age of about 1630 Ma for the Cerro Alto Metadacite. If this age is correct, then the Cerro Alto body is younger than the Rana and Puntiaquido plutons, and field relations need re-examination.

## Metavolcanic Rocks

Vadito Group felsic quartz-eye schist, southern Picuris Range. Original primary stratigraphic relationships between the Vadito Group and the Ortega Group and the felsic schist at Pilar are unknown. The Vadito Group is unlike both the older mafic metavolcanic sequences in the Tusas, Pecos, and Taos areas, and the younger felsic metavolcanic sequences in the Tusas, Rio Mora, and Taos areas. An age of crystallization for felsic metavolcanic rocks in the Vadito Group in the southern Picuris Range may help constrain correlations. One possible complication is that the Vadito Group might actually be a composite package containing tectonic slices of various rock groups of various ages.

Rio Pueblo Schist, Comales campground. These rocks were tentatively correlated with the felsic schist in the Pilar cliffs by Montgomery (1962). Textures in these problematic sheared rocks permit either granitic or volcanic protoliths. Zircons from the Comales rocks yielded a preliminary age of about 1665 Ma (S.A. Bowring, personal communication, 1986). This age is relatively consistent with ages of granitic rocks in the southwestern Picuris Range, and inconsistent with the proposed age/correlations of felsic schist in the Pilar cliffs. Felsic schists at

Comales campground could be sheared granites or a volcanic phase of the southwestern Picuris Range plutons.

Felsic schist, Pilar cliffs. It is unknown how the felsic schist relates to the Vadito Group. Rocks similar to the felsic schist at Pilar in the Tusas Range are around 1700 Ma (Williams, 1987). If the Ortega Group does lie in primary stratigraphic contact with the felsic schist at Pilar in the Picuris Range, then an age of crystallization of felsic schist protolith constrains the maximum age for deposition of the Ortega Group sediments.

#### Metasedimentary Rocks

Marquenas Quartzite Formation, quartzite cobble.

Large, rounded quartzite clasts in the southern conglomeratic member of the Marquenas Quartzite Formation may have already been quartzite when incorporated into the sandy Marquenas protolith. This unit is thought to be older than the Ortega Quartzite. Additionally, Marquenas quartzite clasts are compositionally different from the Ortega Quartzite, so Ortega rocks were not a source for the Marquenas. Detrital zircons in the Ortega Quartzite in the Picuris Range have U-Pb ages of about 1830 Ma (Maxon, 1976). No rocks of this age are recognized in the southwestern U.S.

It is possible that the detrital zircons in Ortega Quartzite originated from the same source as the quartzite clasts in the Marquenas Quartzite. Even if this is not the case, detrital zircons in the Marquenas clasts may aid in the search for a source terrain, and add some perspective to the controversy concerning the stratigraphic position of the Marquenas Quartzite Formation.

R6 schist member, southern Picuris Range. The R6 member of the Rinconada Formation contains grains of rutile that probably isotopically equilibrated during peak metamorphic conditions (M.L. Williams, personal communication, 1986). U-Pb chronology of rutile should yield an absolute age for peak metamorphism.

## APPENDIX 2

Garnet-biotite geothermometry calculations for Picuris Range samples. Equations are from Ferry and Spear (1978). All microprobe data are courtesy of M.L. Williams.

$$T(^{\circ}\text{K}) = \frac{12,454 + 0.057(P)}{4.662 - 3(1.9872)\ln K_D}$$

$$K_D = \frac{(\text{Fe/Mg})_{\text{Bi}}}{(\text{Fe/Mg})_{\text{Gt}}}$$

## Microprobe data for sample HC-64

## GARNET

HCC85 AND 64 E TR EACH 25-Nov-86 12:10 AM  
Garnet Data Set: 4 Trav Length: 256 Step Length: 9.9

Weight Percent:

	FeO	MgO	MnO	CaO	TiO2	Al2O3	SiO2	Total	Beam
1	37.13	1.89	3.03	1.14	0.07	20.96	37.30	101.51	20.04
2	36.91	1.90	2.97	1.13	0.04	20.79	37.47	101.21	20.04
3	36.75	1.94	2.91	1.12	0.02	20.92	37.17	100.81	20.04
4	37.61	1.89	2.86	1.14	0.04	21.11	37.40	102.07	20.04
5	37.21	1.87	2.85	1.11	0.05	20.86	37.46	101.41	20.04
6	37.11	1.89	2.74	1.18	0.03	20.83	37.15	100.95	20.03
7	36.99	1.92	2.75	1.14	0.05	20.93	37.07	100.85	20.04
8	37.72	1.93	2.66	1.08	0.03	21.09	37.21	101.72	20.05
9	37.37	1.94	2.60	1.15	0.06	20.89	37.26	101.27	20.05
10	37.14	1.97	2.48	1.14	0.07	20.86	37.15	100.91	20.03
11	37.64	1.95	2.38	1.08	0.05	21.15	37.25	101.40	20.05
12	37.60	1.98	2.34	1.11	0.04	21.10	37.45	101.62	20.05
13	37.39	2.04	2.31	1.09	0.03	20.79	37.08	100.73	20.04
14	37.84	2.07	2.14	1.12	0.04	20.74	36.76	100.71	20.03
15	37.95	2.02	2.09	1.06	0.04	20.79	36.86	100.81	20.04
16	37.99	2.05	1.95	1.06	0.06	21.05	36.94	101.10	20.05
17	38.25	2.09	1.89	1.01	0.04	20.93	36.86	101.07	20.05
18	38.46	2.14	1.82	1.05	0.06	20.71	37.17	101.41	20.04
19	38.10	2.07	1.63	1.05	0.03	21.13	37.57	101.58	20.04
20	38.49	2.08	1.53	1.11	0.03	21.00	37.15	101.40	20.04
21	38.35	2.10	1.40	1.06	0.03	20.90	36.98	100.82	20.03
22	38.79	2.00	1.32	1.14	0.03	20.75	36.95	100.96	20.03
23	38.80	2.01	1.23	0.79	0.02	20.80	37.24	100.89	20.03
24	39.03	2.00	1.15	0.68	0.04	20.89	36.98	100.76	20.04
25	39.55	1.83	1.10	0.59	0.00	20.85	37.09	100.99	20.04
26	37.01	0.55	0.83	1.51	0.00	16.53	29.00	75.43	20.04
27	1.28	0.40	0.00	0.00	0.21	34.20	45.24	81.33	20.04

## BIOTITE

FL #	FEO	MNO	MGO	TIO2	AL2O3	SiO2	K2O	Na2O	CaO	AN TTL
31	23.02	0.00	7.42	1.65	19.98	34.73	8.34	0.23	0.02	93.76
32	22.43	0.00	7.90	1.50	19.73	34.73	8.47	0.23	0.00	94.33
33	23.33	0.01	7.53	1.68	20.03	34.72	8.46	0.23	0.01	95.04
34	22.88	0.01	7.79	1.44	19.85	35.01	8.45	0.23	0.01	95.75
35	22.33	0.00	7.74	1.52	20.49	34.93	8.19	0.21	0.00	95.31
37	23.41	0.00	7.39	1.89	19.68	34.93	8.41	0.27	0.02	95.79
39	22.80	0.00	7.63	1.62	20.15	34.94	8.46	0.23	0.00	95.35
40	23.76	0.00	7.74	1.61	19.77	34.31	8.57	0.23	0.00	95.19
41	22.67	0.00	7.66	1.56	20.28	34.82	8.44	0.27	0.02	95.72
42	22.51	0.00	7.37	1.61	19.14	36.14	8.34	0.23	0.01	95.34
43	22.56	0.00	7.69	1.64	20.16	34.73	8.53	0.23	0.00	95.97
44	22.29	0.00	7.76	1.68	20.32	35.05	8.62	0.23	0.00	95.95
45	22.84	0.01	7.41	1.57	20.30	34.71	8.39	0.23	0.00	95.40
46	22.77	0.00	7.61	1.67	20.06	34.57	8.45	0.23	0.01	95.43
47	22.03	0.00	7.64	1.53	20.23	34.71	8.37	0.27	0.00	95.00
48	22.37	0.00	7.81	1.51	19.94	34.75	8.37	0.23	0.01	95.03
49	22.64	0.00	7.70	1.54	20.04	34.43	8.23	0.27	0.06	94.93
50	23.24	0.00	7.39	1.73	20.11	35.03	8.46	0.23	0.00	96.17

Statistical summary of 18 points with anal TTL >90.00 WT %  
Students' T (FCN)= 2.1077

	FEO	MNO	MGO	TIO2	AL2O3	SiO2	K2O	Na2O	CaO	AN TTL
Avg	22.73	0.00	7.66	1.61	20.02	34.81	8.43	0.23	0.01	95.82
+-	0.19	0.00	0.06	0.03	0.14	0.19	0.08	0.02	0.01	Count
+-	0.37	0.00	0.16	0.07	0.30	0.42	0.11	0.02	0.01	1-Sigma
+-	0.18	0.00	0.08	0.03	0.15	0.21	0.03	0.01	0.01	FW Count
	23.79	0.00	8.02	1.69	20.76	36.44	8.53	0.27	0.01	Mean wt %

## Microprobe data for sample HC-377

## GARNET

HC377/455 GARNET 23-Feb-87 8:44 PM  
 Garnet Data Set: 2 Trav Length: 232 Step Length: 8.0

Weight Percent:

	FeO	MgO	MnO	CaO	TiO2	Al2O3	SiO2	Total	Beam
1	39.19	2.04	1.06	0.71	0.01	21.04	36.37	100.42	20.01
2	39.58	2.04	1.07	0.71	0.02	20.88	36.53	100.83	20.02
3	39.21	2.11	1.08	0.64	0.02	20.95	36.74	100.75	20.02
4	39.67	2.03	1.07	0.65	0.00	20.89	36.50	100.81	20.02
5	39.27	2.05	0.98	0.60	0.02	20.94	36.60	100.46	20.02
6	39.56	2.09	0.98	0.59	0.00	20.84	36.34	100.40	20.02
7	38.85	2.06	0.97	0.55	0.01	20.91	36.60	99.95	20.02
8	39.54	2.09	0.97	0.55	0.01	20.96	36.38	100.50	20.01
9	39.33	2.08	0.93	0.51	0.01	21.09	36.61	100.56	20.01
10	39.77	2.09	0.91	0.54	0.01	20.75	36.79	100.86	20.01
11	40.34	2.10	0.95	0.48	0.01	21.00	36.73	101.61	19.98
12	40.01	2.11	0.90	0.46	0.02	21.00	36.80	101.30	19.96
13	39.79	2.05	0.91	0.50	0.02	21.14	36.57	100.98	19.98
14	40.09	2.02	0.90	0.50	0.02	20.94	36.41	100.88	20.01
15	40.13	2.08	0.88	0.48	0.02	20.92	36.58	101.09	20.02
16	39.91	2.02	0.88	0.47	0.00	20.88	36.61	100.77	20.01
17	39.50	2.17	0.80	0.44	0.02	20.50	35.59	99.23	20.00
18	39.96	2.03	0.83	0.47	0.01	20.81	36.79	100.90	20.00
19	39.66	2.06	0.83	0.48	0.01	20.83	36.46	100.33	19.98
20	39.40	1.98	0.81	0.42	0.02	20.76	36.67	100.06	19.99
21	40.04	1.99	0.85	0.45	0.00	20.80	37.03	101.16	19.97
22	39.93	1.93	0.82	0.40	0.01	20.79	36.78	100.66	19.97
23	39.92	1.89	0.80	0.40	0.02	21.59	37.80	102.42	19.96
24	40.30	1.86	0.82	0.40	0.02	20.92	36.83	101.15	19.97
→ 25	39.97	1.80	0.83	0.47	0.02	20.92	36.81	100.84	19.97
26	39.85	1.64	0.83	0.60	0.02	20.65	36.56	100.17	19.97
27	39.72	1.44	0.86	0.74	0.01	20.30	35.76	98.83	19.97
28	1.38	0.00	0.00	0.00	0.00	0.27	0.81	2.46	19.96
29	0.12	0.00	0.00	0.00	0.00	0.14	1.93	2.19	19.97
30	0.00	0.00	0.00	0.00	0.00	0.00	0.04	0.04	20.00

## BIOTITE

Point # 18 HC 377/455 BIOTITE 23-Feb-87 5:27 PM  
 BAS, File # 3 X= 13.625 Y= 49.104  
 Ref's: FES MGG MNF T14 ALA SIG X10 NAE CAA  
 Beam 20.05 NA

Oxide	K-ratio	Beta	MDL	Norm'd	Calc'd WT%	Stoic: (11 O's)	( 8 Cat)
FE0	0.2112	1.0863	0.037	24.21	22.94 +- 0.19	FE+ 1.4929	1.5291
MGO	0.0332	1.3308	0.045	7.48	7.09 +- 0.06	MG- 0.8218	0.8418
MNO	0.0000	1.0000	0.034	0.00	0.00 +- 0.00	MN- 0.0000	0.0000
TIO2	0.0156	1.0478	0.018	1.73	1.64 +- 0.05	TI- 0.0958	0.0982
AL2O3	0.1659	1.2136	0.028	21.25	20.13 +- 0.14	AL- 1.8463	1.8911
SIO2	0.2803	1.2063	0.021	35.69	33.81 +- 0.18	SI- 2.6312	2.6951
K2O	0.0821	1.0773	0.036	9.33	8.84 +- 0.10	K- 0.8777	0.8990
NA2O	0.0016	1.3058	0.061	0.30	0.29 +- 0.02	NA- 0.0434	0.0444
CAO	0.0001	1.0481	0.035	0.01	0.01 +- 0.01	CA- 0.0008	0.0008
Total=	0.8100				94.75		

Microprobe data for sample HC-385

**GARNET**

HCC95 AND 64 E TR EACH 24-Nov-86 10:50 PM  
 Garnet Data Set: 2 Trav Length: 194 Step Length: 8.4

Weight Percent:

	FeO	MgO	MnO	CaO	TiO2	Al2O3	SiO2	Total	Beam
1	39.99	1.81	0.46	1.11	0.05	20.95	37.57	101.94	20.05
2	40.07	1.85	0.46	1.07	0.05	21.08	37.48	102.04	20.05
3	39.79	1.89	0.42	1.10	0.02	21.02	37.40	101.63	20.05
4	40.25	1.83	0.36	1.09	0.05	20.96	37.20	101.78	20.05
5	40.10	1.85	0.37	1.10	0.03	21.07	37.14	101.66	20.05
6	40.12	1.89	0.36	1.06	0.02	20.85	37.30	101.61	20.05
7	39.61	1.89	0.38	0.99	0.03	20.81	36.92	100.60	20.06
8	40.08	1.93	0.32	0.99	0.03	21.21	37.41	101.97	20.05
9	39.92	1.95	0.34	1.06	0.01	21.12	37.34	101.75	20.05
10	40.05	1.97	0.31	0.96	0.01	20.96	37.09	101.35	20.05
11	40.38	1.97	0.32	0.96	0.05	21.09	37.44	102.21	20.06
12	40.19	1.96	0.34	0.96	0.04	20.90	37.25	101.64	20.06
13	39.99	2.04	0.35	0.95	0.03	20.94	37.29	101.59	20.06
14	39.89	2.00	0.35	0.91	0.03	21.02	37.25	101.42	20.06
15	40.29	2.09	0.37	0.74	0.01	21.05	37.53	102.08	20.05
16	39.74	2.09	0.34	0.78	0.03	20.99	37.32	101.29	20.05
17	40.06	2.07	0.42	0.66	0.00	21.12	37.61	101.94	20.05
18	39.96	2.02	0.46	0.62	0.04	21.13	37.32	101.55	20.05
19	39.98	2.04	0.45	0.62	0.02	20.96	37.38	101.45	20.05
20	39.70	2.06	0.50	0.62	0.00	21.06	36.97	100.91	20.05
21	40.38	1.98	0.56	0.56	0.00	21.01	37.12	101.61	20.05
22	39.94	1.86	0.59	0.54	0.01	21.37	37.61	101.92	20.05
23	55.64	0.20	0.06	1.05	0.03	5.17	9.78	71.93	20.06
24	1.30	0.31	0.00	0.01	0.19	35.61	46.21	83.63	20.06

**BIOTITE**

PL #	FE2	MNO	MGO	TIO2	AL2O3	SiO2	K2O	Na2O	CaO	AN	TTL
1	22.01	0.00	7.26	1.72	20.21	34.75	8.49	0.17	0.04	93.35	
2	22.06	0.01	7.14	1.67	19.58	34.14	8.73	0.25	0.03	94.25	
3	21.94	0.00	7.17	1.63	19.78	34.20	8.13	0.23	0.13	93.51	
4	22.17	0.00	6.83	1.62	19.67	34.01	7.53	0.21	0.23	91.75	
5	22.35	0.00	6.90	1.57	19.78	34.54	8.54	0.26	0.09	94.02	
6	22.00	0.00	7.01	1.63	19.28	34.21	8.79	0.26	0.04	94.36	
7	22.14	0.00	7.11	1.61	20.25	34.30	8.73	0.26	0.02	94.35	
8	22.04	0.00	7.40	1.64	19.30	33.76	7.43	0.39	0.01	94.13	
9	22.03	0.00	7.23	1.65	20.76	34.56	8.40	0.30	0.03	93.20	
10	22.23	0.00	7.25	1.63	20.07	33.59	7.67	0.33	0.16	93.39	
11	22.55	0.00	6.98	1.68	20.10	34.31	8.75	0.25	0.12	93.73	
12	22.19	0.00	7.15	1.68	20.18	33.97	8.35	0.23	0.12	93.91	
13	22.09	0.00	7.11	1.65	20.69	34.56	8.44	0.31	0.05	93.17	
14	22.39	0.00	7.20	1.64	19.94	34.09	8.77	0.31	0.04	94.39	
15	22.03	0.00	7.51	1.64	20.11	34.30	8.77	0.33	0.04	93.11	
16	20.35	0.00	6.84	1.78	18.78	34.71	8.36	0.15	0.11	91.78	
17	20.31	0.00	7.13	1.74	19.80	34.23	8.44	0.11	0.17	92.00	
18	21.69	0.00	6.98	1.62	19.79	34.43	7.97	0.22	0.01	93.91	
19	19.10	0.00	7.22	1.54	20.27	33.35	9.10	0.10	0.10	93.31	
20	20.35	0.00	7.22	1.59	20.21	34.57	7.67	0.12	0.26	92.27	
21	22.01	0.00	7.34	1.60	20.70	34.43	8.74	0.23	0.04	94.33	
22	22.65	0.02	6.91	1.72	20.11	34.74	8.36	0.23	0.03	93.36	
23	22.00	0.00	6.91	1.71	19.95	34.28	7.45	0.14	0.27	92.16	
24	22.42	0.00	6.92	1.69	20.36	34.94	8.33	0.19	0.12	94.14	
25	22.66	0.00	6.94	1.66	19.71	34.14	8.04	0.17	0.10	93.73	
26	22.95	0.00	7.32	1.66	20.18	33.78	8.49	0.35	0.00	94.32	
27	22.11	0.00	7.32	1.72	20.22	33.58	9.34	0.10	0.07	94.18	
28	22.40	0.00	7.12	1.71	19.44	34.06	8.34	0.13	0.09	92.36	
29	21.81	0.00	7.33	1.65	19.30	33.90	8.33	0.23	0.11	93.10	
30	21.59	0.00	6.90	1.63	19.49	33.84	8.43	0.17	0.18	91.66	

Statistical summary of 30 points with #wt Fe = 51.00 at 8  
 #wt Mn = 0.00

PL #	FE2	MNO	MGO	TIO2	AL2O3	SiO2	K2O	Na2O	CaO	AN	TTL
008	21.74	0.00	7.15	1.70	19.67	34.40	8.45	0.23	0.11	93.71	
11	21.79	0.00	6.90	1.60	19.14	34.19	8.39	0.22	0.11	92.90	
71	21.92	0.00	7.21	1.65	19.38	34.46	8.44	0.23	0.03	93.84	
11	21.77	0.00	6.95	1.66	19.14	34.17	8.37	0.22	0.03	92.90	

## Microprobe data for sample HC-454

## GARNET

HC377/455 GARNET 22-Feb-87 10:05 FM  
 Garnet Data Set: 4 Trav Length: 608 Step Length: 19.0

Weight Percent:

	FeO	MgO	MnO	CaO	TiO2	Al2O3	SiO2	Total	Beam
1	37.36	1.58	3.39	0.94	0.02	20.84	36.71	100.84	20.13
2	36.79	1.63	3.32	0.91	0.03	20.75	36.68	100.11	20.14
3	37.06	1.63	3.26	0.90	0.02	20.66	36.63	100.16	20.13
4	37.13	1.60	3.15	0.89	0.06	20.88	36.99	100.70	20.12
5	36.62	1.63	3.17	0.82	0.02	20.69	36.75	99.70	20.11
6	36.92	1.64	3.12	0.91	0.05	20.84	36.79	100.27	20.11
7	37.36	1.70	3.12	0.84	0.04	20.84	36.31	100.21	20.10
8	37.39	1.63	3.08	0.94	0.04	20.79	37.09	100.96	20.11
9	37.25	1.67	3.09	0.85	0.01	20.94	36.98	100.79	20.10
10	37.29	1.72	2.97	0.89	0.02	20.76	37.25	100.90	20.11
11	37.36	1.65	2.98	0.83	0.04	20.72	36.76	100.34	20.10
12	37.29	1.70	2.91	0.88	0.02	20.76	37.01	100.57	20.09
13	37.69	1.72	2.87	0.84	0.03	21.08	37.17	101.40	20.09
14	37.53	1.74	2.85	0.81	0.03	20.60	36.99	100.58	20.08
15	37.54	1.75	2.85	0.81	0.02	20.79	36.59	100.35	19.97
16	37.50	1.76	2.79	0.84	0.04	20.93	37.12	100.98	20.00
17	37.87	1.76	2.75	0.82	0.04	20.98	37.21	101.43	20.10
18	38.13	1.74	2.66	0.79	0.00	20.68	36.05	100.07	20.09
19	37.36	1.75	2.63	0.82	0.02	20.62	36.53	99.73	20.10
20	37.31	1.77	2.58	0.77	0.05	20.79	37.04	100.31	20.10
21	38.02	1.80	2.53	0.78	0.04	20.80	36.72	100.69	20.09
22	37.98	1.75	2.50	0.77	0.03	20.57	36.73	100.33	20.09
23	37.87	1.79	2.45	0.77	0.02	20.91	37.19	101.00	20.09
24	38.39	1.71	2.34	0.77	0.01	20.67	36.80	100.69	20.09
25	38.02	1.84	2.28	0.76	0.01	20.92	36.93	100.76	20.09
26	37.50	1.86	2.25	0.72	0.00	20.63	37.17	100.13	20.09
27	37.97	1.82	2.13	0.66	0.00	20.94	36.89	100.33	20.10
28	37.91	1.81	2.08	0.61	0.01	20.73	37.11	100.26	20.10
29	38.41	1.94	2.01	0.56	0.00	20.77	37.27	100.96	20.10
30	38.84	1.91	1.75	0.55	0.03	20.52	36.97	100.57	20.10
31	39.32	1.93	1.17	0.58	0.01	20.90	37.34	101.25	20.01
32	38.53	1.57	0.81	0.56	0.00	22.06	38.38	101.91	20.03
33	14.20	1.14	0.00	0.00	0.38	53.38	26.66	95.76	20.12

## BIOTITE

Point # 29 HC 377/455 BIOTITE 23-Feb-87 3:49 PM  
 BAs, File # 3 X= 22.310 Y= 16.070  
 Ref's: FE3 H65 MNF TI4 ALA SIG K10 NAE CAE  
 Beam 20.13 NA

Oxide	K-ratio	Beta	MDL	Norm'd	Calc'd WTX	Stoic: (11 Ox)	(8 Cat)
FE0	0.1936	1.0889	0.037	22.18	21.03 +- 0.19	FE-	1.3491 1.3873
MGO	0.0633	1.3088	0.044	9.01	8.57 +- 0.36	MG-	0.9774 1.0051
MNO	0.0003	1.1050	0.037	0.03	0.03 +- 0.02	MN-	0.0018 0.0018
TIO2	0.0151	1.0516	0.018	1.67	1.59 +- 0.04	TI-	0.0913 0.0939
AL2O3	0.1656	1.2123	0.028	21.13	20.08 +- 0.14	AL-	1.8113 1.8626
SIO2	0.2887	1.2062	0.021	36.64	34.82 +- 0.19	SI-	2.6650 2.7405
K2O	0.0792	1.0803	0.035	9.01	8.56 +- 0.10	K-	0.8358 0.3595
NA2O	0.0018	1.7625	0.060	0.34	0.32 +- 0.02	NA-	0.0475 0.0489
CAO	0.0000	1.0000	0.034	0.00	0.00 +- 0.00	CA-	0.0000 0.0000
Total=	0.8097				95.03		

## REFERENCES CITED

- Aldrich, L.T., Wetherill, G.W., Davis, G.L., and Tilton, G.R., 1958, Radioactive ages of micas from granitic rocks by Rb-Sr and K-Ar methods: American Geophysical Union Transactions, v. 39, p. 1124-1134.
- Aleinikoff, J.N., Reed, J.C., Jr., and Pallister, J.S., 1985, Tectonic implications from U-Pb dating of detrital zircons from the Early Proterozoic terrain of the central Rocky Mountains: Geological Society of America Abstracts with Programs, v. 17, p. 510.
- Baldwin, B., 1956, The Santa Fe group of north-central New Mexico: New Mexico Geological Society Guidebook 7, p. 115-121.
- Baltz, E.H., 1978, Resume of Rio Grande depression in north-central New Mexico; in J.W. Hawley, ed., Guidebook to Rio Grande rift in New Mexico and Colorado: New Mexico Bureau of Mines and Mineral Resources Circular 163, p. 210-228.
- Barker, F., 1958, Precambrian and Tertiary geology of Las Tablas quadrangle, New Mexico: New Mexico Bureau of Mines and Mineral Resources Bulletin 45, 104 p.
- Bauer, P.W., 1984, Stratigraphic summary and structural problems of Precambrian rocks, Picuris Range, New Mexico: New Mexico Geological Society, Guidebook 35, p. 199-204.
- Bauer, P.W., 1987, Structural and stratigraphic relationships between the early Proterozoic Vadito and Ortega groups, Picuris Range, northern New Mexico: Geological Society of America Abstracts with Programs, v. 19, p. 259.
- Bauer, P.W. and Williams, M.L., 1985, Structural relationships and mylonites in the Proterozoic rocks of the northern Pedernal Highlands, central New Mexico: New Mexico Geological Society, Guidebook 36, p. 140-145.
- Bell, D.A., 1985, Structural and age relationships in the Embudo Granites, Picuris Mountains, New Mexico [M.S. thesis]: University of Texas, Dallas, 175 p.

- Bell, D.A. and Nielsen, K.C., 1985, Intrusion and deformation sequence of the Embudo granites, northcentral New Mexico: Geological Society of America Abstracts with Programs, v. 17, p. 151.
- Bell, T.H., 1981, Foliation development - the contribution, geometry and significance of progressive bulk inhomogeneous shortening: Tectonophysics, v. 75, p. 273-296.
- Bell, T.H., 1985, Deformation partitioning and porphyroblast rotation in metamorphic rocks: A radical reinterpretation: Journal of Metamorphic Geology, v. 3, p. 109-118.
- Bell, T.H. and Rubenach, M.J., 1980, Crenulation cleavage development - evidence for progressive bulk inhomogeneous shortening from "millipede" microstructures in the Robertson River Metamorphics: Tectonophysics, v. 68, T9-T15.
- Bell, T.H. and Rubenach, M.J., 1983, Sequential porphyroblast growth and crenulation cleavage development during progressive deformation: Tectonophysics, v. 92, p. 171-194.
- Bell, T.H. and Hammond, R.L., 1984, On the internal geometry of mylonite zones: Journal of Geology, v. 92, p. 667-686.
- Bell, T.H., Rubenach, M.J., and Fleming, P.D., 1986, Porphyroblast nucleation, growth and dissolution in regional metamorphic rocks as a function of deformation partitioning during foliation development: Journal of Metamorphic Geology, v. 4, p. 37-67.
- Berthé, D. and Brun, J.P., 1980, Evolution of folds during progressive shear in the South Armorican shear zone, France: Journal of Structural Geology, v. 2, p. 127-134.
- Berthé, D., Choukroune, P., and Jegouzo, P., 1979, Orthogneiss, mylonite, and non-coaxial deformation of granites: the example of the South Armorican Shear Zone: Journal of Structural Geology, v. 1, p. 31-42.
- Bingler, E.C., 1974, Precambrian rocks of the Tusas Mountains: New Mexico Geological Society Guidebook 25, p. 109-113.

- Black, L.P., Bell, T.H., Rubenach, M.J., and Withnall, I.W., 1979, Geochronology of discrete structural-metamorphic events in a multiply deformed Precambrian terrain: *Tectonophysics*, v. 54, p. 103-137.
- Borradaile, G.J., 1978, Transected folds: A study illustrated with examples from Canada and Scotland: *Geological Society of America Bulletin* v. 89, p. 481-493.
- Bowring, S.A. and Condie, K.C., 1982, U-Pb zircon ages from northern and central New Mexico: *Geological Society of America Abstracts with Programs*, v. 14, p. 304.
- Cabot, E.C., 1938, Fault border of the Sangre de Cristo Mountains north of Santa Fe, New Mexico: *Journal of Geology*, v. 46, p. 88-105.
- Callender, J.F., Robertson, J.M. and Brookins, D.G., 1976, Summary of Precambrian geology and geochronology of northeastern New Mexico: *New Mexico Geological Society Guidebook 27*, p. 129-135.
- Carreras, J., Estrada, A., and White, S., 1977, The effects of folding on the c-axis fabrics of a quartz mylonite: *Tectonophysics*, v. 39, p. 3-24.
- Cobbold, P.R. and Quinquis, H., 1980, Development of sheath folds in shear regimes: *Journal of Structural Geology*, v. 2, p. 119-126.
- Codding, D.B., Grambling, J.A., and Williams, M.L., 1933, Geochemistry of minor element and rare earth-rich horizons in Precambrian metamorphic rocks of the southern Sangre de Cristo Mountains, New Mexico: *Geological Society of America Abstracts with Programs*, v. 15, p.
- Condie, K.C., 1978a, Geochemical evidence for undepleted mantle beneath New Mexico during the Proterozoic: *Geological Society of America Abstracts with Programs*, v. 10, p. 100.
- Condie, K.C., 1978b, Geochemistry of Proterozoic granitic plutons from New Mexico: *Chemical Geology*, v. 21, p. 131-149.
- Condie, K.C., 1982, Plate-tectonics model for Proterozoic continental accretion in the southwestern United States: *Geology*, v. 10, p. 37-42.

- Condie, K.C., 1982, Early and Middle Proterozoic supracrustal successions and their tectonic settings: *American Journal of Science*, v. 282, p. 341-357.
- Condie, K.C., 1984, Early Proterozoic supracrustal associations in the southwest: An update: *Geological Society of America Abstracts with Programs*, v. 16, p.
- Condie, K.C., 1985, Early Proterozoic continental accretion in southwestern North America: Sixth International Conference on Basement Tectonics, Abstracts with Programs, v. 6, p. 13-14.
- Condie, K.C., 1986, Geochemistry and tectonic setting of early Proterozoic supracrustal rocks in the southwestern United States: *Journal of Geology*, v. 94, p. 845-864.
- Condie, K.C., 1987, Early Proterozoic arc terranes and continental accretion in the southwestern U.S.: *Geological Society of America Abstracts with Programs*, v. 19, p. 625.
- Conway, C.M. and Silver, L.T., 1986, 1700-1610 Ma Proterozoic rocks in central to southeastern Arizona: *Arizona Geological Digest*, in press.
- Coward, M.P., 1983, Thrust tectonics, thin skinned or thick skinned, and the continuation of thrusts to deep in the crust: *Journal of Structural Geology*, v. 5, p. 113-123.
- Duncan, A.C., 1985, Transected folds: a re-evaluation, with examples from the "type area" at Sulphur Creek, Tasmania: *Journal of Structural Geology*, v. 7, p. 409-419.
- Duncan, I.J. and Shore, P.J., 1984, The Vadito melange: A new perspective on the tectonic evolution of northern New Mexico: *Geological Society of America Abstracts with Programs*, v. 16, n. 4, p. 220.
- Ferry, J.M. and Spear, F.S., 1978, Experimental calibration of the partitioning of Fe and Mg between biotite and garnet: *Contributions to Mineralogy and Petrology*, v. 66, p. 113-117.
- Fullagar, P.D. and Shiver, W.S., 1973, Geochronology and petro-chemistry of the Embudo Granite, New Mexico: *Geological Society of America Bulletin*, v. 84, p. 2705-2712.

- Grambling, J.A., 1979, Precambrian geology of the Truchas Peak region, north-central New Mexico, and some regional implications: New Mexico Geological Society, Guidebook 30, p. 135-143.
- Grambling, J.A., 1986, Crustal thickening during Proterozoic metamorphism and deformation in New Mexico: *Geology*, v. 14, p. 149-152.
- Grambling, J.A., 1986b, A regional gradient in the composition of metamorphic fluids in pelitic schist, Pecos Baldy, New Mexico: *Contributions to Mineralogy and Petrology*, v. 94, p. 149-164.
- Grambling, J.A. and Ward, D.B., 1987, Thrusting of the Pecos Greenstone belt over younger supracrustal rocks, Rio Mora area, New Mexico: *Geological Society of America Abstracts with Programs*, v. 19, p. 278.
- Grambling, J.A. and Williams, M.L., 1985a, The effects of  $Fe^{3+}$  and  $Mn^{3+}$  on aluminum silicate phase relations in north-central New Mexico, U.S.A.: *Journal of Petrology*, v. 26, p. 324-354.
- Grambling, J.A. and Williams, M.L., 1985b, Correlation of Proterozoic stratigraphy across northern New Mexico: Sixth International Conference on Basement Tectonics Abstracts with Programs, v. 6, p. 19.
- Grambling, J.A., Williams, M.L., and Coddling, D.B., 1983, Mn and Cr-rich marker horizons in multiply-deformed Proterozoic metamorphic rocks, northern New Mexico: *Geological Society of America Abstracts with Programs*, v. 15, p. 424.
- Green, A.G., Weber, W., and Hajnal, Z., 1985, Evolution of Proterozoic terrains beneath the Williston Basin: *Geology*, v. 13, p. 624-628.
- Gresens, R.L., 1972, Staurolite-quartzite bands in kyanite at Big Rock, Rio Arriba County, New Mexico - A discussion: *Contributions to Mineralogy and Petrology*, v. 35, p. 193-199.
- Gresens, R.L., 1975, Geochronology of Precambrian rocks, north-central New Mexico: *Geological Society of America Bulletin*, v. 86, p. 1444-1448.
- Gresens, R.L. and Stensrud, H.L., 1974, Recognition of more metarhyolite occurrences in northern New Mexico and a

- possible Precambrian stratigraphy: *Mountain Geologist*, v. 11, p. 109-124.
- Hobbs, B.E., Means, W.D. and Williams, P.F., 1976, An outline of structural geology: Wiley, New York, 571 p.
- Hoffman, P.F. and Bowring, S.A., 1984, Short-lived 1.9 Ga continental margin and its destruction, Wopmay orogen, northwest Canada: *Geology*, v. 12, p. 68-72.
- Holcombe, R.J. and Callender, J.F., 1982, Structural analysis and stratigraphic problems of Precambrian rocks of the Picuris Range, New Mexico: *Geological Society of America Bulletin*, v. 93, p.138-149.
- Holcombe, R.J., Bauer, P.W., and Callender, J.F., 1985, A kinematic model for the polyphase evolution of the Precambrian rocks in the Picuris Range, northern New Mexico: Sixth International Conference on Basement Tectonics Abstracts with Programs, v. 6, p. 20.
- Holdaway, M.J., 1971, Stability of andalusite and the aluminum silicate phase diagram: *American Journal of Science*, v. 271, p. 97-131.
- Holdaway, M.J., 1978, Significance of chloritoid-bearing and staurolite-bearing rocks in the Picuris Range, New Mexico: *Geological Society of America Bulletin*, v. 89, p. 1404-1414.
- Holst, T.B., 1985, Implications of a large flattening strain for the origin of a bedding-parallel foliation in the Early Proterozoic Thomson Formation, Minnesota: *Journal of Structural Geology*, v. 7, p. 375-383.
- Hudleston, P.J., 1986, Extracting information from folds in rocks: *Journal of Geological Education*, v. 34, p.237-245.
- Hurd, R.L., 1982, The deformational history and contact relationships in the central Hondo syncline, Picuris Mountains, New Mexico [M.S. thesis]: University of Texas, Dallas, 82 p.
- Just, E., 1937, Geology and economic features of the pegmatites of Taos and Rio Arriba counties, New Mexico: *New Mexico Bureau of Mines and Mineral Resources Bulletin* 13, 73 p.
- Klich, I., 1983, Precambrian geology of the Elk Mountain - Spring Mountain area, San Miguel county, New Mexico [M.S. thesis]: *New Mexico Institute of Mining and Technology*, 147 p.

- Lister, G. and Snoke, A.W., 1984, S-C mylonites: *Journal of Structural Geology*, v. 6, p. 617-638.
- Long, L.E., 1972, Rb-Sr chronology of Precambrian schist and pegmatite, La Madera quadrangle, northern, New Mexico: *Geological Society of America Bulletin*, v. 83, p. 3425-3432.
- Long, P.E., 1974, Contrasting types of Precambrian granitic rocks in the Dixon-Penasco area, northern New Mexico: *New Mexico Geological Society Guidebook 25*, p. 101-108.
- Long, P.E., 1976, Precambrian granitic rocks of the Dixon-Penasco area, northern New Mexico [PhD thesis]: Stanford University, Stanford, 533 p.
- Manley, K., 1976, The late Cenozoic history of the Espanola Basin, New Mexico [Ph.D. thesis]: University of Colorado, 171 p.
- Marjoribanks, R.W. and Black, L.P., 1974, Geology and geochronology of the Arunta complex, north of Ormiston Gorge, Central Australia: *Journal of the Geological Society of Australia*, v. 21, p. 291-300.
- Maxon, J.R., 1976, The age of the Tres Piedras Granite, New Mexico: A case of large scale isotopic homogenization [M.S. thesis]: Florida State University, 101 p.
- McCarty, R.M., 1983, Structural geology and petrography of part of the Vadito Group, Picuris Mountains, New Mexico [M.S. thesis]: Univ. of New Mexico, Albuquerque, 159 p.
- McLelland, J.M. and Isachsen, Y.W., 1985, Geological evolution of the Adirondack Mountains: A review, *in* Tobi, A., and Touret, J., eds., *The deep Proterozoic crust in the North Atlantic provinces*: NATO Advanced Study Institute Series C, v. 158, p. 175-215.
- Miller, E.L., Kanter, L.R., Larue, D.K., Turner, R.J., Murchey, B., and Jones, D.L., 1982, Structural fabric of the Paleozoic Golconda allocthon, Antler Peak Quadrangle, Nevada; progressive deformation of an oceanic sedimentary assemblage: *Journal of Geophysical Research*, v. 87, p. 3795-3804.
- Miller, J.P., Montgomery, A., and Sutherland, P.K., 1963, Geology of part of the Sangre de Cristo Mountains, New Mexico: *New Mexico Bureau of Mines and Mineral Resources Memoir 11*, 106 p.

- Montgomery, A., 1953, Precambrian geology of the Picuris Range, north-central New Mexico: New Mexico Bureau of Mines and Mineral Resources Bulletin 30, 89 p.
- Montgomery, A., 1963, Precambrian geology, in Miller, J.P., Montgomery, A., and Sutherland, P.K., Geology of part of the Sangre de Cristo Mountains, New Mexico: New Mexico Bureau of Mines and Mineral Resources Memoir 11, p. 7-21.
- Nelson, B.K. and DePaolo, D.J., 1985, Rapid production of continental crust 1.7 to 1.9 b.y. ago: Nd isotopic evidence from the basement of the North American mid-continent: Geological Society of America Bulletin. v. 96, p. 746-754.
- Nielsen, K.C., 1972, Structural evolution of the Picuris Mountains, New Mexico [M.S. thesis]: University of North Carolina, Chapel Hill, 47 p.
- Nielsen, K.C. and Scott, T.E., Jr., 1979, Precambrian deformational history of the Picuris Mountains, New Mexico: New Mexico Geological Society Guidebook, v. 30, p. 113-120.
- Olesen, N.O., 1978, Distinguishing between inter-kinematic and syn-kinematic porphyroblastesis: Geologische Rundschau, v. 67, p. 278-287.
- Passchier, C.W. and Simpson, C., 1986, Porphyroclast systems as kinematic indicators: Journal of Structural Geology, v. 8, p. 831-843.
- Pfiffner, O.A., 1981, Fold and thrust tectonics in the Helvetic nappes: In K.R. McClay and N.J. Price, eds., Thrust and Nappe Tectonics: Geological Society of London, Special Publication 9, p. 319-327.
- Powell, C. McA., 1974, Timing of slaty cleavage during folding of Precambrian rocks, Northwest Tasmania: Geological Society of America Bulletin, v. 85, p. 1043-1060.
- Powell, C. McA. and Vernon, R.H., 1979, Growth and rotation history of garnet porphyroblasts with inclusion spirals in a Karakoram schist: Tectonophysics, v. 54, p. 25-43.
- Quinquis, H., Andren, C., Brun, J.P., and Cobbold, P.R., 1978, Intense progressive shear in Ile de Groix blueschists and compatibility with subduction or

- obduction: *Nature, Lond.* 273, 43-45.
- Reed, J.C., Jr., 1984, Proterozoic rocks of the Taos Range, Sangre de Cristo Mountains, New Mexico: *New Mexico Geological Society Guidebook 35*, p. 179-185.
- Register, M.E., 1979, Geochemistry and geochronology of the Harding pegmatite, Taos County, New Mexico [M.S. thesis]: University of New Mexico, Albuquerque, 145 p.
- Rivers, T., 1983, The northern margin of the Grenville Province in western Labrador - Anatomy of an ancient orogenic front: *Precambrian Research*, v. 22, p. 41-73.
- Robertson, J.M. and Moench, R.H., 1979, The Pecos greenstone belt: A Proterozoic volcano-sedimentary sequence in the southern Sangre de Cristo Mountains, New Mexico: *New Mexico Geological Society Guidebook 30*, p. 165-173.
- Roering, C. and Smit, C.A., 1987, Bedding-parallel shear, thrusting and quartz vein formation in Witwatersrand quartzites: *Journal of Structural Geology*, v. 9, p. 419-427.
- Rosenfeld, J.L., 1968, Garnet rotations due to the major Paleozoic deformations in southeastern Vermont: *In Studies of Appalachian Geology: Northern and Maritime*, W.S. White, E. Zen, J.B. Hadley, and J.B. Thompson, eds., Wiley Interscience, New York, p. 195-202.
- Rosenfeld, J.L., 1970, Rotated garnets in metamorphic rocks: *Geological Society of America Special Paper 129*.
- Sanderson, D.J., 1973, The development of fold axes oblique to the regional trend: *Tectonophysics*, v. 16, p. 55-70.
- Schoneveld, C., 1977, A study of some typical inclusion patterns in strongly paracrystalline rotated garnets: *Tectonophysics*, v. 39, p. 453-471.
- Scott, T.E., Jr., 1980, A strain analysis of the Marquenas Quartzite and contact relationships of Ortega-Vadito Groups [M.S. thesis]: University of Texas, Dallas, 173 p.
- Sedlock, R.L. and Larue, D.K., 1985, Fold axes oblique to the regional plunge and Proterozoic terrane accretion in the southern Lake Superior region: *Precambrian Research*, v. 30, p. 249-262.

- Silver, L.T., 1984, Observations on Precambrian evolution of northern New Mexico and adjacent regions: Geological Society of America Abstracts with Programs, v. 16, p. 256.
- Silver, L.T., 1987, A Proterozoic history for southwestern North America: Geological Society of America Abstracts with Programs, v. 19, n. 7, p. 845.
- Silver, L.T., Crittenden, M., and Robertson, J.M., 1977, Chronostratigraphic elements of Precambrian rocks of the southwestern and far western U.S.: Geological Society of America Abstracts with Programs, v. 9, p. 1176.
- Simpson, C., 1986, Determination of movement sense in mylonites: Journal of Geological Education, v. 34, p. 246.
- Simpson, C. and Schmid, S.M., 1983, An evaluation of criteria to deduce the sense of movement in sheared rocks: Geological Society of America Bulletin, v. 94, p. 1281-1288.
- Soegaard, K. and Eriksson, K.A., 1985, Evidence of tide, storm, and wave interaction on a Precambrian siliclastic shelf: the 1,700 m.y. Ortega Group, northern New Mexico: Journal of Sedimentary Petrology, v. 55, p. 672-684.
- Soegaard, K. and Eriksson, K.A., 1986, Transition from arc volcanism to stable-shelf and subsequent convergent-margin sedimentation in northern New Mexico from 1.76 Ga: Journal of Geology, v. 94, p. 47-66.
- Speed, R.C. and Larue, D.K., 1982, Barbados: architecture and implications for accretion: Journal of Geophysical Research, v. 87, p. 3633-3643.
- Spry, A., 1969, Metamorphic textures: Pergamon Press, 350 p.
- Stacey, J.S. and Hedlund, D.C., 1983, Lead-isotopic compositions of diverse igneous rocks and ore deposits from southwestern New Mexico and their implications for Early Proterozoic crustal evolution in the western U.S.: Geological Society of America Bulletin, v. 94, p. 43-57.
- Stacey, J.S. and others, 1976, Plumbotectonics II A, Precambrian massive sulfide deposits: United States Geological Survey Open-File Report 76-476, 26 p.

- Steiger, R.H. and Jager, E., 1977, Subcommittee on geochronology: Convention on the use of decay constants in geo- and cosmochronology: Earth and Planetary Science Letters, v. 36, p. 359-362.
- Steinpress, M.G., 1980, Neogene stratigraphy and structure of the Dixon area, Espanola basin, north-central New Mexico [M.S. thesis]: University of New Mexico, Albuquerque, 127 p.
- Sutherland, P.K., 1963, Precambrian structure, key to Pennsylvanian depositional history in the southern Sangre de Cristo mountain area, New Mexico: Abstracts for 1962, Geological Society of America Special Paper 73, p. 251-252.
- Tullis, J., Snoke, A.W., and Todd, V.R., 1982, Significance and petrogenesis of mylonitic rocks: Geology, v. 10, p. 227-230.
- Van Schmus, W.R. and Bickford, M.E., 1981, Proterozoic chronology and evolution of the midcontinent region, North America; in Kroner, A., ed., Precambrian Plate Tectonics: Amsterdam, Elsevier, p. 261-296.
- Vernon, R.H., 1978, Porphyroblast-matrix microstructural relationships in deformed metamorphic rocks: Geologische Rundschau, v. 67, p. 288-305.
- Vernon, R.H., 1986, Evaluation of the "quartz-eye" hypothesis: Economic Geology, v. 81, p. 1520-1527.
- Vernon, R.H., 1987, Growth and concentration of fibrous sillimanite related to heterogeneous deformation in K-feldspar-sillimanite metapelites: Journal of Metamorphic Geology, v. 5, p. 51-68.
- Ward, D.B. and Grambling, J.A., 1985, Dating a Proterozoic metamorphic event using Rb-Sr geochronology: An example from northern New Mexico: Geological Society of America Abstracts with Programs, v. 17, p. 744.
- White, S.H., Burrows, S.E., Carreras, J., Shaw, Nd., and Humphreys, F.J., 1980, On mylonites in ductile shear zones: Journal of Structural Geology, v. 2, p. 175-187.
- Williams, G.D., 1978, Rotation of contemporary folds in the X direction during overthrust processes in Laksefjord, Finnmark: Tectonophysics, v. 48, p. 29-40.

- Williams, M.L., 1982, Geology of the copper occurrence at Copper Hill, Picuris Mountains, New Mexico [M.S. thesis]: University of Arizona, Tucson, 104 p.
- Williams, M.L., 1987, Stratigraphic, structural, and metamorphic relationships in Proterozoic rocks from northern New Mexico [Ph.D. thesis]: University New Mexico, Albuquerque, 138 p.
- Williams, M.L., Grambling, J.A., and Bowring, S.A., 1986, Redefinition of the Vadito Group, an extensive felsic volcanic-sedimentary sequence in the Proterozoic of northern New Mexico: Geological Society of America Abstracts with Programs, v. 18, p. 422.
- Williams, P.F., 1985, Multiply deformed terrains - problems of correlation: Journal of Structural Geology, v. 7, p. 269-280.
- Williams, P.F. and Schoneveld, C., 1981, Garnet rotation and the development of axial plane crenulation cleavage: Tectonophysics, v. 70, p. 307-334.
- Wilson, M.R., 1971, On syntectonic porphyroblast growth: Tectonophysics, v. 11, p. 231-260.
- Wobus, R.A. and Manley, K., 1982, Reconnaissance geologic map of the Burned Mountain quadrangle, Rio Arriba County, New Mexico: U. S. Geological Survey Miscellaneous Field Studies Map MF-1409, scale 1:24,000.
- Zwart, H.J., 1962, On the determination of polymetamorphic associations and its application to the Bosost area (central Pyrenees): Geologische Rundschau, v. 52, p. 38-65.

This dissertation is accepted on behalf of the faculty  
of the Institute by the following committee:

James M. Roberts  
\_\_\_\_\_  
Advisor  
Jonathan J. Collins  
\_\_\_\_\_  
W. A. Grandis  
\_\_\_\_\_  
Kenneth J. Louden  
\_\_\_\_\_  
C. K. Mauer  
\_\_\_\_\_  
12/15/87  
\_\_\_\_\_  
Date

- Exposed contact.
- - - Inferred or covered contact.
- Buried contact.
- Exposed fault, with sense of motion where known.
- - - Inferred fault, with sense of motion where known.
- ..... Buried fault, with sense of motion where known.
- Strike and dip of compositional layering (So), younging unknown. Generally sub-parallel to S1.
- Strike and dip of right-side-up compositional layering.
- Strike and dip of overturned compositional layering.
- Strike and dip of dominant foliation, generally S3\*.
- ← Trend and plunge of intersection lineation, generally L2\*.
- ← Overturned F2 syncline.
- ← Overturned F3 syncline.
- ← Overturned F3 anticline.
- ← Overturned F2 anticline.
- ← Area of many minor folds.
- ← Minor syncline.
- ← Minor anticline.

LITHOLOGIES

- QT Quaternary and Tertiary rocks. Includes volcanicslastics, alluvial and fluvial sediments, and recent sands and gravels.
- Pz Paleozoic sedimentary rocks. Mississippian-Pennsylvanian arkose, quartzite, conglomerate, shale, and limestone.
- Fault breccia. Zone of highly brecciated mixed metasedimentary rocks along the Picuris-Pecos fault.
- Pegmatite. Small, concordant, simple pegmatites of quartz, microcline, albite, and muscovite.
- Granite of Picuris Peak. Strongly foliated, medium- to coarse-grained granitic rocks interlayered with supracrustal rocks.
- Granite of Alamo Canyon. Pink to orange, fine- to medium-grained, crumbly, equigranular granitic rocks. Ga - Thin, discontinuous amphibolite bodies in Ga.
- Piedra Lumbre Formation. PL - Thinly laminated garnet-staurolite schists and phyllites. PL0 - Dark gray to black garnet phyllite. PLq - Massive to layered schistose cross-bedded quartzite.
- Pilar Phyllite Formation. Very fine-grained, black, compact, quartz-rich carbonaceous slaty phyllite. Separated from R6 by distinctive blue-black garnet quartzite.
- R6 Schist. Well-layered, gray to red, quartz-muscovite-biotite-garnet-(staurolite) phyllites and schists. Commonly strongly crenulated.
- R5 Quartzite. Resistant, massive, locally micaceous, white to gray to blue, crystalline quartz arenite with local cross-beds.
- R4 Schist. Fine- to medium-grained, reddish weathering, gray to silver, garnet-staurolite-muscovite-biotite-quartz schists.
- R3 Quartzite. Resistant, massive to thinly-layered, cross-bedded, white to gray to tan to blue quartz arenites. Local thin schistose layers.
- R12 Schists. Poorly resistant, biotite-muscovite "salt and pepper" schist with large andalusite porphyroblasts, overlie by garnet-staurolite schists.
- Ortega Quartzite. Resistant, massive, cross-bedded quartz arenite. Oqu - Upper quartzite. Oql - Lower red quartzite. Osa - Aluminous schist. Oab - Biotite schist. Oqm - Massive, dark quartzite. Osl - Red laminated schist.
- Rio Pueblo Schist. RP - White, feldspathic quartz-eye schist. RPp - Red muscovite quartz-eye schist. RPaw - White quartz-muscovite schist. RPo - Piemontite schist. Units may have no stratigraphic significance. Felsic schist at Pilar. White to pink, feldspathic, quartz-muscovite, quartz-eye schist. May be equivalent to Rio Pueblo Schist.
- Felsite. White, fine-grained, dense, quartz-muscovite schists that commonly contain rounded quartz-eyes.
- Amphibolite. Strongly layered, black, amphibole-plagioclase rocks with wide range of textures. Locally grade into black biotite schists.
- Quartzite and conglomerate. Massive, cross-bedded quartz arenite, thin-bedded schistose quartzite, and polystratic quartzose conglomerates with rounded clasts. Equivalent to Marquenas Quartzite to the west.
- Schist. Interlayered schists and immature quartzites. Vsw - White quartz-muscovite schist. Vsa - Andalusite schist. Vab - Biotite schist. Vsg - Garnet-biotite-andalusite schist.

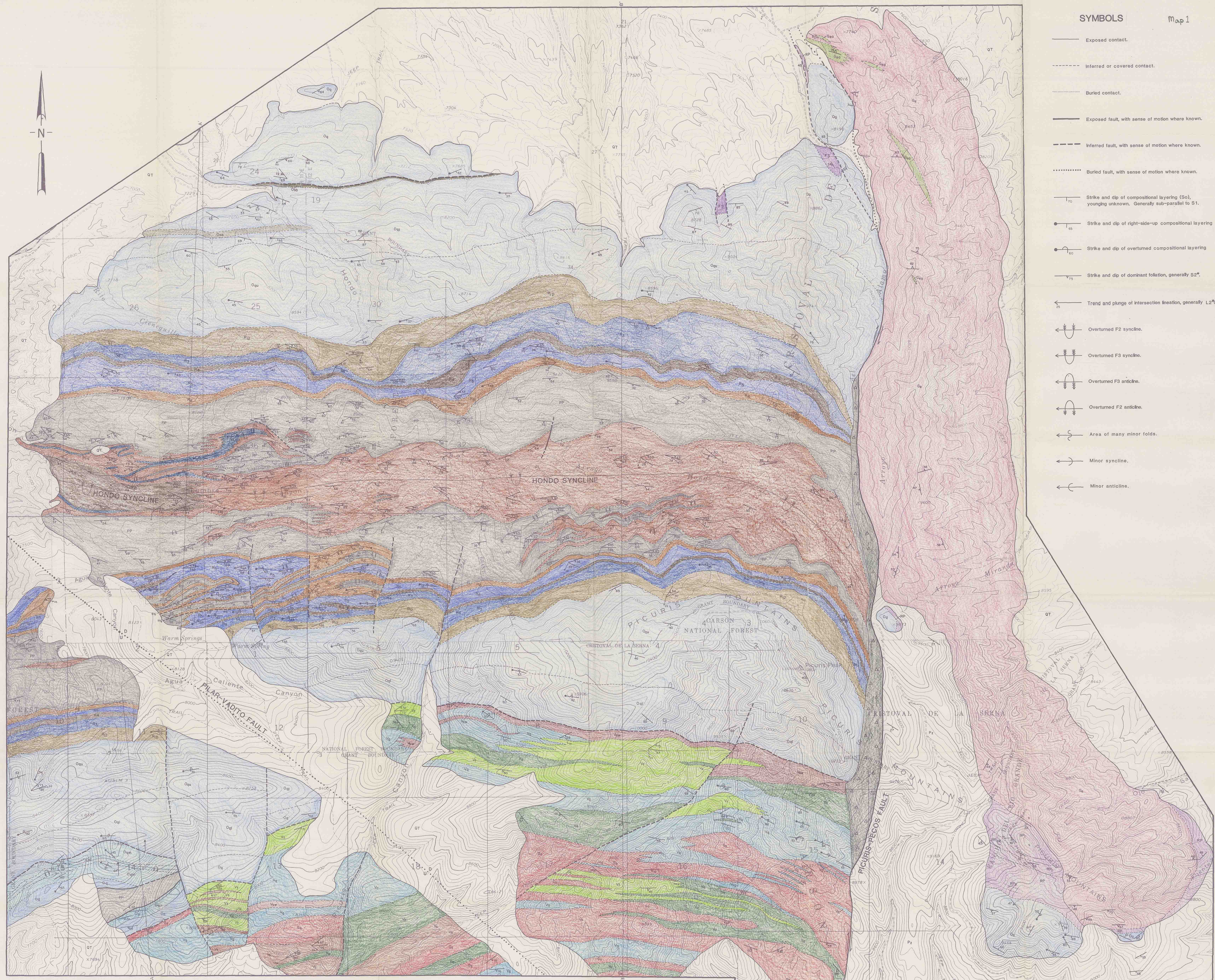
PHANEROZOIC

PRECAMBRIAN

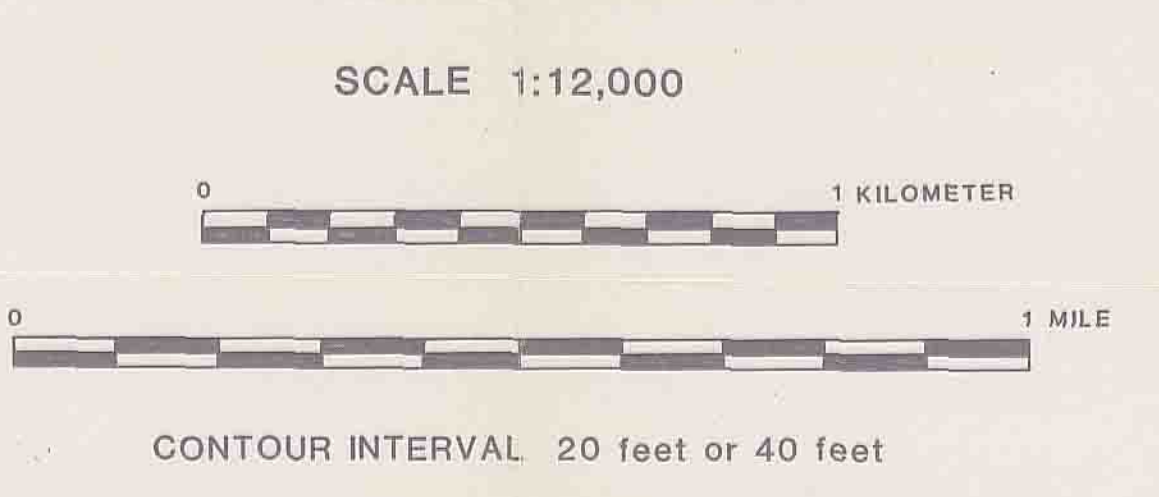
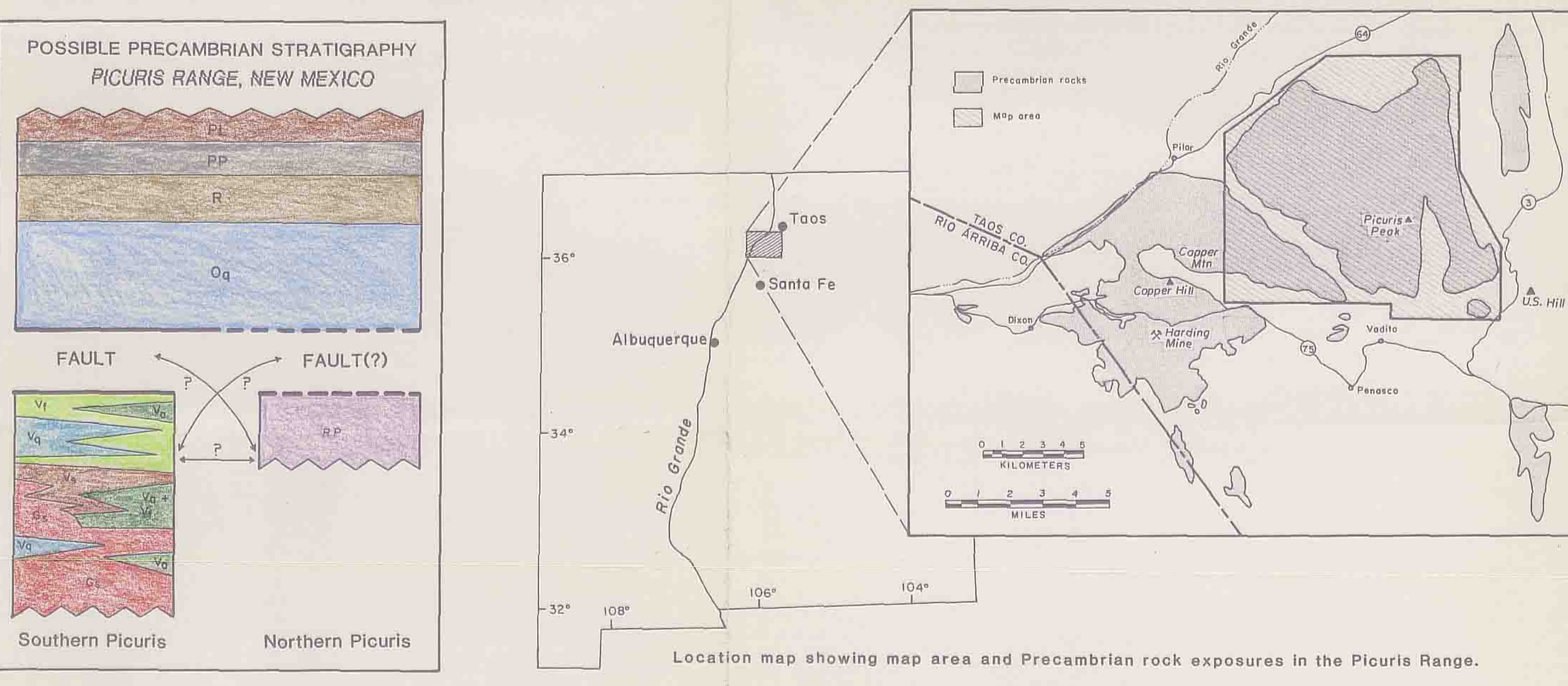
- PIEDRA LUMBRE FORMATION
- PILAR PHYLLITE FORMATION
- ORTEGA GROUP
- RINCONADA FORMATION
- ORTEGA QUARTZITE FORMATION

RIO PUEBLO SCHIST & FELSIC SCHIST AT PILAR  
SEE STRAT. CHART BELOW

VADITO GROUP



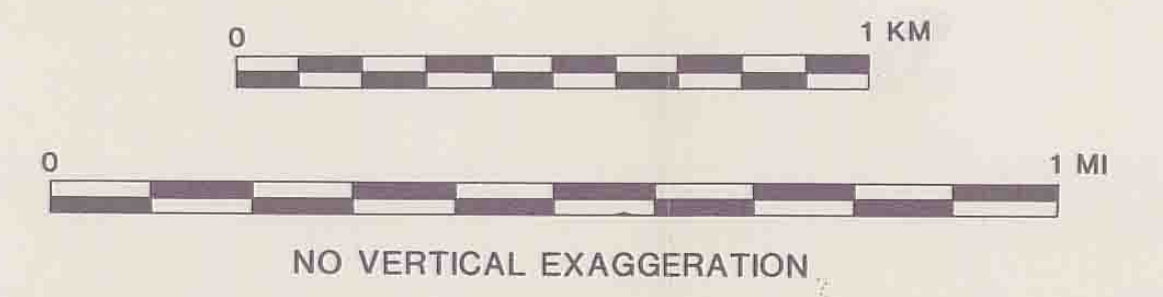
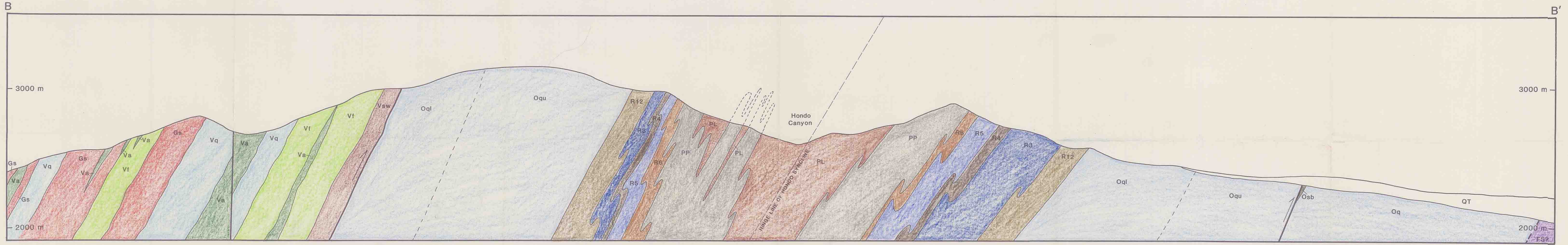
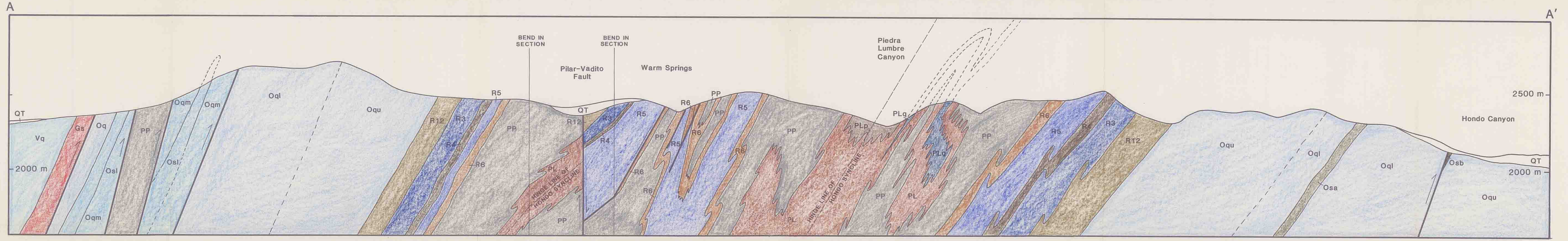
GEOLOGIC MAP OF PRECAMBRIAN ROCKS IN THE EASTERN PICURIS RANGE, NORTHERN NEW MEXICO



Paul W. Bauer  
1987



Drafted by P. W. Bauer



CROSS-SECTIONS TO ACCOMPANY GEOLOGIC MAP OF PRECAMBRIAN ROCKS OF THE EASTERN PICURIS RANGE, NEW MEXICO

PAUL W. BAUER  
1987